

Ditton Geotechnical Services Pty Ltd  
80 Roslyn Avenue Charlestown NSW 2290  
PO Box 5100 Kahibah NSW 2290



## **Donaldson Coal Pty Ltd**

### **Subsidence Predictions and Impact Assessment for the Proposed SMP Area 2 Pillar Extraction Panels at Abel Mine, Black Hill**

**DGS Report No. ABL-002/1**

**Date: 1 June 2011**



1 June 2011

Mr Tony Sutherland  
Technical Services Manager - Underground Operations  
Donaldson Coal  
Abel Mine  
1132 John Renshaw Drive,  
Black Hill NSW 2322

DGS Report No. ABL-002/1

Dear Tony,

**Subject: Subsidence Predictions and Impact Assessment for the Proposed SMP Area 2  
Pillar Extraction Panels at Abel Mine, Black Hill**

This report has been prepared in accordance with the brief provided on the above project.

Please contact the undersigned if you have any questions regarding this matter.

For and on behalf of  
**Ditton Geotechnical Services Pty Ltd**

A handwritten signature in black ink, appearing to read 'Steven Ditton', is written over a light grey horizontal line.

Steven Ditton  
Principal Engineer

## Executive Summary

This report presents predictions of worst-case mine subsidence effects and impact management strategies for natural and man-made features in SMP Area 2 of the Abel Mine, John Renshaw Drive, Black Hill. The report will be used for the purpose of preparing a Subsidence Management Plan (SMP) submission to the NSW Department of Industry and Investment.

The report has assessed the proposed mining layout of thirteen, 160.5 m wide pillar extraction panels (Panels 14 - 26) in the 1.8 m to 4.2 m thick Upper Donaldson Seam. It is also proposed to extract the pillars in the 89 m, 105 m and 140 m wide Tailgate, East Install and South East Mains Headings respectively after completion of the production panels.

The proposed mining area (Area 2) has been defined by an approximate 26.5° angle of draw line outside of the proposed second workings panel limits. The area is partially bounded by Area 1 to the north, the F3 Freeway to the east and generally Black Hill Road to the south. The land within Area 2 is semi-cleared, dry-sclerophyll forest with generally flat to gently undulated terrain.

The surface of the Area 2 SMP application area is contained within land owned by Black Hill Land Pty Limited, Catholic Diocese of Maitland-Newcastle, private rural-residential land holdings and a narrow strip traversing the area owned by Hunter Water Corporation.

The surface slopes range from 1° to 10° and steepen locally to 15° along Viney Creek (a Schedule 2 Stream (**DIPNR, 2005**)), which drains the site towards the north-east. Topographic relief ranges from 16 m to 68 m AHD across the panels.

Land use in Area 2 includes the following:

- Native bushland with ephemeral and perennial streams
- Livestock Grazing
- Rural Residential

Infrastructure within Area 2 includes:

- Transgrid 330kV transmission line with five suspension towers (26B to 30B)
- Energy Australia 132kV transmission line with seven pairs of timber power poles (EA8 to EA14)
- Energy Australia 11 kV and 415 V domestic supply lines with twenty-three power poles
- Hunter District Water Board pipeline

- Optus fibre optic cable within the Transgrid 330kV powerline Easement
- Active and redundant buried Telstra copper cables
- Two Permanent Survey Control Marks
- Four Principal Residences (as defined in the Project Approval)
- Other structures within the proposed Catholic High School (which is located on the south-eastern section of Lot 131 DP 1057179)
- Two Non-Principal Residences and various out buildings (defined in the Project Approval as “All Other Surface Structures”)
- Disused, unoccupied residences/office buildings
- Buried stock and domestic water supply pipe lines
- Two Public Roads (Black Hill and Taylors Road)
- Private access roads and tracks
- Cattle stockyard and holding areas
- Various property boundary and internal paddock fences, gates and cattle grids
- Several (< 1ML storage capacity) stock watering dams
- Two reinforced concrete pipe culverts in fill along Black Hill Road
- Several buried and clay liner capped contaminated material areas (hazardous waste from previous land users)

SMP Area 2 was classified as a subsidence district until 1994 when the Ironbark and Ironbark subsidence districts were revoked. The Mine Subsidence Board is in the process of re-classifying the area as a Mine Subsidence District.

The Catholic Diocese land is presently used to graze cattle (and previous to that was the Steggle's Poultry Farm). Disruption of the existing stock watering and domestic supply system is a significant business risk and will need to be managed carefully during mining.

The Black Hill Land Pty Ltd land is currently partially developed in SMP Area 1 only and has a Boral Asphalt plant and the remediated Iron Bark Colliery pit top area. The Black Hill Land Pty Ltd land is likely to be redeveloped into industrial lots with sealed access roads. No development proposals have been indicated for the Catholic Diocese land at this stage.

Based on the predicted post-mining subsidence contours prepared for this study, it is estimated that the areal extent of flooding due to the 1 in 100 year ARI event may increase by up to 5% after mining of Areas 1 and 2 is completed.

Aboriginal Artefact scatters (silcrete stone axe flakes) have been identified at three locations within Areas 1 and 2, but all are outside the limits of proposed secondary extraction. It has also been assessed that there are likely to be further archaeological sites with 'moderate cultural significance' along the Viney Creek corridor to the south of the proposed SMP area.

A 330 kV power line corridor traverses SMP Areas 1 and 2 with a total of eleven transmission towers (No.s 26B to 36B), including five suspension-type towers (26B to 30B) in Area 2. The towers were constructed with cruciform footings in the early 1980's in anticipation of mine subsidence from the Iron Bark Colliery (which did not proceed). Transgrid are currently reviewing the adequacy of the cruciforms and the need for further subsidence mitigation works prior to the proposed Area 1 and 2 subsidence effects.

Based on consultation with the stakeholders to-date, Subsidence Control Zones (SCZ) will be required for Viney Creek (DECCW) and the four Principal Residences within the application area.

The pillar extraction panels will have cover depths ranging from 100 m to 150 m and average mining heights ranging from 1.8 m to 2.8 m. The East Install, South East Main and Tailgate Headings will also be extracted on retreat after the production panels 14 to 26 are completed. The mining height in the main headings panels will range from 2.0 m to 2.8 m.

Panel development headings will be 5.5 m wide and range from 2.4 m to 2.6 m high (depending on seam thickness).

Barrier pillars between production panels will generally have widths of 24.5 m and pillar width/height ratios of 9.4 to 11.1 and are expected to behave elastically in the long term (i.e. strain hardening characteristics are likely to develop if the pillars are overloaded).

A solid barrier between the finishing ends of the production panels and the adjacent East Mains, East Install and South East Mains will be 21.5 m to 23 m wide with pillar width/height ratios of 8.3 to 9.2. Barrier pillars between Panel 1, Tailgate Headings and South East Main Headings will have widths of 16.5 m and 21 m with pillar width/height ratios of 6.6 and 8.1 respectively. These pillars are also expected to behave elastically in the long term due to their strain hardening characteristics.

The overburden comprises thinly bedded sandstone, siltstone and mudstones (shale) of the Dempsey Formation, which is part of the Permian Aged Tomago Coal Measures. A persistent geological structure (reverse fault) with an 8 m throw intersects the eastern SMP area on a north westerly strike.

The panel width to cover depth (W/H) ratios for the proposed 160.5 m wide pillar extraction panels 14 to 26 will range from 0.90 to 1.97, indicating 'critical' to 'supercritical' subsidence

behaviour, which are assumed to occur at Abel when panel W/H ratios are  $> 0.6$  and  $> 1.4$  respectively.

The panel width to cover depth (W/H) ratios for the Tailgate Headings, East Main and South East Mains will range from 0.90 to 1.46, indicating 'critical' overburden behaviour in regards to subsidence development.

The following subsidence effect parameters for all of the proposed pillar extraction panels are predicted:

- Predicted first and final maximum subsidence for the production panels 14 to 26 range from 0.75 m to 1.41 m and from 0.76 m to 1.45 m respectively (i.e. 28% to 55% of the effective mining height).
- Predicted first and final maximum subsidence for the 89 m to 140 m wide East Install, TG and SE Mains panels range from 0.69 m to 1.21 m and from 0.87 m to 1.36 m (i.e. 26% to 51% of the effective mining height).
- First and Final barrier pillar subsidence ranges from 0.03 m to 0.17 m due to total pillar stresses after mining of 5.8 MPa to 11.7 MPa. The post-mining factors of safety for the barrier pillars are estimated to range from 2.34 to 24.1 and likely to behave elastically in the long-term.
- Final maximum panel tilt ranges from 14 mm/m to 36 mm/m.
- Final maximum panel hogging curvature ranges from  $0.51 \text{ km}^{-1}$  to  $1.89 \text{ km}^{-1}$ .
- Final maximum panel sagging curvature will range from  $0.65 \text{ km}^{-1}$  to  $2.39 \text{ km}^{-1}$ .
- Final tensile strains associated with the hogging curvatures will range from 5 mm/m to 19 mm/m.
- Compressive strains associated with the sagging curvatures will range from 7 mm/m to 24 mm/m.
- Final maximum panel horizontal displacement from 140 mm to 360 mm.
- Final goaf edge subsidence ranging from 35 mm to 170 mm.
- Distance from goaf edges to maximum panel tilt (inflexion point) ranges from 16 m to 50 m.
- The angle of draw to the 20 mm subsidence contour ranges from  $7^\circ$  to  $21^\circ$ .

- Predictions of subsidence development curves for 10 m/week, 30 m/week and 50m/week have been derived using the dynamic subsidence analysis module provided in the SDPS program.

The predicted curves are consistent with the measured curves for Area 1 panels in regards to subsidence development, and indicate that 90% to 95% of First maximum panel subsidence will occur within 4 to 6 weeks after undermining, depending on the inevitable variation in retreat rates that will occur during second workings.

The key outcomes of the impact assessment are as follows:

- Based on the predicted range of maximum transverse tensile strains (i.e. 5 to 19 mm/m), surface cracking widths of between 50 mm and 190 mm (based on the Upper 95% Confidence limit) could occur above Panels 14 to 26 and within the limits of extraction (i.e. goaf) beneath the SMP Area 2. The Upper 95% Confidence Limit used in these predictions considers that these values may be exceeded 5% of the time.
- Therefore on a small number of occasions, the predicted crack widths may be exceeded (as has been the case with the panels extracted to date in SMP Area 1). These are generally found to be related to the presence of adverse or anomalous geological or topographical conditions. Strain concentration in near surface rock could also double the above crack widths locally to 100 mm and 380 mm respectively.
- The tensile cracks will probably be tapered and extend to depths ranging from 5 to 10 m, and possibly deeper in near surface sandstone exposures, if present. The cracking is likely to develop in the tensile strain zone just behind the retreating pillar extraction face and soon after undermining occurs. These cracks are termed *transient* as they may close once full subsidence and compressive strains develops in the central areas of the completed panels. Additional cracks are also likely to occur within the tensile strain zones that will form inside and parallel to the rib-sides of the completed panels.
- The previous Area 1 SMP report indicated that the transient cracks widths would be < final crack widths on average. However, based on the similarity in width observed between the transient and final cracks, and the measured average retreat rates for Panels 1 to 4 of 23 m/week to 37 m/week, it is assessed that the extraction face does not move fast enough for the transient crack width reduction to occur generally. The face retreat rates can also vary significantly from < 10 m/week to 50 m/week, depending on mine roof conditions and operational factors, so it is possible that transient cracking will vary between dynamic and final static magnitudes.

It has therefore been assumed in this study that the transient crack widths will be similar in width to final subsidence crack width predictions above the proposed Area 2 Panels.

- The predicted range of maximum transverse compressive strains (7 to 24 mm/m) above the pillar extraction panels may result in shear displacements or 'shoving' of between 70 mm and 240 mm within the central limits of extraction.

- Uplift movements of between 100 mm and 150 mm have occurred in compressive strain zones above Area 1 panels to-date. Uplift movements of between 10 mm and 35 mm have also occurred just outside the limits of mining above the Area 1 panels. These movements are not due to the valley closure mechanism, but related to systematic subsidence development of compressive strains and cantilevering of the bending rock mass. Similar movements may occur again above the Area 2 Panels.
- The **ACARP, 2003** model predicts that mean to U95%CL heights of continuous sub-surface fracturing of 46 m to 89 m (22 to 33 times the effective mining heights of 2.10 to 2.66 m). The likelihood that continuous fracturing will extend to within 10 m of the surface is considered 'likely' for cover depths <50 m and 'possible' for cover depths of 50 to 80 m. Connective cracking to the surface is 'unlikely' to occur where cover depth exceeds 80 m, and 'very unlikely' where cover depth exceeds 100 m.
- The **Forster, 1995** model indicates a similar range of connective cracking heights from 43 m to 88 m for the pillar extraction panels with an effective mining height of 2.1 to 2.66 m.
- Discontinuous fracturing is likely to interact with surface fractures and open joints in the rock mass for cover depths <100m. It is possible that the interaction could continue for cover depths up to 140 m for the given mining geometries.
- In regards to changes to rock mass permeability, **Forster, 1995** indicates that horizontal permeabilities in the fractured zones above longwall mines (see **Figure 30**) could increase by 2 to 4 orders of magnitude (e.g. pre-mining  $k_h = 10^{-9}$  to  $10^{-10}$  m/s; post-mining  $k_h = 10^{-7}$  to  $10^{-6}$  m/s).
- Discontinuous fracturing would be expected to increase rock mass storage capacity and horizontal permeability without direct hydraulic connection to the workings. Rock mass permeability is unlikely to increase significantly outside the limits of extraction.
- The measurement of the A-Zone horizon above Panels 1 and 2 indicates the height of continuous sub-surface fracturing in the Fractured Zone has occurred to between 45 and 50 m above the 120 m and 150 m wide panels with cover depths of 73 m to 95 m.
- The discontinuous subsurface fracturing in the Constrained Zone has lowered the near surface water table by approximately 15.3 m above Panel 1, however it is anticipated that it will recover in the medium to long term after mining is completed. The near surface water table above Panel 2 appears to have dropped below the piezo to a depth > 19.7 m on the western side of a NW striking fault but fell only 4.5 m on the eastern side of the fault.
- Based on the results, it appears that approximately six closed form depressions with volumes ranging from 0.36 ML to 1 ML could develop along the Viney Creek tributaries or gullies above the central areas of Panels 23 to 26. The 'ponds' are estimated to have maximum potential depths of 0.8 to 1.0 m.



- Two of the pond locations exist above Panels 24 and 25 and are already depressions, with one of the depressions above Panel 24 expected to decrease (after mining) from 0.77 ML to 0.63 ML.
- It is considered unlikely that valley closure movements will occur in the gullies / broad crested valleys above the proposed panels. The lack of thick, massive beds of conglomerate and sandstone units along the creeks / valleys at the surface will also mean the development of these phenomena is likely to be limited to < 100 mm. Minor cracking in creek beds may cause some shallow sub-surface re-routing of surface flows due to the valley closure mechanism.
- To-date, local longwall mining experiences in undulating terrain with ground slopes up to 25° has not resulted in any large scale, *en-masse* sliding instability due to mine subsidence (or other natural weathering processes etc.). In general, it is possible that localised instability could occur where ground slopes are > 15°, if the slopes are also affected by mining-induced cracking and increased erosion rates.
- The rate of erosion is expected to increase significantly in areas with exposed dispersive / reactive alluvial or residual soils and slope gradients are increased by more than 2% (i.e. tilts >20 mm/m). It is estimated that the gradients above the site will increase or decrease by 0.5% to 2.5%.
- An empirical model for predicting far-field displacement (FFDs) in the Newcastle Coalfield indicates that measurable FFD movements (i.e. 20 mm) generally occur in relatively flat terrain for distances up to 3 to 4 times the cover depth. Predicted lateral curvature radii for each road after mining are > 200 km for horizontal displacements of < 15 mm.

An empirical model for predicting far-field strains (FFSs) in the Newcastle Coalfield indicates that measureable (but diminishing) strains can also occur outside the limits of longwall extraction for distances up to one cover depth (based on the Upper 95% Confidence limit curve). It is assessed, however, that strains will be <0.5 mm/m at a distance equal to 0.5 x cover depth from the pillar extraction panels at Abel.

Based on the above, no impacts due to the proposed mining layout are likely to develop along John Renshaw Drive and the F3 Freeway.

- Nine of eleven Transgrid 330 kV transmission towers (26B to 36B) are within the proposed limits of the pillar extraction panels for Area 1 (five out of six towers) and Area 2 (four out of five towers). The towers above the proposed extraction limits are likely to be subjected to subsidence ranging from 0.02 m to 1.45 m at the tower centres.
- Transient tilts at the Transgrid Towers above the pillar extraction panels are estimated to range from 4 to 43 mm/m for the possible range of retreat rates (30 m/week or less) in Areas 1 and 2. Transient tensile and compressive strains are expected to range from 1 mm/m to 19 mm/m, depending on face retreat rates.

- Final Transgrid Tower tilts are estimated to range between 2 mm/m and 43 mm/m in Areas 1 and 2. Horizontal displacements are estimated to range between 20 mm and 430 mm. Four or five of the tower locations are expected to have residual compressive strains ranging from 2 mm/m to 16 mm/m, with the other towers expected to have residual tensile strains ranging from 1 to 19 mm/m.
- Whilst the Transgrid Towers already have cruciform footings installed, the design limits for the footings (and towers) to resist the predicted movements are uncertain and should be checked by a structural engineer before mine subsidence occurs. Advice from Transgrid is that their preliminary engineering analysis indicates that the cruciform footings are adequate for the predicted levels of subsidence, tilt and strain. It is also likely that flexible conductor strings will need to be installed prior to pillar extraction.
- Mitigation, repair or replacement works may be required after mining impacts for the other features, which include a buried 200 mm diameter UPVC Hunter Water Pipeline, the stock watering system on Catholic Diocese Land, the buried PVC sheathed Optus Fibre Optic cable, fourteen pairs of timber poles, which suspend the Energy Australia 132 kV power lines (seven pairs in Area 1 and seven pairs in Area 2), forty-nine timber poles (twenty six in Area 1 and twenty three in Area 2), which suspend the Energy Australia 11 kV and 415 V domestic power lines, and buried Telstra copper telecommunications cabling.
- The likely impacts of 0.75 m to 1.45 m of mine subsidence and up to 19 mm/m of horizontal tensile strain on the Optus Fibre Optic Cable and Hunter Water pipeline are likely to be significant. Further analysis of the predicted deflected shapes provided in this report and likely stress / strain transfer into each feature will need to be undertaken by the stakeholders or their nominated consultants.

Draft impact management strategies have been developed to allow for sections of each of these features to be uncovered and relocated or replaced either before, during or after mining.

- It is assessed that damage to joints/couplings along the buried stock watering and domestic pipelines and at connections between troughs and residences should be anticipated during mining.

Isolating affected lines and providing alternative water supplies may be necessary if flexible couplings can't be installed prior to mining impact.

- No mining related impacts are predicted for the Aboriginal artefact scatters sites identified outside the limits of secondary extraction and angle of draw.
- Due to the proposed location and extent of the proposed first workings only buffer zones within a 26.5° angle of draw (i.e. 0.5 x cover depth) of the four Principal Residences plus other structures on the proposed Catholic High School site, it is

assessed that the subsidence effects are 'very unlikely' to result in significant impact to the structures. The predicted subsidence effects at the Principal Residences are likely to be < 20 mm subsidence, < 2 mm/m tilt, < 0.1 km<sup>-1</sup> curvature and < 2 mm/m tensile and compressive strain. It is considered unlikely that any subsidence related impacts will not exceed the 'Negligible' to 'Slight' Damage Categories as defined in **AS2870, 1996**.

- The non-principal residences and buildings on Catholic Diocese Land may be subject to subsidence ranging from 0.07 m to 1.3 m, tilts of 6 to 33 mm/m, sagging and hogging curvatures of 1.5 and 1.1 km<sup>-1</sup>, horizontal compressive and tensile strains of 15 and 11 mm/m and horizontal displacements of 60 mm to 330 mm.

It is assessed that the buildings will sustain 'moderate' to 'severe' damage (or Category 3 to 4 Damage, as defined in **AS2870, 1996**) by the associated tilts, strains and curvatures.

These residences are considered as “All Other Surface Structures” under the Project Approval and will have a management plan prepared and implemented as outlined in the Subsidence Specific Commitments (Section E of the Project Approval).

- Panel cross lines and centre lines should be installed above each panel and surveyed before, during and after mine subsidence develops for the purpose of providing relevant monitoring data for end of panel reports and stakeholders. Subsidence monitoring will also be necessary at specific surface features as required by individual Property SMPs.
- Black Hill Road will be undermined by the proposed Area 2 Panels 23 to 26. The road is bitumen sealed, dual carriageway within the Cessnock City Council (CCC) district.

The road is 7 m wide with 1m wide unsealed shoulders. The road formation is generally on-grade with two filled embankments up to 3 m high and RCP culverts placed where the road crosses ephemeral drainage gullies associated with Viney Creek.

The road is likely to be subsided by up to 1.39 m, with tilts of 7 to 30 mm/m, tensile strains of 4 to 12 mm/m and compressive strains of 5 to 10 mm/m. Worst-case impacts to the road and its associated infrastructure are assessed to include 40 mm to 120 mm wide cracks, shearing of 50 to 100 mm and +/- 1 to 2.5% change in superelevation.

- Taylors Road is estimated to be subsided by 1.34 m, with tilts up to 27 mm/m and tensile and compressive strains of mm/m. Impacts to the road are likely to be similar to Black Hill Road.
- Impact management strategies for the Black Hill and Taylors Road may require a pre-mining condition survey of road and drainage infrastructure prior to commencement of second workings. On-going consultation with Cessnock City Council in regards to



preparation of a Public Roads Management Plan for managing mine subsidence impacts within the road corridors will be necessary.

- Some of the property fences, dams and private access roads from Black Hill Road that are outside of the proposed Subsidence Control Zones for the Principal Residences may be 'moderately' impacted by mine subsidence. Management of impact to these features will be included in the appropriate property management plan.

It is considered that as the proposed SMP Area 2 mining layout is similar to the layout presented in the Environmental Assessment (EA) Report for the Abel Mining Lease Application. The mining geometry and resulting impacts to the natural and man-made features will therefore be similar in magnitude and location to the EA study outcomes.

## Table of Contents

### Glossary of Terms

1.0	Introduction .....	23
2.0	Available Information .....	24
3.0	Mining Geometry .....	25
3.1	Pillar Extraction Panels .....	25
3.2	Subsidence Control Zones.....	26
4.0	Site Conditions .....	27
4.1	Land Use and Surface Features .....	27
4.2	Sub-Surface Conditions.....	30
5.0	Subsidence Prediction Methodology.....	32
5.1	General .....	32
5.2	Subsidence Prediction Model Details .....	32
5.3	Design of Subsidence Control Zones .....	36
5.3.1	General .....	36
5.3.2	Minimum Design Set-Back Distances for SCZs.....	36
5.3.3	Pillar Stability .....	39
6.0	Results of Subsidence Assessment.....	41
6.1	Subsidence Reduction Potential .....	41
6.2	Single Panel Subsidence Predictions.....	41
6.3	Predicted v. Measured Single Panel Subsidence Data for Area 1 Panels 1 to 4 .....	43
6.4	Barrier Pillar Subsidence Predictions.....	49
6.4.1	Empirical Model Development.....	49
6.4.2	Inter-Panel Barrier Pillars .....	50
6.5	Bearing Capacity of Roof and Floor Strata.....	52
6.6	Analytical Pillar Subsidence .....	52
6.6.1	Model Development.....	52
6.6.2	Analytical Model Outcomes .....	54
6.7	Goaf Edge Subsidence Prediction .....	55
6.8	Angle of Draw Prediction .....	55
6.9	Inflexion Point and Peak Strain Locations.....	56
6.10	Multiple Panel Subsidence Predictions .....	57

6.10.1	Maximum Subsidence above Pillar Extraction Panels .....	57
6.10.2	Maximum Panel Tilts and Horizontal Displacements .....	59
6.10.3	Maximum Panel Curvature and Strains .....	61
6.11	Prediction of Subsidence Impact Parameter Contours .....	66
6.11.1	Calibration of the SDPS® Model .....	66
6.11.2	Predicted Subsidence Contours .....	67
7.0	Subsidence Impacts and Management Strategies .....	68
7.1	General .....	68
7.2	Surface Cracking .....	69
7.2.1	Predicted Impacts .....	69
7.2.2	Impact Management Strategies .....	71
7.3	Sub-Surface Cracking .....	71
7.3.1	Sub-Surface Fracturing Zones .....	71
7.3.2	Sub-Surface Fracture Height Predictions .....	73
7.3.3	Discussion of A-Zone Horizon Model Predictions Above Pillar Extraction Panels .....	74
7.3.4	Discussion of B-Zone Horizon Model Predictions Above Pillar Extraction Panels .....	75
7.3.5	Impact on Rock Mass Permeability .....	75
7.3.6	Discussion of Prediction Model Uncertainties .....	76
7.3.7	Measured v. Predicted Heights of Fracturing above Panels 1 and 2 .....	76
7.3.8	Impact Management Strategies .....	80
7.4	Ponding .....	81
7.4.1	Potential Impacts .....	81
7.4.2	Impact Management Strategies .....	82
7.5	Flood Levels on Black Hill Land Pty Ltd Land .....	83
7.5.1	Potential Impacts .....	83
7.5.2	Impact Mitigation Strategies .....	83
7.6	Slope Instability and Erosion .....	83
7.6.1	Potential Impacts .....	83
7.6.2	Impact Management Strategies .....	84
7.7	Valley Uplift and Closure .....	84
7.7.1	Potential Impacts .....	84
7.7.2	Impact Management Strategy .....	85

7.8	Far-Field Horizontal Displacements and Strains .....	85
7.8.1	Background to Prediction Model Development.....	85
7.8.2	Potential Impacts .....	86
7.8.3	Impact Management Strategies .....	87
7.9	Transgrid Towers .....	88
7.9.1	Predicted Subsidence and Potential Impacts.....	88
7.9.2	Towers above the Proposed Pillar Extraction Panels.....	90
7.9.3	Towers outside of the Proposed Mining Limits.....	91
7.9.4	Impact Management Strategies .....	91
7.10	Black Hill Road and Drainage Infrastructure.....	92
7.10.1	Details and Potential Impacts.....	92
7.10.2	Impact Management Strategies .....	93
7.11	Energy Australia Power Line Easements .....	93
7.11.1	Potential Impacts to 132 kV Line.....	93
7.11.2	Potential Impacts to 11 kV and 415 V Line.....	95
7.11.3	Impact Management Strategies .....	97
7.12	Optus Fibre Optic Cable.....	98
7.12.1	Potential Impacts .....	98
7.12.2	Impact Management Strategies .....	99
7.13	Hunter Water Pipeline .....	99
7.13.1	Potential Impacts .....	99
7.13.2	Impact Management Strategies .....	101
7.14	Telstra Copper Cables .....	101
7.14.1	Potential Impacts .....	101
7.14.2	Impact Management Strategies .....	101
7.15	Farm Dams .....	101
7.15.1	Potential Impacts .....	101
7.15.2	Impact Management Strategies .....	102
7.16	Stock Watering System on the Catholic Diocese Land.....	103
7.16.1	Potential Impacts .....	103
7.16.2	Impact Management Strategies .....	104
7.17	Principal Residences .....	105
7.17.1	Details and Potential Impacts.....	105

7.17.2	Impact Management Strategies .....	108
7.18	Non-Principal Residences (All Other Surface Structures).....	108
7.18.1	Details and Potential Impacts.....	108
7.18.2	Impact Management Strategies .....	110
7.19	Property Fences and Livestock Grazing on Catholic Diocese Land.....	111
7.19.1	Potential Impacts.....	111
7.19.2	Impact Management Strategies .....	111
7.20	Disused Buildings on Catholic Diocese Land.....	111
7.20.1	Potential Impacts.....	111
7.20.2	Impact Management Strategies .....	111
7.21	Proposed Re-Development of Black Hill Land Pty Ltd Land .....	112
7.21.1	Predicted Impacts.....	112
7.21.2	Impact Management Strategies .....	112
7.22	Aboriginal Heritage Sites .....	113
7.22.1	Potential Impacts.....	113
7.22.2	Impact Management Strategies .....	113
7.23	F3 Freeway and John Renshaw Drive.....	113
7.23.1	Potential Impacts.....	113
7.23.2	Impact Management Strategies .....	114
7.24	Comparison of Subsidence Profile Predictions to the Environmental Assessment ...	114
8.0	Monitoring Requirements .....	115
8.1	Subsidence Development .....	115
8.2	Surface Monitoring Plans.....	117
8.3	Survey Accuracy .....	118
8.4	Sub-Surface Monitoring.....	118
9.0	Conclusions .....	119
10.0	References .....	120

## **Figures 1 to 46**

## **Appendix A - Summary of the Modified ACARP, 2003 Empirical Model**

## **Appendix B - Extract from SDPS<sup>®</sup> User Manual**

## **Appendix C - Barrier Pillar Stability Calculations**



## Glossary of Terms

<b>Angle of Draw</b>	The angle to the vertical from the sides or ends of an extracted panel and the line drawn from the limits of extraction at seam level to the 20 mm subsidence contour at the surface. The 20 mm subsidence contour is an industry defined limit and represents the practical measurable limit of subsidence.
<b>Barrier Pillar</b>	The pillar of coal left between adjacent pillar extraction panels. This forms a barrier that allows the goaf to be sealed off and facilitates regional workings stability during pillar extraction.
<b>Compressive Strain</b>	A decrease in the distance between two points on the surface. Compressive strains may cause shear cracking or steps at the surface if $> 3 \text{ mm/m}$ and are usually associated with concave curvatures near the middle of the panels.
<b>Confidence Limits</b>	A term used to define the level of confidence in a predicted <i>Subsidence Effect</i> (see definition below) subsidence impact parameter and based on a database of previously measured values above geometrically similar mining layouts.
<b>Cover Depth</b>	The depth (H) from the surface to the mine workings roof horizon.
<b>Critical Panels</b>	<p>Pillar extraction panels that are almost as deep as they are wide (W) (ie <math>0.9 &lt; W/H &lt; 1.4</math>) and is the point where failure of the overburden starts to occur if no massive strata is present (i.e. panel geometries are transitional between sub and super critical panels).</p> <p>Massive strata may continue to span but the maximum subsidence will be greater due to the bending action rather than the natural arching mechanism. Maximum subsidence above panels with non-spanning strata will approach values that are proportional to the mining height.</p>
<b>Curvature</b>	<p>The rate of change of tilt between three points (A, B and C), measured at set distances apart (usually 10 m). The curvature is plotted at the middle point or point B and is usually concave in the middle of the panel and convex near the panel edges.</p> <p>i.e. <math>\text{curvature} = (\text{tilt between points A and B} - \text{tilt between points B and C}) / (\text{average distance between points A to B and B to C})</math> and usually expressed in 1/km.</p>

Radius of curvature is the reciprocal of the curvature is usually measured in km (i.e.  $\text{radius} = 1/\text{curvature}$ ). The curvature is a measure of surface 'bending' and is generally associated with cracking.

**Credible Worst Case**

The Credible Worst-Case (CWC) prediction for a given *Subsidence Effect* and is normally the Upper 95% Confidence Limit determined from measured data and the line of 'best fit' or mean used to calculate the mean value. The CWC values are typically 1.5 to 2 times the mean values.

**Design Angle of Draw (Design AoD)**

The 'practical' angle of draw used to define minimum or allowable distances from the sides and ends of an extracted pillar panel to sensitive surface features. It is considered to be an effective impact management tool in which to minimise impact from differential subsidence effects parameters such as tilt, curvature and strain, which may cause cracking or instability. A Design Angle of Draw of  $26.5^\circ$  has been used with negligible impact to surface features at the Abel Mine to-date.

**Development Height**

The height at which the first workings (i.e. the main headings) are driven; usually equal to or less than the pillar extraction height in the production panels or second workings areas.

**Dry-schlerophyll Forest**

Multi-aged stands of eucalypts with a forest floor dominated by hard leafed shrubs such as banksias, wattle and tea trees.

**Extraction Height**

The height at which the seam is mined or extracted across a pillar extraction face by the continuous miner.

**Factor of Safety (FoS)**

The ratio between the strength of a pillar divided by the load applied to the pillar.

**Far-Field Displacement**

Horizontal displacement outside of the angle of draw, associated with movement are due to horizontal stress relief above an extracted panel of coal. The strains due to these movements are usually  $< 0.5$  mm/m outside a  $26.5^\circ$  angle of draw and do not cause damage directly. Such displacements have been associated with differential movement between bridge abutments and dam walls in the Southern Coalfield, but generally have not caused any damage to structures in the Western Coalfield.

**First Workings**

The tunnels or roadways driven by a continuous mining machine to provide access to the production panels in a mine (i.e. main headings). The roof of the roadways is generally supported by high strength steel rock bolts encapsulated in chemical resin. Subsidence above first workings pillars and roadways is generally  $< 20$  mm.

<b>Goaf</b>	The extracted area that the immediate roof of the overburden collapses into, following the extraction of the coal. The overburden above the 'goaf' sags as the goaf compresses under load, resulting in a subsidence 'trough' at the surface.
<b>Horizontal Displacement</b>	Horizontal displacement of a point after subsidence has occurred above an underground mining area within the angle of draw. It can be predicted by multiplying the tilt by a factor derived for the near surface lithology at a site (e.g. a factors of around 7 to 10 are normally applied in the Newcastle Coalfield).
<b>Inbye</b>	An underground coal mining term used to describe the relative position of some feature or location in the mine that is closer to the workings coal face than the reference location.
<b>Inflexion Point</b>	The point above a subsided area where tensile strain changes to compressive strain along the deflected surface. It is also the point where maximum tilt occurs above an extracted longwall panel. It is typically located between 0.25 and 0.4 x cover depth from the panel sides, depending on panel W/H ratio.
<b>Longitudinal Subsidence Profile</b>	Subsidence measured (or predicted) along an extraction panel or centre line.
<b>Mean Values</b>	The average value of a given <i>Subsidence Effect</i> value (i.e. of subsidence, tilt and strain) predicted using a line of 'best fit' through a set of measured data points against key independent variables (e.g. panel width, cover depth, extraction height). The mean values are typically two-thirds to half of the Credible Worst-case values and sometimes lower.
<b>Mining Height</b>	Refers to the height or thickness of coal extracted in a production panel or second workings area.
<b>Outbye</b>	An underground coal mining term used to describe the relative position of some feature or location in the mine that is closer to the point of mine entry than the reference location.
<b>Outlier</b>	A data point well outside the rest of the observations, representing an anomaly (e.g. a measurement related to a structural discontinuity or fault in the overburden that causes a compressive strain concentration at the surface, in an otherwise tensile strain field).
<b>Panel Width</b>	The width of an extracted area between chain pillars.

<b>Primary Subsidence</b>	<p>The subsidence which is directly caused by second workings and the sagging of overburden or compression of adjacent barrier pillars. Primary subsidence usually occurs after undermining of a given surface location and then again after three or four adjacent pillar extraction panel face pass the point.</p>
<b>Residual Subsidence</b>	<p>The last 5% to 10% of subsidence that occurs after primary subsidence is complete and is due to the re-consolidation or re-compaction of goaf and overburden. It is a time dependent component of the subsidence and is unlikely to cause further impact to surface features.</p>
<b>Secondary Subsidence</b>	<p>See <i>Residual Subsidence</i>.</p>
<b>Second Workings</b>	<p>Refers to the removal of part or all of first workings pillars and usually results in goaf formation as spans between pillars are increased. Second workings are therefore performed on retreat out of a production panel or main headings area that will no longer be required to provide access or ventilation to a given section of mine.</p>
<b>Shoving</b>	<p>The shortening effect of compressive strains due to mine subsidence on surface terrain, which results in localised shearing movements and localised uplift of soils and rock.</p>
<b>Strain</b>	<p>The change in horizontal distance between two points at the surface after mining, divided by the pre-mining distance between the points.</p> <p>i.e. <math>\text{Strain} = ((\text{post-mining distance between A and B}) - (\text{pre-mining distance between A and B})) / (\text{pre-mining distance between A and B})</math> and is usually expressed in mm/m.</p> <p>Strain can be estimated by multiplying the curvature by a factor derived for the near surface lithology at a site (e.g. a factor of around 7 to 10 is normally applied in the Newcastle Coalfield).</p> <p>Discontinuous overburden behaviour however, can result in local strain and curvature concentrations at cracks, making accurate predictions difficult. A rule of thumb is normally applied to allow for these effects, which is to increase smooth profile strains (and curvatures) by 2 to 4 times occasionally at a given location. The increase in strain also usually develops at locations with shallow rock profiles, as opposed to areas with deep soil profiles.</p>
<b>Study Area</b>	<p>The area which may be influenced by mine subsidence from the extraction of the proposed pillar extraction panels.</p>

<b>Sub-critical Panels</b>	Pillar Extraction panels that are deeper than they are wide ( $W/H < 0.6$ ) and cause lower magnitudes of subsidence than shallower panels due to natural arching of the overburden across the extracted coal seam and regardless of geology.
<b>Subsidence</b>	The difference between the pre-mining surface level and the post-mining surface level at a point, after it settles above an underground mining area.
<b>Subsidence Control</b>	Reducing the impact of subsidence on a feature by modifying the mining layout and set back distances from the feature (normally applied to sensitive natural features that can't be protected by mitigation or amelioration works).
<b>Subsidence Effect</b>	The term used to define the subsidence and differential subsidence parameters (i.e. subsidence, tilt, strain and horizontal displacement) that may or may not have an impact on natural or man-made surface and sub-surface features above a mining area.
<b>Subsidence Impact</b>	The impact that a subsidence effect has on natural or man-made surface and sub-surface features above a mining area.
<b>Subsidence Management Plan</b>	Refers to the approval process for managing mine subsidence impacts, in accordance with the Department of Industry and Investment Guidelines. The mine must prepare a Subsidence Management Plan (SMP) to the satisfaction of the Director-General, before the commencement of operations that will potentially lead to subsidence of the land surface.
<b>Subsidence Mitigation/Amelioration</b>	Modifying or reducing the impact of subsidence on a feature, so that the impact is within safe, serviceable, and repairable limits (normally applied to moderately sensitive man-made features that can tolerate a certain amount of subsidence).
<b>Subsidence Reduction Potential</b>	Refers to the potential reduction in subsidence due to massive strata in the overburden being able to either 'bridge' across an extracted panel or have a greater bulking volume when it collapses into the panel void (if close enough to seam level). The term was defined in an <b>ACARP, 2003</b> study into this phenomenon and is common in NSW Coalfields.
<b>Super-Critical Panels</b>	Pillar Extraction panels that are not as deep (H) as they are wide (W) (ie $W/H > 1.4$ ) and will cause complete failure of the overburden and maximum subsidence that is proportional to the mining height (i.e 0.5 to 0.6 T).
<b>Tilt</b>	The rate of change of subsidence between two points (A and B), measured at set distances apart (usually 10 m). Tilt is plotted at the

mid-point between the points and is a measure of the amount of differential subsidence.

i.e.  $\text{Tilt} = (\text{subsidence at point A} - \text{subsidence at point B}) / (\text{distance between the points})$  and is usually expressed in mm/m.

<b>Tensile Strain</b>	An increase in the distance between two points on the surface. Tensile strains > 2 mm/m are likely to cause cracking at the surface with shallow soil profiles over rock and are usually associated with convex curvatures near the sides (or ends) of the panels. Tensile strain also usually develops above barrier pillars.
<b>Transverse Subsidence Profile</b>	Subsidence measured (or predicted) across a pillar extraction panel or cross line.
<b>Valley Closure</b>	The inward (or outward) movement of valley ridge crests due to subsidence trough deformations or changes to horizontal stress fields associated with longwall mining. Measured movements have ranged between 10 mm and 400 mm in the NSW Coalfields and are usually visually imperceptible.
<b>Valley Uplift</b>	The phenomenon of upward movements along the valley floors due to <b>Valley Closure</b> and buckling of sedimentary rock units. Measured movements have ranged between 10 mm and 400 mm in the NSW Coalfields and may cause surface cracking in exposed bedrock on the floor of the valley (or gorge).

## 1.0 Introduction

This report presents a mine subsidence impact assessment for the proposed Area 2 pillar extraction panels in the Upper Donaldson Seam at Abel Underground Coal Mine, Black Hill. The report will be used for the purpose of preparing a Subsidence Management Plan (SMP) submission to the NSW Department of Industry and Investment.

The report has assessed the proposed mining layout of thirteen pillar extraction panels (Panels 14 - 26) and three main headings panels (Tailgate Headings, South East Mains and East Install Headings), as shown in **Figure 1**. Area 2 is located south of Area 1 (Panels 1 to 13 and East Mains Headings). In regards to surface feature impacts, up-dated subsidence predictions for Area 1 have been included where the effects of Areas 1 and 2 will overlap.

The scope of work for the report includes predictions of the following:

- (i) Maximum surface subsidence impact parameters;
- (ii) Surface subsidence impact parameter profiles and contours;
- (iii) Pre and post mining topography;
- (iv) Sub-surface heights of continuous and discontinuous fracturing above the panels.
- (v) Potential cracking width locations;
- (vi) Potential ponding depth locations and impacts on the 1 in 100 Year Average Recurrence Interval (ARI) flood levels along creeks within the site;
- (vii) Potential surface gradient changes;
- (viii) Far-field horizontal displacements and strains
- (ix) Predicted impacts on man-made developments and Aboriginal heritage sites
- (x) Design of Subsidence Control Zones (SCZ) beneath sensitive surface features (ie. Principal residences).

The predictions in this study have been based on three empirical models developed for the Newcastle and US Coalfields (refer to **Holla, 1987, ACARP, 2003** and **SDPS, 2007**). Reference has also been made to relevant information provided in the Abel Mine's Environmental Impact Assessment submission to the NSW Department of Planning (Oct, 06).

Mean and Credible Worst-case subsidence impact parameter predictions, with or without impact management controls, have been estimated in this study to assist specialist consultants assess the potential impact to a given feature. The necessary mine planning adjustments or mitigation measures will then be implemented to deliver satisfactory outcomes to the feature (and stakeholders).

## 2.0 Available Information

The following information was provided by the mine to prepare this report:

- The proposed mining layout.
- Cover depth contours to the Upper Donaldson Seam and seam thickness isopachs.
- Borehole log and core testing data from the SMP Area.
- Geological structure (fault and dyke) locations.
- Surface topographic levels and existing drainage regime locations.
- Locations of surface developments and infrastructure in the study area.
- Locations of Aboriginal Artefact Scatter sites.
- Subsidence results from the SMP Area 1 extracted panels.

Plans of the proposed mining layout with cover depth contours, seam thickness isopachs and pre-mining surface topography are presented in **Figures 1 to 3**.

Bore core log and testing data from the boreholes shown in **Table 1** were also included in this assessment.

**Table 1 - Borehole Log Data**

<b>BH#</b>	<b>Easting</b>	<b>N</b>	<b>Collar RL</b>	<b>Date</b>
C153	369525	6366791	40.21	10/03/09
C155	370012	6367148	30.85	19/03/09
C156	369569	6366357	49.28	23/03/09
C158	370111	6366526	41.12	30/03/09
C159R	370444	6367172	30.68	08/04/09
C161	370656	6367523	36.24	23/04/09



### **3.0 Mining Geometry**

#### **3.1 Pillar Extraction Panels**

The following mine workings details have been assumed in this assessment for the pillar extraction panels beneath non-sensitive features:

##### Production Panels

- (i) The pillar extraction panels (Panels 14 to 26) will be located at depths ranging from 100 m to 150 m and will be 160.5 m wide (rib to rib).
- (ii) The development headings and first workings pillars will be located in the C-G plies within the Upper Donaldson Seam. In some areas the working section will be the C-E plies. In other areas the F-G horizons are present in the immediate floor of the mine workings, and increase the mineable seam thickness up to a range of 3.2 to 3.4 m. First workings roadways are driven at 2.4 to 2.6m in height. The A ply coal is located above the Upper Donaldson Seam (ranging in height from 5 to 20m above the Upper Donaldson Seam) and will not be mined.
- (iii) The pillar extraction panels will be developed to the south from the East Main and South East Main headings. The first workings in each production panel will consist of a four heading layout with 45 m and 65 m centre spacing across the panel with 25 m cut through spacing. Based on a nominal roadway width of 5.5 m, the solid pillar geometries will be 19.5 m wide x 39.5 m and 59.5 m in length.
- (iv) The barriers between the extracted pillar panels will be 24.5 m wide (solid) and 0.25 km to 0.55 km long. The pillar height will range from 2.3 m to 2.6 m, depending on the thickness of the C-E seam sections. The inter-panel barriers will therefore have width to height (w/h) ratios ranging from 9.4 to 11.1.
- (v) Based on previously extracted panels in Area 1 (i.e. Panels 1 and 2), it has been assumed that approximately 95% of the pillars (high extraction mining) will be extracted during second workings, using continuous miners and Mobile Breaker Line Supports (MBLS) to provide temporary roof control.
- (vi) The panel pillars and adjacent solid ribs will be extracted (i.e. lifted) on retreat to a maximum distance of 9.75 m. At some locations the F-G horizons are present in the immediate floor of the mine workings, and increase the mineable seam thickness up to a range of 3.2 to 3.4 m. At these locations, the continuous miner may cut or 'ramp' down into the floor a further 0.5 m to 0.6 m and increase the effective mining height to 2.8 m across the panel.
- (vii) Either one or two rows of remnant pillars (referred to as 'Stook X') will be left at the intersection between extracted panel pillars, and will have an average plan dimension of 3.8 x 19.5 m. For the case of Panels 1 and 2, it was also necessary to leave similar size remnants directly beneath sub-vertical fault lines for roof control purposes. The

extraction ratio for the panel was effectively reduced to between 75% and 85% along the fault lines.

- (viii) A solid barrier between the finishing ends of the panels and the adjacent East Mains will be 16.3 m to 21.4 m wide (after allowing for a similar 9.75 m wide rib strip during retreat along the East and South East Mains).

### Main Headings Panels

- (ix) The East Install Headings and South East Mains will be developed on a 5 to 6 heading layout respectively with pillars formed at 25 m wide x 45 m long centre spacing. The pillars may also be lifted to a depth of 9.75 m on retreat after completion of mining in the production panels.

The final rib-rib width of the above main headings panels will be 105.5 m and 140 m respectively, with solid pillar barrier widths of between 21 m and 23.5 m left between the adjacent pillar extraction panels. These pillars will have 'squat' w/h ratios ranging from 8.4 to 9.4 and are expected to yield gradually and strain-harden if overloading occurs.

- (x) Another first workings panel called the Tailgate Headings, will be developed and extracted between Panel 1 (Area 1) and the South East Mains. The panel will have a rib-rib width of 89 m and effective mining height of 2.8 m. The solid barrier between Panel 1 and South East Mains will be 16.5 m and 21 m respectively. These pillars are have w/h ratios ranging from 6.6 to 8.1 and are also expected to yield gradually and strain-harden if overloading occurs.

The panel width to cover depth ratio (W/H) for the proposed pillar extraction panels will range from 0.9 to 2.0, indicating critical to supercritical subsidence behaviour is likely to occur. Similar behaviour is also expected after the secondary extraction of the South East Mains and Tailgate headings, which will have W/H ratios ranging from 0.9 to 1.2.

*Note: Critical subsidence refers to the point where sub-critical or natural overburden 'arching' behaviour stops (i.e. when  $W/H > 0.6$ ) and the development of maximum subsidence or super-critical overburden behaviour starts (i.e. maximum possible subsidence occurs when  $W/H > 1.4$  and is a function of mining height and goaf stiffness).*

## **3.2 Subsidence Control Zones**

For mine workings below sensitive surface features or a designated Subsidence Control Zone (SCZ), the following design assumptions have been applied:

- (i) The panels will have either first workings or partial extraction pillars that have adequate long-term stability.
- (ii) The pillars will be designed to behave elastically under abutment loading conditions from adjacent high extraction ratio panels.

## 4.0 Site Conditions

### 4.1 Land Use and Surface Features

The proposed mining area is zoned as rural residential and commercial property with several public utility easements and Council roads.

The land is semi-cleared, dry-sclerophyll forest and the terrain is flat to gently undulated. The surface slopes range from 1° to 10° and steepen locally to 15° along Viney Creek (a Schedule 2 Stream, **DIPNR, 2005**), which drains the site towards the north-east. Topographic relief ranges from 16 m AHD to 68 m AHD across the panels.

The natural and archaeological features of significance within the study area include:

- Gently undulating terrain and mild slopes.
- Headwaters of Viney Creek (a Schedule 2 Stream) and several unnamed drainage gullies (DECCW listed Schedule 1 watercourses).
- Sandy alluvial deposits (up to 3 m deep) exist along the lower reaches of the creek with no rock exposures evident.
- Silty sand and sandy clay surface soils present on the site are likely to be mildly to highly erosive / dispersive if exposed to concentrated runoff during storm flow events.
- The 1 in 100 Year ARI flood levels along the creeks within the site (see **Figure 3**)
- Vegetation on the site consists of dense stands of dry schlerophyll forest with shrubs, ferns and grasses. The riparian zones along creeks have sparse to dense stands of melaleucas, vines and grasses.
- Common flora/fauna habitats within the study area.
- Reference to three separate studies of the area (**Parsons Brinkerhoff, 2003, South Eastern, 2006** and **ERM, 2008**) have identified three scattered Aboriginal artefact sites in the SMP area that are located outside the limits of proposed secondary extraction (see **Figure 3**). The artefacts are listed as silcrete stone axe flakes and were identified by the Mindaribba Local Aboriginal Land Council and Awabakal Traditional Owners.

Existing developments within Area 2 include the following:

#### Land Use

- Semi-cleared and undeveloped land (Catholic Diocese and Black Hill Land Pty Ltd) to the North of Black Hill Road.

The Catholic Diocese Land is presently being used for cattle grazing with one area designated a future high school development area. At this stage, the Black Hill Land Pty Ltd land is likely to be redeveloped into industrial lots with sealed access roads and drainage works. No development applications have been indicated yet for the Catholic Diocese land.

- Semi-cleared rural-residential zoned land to the south of Black Hill Road

The land is currently used for cattle grazing with some domestic vegetable growing adjacent to the Principal Residences.

#### Public Roads and Infrastructure

- Black Hill Road and Taylors Road (Cessnock City Council).

Black Hill road is a bitumen spray sealed dual carriageway with gravel shoulders. The road is mainly on-grade, with some sections in cut and fills up to 3 m deep. The condition of the road is considered good to fair, with only minor 'crocodile' cracking and rutting observed.

Taylors Road is an unsealed gravel dual carriageway which provides access to private residences to the south of the Area 2.

- Two concrete pipe culverts (No.s 1 and 2) in up to 3 m of fill below Black Hill Road (Cessnock City Council).

Culvert No.1 has twin 1200 mm diameter pipes with a 1.8 m high x 2.5m long gabion head wall and cobble-sized dolerite rip-rap on the downstream side.

Culvert No.2 is a single 900 mm diameter pipe. Both culverts have upstream and downstream reinforced concrete head walls, and the pipe segments are 3 m long.

#### Private Structures

- Three Principal Residences and associated All Other Surface Structures south of Black Hill Road on rural residential zoned land (privately owned). The associated structures include sheds, cottages, above ground concrete water tanks, in-ground septic tanks and on-site effluent disposal fields.

- One Principal Residence and other structures within the future proposed high school development area (Catholic Diocese Land). A second Principal Residence is within the Catholic Diocese site but not within SMP Area 2.
- Two non-Principal residences (rental properties) and associated sheds (Catholic Diocese Land).
- Two buildings associated with the former chicken farm (Catholic Diocese Land) which are currently used as storage facilities and/or meeting rooms by the Catholic Diocese).
- Demolished former chicken farm building rubble and disused houses / office buildings (Catholic Diocese Land).
- Areas within the Catholic Diocese land where rehabilitation, including capping of contaminated areas, has been conducted.

#### Utilities

- Five 330kV Transgrid Transmission towers (26B to 30B).
- A buried fibre optic cable in the Transgrid easement (Optus).
- One buried 200 mm diameter UPVC water supply pipeline (pressurised) with rubber ring joints and a disused 375 mm diameter welded steel pipeline (Hunter Water).
- A 132 kV transmission line suspended on seven pairs (EA9 to EA15) of un-guyed, timber poles with bolted steel cross bracing (Energy Australia).
- Domestic 11 kV and 415V suspended power lines suspended on twenty-three timber poles (No.s 24 to 49) (Energy Australia).
- Domestic buried copper cable telephone lines to the residents along Black Hill Road (Telstra).
- Redundant domestic buried copper cable telephone lines (Telstra). This local cable reticulation was used when the property was functioning as a chicken farm and the cable provided services to the individual properties located on the land.
- Two Permanent Survey Control Marks
- Buried water reticulation pipelines and above ground troughs for livestock watering and supply to Principal and non-principal residences (Catholic Diocese Land).

#### Private dams, property access roads and fences

- Several abandoned earth embankment dams with < 1ML capacity (Black Hill Land Pty Ltd and Catholic Diocese Land). The dams have been filled in and are dry.
- Several earth embankment dams with < 1ML capacity (Private Residences). The dams are generally full of water (except for one dam with numerous piping failures) and used for stock watering.
- Unsealed and bitumen sealed property access roads, driveways and fences (Catholic Diocese, Black Hill Land Pty Ltd and other Principal Residences).

Based on consultation with stakeholder's to-date, Subsidence Control Zones (SCZ) will be required for Viney Creek and the Principal Residences plus other structures within the proposed Catholic High School Development.

The locations of the above features (and surface gradients) are shown in **Figures 1 and 3**.

## 4.2 Sub-Surface Conditions

Reference to the 1:100,000 Geological Sheet for the Newcastle Coalfield (**DMR, 1995**), indicates the proposed SMP layouts are located within the Dempsey Formation of the Permian Tomago Coal Measures.

The overburden for the area will consist of gently, south-west dipping (i.e. 2 to 5 degrees) sedimentary strata of the Tomago Coal Measures, which generally comprise interbedded sandstone, shale, carbonaceous mudstone, tuffaceous claystone and coal. The coal seams present in the overburden (in descending order) include the Sandgate, Buttai, Beresfield, Upper and Lower Donaldson, Big Ben and Ashtonfield Seams.

Based on reference to the DMR Geological Sheet, there are several significant NW:SE striking geological structure zones (i.e. faults and dykes) which occur along Buttai Creek and Long Gully Creek to the west of the site, and also an 8 m throw reverse fault in the north-east corner of the SMP area (see **Figure 1**). The south-eastern bedding dip across the site is associated with the southern arm of the Four Mile Creek Anticline, which is located to the west of the site.

Surface joint patterns measured on the sandstone cliff lines and outcrops to the south of the SMP area consist of a sub-vertical, widely spaced, planar to wavy, persistent joint sets striking between 025° and 035° (NNE to NE). A sub-vertical joint set striking at approximately 135° (NW:SE) is also present. The trends of the cliff faces are similar to the above joint sets.

The Upper Donaldson Seam has low strength with sonic derived unconfined compressive strength (UCS) values ranging from 7 to 15 MPa. Some medium to high strength stone bands up to 0.5 m thick are present within the coal seam, with UCS values ranging between 30 and 90 MPa.

The immediate roof and floor of the proposed mining horizon will typically consist of 5 to 10 m or more of thin to medium interbedded shale and sandstone with low to medium strength (10 to 50 MPa). The weaker materials, such as carbonaceous mudstone, mudstone and claystone are very thin (< 0.1 m thick) and exist in both the roof and floor.

Low strength immediate roof and floor materials were also generally noted in several boreholes in the north, where the cover depths are less than 40 m. This is also considered to be the depth of weathering on the Donaldson open cut mine to the north of the underground mining area. The sonic UCS results indicated thinly bedded strata with strengths ranging between 10 and 50 MPa and generally from 30 to 50 MPa for the overburden materials at depths > 40 m.

The UCS and stiffness properties of the immediate roof and floor materials have been derived from laboratory and point load strength test results from core taken from six boreholes and in-situ geophysical testing data. Good correlation was apparent between the laboratory derived and *in situ* sonic UCS results presented in the Environmental Assessment.

Estimates of the range of material strength and stiffness properties present in the roof and floor of the Upper Donaldson Seam are summarised in **Table 2**.

**Table 2 - Strength Property Estimates for Upper Donaldson Seam, Roof and Floor Lithology**

Lithology	Strata Thickness (m)	UCS Range <sup>+</sup> [Average] (MPa)	Elastic Moduli Range* (GPa)	Average Moisture Sensitivity <sup>^</sup>
Interbedded sandstone/shale beds above the UD Seam	<10	10.5 - 93 [18 - 51]	3 - 20 [5 - 15]	Non-Sensitive to Moderately Sensitive
Interbedded sandstone/shale beds below the UD Seam	<10	11.5 - 130 [31 - 72]	3 - 15 [5 - 10]	Non-Sensitive to Slightly Sensitive
Upper Donaldson Seam	1.9 - 3.2	5 - 15 [10]	2 - 4 [3]	Non- Sensitive to slightly sensitive stone bands

Note:

+ - Unconfined Compressive Strength derived from point load testing to **ISRM, 1985** on bore core samples taken from SMP area.

\* - Laboratory Young's Modulus (E) derived from laboratory and sonic UCS data,  $E = 300 \times \text{UCS}$  (units are in MPa).

<sup>^</sup> - Moisture sensitivity testing determined from the Immersion Test procedure presented in **Mark & Molinda, 1996**.

## **5.0 Subsidence Prediction Methodology**

### **5.1 General**

The study included the following activities and the application of several industry established empirical models to predict the ‘mean’ and ‘credible worst-case’ subsidence for a given mining layout:

- (i) Development of a geotechnical model for the study area (i.e. mining geometry, geology, material properties etc).
- (ii) Calculation of maximum subsidence impact parameter predictions and representative parameter profiles using the **ACARP, 2003** and **Holla, 1987** empirical subsidence models and the mining geometries proposed.
- (iii) Assessment of barrier and chain pillar stability, based on **ACARP, 1998a** and **ACARP, 1998b**.
- (iv) Development and calibration of **SDPS<sup>®</sup>** models (using the subsidence, tilt and strain profiles from (ii)) to generate subsidence and associated impact parameter contours above the proposed mining layouts.
- (v) Generation of subsidence, tilt, strain, horizontal displacement, post mining topography, potential cracking width, ponding location and surface slope gradient change contours for the proposed mining layouts using **Surfer8<sup>®</sup>** contouring software.
- (vi) Estimation of sub-surface fracturing heights above the panels using empirically based models in **ACARP, 2003**, **Forster, 1995** and **Mark, 2007**.
- (vii) Estimation of the extent and magnitude of far-field displacements (FFD) and strains (FFE), based on empirically based models developed from Newcastle Coalfield data by **DgS, 2008**.

The terms ‘mean’ and ‘Upper 95% Confidence Limit’ used in these predictions consider that the predicted maximum subsidence effect values may be exceeded by 50% and 5% respectively for the panels mined. Therefore on a small number of occasions, the predicted values and impacts may be exceeded generally by a range of 5-20% (as has been the case with the panels extracted to date in SMP Area 1). These are generally found to be related to the presence of adverse or anomalous geological or topographical conditions.

### **5.2 Subsidence Prediction Model Details**

The two subsidence predictions models used in this study are summarised below:

- **ACARP, 2003** - An empirical model that was originally developed for predicting maximum single and multiple longwall panel subsidence, tilt, curvature and strain in



the Newcastle Coalfield. The model database includes measured subsidence parameters and overburden geology data, which have been back analysed to predict the subsidence reduction potential (SRP) of massive lithology in terms of 'Low', 'Moderate' and 'High' SRP categories.

- The model database also includes chain or barrier pillar subsidence, inflexion point distance from panel edges, inflexion point subsidence, goaf edge subsidence and angle of draw prediction models. These models allow subsidence profiles to be generated for any number of panels within a range of appropriate statistical confidence limits. The mean and Upper 95% Confidence Limit (U95%CL) values have been adopted in this study for predictions of the average and Credible Worst-Case values expected, due to the proposed mining activities.

The **ACARP, 2003** model may also be used for predicting maximum subsidence above pillar extraction panels by applying the 'effective' mining height principle (i.e. extraction ratio x mining height) defined in **Van de Merwe and Madden, 2002**. The principle allows for subsidence reducing effect of crushed out remnant coal that will be left behind in the workings.

Based on a comparison between high extraction panel and longwall panel subsidence databases in **ACARP, 2003** and **Holla, 1987**, a conservative extraction ratio of 95% and a maximum longwall panel subsidence of 58% of the mining height, give a maximum pillar extraction panel subsidence of 55% of the mining height for supercritical panels.

It is also apparent from mining experience in Panel 1 and 2 in Area 1 that additional stooks have been left to support mine roof where sub-vertical faults have intersected the workings. The stooks at these locations are estimated to have decreased maximum subsidence to a range of 40% to 44% of the mining height with panel extraction ratios of approximately 75% to 85%.

A summary of the **ACARP, 2003** model, which defines the parameters and terms used, is presented in **Appendix A**.

- **SDPS<sup>®</sup>, 2007** - A US developed (Virginia Polytechnical Institute) influence function model for subsidence predictions above longwalls or pillar extraction panels. The model requires calibration to measured subsidence profiles to reliably predict the subsidence and differential subsidence profiles required to assess impacts on surface features.
- The model also includes a database of percentage of hard rock (i.e. massive sandstone / conglomerate) that effectively reduces subsidence above super-critical and sub-critical panels, due to either bridging or bulking of collapsed material. An extract from the **SDPS<sup>®</sup>** user manual defining the parameters and terms used is presented in **Appendix B**.

Overall, the **SDPS<sup>®</sup>** model should preferably be calibrated to measured subsidence profiles above pillar extraction workings with similar conditions as Abel. However, due to the lack of

similar mining data, the calibration procedure applied in this study is considered best practice for a ‘green fields’ study. A re-calibration of the model may be necessary, however, if the predicted outcomes of this study are significantly different to measured ones.

The modifications to the **ACARP, 2003** model by DgS included adjustments to the following key parameters, which were made to improve compatibility between the two models used in this study:

- Chain (and barrier) pillar subsidence prediction is now based on pillar subsidence over extraction height ( $S_p/T$ ) v. pillar stress (under double abutment loading conditions).
- Distance of the inflexion point from rib sides and inter-panel pillars in similar terms to **SDPS**<sup>®</sup> software (i.e.  $d/H$  v.  $W/H$ ).
- The horizontal strain coefficient ( $\beta_s$ ) is the linear constant used to estimate strain based on predicted curvature, and is equivalent to the reciprocal of the neutral axis of bending,  $d_n$  used in **ACARP, 2003**. Based on local Abel data, a value of  $d_n = 10$  m or a  $\beta_s = 0.1 \text{ m}^{-1}$  has been applied to predict ‘smooth’ profile strains using the calibrated **SDPS**<sup>®</sup> model.

Multiple-panel effects are determined by the **ACARP, 2003** model by adding a proportion of the chain (or barrier) pillar subsidence to the predicted single panel subsidence. Estimates of first and final subsidence above a given set of pillar extraction panels use this general approach. The definition of First and Final  $S_{\max}$  is as follows:

First  $S_{\max}$  = the first maximum subsidence after the extraction of a panel, including the effects of previously extracted panels adjacent to the subject panel;

Final  $S_{\max}$  = the final maximum subsidence over an extracted panel, after at least three more panels have been extracted, or when mining is completed.

First and Final  $S_{\max}$  for a panel are predicted by adding 50% and 100% of the predicted subsidence over the respective barrier pillars (i.e. between the previous and current panel), less the goaf edge subsidence (which occurs before the barrier pillar is loaded from both sides). The maximum subsidence is limited to 58% of the effective mining height for the panels.

The subsidence above chain and barrier pillars has been defined in this study as follows:

First  $S_p$  = the first subsidence over a pillar after panels have been extracted on both sides of the pillar;

Final  $S_p$  = the final subsidence over a pillar after at least another three more panels have been extracted, or when mining is completed.

A conceptual model of the multiple panel subsidence mechanism is given in **Figure 4a**.

Residual subsidence above chain (and barrier) pillars and extracted panels tend to occur after mining of adjacent panels due to (i) increased overburden loading on the pillars, and (ii) on-going goaf consolidation or creep of the collapsed roof or goaf in the panel. The residual movements can increase subsidence by a further 10 to 30% above chain (and barrier) pillars after the first pillar subsidence occurs. Residual subsidence is likely to decrease exponentially as mining moves further away from a given panel. A subsidence increase of 20% after double abutment loading occurs (i.e. First  $S_p$ ) has been assumed in this study to allow for long-term loading effects (i.e. Final  $S_p$ ).

Unless otherwise stated the predicted values presented in the following sections of this report are given as a range from the mean to the U95%CL values. The measured subsidence will be expected to be somewhere between these values.

Tilts and curvatures have been assessed using the empirical techniques presented in **ACARP, 2003** and by also taking first and second derivatives of the predicted subsidence profiles for comparative purposes.

Predictions of strain and horizontal displacement were made based on the relationship between the measured curvatures and tilt respectively as discussed in **ACARP, 1993** and **ACARP, 2003**.

Structural and geometrical analysis theories indicate that strain is linearly proportional to the curvature of an elastic, isotropic bending 'beam'. This proportionality actually represents the depth to the neutral axis of the beam, or in other words, half the beam thickness. **ACARP, 1993** studies returned strain over curvature ratios ranging between 6 and 11 m for NSW and Queensland Coalfields. Near surface lithology strata unit thickness and jointing therefore dictate the magnitude of the proportionality constant between curvature and strain. Similar outcomes are found for tilt and horizontal displacement.

**ACARP, 2003** continued with this approach and introduced the concept of secondary curvature and strain concentration factors due to cracking. The mean and median peak strain / curvature ratios for the Newcastle Coalfield was assessed to equal 5.2 m and 7.3 m respectively, with strain concentration effects increasing the 'smooth-profile' strains by 2 to 4 times occasionally. A review of the local strain database for Area 1 at Abel Mine has lead to the value of 10 m being adopted as a more appropriate value for impact prediction purposes.

A  $d_n$  value of 10 m has also been applied to the predicted 'smooth' curvature and tilt profiles to estimate strain and horizontal displacement respectively above the proposed Abel panels in the Area 2. These values may then be compared to the empirical model outcomes to estimate localised, concentrated strain effects due to cracking. Cracking is expected to occur in zones of peak tensile (or compressive) strains when tensile and compressive strains exceed 1 to 3 mm/m respectively and where surface rock exposures are present.

Surface crack widths (in mm) may be estimated by multiplying the predicted strains by 10, which is an empirical factor based on the distance between the pegs in the **ACARP, 2003** model database and the measured strains and crack widths above extracted panels. As

mentioned earlier these predictions may be exceeded from time to time by anomalous conditions.

### **5.3 Design of Subsidence Control Zones**

#### **5.3.1 General**

The design of a reliable Subsidence Control Zone (SCZ) will require consideration of the following issues:

- The minimum set-back distance from total pillar extraction panels (i.e. panels with > 85% of coal extracted) to control subsidence deformation to below tolerable design limits for the feature.
- The long-term stability of the pillars in the SCZ under abutment loading conditions from adjacent high extraction areas.
- The use of narrower total extraction panels that are sub-critical (i.e.  $W/H < 0.6$ ) or partial extraction panels with long term stable remnant pillars left beneath sensitive surface features to control subsidence impacts to within tolerable limits.
- Whether the performance of the SCZ needs to be trialled in non-sensitive panels.

Further design criteria, specific to the feature being protected, are provided in the following sections.

#### **5.3.2 Minimum Design Set-Back Distances for SCZs**

Minimum set back distances required for SCZs will depend upon the type of feature and the consequences of excessive damage, if it occurs. Based on the statement of commitments in the Project Approval, it will be necessary to protect the Schedule 2 section of Viney Creek and all Principal Residences and structures from mining related impacts.

##### Viney Creek

The minimum set-back distance from Viney Creek to total extraction mining has been defined in the Abel Mine's Environmental Assessment Report documents and Project Approval as a distance  $26.5^\circ$  Angle of Draw (AoD) + 40 m, to limit subsidence of the creek bed and banks to < 20 mm.

Based on consultation with the surface water consultant for the project, it is understood that Viney Creek will tolerate higher magnitudes of subsidence if no hydraulic connection or change in drainage patterns and watercourse ecology occur.

For the Abel mining lease and reference to nearby mine sites, it is assessed that the development of significant surface cracking (i.e. > 20 mm wide) may be defined as the point

where tensile strains exceed 2 mm/m in areas with relatively deep soil cover. Provided the proposed mining method does not result in widespread exceedences of 2 mm/m tensile (or compressive) strains, then it is assessed that the creek may be subsided by up to 0.3 m without significant impact.

Based on the above, it is also considered the following techniques may be adopted to control subsidence impacts to within tolerable limits for Viney Creek:

- (i) Extract sub-critical total extraction panels (i.e. with  $W/H < 0.6$ ) beneath the creek with squat chain pillars (i.e. with pillar  $w/h$  ratios  $> 5$ ) between the panels.
- (ii) Alternatively it will be possible to conduct partial pillar extraction beneath the creek, which results in similar minimal subsidence magnitudes and impacts as defined above.
- (iii) Adopt an angle of draw of  $26.5^\circ$  or  $0.5 \times$  cover depth from the creek centreline to define a 'low' impact set-back distance from total extraction mining limits, pending confirmation from earlier panel monitoring data (see **Section 12**).

#### Principal Residences and Designated Structures

Principal residences and designated structures will require adequate set-back distances from total extraction mining panels to protect the structures from differential displacements (pending confirmation of tolerable limits from MSB).

The general advice given by the MSB is to ensure that any damage to the structures due to mining is 'safe, serviceable and repairable and that the tilt of the structures due to mining is not to exceed 5 mm/m (so that the buildings are unlikely to require re-levelling).

The above design criteria for the SPZs is indicative of 'negligible' to 'slight' (i.e. Category 0 to 2 damage), as defined in **AS2870, 1996**. These damage categories are defined as 'minor' and would be considered normal in regards to footing performance over the life of similar types of buildings with moderately reactive clay (Class M) or controlled fill beneath shallow footings.

Another consideration is that the houses within the Abel Mining Lease are not within a proclaimed mine subsidence district, and as a result, the MSB have been unable to impose any development restrictions on the houses built within the lease. As a result, some of the houses may not have been built with a level of articulation that would be considered appropriate for a limited amount of mine subsidence movement, or similar to that for a Class M reactive clay site.

*Note: A Class M site is defined by **AS2870, 1996** as having 20 to 40 mm of vertical surface movement due to natural soil moisture content changes over seasonal cycles of 'wet' and 'dry' conditions.*

It is therefore recommended that the design set-back distances from Principal Residences to total extraction mining will need to consider the surface topography, structure and footing type, the level of building articulation present, performance history of the structure, and clay reactivity to moisture change potential in foundation materials beneath footings.

The following set-back distances from Principal Residences presented in **Table 3** have been adopted at this stage to control subsidence, tilt, curvature and strain to the limits recommended in **Appleyard, 2001** for a given residential structure type and ground slope condition.

**Table 3 - Summary of Recommended Design Angles of Draw to Various Principal Residence Structures**

Principal Residence Structure Type <sup>+</sup>	Tolerable Subsidence Impact Parameters (i.e. 'Negligible' to 'Slight' Damage Category in AS2870 - 1996)				Minimum Design Angle of Draw (degrees) [setback distance in terms of cover depth, H]	
	Subsidence <sup>#</sup> (m)	Tilt (mm/m)	Curvature (1/km)	Strain (mm/m)	Flat-Moderate Topography*	Steep Topography <sup>^</sup>
Clad Frame on Strip/Pad Footings	<0.05	<4	<0.25	<3	17 [0.3H]	26.5 [0.5H]
Articulated Masonry Veneer on Strip/Pad/Slab Footings	<0.03	<3	<0.2	<2	20 [0.35H]	30 [0.6H]
Non-articulated Masonry Veneer on Strip/Pad/Slab Footings	<0.02	<2	<0.1	<1.0	26.5 [0.5H]	35 [0.7H]
Articulated Full Masonry Strip/Pad/Slab Footings	<0.02	<2	<0.1	<1.0	26.5 [0.5H]	35 [0.7H]
Non-articulated Full Masonry on Strip/Slab Footings	<0.01	<1	<0.05	<0.5	35 [0.7H]	45 [1H]

Notes:

+ - Buildings are single or double storey and have wall lengths ranging between 10 m and 30 m.

# - subsidence limits applied to limit associated tilts, strains and curvatures.

\* - ground slopes < 15° between mining limits and structure.

^ - ground slopes > 15° between mining limits and structure.

Further justification for the above design set-back distances are provided in **Section 7** of this report in regards to measured subsidence impact parameters outside the limits of total extraction mining observed for the Area 1 panels. Results of monitoring and any impacts may require further review of these values.

### 5.3.3 Pillar Stability

The stability of the SCZ will be controlled by mine design. The total stress acting on the first and subsequent row of pillars in the SCZ has been estimated using the abutment load concept defined in **ACARP, 1998a** for estimating single abutment loads on barrier pillars with an adjacent goaf. The load model is shown schematically in **Figure 4b**.

The total stress acting on the pillars after mining may be estimated as follows:

$$\sigma_{\text{pillar}} = \text{pillar load/area} = (P+RA)/wl$$

where:

$P/wl$  = Full tributary area load of column of rock above each pillar;

$$= (w+r)(l+r) \cdot \rho \cdot g \cdot H;$$

$RA/wl$  = Single Abutment load due to cantilever action of overburden over goaf

$$= 0.5 u H^2 \tan(\theta)(l+r)/(wl) \quad \begin{array}{l} \text{(where } u = \text{unit weight of overburden } 0.025 \text{ MPa/m} \\ \theta = \text{abutment angle (normally taken as } 21^\circ) \end{array}$$

$R$  = Proportion of abutment load acting on first row of SPZ pillars;

$$= 1 - [(D-w-r)/D]^3 \quad \begin{array}{l} \text{(where } D = \text{distance (m) that load distribution will} \\ \text{extend from goaf edge according to } \mathbf{Peng \& Chiang,} \\ \mathbf{1986: } D = 5.13\sqrt{H} \end{array}$$

$$= 1 \text{ (assumed for Abel SCZs)}$$

$w$  = pillar width (solid);

$l$  = pillar length (solid);

$r$  = roadway width;

$H$  = depth of cover;

The FoS of the SCZ pillars were based on the strength formula presented in **ACARP, 1998b** (i.e. UNSW Power Rule) for 'squat' pillars with  $w/h$  ratios  $> 5$  as follows:

$$S = 27.63 \Theta^{0.51} (0.29((w/5h)^{2.5} - 1) + 1) / (w^{0.22} h^{0.11})$$

where:

$h$  = pillar height;

$\Theta$  = a dimensionless 'aspect ratio' factor or  $w/h$  ratio.

The FoS is then calculated by dividing the pillar strength,  $S$ , with the pillar stress,  $\sigma_{\text{pillar}}$ :

$$\text{FoS} = S / \sigma_{\text{pillar}}.$$

The next row of pillars inside the SCZ will be subject to significantly lower stress (<20% A).

For long-term stability it is recommended that a minimum Design FoS of 2.11 under worst-case service load conditions be adopted for sensitive surface features. Based on **ACARP 1998b**, the probability of failure of the SCZ pillars will be < 1 in 1 million.

The pillar width/height ratio is also a very important factor that indicates the post-yield behaviour of the pillars if they are overloaded.

Pillars with w/h ratios < 3 are considered most likely to 'strain-soften' if overloaded and result in rapid failure and pillar runs, whereas w/h ratios > 5 are more likely to 'strain-harden' and yield slowly or 'squeeze'. These types of post-yield behaviour have been discussed in **ACARP, 2005** and demonstrated in **Figure 6c** for various in-situ observations and laboratory experiments.

The proposed pillars in the SCZs will have width/height ratios that are between 5 and 10 for the nominal mining height ranges. The pillars are therefore likely to remain stable as a group and strain harden if local overloading occurs. A summary of design calculations for the currently proposed SCZs at the Abel mine are presented in **Table 4**.

The above formulae have also been applied in the subsidence assessment that follows for the proposed Area 2 mining layout.

**Table 4 - Design Calculation Summary for Proposed Subsidence Control Zones**

Cover Depth (m)	Pillar Area w x l (m)	Pillar Height h (m)	Pillar Strength (MPa)	FTA Stress (MPa)	Service Load Stress* (MPa)	Pillar FoS	Pillar w/h
100	19.5 x 39.5	2.5	24.00	3.65	6.08	3.95	7.8
120		2.5	24.00	4.38	7.73	3.11	7.8
125		2.5	24.00	4.56	8.16	2.94	7.8
130		2.5	24.00	4.75	8.60	2.79	7.8

\* - Service load is assumed to equal to full single abutment load from an adjacent high extraction panel goaf.



## **6.0 Results of Subsidence Assessment**

### **6.1 Subsidence Reduction Potential**

The Subsidence Reduction Potential (SRP) refers to the subsidence reducing effect that massive conglomerate / sandstone units above longwall or pillar extraction panels of a given width. The typical stratigraphy over the SMP area is shown in **Figure 5a** and indicates the strata units are < 10 m thick.

The thickness (t) of the sandstone units above the proposed Abel Mine panels were plotted against panel width (W) and distance (y) of the unit above the panels (and normalised to cover depth, H) as shown in **Figure 5b**.

Based on the database, the sandstone units within the overburden are likely to have 'Low' SRP for unit thicknesses < 10 m. This outcome generally applies to all of the 89 m to 160.5 m wide panels with cover depths ranging from 100 m to 150 m.

It is also considered prudent at this stage to assume 'Low' SRP exists for all panels until sufficient local subsidence data becomes available to change this report's assessment of the strata properties.

### **6.2 Single Panel Subsidence Predictions**

Based on the SRP assessment, the range of subsidence for the 'Low' SRP limit lines was determined from the subsidence prediction curves for the 100 m +/- 50 m panel depth category, as shown in **Figure 6a**. The results are also summarised in **Table 5**.

The predictions of maximum single panel subsidence for the pillar extraction Panels 14 to 26, range between 0.75 m and 1.45 m for W/H ratios of 0.9 to 1.97 and a mining height range of 2.2 m to 2.8 m.

The secondary extraction of the Tailgate, South East Mains and East Install Headings will have critical panel W/H ratios of 0.90 to 1.46, with predictions of maximum single panel subsidence ranging from 0.69 m to 1.27 m for mining heights ranging from 2.0 m to 2.8 m.

Subsequent mining of adjacent panels will result in further subsidence increases due to barrier pillar compression and are presented in **Section 6.10**.

**Table 5 - Predicted Single Panel Subsidence (based on ACARP, 2003 Empirical Model)**

Panel #	XL #	Panel Width W (m)	Cover Depth H (m)	W/H	Mining Height T (m)	Extraction Ratio e (%)	Effective Mining Height Te (m)	S <sub>max</sub> Single (mean) (m)	S <sub>max</sub> Single (U95 % CL) (m)
<b>Pillar Extraction Panels 14 to 26</b>									
14	9	96	110	0.87	2.8	95	2.66	0.75	0.88
15	9	160.5	110	1.46	2.8	95	2.66	1.19	1.32
15	10	160.5	120	1.34	2.8	95	2.66	1.12	1.26
16	9	160.5	105	1.53	2.8	95	2.66	1.23	1.36
16	10	160.5	115	1.40	2.8	95	2.66	1.16	1.29
17	9	160.5	107	1.50	2.8	95	2.66	1.21	1.34
17	10	160.5	120	1.34	2.8	95	2.66	1.12	1.26
18	9	160.5	110	1.46	2.8	95	2.66	1.19	1.32
18	10	160.5	120	1.34	2.8	95	2.66	1.12	1.26
19	9	160.5	110	1.46	2.8	95	2.66	1.19	1.32
19	10	160.5	120	1.34	2.8	95	2.66	1.12	1.26
20	7	270.5	137	1.97	2.2	95	2.09	1.16	1.25
21	7	160.5	137	1.17	2.3	95	2.19	0.89	1.00
22	7	160.5	133	1.21	2.5	95	2.38	0.97	1.09
23	6	160.5	112	1.43	2.8	95	2.66	1.18	1.31
23	7	160.5	127	1.26	2.8	95	2.66	1.09	1.22
24	6	160.5	112	1.43	2.8	95	2.66	1.18	1.31
24	7	160.5	124	1.29	2.8	95	2.66	1.10	1.23
24	8	160.5	130	1.23	2.8	95	2.66	1.09	1.22
25	6	160.5	111	1.45	2.8	95	2.66	1.18	1.32
25	7	160.5	120	1.34	2.8	95	2.66	1.12	1.26
25	8	160.5	125	1.28	2.8	95	2.66	1.09	1.22
26	6	160.5	112	1.43	2.7	95	2.57	1.14	1.26
26	7	160.5	117	1.37	2.8	95	2.66	1.14	1.28
26	8	160.5	130	1.23	2.8	95	2.66	1.09	1.22
<b>Tailgate, South East Main and East Install Headings</b>									
TG	5A	89	97	0.92	2.8	95	2.66	0.79	0.92
TG	5B	89	100	0.89	2.8	95	2.66	0.76	0.90
TG	5C	89	110	0.81	2.8	95	2.66	0.69	0.82
SEM	5A	140	105	1.33	2.8	95	2.66	1.12	1.25
SEM	5B	140	103	1.36	2.8	95	2.66	1.14	1.27
EI	5D	105	100	1.06	2.7	95	2.57	0.89	1.02

\* - Pillar FoS based on development height of 2.5 m.

*italics* - barrier pillar FoS < 1 and likely to yield after mining is completed (U95%CL of First S<sub>p</sub> assumed = 2 x mean values and U95%CL of Final S<sub>p</sub> assumed = 30% mining height)

### 6.3 Predicted v. Measured Single Panel Subsidence Data for Area 1 Panels 1 to 4

As a model validation exercise for the above predictions, predicted values of subsidence for the Area 1 Panels 1 to 4 have been compared to the measured values in **Table 6A**.

**Table 6A - Summary of Area 1 Predicted v. Measured Maximum Subsidence**

Panel No.	Line/Chain from start	Panel Width W (m)	Cover Depth H (m)	Panel W/H	Mining Height T (m)	Panel <sup>#</sup> e%	Predicted (mean -U95% CL)		Measured	
							Subsidence S <sub>max</sub> (m)	S <sub>max</sub> /Te (m/m)	Subsidence S <sub>max</sub> (m)	S <sub>max</sub> /Te (m/m)
1	CL 60	120	105	1.14	2.8	98	1.03 - 1.17	0.38 - 0.43	1.193	0.42
	CL 137	120	100	1.20	2.35	93	0.85 - 0.96	0.39 - 0.44	0.788*	0.30*
	CL 626	120	90	1.33	2.35	98	0.97 - 1.08	0.42 - 0.47	1.027	0.45
	XL 275	120	98	1.22	2.35	98	0.91 - 1.00	0.40 - 0.45	0.99	0.43
2	CL 75	150	67	2.24	2.5	92	1.29 - 1.33	0.56 - 0.58	1.004	0.44
	XL 124	150	75	2.00	2.5	83	1.14 - 1.20	0.52 - 0.58	0.900	0.43
3	CL 73	160.5	60	2.68	2.5	95	1.33 - 1.38	0.56 - 0.58	0.835	0.35
	CL 260	160.5	78	1.89	2.5	95	1.33 - 1.38	0.56 - 0.58	0.933	0.39
	XL 170	160.5	70	2.29	2.5	95	1.33 - 1.38	0.56 - 0.58	0.817	0.34
4	CL 45	160.5	55	2.92	2.5	95	1.22 - 1.27	0.56 - 0.58	0.900	0.41

Notes:

# - e% = panel extraction ratio. Panel 1 had only one central row of 3 m wide (average) x 19 m long stooks.

Panels 2 to 4 had 2 stook rows with additional stooks left adjacent to the fault through Panel 2.

\* - subsidence in Panel 1 reduced by additional coal stooks left beneath a fault and where the Breaker Line supports were buried by a goaf fall.

**Bold** - Measured value exceeded predictions by > 10%.

The outcome of the subsidence review indicates that in general, the measured maximum subsidence values plot below the predicted upper 95% confidence limits for a given panel geometry; see **Figure 6b**.

The typical effective mining heights for Panel 1 were assumed to be 98% of the actual mining heights of 2.25 m to 2.8 m, due to the single row of remnant pillars (stook 'X') left in the goaf. The stooks have effectively reduced the available volume in which the fallen roof and crushed out remnant pillars could occupy, and is in proportion to the overall coal pillar extraction ratio for the panel (i.e. 98%). The typical effective mining heights for Panels 2 to 4 was assumed to be 95% of the actual mining heights of 2.25 m to 2.5 m, due to the two rows of remnant pillars (stook 'X') left in the goaf.

The measured subsidence for Panel 1 ranged between 30% to 45% of the effective mining height, and correlates well with the predicted mean and U95%CL range of 33% to 47% of the effective mining height.

The extra stooks left below the fault through Panel 1 (and where the BLS's were buried by an intersection roof fall) appear to have reduced subsidence by approximately 30%. The effective mining height at this location was 93% of the average mining height of 2.8 m.

The measured subsidence for Panel 2 ranged from 42% to 44% of the effective mining height, and appears to be significantly lower than the predicted mean and U95%CL range of 52% to 58% of the effective mining height, despite the allowance for the additional stooks that were required for roof control (the effective mining heights for the panel ranged from 83% to 92%).

A similar outcome has also been noted for the supercritical Panels 3 and 4, where measured subsidence has ranged from 35% to 41% of the effective mining heights significantly lower than the predicted values of 58% of the effective mining height.

Based on a review of the prediction model databases (**Holla, 1987** and **ACARP, 2003**), it is considered that the prediction models are conservative for supercritical panels where cover depths are relatively shallow (i.e. < 80 m). This is likely to be caused by significantly lower overburden pressures acting on the goaf, which has resulted in a reduced level of subsidence compared to the deeper panels.

It is however, not considered necessary to adjust the prediction models at this stage, as the prediction of tilt, strain and curvature have higher levels of uncertainty associated with the shallower cover depths.

Predicted values of maximum tilt for the Area 1 Panels 1 to 4 have been compared to the measured values in **Table 6B**.

**Table 6B - Summary of Area 1 Predicted v. Measured Maximum Tilts**

Panel No.	Line/Chain from start	Panel Width W (m)	Cover Depth H (m)	Panel W/H	Mining Height T (m)	Panel <sup>#</sup> e%	Predicted Tilts (mean - U95% CL) (mm/m)	Measured (mm/m)
1	CL 60	120	105	1.14	2.8	98	26 - 39	<b>49.5</b>
	CL 137	120	100	1.20	2.8	93	20 - 30	27
	CL 626	120	90	1.33	2.35	98	24 - 36	22
	XL 275	120	98	1.22	2.35	98	22 - 33	34 - <b>42</b>
2	CL 75	150	67	2.24	2.5	92	47 - 70	44
	XL 124	150	75	2.00	2.5	83	36 - 54	19 - 27
3	CL 73	160.5	60	2.68	2.5	95	49 - 73	41
	CL 260	160.5	78	1.89	2.5	95	43 - 64	29
	XL 170	160.5	70	2.29	2.5	95	49 - 73	14 - 45
4	CL 45	160.5	55	2.92	2.5	95	43 - 65	58

# - e% = panel extraction ratio. Panel 1 had only one central row of 3 m wide (average) x 19 m long stooks.

Panels 2 to 4 had 2 stook rows with additional stooks left adjacent to the fault through Panel 2.

**Bold** - Measured value exceeded predictions by > 10%.

The outcome of the review indicates that 88% of the measured maximum tilts plot within the upper and lower 95% confidence limits for the predicted values. Predicted tilts were exceeded by 1.27 times the measured values at two locations (see below for further discussion).

Predicted values of maximum convex and concave curvature for the Area 1 Panels 1 to 4 have also been compared to the measured values in **Table 6C**.

**Table 6C - Summary of Area 1 Predicted v. Measured Maximum Curvature Data**

Panel No.	Line/Chain from start Line	Panel Width W (m)	Cover Depth H (m)	Panel W/H	Mining Height T (m)	Panel <sup>#</sup> e%	Predicted Curvatures (mean - U95% CL)		Measured Curvatures	
							Convex C <sub>max</sub> (km-1)	Concave C <sub>min</sub> (km-1)	Convex C <sub>max</sub> (km-1)	Concave C <sub>min</sub> (km-1)
1	CL 60	120	105	1.14	2.8	98	1.13 - 1.68	1.43 - 2.15	<b>2.56</b>	2.32
	CL 137	120	100	1.20	2.8	93	0.94 - 1.38	1.19 - 1.78	1.09	0.93
	CL 626	120	90	1.33	2.35	98	1.06 - 1.58	1.35 - 2.03	2.20	2.10
	XL 275	120	98	1.22	2.35	98	1.00 - 1.48	1.27 - 1.90	2.3 - <b>3.55</b>	1.74 - <b>2.16</b>
2	CL 75	150	67	2.24	2.5	92	2.02 - 3.01	2.56 - 3.84	3.21	3.22
	XL 124	150	75	2.00	2.5	83	1.62 - 2.41	2.05 - 3.08	1.23 - 2.43	0.97 - 2.17
3	CL 73	160.5	60	2.68	2.5	95	2.09 - 3.11	2.65 - 3.97	1.96	3.27
	CL 260	160.5	78	1.89	2.5	95	1.74 - 2.59	2.21 - 3.31	2.30	1.58
	XL 170	160.5	70	2.29	2.5	95	2.09 - 3.11	2.65 - 3.97	<b>4.43</b>	2.40
4	CL 45	160.5	55	2.92	2.5	95	1.92 - 2.86	2.43 - 3.65	<b>5.29</b>	3.43

# - e% = panel extraction ratio. Panel 1 had only one central row of 3 m wide (average) x 19 m long stooks.

Panels 2 to 4 had 2 stook rows with additional stooks left adjacent to the fault through Panel 2.

\* - subsidence in Panel 1 reduced by additional coal stooks left beneath a fault and where the Breaker line supports were buried by a goaf fall.

**Bold** - Measured value exceeded predictions by > 10%.

The outcome of the review indicates that 80% of the measured maximum curvatures plot within the upper and lower 95% confidence limits for the predicted values. Predicted curvatures were exceeded by 1.13 to 2.40 times the measured values at five locations above Panels 1, 3 and 4 where (see below for further discussion).

The prediction exceedences for tilt and curvatures above Panels 1, 3 and 4 may have been due to 'discontinuous' subsidence behaviour exacerbated by sloping surface topography near water courses and/or secondary subsidence profile development due to irregular stook geometry or face extraction height variation in the workings. Further data is required to determine if the model is actually under-predicting tilt and curvature significantly and therefore require re-calibration.

Predicted values of maximum tensile and compressive strain for the Area 1 Panels 1 to 4 have been compared to the measured values in **Table 6D**.

**Table 6D - Summary of Area 1 Predicted v. Measured Maximum Horizontal Strain Data**

Panel No.	Line	Panel Width W (m)	Cover Depth H (m)	Panel W/H	Mining Height T (m)	Panel <sup>#</sup> e%	Predicted Strains <sup>^</sup> (mean - U95 % CL)		Measured Strains	
							Tensile +E <sub>min</sub> (mm/m)	Compressive -E <sub>max</sub> (mm/m)	Tensile +E <sub>min</sub> (mm/m)	Compressive -E <sub>max</sub> (mm/m)
1	CL 60	120	105	1.14	2.8	98	11 - 17	14 - 22	11	11
	CL 137	120	100	1.20	2.8	93	9 - 14	12 - 18	4	5
	CL 626	120	90	1.33	2.35	98	11 - 16	14 - 20	4	9
	XL 275	120	98	1.22	2.35	98	10 - 15	13 - 19	8	11
2	CL 75	150	67	2.24	2.5	92	20 - 30	25 - 38	6	9
	XL 124	150	75	2.00	2.5	83	16 - 24	21 - 31	5	7
3	CL 73	160.5	60	2.68	2.5	95	21 - 31	27 - 40	7	2
	CL 260	160.5	78	1.89	2.5	95	21 - 31	24 - 36	8	6
	XL 170	160.5	70	2.29	2.5	95	19 - 28	27 - 40	n.a.	n.a.
4	CL 45	160.5	55	2.92	2.5	95	19 - 29	24 - 37	n.a.	n.a.

# - e% = panel extraction ratio. Panel 1 had only one central row of 3 m wide (average) x 19 m long stooks.

Panels 2 to 4 had 2 stook rows with additional stooks left adjacent to the fault through Panel 2.

**Bold** - Measured value exceeded predictions by > 10%.

<sup>^</sup> - Strains calculated by multiplying predicted curvatures (see **Table 6C**) by 10.

To-date, maximum measured tensile and compressive strains above Panels 1 to 4 have ranged between +/- 11 mm/m, with local strains of up to 30 mm/m indicated by observed crack widths of 180 mm (Panel 1), 50 mm (Panel 2) 260 mm (Panel 3), 300 mm (Panel 4).

Some compressive shear failures with associated uplift of 100 mm to 150 mm have also been observed above Panel 3.

Predicted values of goaf edge subsidence and angle of draw for the Area 1 Panels 1 to 4 have also been compared to the measured values in **Table 6E**.

**Table 6E - Summary of Area 1 Predicted v. Measured Goaf Edge and AoD Data**

Panel No.	Line	Panel Width W (m)	Cover Depth H (m)	Panel W/H	Mining Height T (m)	Panel# e%	Predicted Goaf Edge Subsidence and AoD (mean - U95% CL)		Measured Goaf Edge Subsidence and AoD	
							S <sub>goe</sub> (m)	AoD (degrees)	S <sub>goe</sub> (m)	AoD (degrees)
1	CL 60	120	105	1.14	2.8	98	0.05 - 0.14	10 - 19	0.049	10
	CL 861	120	85	1.41	2.25	98	0.04 - 0.10	8 - 16	0.050	8
	XL 275	120	98	1.22	2.35	98	0.05 - 0.14	8 - 16	0.026 0.05	6 - <b>23</b>
2	CL 75	110	65	2.25	2.5	94	0.03 - 0.09	6 - 15	0.025	2
	CL 264	160	85	1.88	2.5	88	0.04 - 0.10	7 - 16	0.05	7
	XL 124	150	75	2.00	2.5	83	0.035 - 0.10	7 - 15	-0.035 0.045	7 - 9
3	CL 73	160.5	60	2.68	2.5	95	0.04 - 0.12	8 - 17	0.12	20
	CL 260	160.5	78	1.89	2.5	95	0.04 - 0.12	8 - 17	0.036	3
	XL 170	160.5	70	2.29	2.5	95	0.04 - 0.12	8 - 17	0.001 0.05	0 - 4
4	CL 45	160.5	55	2.92	2.5	95	0.04 - 0.11	7 - 16	0.006	0

Notes:

AoD - Angle of draw to 20 mm subsidence contour.

# - e% = panel extraction ratio. Panel 1 had only one central row of 3 m wide (average) x 19 m long stooks.

Panels 2 to 4 had 2 stook rows with additional stooks left adjacent to the fault through Panel 2.

**Bold** - Measured value exceeded predictions by > 10%.

*italics* - negative goaf edge subsidence values indicate uplift.

The measured goaf edge subsidence has ranged from 35 mm of uplift to 120 mm with angles of draw to the 20 mm subsidence contour ranging between 0° and 23° (mean of 8°).

The outcome of the review indicates that 100% of the measured goaf edge and 92% of the angle of draw (to 20 mm subsidence) values plot below the upper 95% confidence limits for the predicted values. The one exceedence in AoD that did occur was < design angle of draw of 26.5°.

Overall, it is assessed that the **ACARP, 2003** model with the inclusion of the effective mining height, is likely to provide reasonably reliable subsidence impact parameter predictions for the Area 2 Panels.



## 6.4 Barrier Pillar Subsidence Predictions

### 6.4.1 Empirical Model Development

The predicted subsidence values above the barrier pillars have been estimated based on an empirical model and an analytical model of the roof-pillar-floor system.

The empirical model has been developed from measured NSW Coalfields subsidence data over chain pillars ( $S_p$ ) divided by the mining height (T) v. total pillar stress after longwall panel extraction on both sides.

Reference to the longwall chain pillar database indicates that the subsidence measured above 'squat' chain pillars (i.e.  $w/h > 5$ ) may increase significantly when total average pillar stresses exceed 25 MPa (see **Figure 7a**) or when the pillar stress exceeds 0.5 times the pillar strength (see **Figure 7b**). This is equivalent to a Factor of Safety (FoS) of  $< 2.0$ .

The estimate of the total stress acting on the proposed barrier pillars under double abutment loading conditions (which will occur after the mining of high pillar extraction panels along both sides) is based on the abutment angle concept described in **ACARP, 1998a** as follows:

$$\sigma = \text{pillar load/area} = (P + A_1 + A_2)/wl$$

where:

$P$  = full tributary area load of column of rock above each pillar;

$$= (l + r)(w + r).p.g.H;$$

$A_{1,2}$  = total abutment load from each side of pillar in MN/m, and

$$= (l+r)pg(0.5W'H - W'^2/8\tan\phi) \quad (\text{for sub-critical panel widths}) \text{ or}$$

$$= (l+r)(pgH^2\tan\phi)/2 \quad (\text{for super-critical panel widths});$$

$w$  = pillar width (solid);

$l$  = pillar length;

$r$  = roadway width;

$H$  = depth of cover;

$\phi$  = abutment angle (normally  $21^\circ$  adopted for cover depths  $< 350$  m in the NSW Coalfields);

$W'$  = effective panel width (rib to rib distance minus the roadway width).

A panel is deemed sub-critical when  $W'/2 < H \tan \phi$ .

As presented in **ACARP, 1998b** the FoS of the barrier and chain pillars were based on the strength formula for 'squat' pillars with w/h ratios > 5 as follows:

$$S = 27.63 \Theta^{0.51} (0.29((w/5h)^{2.5} - 1) + 1) / (w^{0.22} h^{0.11})$$

where:

h = pillar height;

$\Theta$  = a dimensionless 'aspect ratio' factor or w/h ratio in this case.

The FoS was calculated by dividing the pillar strength, S, with the pillar stress,  $\sigma$ .

#### 6.4.2 Inter-Panel Barrier Pillars

Predictions of the maximum first and final barrier pillar subsidence for Panels P14 to P26 have been based on the mean and U95%CL curves shown in **Figure 7a** and the total stress acting on the pillars under double abutment loading conditions. Due to the method of pillar lifting employed at Abel, the development height of the pillars has been used instead of the face extraction height.

A summary of the subsidence predictions for the barrier pillars is presented in **Table 7A**.

For comparative purposes the pillar subsidence database was plotted against 1/FoS (or pillar stress / strength) in **Figure 7b** and shows that the chain pillar subsidence follows a similar trend to the increasing 1/FoS parameter as it does to the pillar stress:

- Firstly, the subsidence increases slowly up to an 1/FoS of 0.5 (the elastic zone), and then
- increases more rapidly to an 1/FoS of 1 (the transition zone between elastic and yielded zones), before
- 'rolling over' to a for 1/FoS values > 1 (the yielded zone).

Based on **Figure 7b**, the proposed 55 m wide chain pillar subsidence predictions in the elastic zone (i.e. FoS > 2) may be conservative.

It is also apparent from the measured data **Figure 7a** that the subsidence above the pillars is not just a function of the strength and stiffness of the coal pillars and surrounding rock mass (i.e. higher subsidence is measured above weak shale roof compared to a strong sandstone one).

**Table 7A - Predicted Pillar Subsidence under Double Abutment Loading (based on Modified ACARP, 2003 Empirical Model)**

Panel #	XL#	Pillar Width (m)	Cover Depth H (m)	Pillar Stress (MPa)	Pillar* FoS	Sp First (mean)	Sp First (U95 % CL)	Sp Final (mean)	Sp Final (U95 % CL)
<b>Pillar Extraction Panels 14 to 26</b>									
14	9	24.5	110	8.20	4.76	0.06	0.13	0.08	0.14
15	9	24.5	110	7.98	4.88	0.06	0.13	0.08	0.14
15	10	24.5	120	9.18	4.24	0.07	0.14	0.09	0.15
16	9	24.5	105	7.70	5.06	0.06	0.13	0.07	0.14
16	10	24.5	115	9.03	4.32	0.07	0.14	0.09	0.15
17	9	24.5	107	7.97	4.89	0.06	0.13	0.08	0.14
17	10	24.5	120	10.47	3.05	0.08	0.15	0.10	0.17
18	9	24.5	110	8.20	4.76	0.06	0.13	0.08	0.14
18	10	24.5	120	9.42	4.14	0.07	0.14	0.09	0.16
19	9	24.5	110	5.80	6.72	0.05	0.12	0.06	0.13
20	7	24.5	137	11.67	3.34	0.09	0.15	0.10	0.16
21	7	24.5	137	11.46	3.40	0.08	0.14	0.10	0.16
22	7	24.5	133	10.81	3.61	0.08	0.14	0.09	0.15
23	6	24.5	112	8.43	4.62	0.07	0.13	0.08	0.15
23	7	24.5	127	10.17	3.83	0.08	0.15	0.10	0.16
24	6	24.5	112	8.39	4.65	0.07	0.13	0.08	0.15
24	7	24.5	124	9.73	4.01	0.08	0.14	0.09	0.16
24	8	24.5	130	10.46	3.73	0.08	0.15	0.10	0.17
25	6	24.5	111	8.36	4.66	0.07	0.13	0.08	0.15
25	7	24.5	120	9.28	4.20	0.07	0.14	0.09	0.15
25	8	24.5	125	10.31	3.78	0.08	0.15	0.10	0.17
<b>Tailgate, South East Main and East Install Headings</b>									
1	5A	16.5	90	8.21	2.96	0.06	0.12	0.07	0.13
1	5B	16.5	98	9.10	2.67	0.07	0.13	0.08	0.14
1	5C	16.5	105	10.38	2.34	0.08	0.15	0.10	0.17
TG	5A	21.0	97	7.78	4.09	0.06	0.13	0.07	0.14
TG	5B	21.0	100	7.92	4.02	0.06	0.13	0.07	0.14
SEM	5A	23.5	105	8.95	3.38	0.07	0.13	0.08	0.14
SEM	5B	23.5	103	8.75	3.45	0.07	0.13	0.08	0.14
EI	5D	21.0	100	5.60	5.39	0.05	0.11	0.05	0.12
<b>End Barriers between Panels 19 to 14 and East Mains</b>									
18,19	11A,B	21.5	100	8.66	3.07	0.07	0.14	0.08	0.15
17	11C	22.5	103	8.71	3.23	0.07	0.14	0.08	0.15
16,15	11D,E	22.5	101	8.59	3.27	0.06	0.12	0.07	0.13
14	11F	22.5	100	5.97	4.70	0.04	0.10	0.05	0.11

\* - Pillar FoS based on development height of 2.5 m.

*italics* - barrier pillar FoS < 1 and likely to yield after mining is completed (U95%CL of First  $S_p$  assumed = 2 x mean values and U95%CL of Final  $S_p$  assumed = 30% mining height)

The predictions of first and final subsidence above the 24.5 m wide barriers between Panels 14 to 26 ranges from 0.05 m to 0.17 m for a development height of 2.5 m. Pillar stresses are estimated to range from 5.8 MPa to 11.7 MPa for cover depths of 105 m to 137 m. The post-

mining factors of safety for these barrier pillars are estimated to range from 3.05 to 6.72 and likely to behave elastically in the long-term.

The predictions of first and final pillar subsidence for the 16.5 m to 24.5 m wide barrier pillars between Panel 1, Tailgate, East Install Headings, South East Mains and Area 2 production panels (Panels 14 to 26) range from 0.04 m to 0.17 m. The pillar stresses are estimated to range from 5.6 MPa to 10.4 MPa for cover depths of 97 m to 110 m. The post-mining factors of safety for these barrier pillars are estimated to range from 2.34 to 5.39 and the pillars are very likely to behave elastically over the long term.

The w/h ratio range of 6.6 to 9.4 for all the barrier pillars assessed indicates that the barrier pillars are likely to strain-harden if overloaded, and limit maximum subsidence to < 10% of the pillar development heights (see **Figure 7c**).

## 6.5 Bearing Capacity of Roof and Floor Strata

The bearing capacity of the roof and floor strata should be considered when designing the barrier pillars for long-term subsidence control.

Reference to **Pells *et al*, 1998** indicates that the bearing capacity of sedimentary rock under shallow footing type loading conditions is 3 to 4 times its UCS strength. Based on the estimated average UCS values in the immediate floor and roof strata of 18 to 72 MPa, the general bearing capacity of the strata is estimated to range between 54 and 288 MPa.

Based on the predicted average pillar stress range of 5.6 to 11.7 MPa after the mining of the pillar extraction panels, an overall FoS against roof and floor bearing failure of > 4.5 is assessed. The roof and floor strata are therefore likely to behave elastically in the long term.

Some local shear failure may occur in the wetter areas of the mine with weaker floor units however, but unlikely to lead to significant time dependent subsidence increases.

The observed behaviour of longwall chain pillars and roof / floor system has also been used to develop a simple analytical model in **Section 6.6**.

## 6.6 Analytical Pillar Subsidence

### 6.6.1 Model Development

The compression of the barriers, chain pillars and immediate roof and floor strata has also been estimated analytically using two relatively simple models. The purpose of this exercise is to check that the empirical model predictions are reasonable based on the range of measured physical parameters of the rock mass and coal seam.

Given that the stress on the barrier or chain pillars may exceed the in-situ strength of the coal and/or roof / floor materials, the analytical models needed to consider both the elastic and post-yield stiffness moduli of the pillar-roof-floor system as defined in **ACARP, 2005**.

Reference to **Figure 7b** indicates that the proposed barrier pillars (that will generally have w/h ratios > 5) would be expected to strain-harden if they are over-loaded and go into yield. The post-yield stiffness of the coal pillars has been assumed to equal 15% of the peak Young's Modulus value of 3 GPa (i.e. 450 MPa) and limit subsidence to within the observed range of subsidence values for Australian longwall mines; as shown in **Figure 7a**.

The roof and floor strata FoS values estimated in the previous sections of this report indicate that the compression of these materials may be estimated using laboratory test results that have been adjusted to reflect the stiffness of the overall rock mass.

Average rock mass elastic moduli for the floor and roof materials within the significant area of influence of the pillars (i.e. approximately the pillar width or 20 to 25 m above and below the pillars) were estimated based on the laboratory data and the relationship established by **Hoek and Diederichs, 2006** below:

$$E_{\text{rockmass}} = E_{\text{laboratory}}(0.02 + 1/(1 + e^{(60 - \text{GSI})/11}))$$

The upper and lower bound Young's Modulus for each of the above have been estimated for an assessed Geological Strength Index (GSI) range of 50 to 60 (very blocky or jointed strata with fair to good bedding party surface quality (i.e. rough and slightly to moderately weathered) as follows:

$$E_{\text{rockmass}} = 0.3 - 0.5 E_{\text{laboratory}}$$

$$E_{\text{roof}} = 5 - 10 \text{ GPa (for an estimated laboratory stiffness range 10 to 20 GPa)}$$

$$E_{\text{floor}} = 5 - 10 \text{ GPa (for an estimated laboratory stiffness range of 10 to 20 GPa)}$$

$$E_{\text{coal}} = 2 - 4 \text{ GPa (back analysis from field measurements as laboratory stiffness is not possible to measure)}$$

The compression of the pillars in the elastic and post-yielded regimes has been calculated by assuming the pillar will behave like a spring under load and then strain-harden as follows:

$$S_{\text{pillar}} = \sigma_{\text{net}} T_s / E_c + (\sigma_{\text{max}} - S_p) T_s / 0.15 E_c \quad (1)$$

where:

$$S_{\text{pillar}} = \text{pillar compression};$$

$$\sigma_{\text{net}} = \text{pillar stress increase} = \text{total pillar stress} - \text{virgin stress};$$

$$T_s = \text{seam thickness};$$

$$E_c = \text{Young's Modulus of Coal};$$

$\sigma_{\max}$  = maximum stress on pillar after load redistribution to the goaf (if applicable).

$S_p$  = pillar strength (**ACARP, 1998b**)

The analytical model adopted to estimate the immediate compression of the floor and roof was taken from Boussinesq's elastic pressure bulb theory beneath strip footings of varying aspect ratio, see **Das, 1998**:

$$S_{\text{roof}} = \sigma_{\text{net}} w(1-v^2)I/E_{\text{roof}} \quad (2)$$

$$S_{\text{floor}} = \sigma_{\text{net}} w(1-v^2)I/E_{\text{floor}} \quad (3)$$

where:

$S_{\text{roof}}$  = roof compression above pillar;

$S_{\text{floor}}$  = floor compression below pillar;

$\sigma_{\text{net}}$  = net pillar stress increase (= total stress - pre-mining stress);

$w$  = pillar width;

$E_{\text{roof}}$  = average Young's Modulus of roof material for a distance  $w$  above the pillar;

$E_{\text{floor}}$  = average Young's Modulus of floor material for a distance  $w$  below the pillar;

$v$  = Poisson's Ratio (0.25 assumed for all materials);

$I$  = Influence Function for various footing shape geometries (1.5 in this case).

Lower and upper bound estimates of long-term surface subsidence ( $S_{\text{total}}$ ) above a pillar subject to the assumed loading may be estimated by summing equations (1), (2) and (3):

$$S_{\text{total}} = S_{\text{pillar}} + S_{\text{roof}} + S_{\text{floor}}$$

Where the lower bound solution assumes the upper limit estimate of *insitu* rock mass stiffness properties and the upper bound solution assumes the lower limit estimate of the *insitu* rock mass stiffness properties.

## 6.6.2 Analytical Model Outcomes

Lower and upper bound barrier pillar subsidence predictions are presented in **Table 7B** for the proposed 2.5 m high pillars left between the total pillar extraction panels No. 14 to 26. Calculation details are presented in **Appendix C**.

The results of the analytical subsidence prediction analysis for the lower bound material properties and cover depth ranges indicate that the worst-case subsidence over the proposed barrier pillars between Panels 14 to 26 will range between 0.05 and 0.24 m after mining is completed. The pillar FoS values are all > 2 and are therefore expected to behave elastically in the long term.

The predictions for the 24.5 m wide barriers are compared to the empirical model values in **Figure 7d**. Overall, the results generally plot between the mean and U95%CL values predicted by the empirical model, and are therefore considered reasonable for impact analysis purposes.

**Table 7B - Analytical Model Subsidence Predictions Above the Proposed Barrier Pillars for the Pillar Extraction Panels 14 to 26**

Cover Depth (m)	Pillar Height h (m)	Pre-Mining Stress (MPa)	Applied Pillar Stress (MPa)	Pillar FoS Under Final Loading	Subsidence Predictions Based on Non-Linear Pillar and Strata System Compression (m)				
					Pillar	Roof	Floor	Total (Lower & Upper Bounds)*	
Panels 14 to 26 Inter-panel Barrier Pillar width = 24.5 m									
100	2.5	2.25	7.06	5.52	0.00	0.03	0.03	<b>0.07</b>	<b>0.13</b>
110	2.5	2.50	8.20	4.75	0.00	0.04	0.04	<b>0.08</b>	<b>0.16</b>
120	2.5	2.75	9.42	4.14	0.00	0.04	0.04	<b>0.09</b>	<b>0.18</b>
130	2.5	3.00	10.72	3.64	0.00	0.05	0.05	<b>0.11</b>	<b>0.21</b>
140	2.5	3.25	12.10	3.22	0.01	0.06	0.06	<b>0.12</b>	<b>0.25</b>

Notes:

\* - the Upper Bound Total value = 2 x Lower Bound Total value.

*Italics* - Coal pillar stiffness modulus reduced to 10% of peak or elastic value if pillar FoS < 2 under design loading conditions.

## 6.7 Goaf Edge Subsidence Prediction

The predictions of goaf edge subsidence have been derived from the modified **ACARP, 2003** model's curves shown in **Figure 8**.

The goaf edge subsidence predictions for Panels 14 to 26 and the extracted mains headings panels range from 0.035 m to 0.17 m for cover depths from 100 m to 150 m.

## 6.8 Angle of Draw Prediction

The angle of draw values have been estimated from the prediction curves shown in **Figure 9** and range from 7° to 21° for cover depths of 100 to 150 m.

The Angle of Draw predictions have been derived from the goaf edge subsidence predictions given in **Section 6.6** for Panels 14 to 26 and the extracted main headings panels.

## 6.9 Inflexion Point and Peak Strain Locations

The subsidence development process causes tensile and compressive strains to develop above an extracted high pillar extraction panel, due to the sagging and bending of the overburden strata.

Tensile strains are generally located in the outer third zone above an extracted panel and the compressive strains will occur above the central or middle third area. The point where the tensile strains become compressive is called the inflexion point. The relative locations of the peak surface impact parameters above an extracted panel are shown schematically in **Figure 10a**.

The Newcastle Coalfield database of pillar extraction and longwall inflexion point and tensile/compressive strain or convex/concave curvature peak locations, are shown in **Figure 10b**. The measured values for Area 1 are shown on **Figures 10c to 10e** and generally plot within the Newcastle database, but near the lower bound limit. It is considered that the difference between the coalfield and Abel mine data is indicative of the lack of massive units in the overburden strata at Abel.

The predicted locations of the inflexion and peak strain location points for the proposed Area 2 Panels are given in **Table 8** and derived from the Newcastle Coalfield database curves less 10 m (to be consistent with the Abel Mine data).

**Table 8 - Predicted Inflexion and Strain Peak Location Summary**

Panel #	XL #	Cover Depth H (m)	Panel W/H	Inflexion Point Location Factor $d/H$	Inflexion Point Location from Panel Rib, $d$	Tensile Strain Peak Location Factor $d_t/H$	Tensile Strain Peak Location From Panel Rib, $d_t$	Compressive Strain Peak Location Factor $d_c/H$	Compressive Strain Peak Location from Panel Rib, $d_c$
<b>Pillar Extraction Panels 14 to 26</b>									
14	9	110	0.87	0.19	20	0.11	12	0.27	29
15	9	110	1.46	0.30	33	0.18	20	0.41	45
15	10	120	1.34	0.30	36	0.18	22	0.40	49
16	9	105	1.53	0.30	31	0.18	19	0.41	43
16	10	115	1.40	0.30	35	0.19	22	0.41	48
17	9	107	1.50	0.30	32	0.18	19	0.41	44
17	10	120	1.34	0.30	36	0.18	22	0.40	49
18	9	110	1.46	0.30	33	0.18	20	0.41	45
18	10	120	1.34	0.30	36	0.18	22	0.40	49
19	9	110	1.46	0.30	33	0.18	20	0.41	45
19	10	120	1.34	0.30	36	0.18	22	0.40	49
20	7	137	1.97	0.32	44	0.20	28	0.43	59
21	7	137	1.17	0.28	38	0.17	24	0.37	51
22	7	133	1.21	0.28	37	0.18	23	0.38	51
23	6	112	1.43	0.30	34	0.19	21	0.41	46



**Table 8 (cont...) - Predicted Inflexion and Strain Peak Location Summary**

Panel #	XL #	Cover Depth H (m)	Panel W/H	Inflexion Point Location Factor d/H	Inflexion Point Location from Panel Rib, d	Tensile Strain Peak Location Factor d <sub>t</sub> /H	Tensile Strain Peak Location From Panel Rib, d <sub>t</sub>	Compressive Strain Peak Location Factor d <sub>c</sub> /H	Compressive Strain Peak Location from Panel Rib, d <sub>c</sub>
<b>Pillar Extraction Panels 14 to 26</b>									
23	7	127	1.26	0.29	37	0.18	23	0.39	50
24	6	112	1.43	0.30	34	0.19	21	0.41	46
24	7	124	1.29	0.29	36	0.18	23	0.40	49
24	8	130	1.23	0.28	37	0.18	23	0.39	50
25	6	111	1.45	0.30	34	0.19	21	0.41	46
25	7	120	1.34	0.30	36	0.18	22	0.40	49
25	8	125	1.28	0.29	36	0.18	23	0.40	49
26	6	112	1.43	0.30	34	0.19	21	0.41	46
26	7	117	1.37	0.30	35	0.19	22	0.41	48
26	8	130	1.23	0.28	37	0.18	23	0.39	50
<b>Tailgate, South East Main and East Install Headings</b>									
TG	5A	97	0.92	0.19	19	0.10	10	0.27	26
TG	5B	100	0.89	0.18	18	0.10	10	0.26	26
TG	5C	110	0.81	0.14	16	0.09	10	0.24	27
SEM	5A	105	1.33	0.41	43	0.17	18	0.39	41
SEM	5B	103	1.36	0.43	44	0.17	18	0.40	41
25	5A	110	1.46	0.46	50	0.18	20	0.41	45
23	5B	110	1.46	0.46	50	0.18	20	0.41	45
EI	5F	100	1.05	0.24	24	0.13	13	0.32	32

## 6.10 Multiple Panel Subsidence Predictions

Maximum subsidence predictions for multiple panels may be estimated by adding 50% to 100% of the chain or barrier pillar subsidence predictions to the mean single panel  $S_{max}$ . The predicted goaf edge subsidence is subtracted from the chain pillar subsidence (as it is included in the single panel predictions).

The maximum subsidence impact parameter predictions (i.e. tilt, curvature and strain etc) for multiple panels may then be derived using the empirical relationships defined in **ACARP, 2003** (see the following sections).

### 6.10.1 Maximum Subsidence above Pillar Extraction Panels

The maximum first and final subsidence predictions for the proposed 160.5 m wide extraction Panels 14 to 26 are summarised in **Table 9** for the range of cover depths of 100 m to 150 m. An average panel mining heights of 2.2 to 2.8 m has been assumed together with an extraction ratio of 95% (i.e. effective mining heights range from 2.09 m - 2.66 m).

Predicted first and final maximum subsidence for the production panels 14 to 26 range from 0.75 m to 1.41 and from 0.76 to 1.45 m respectively (i.e. 28% to 55% the effective mining height).

Predicted first and final maximum subsidence for the 89 m to 140 m wide East Install, TG and SE Mains panels range from 0.69 m to 1.21 m and from 0.87 m to 1.36 m (i.e. 26% to 51% the effective mining height).

Representative first and final subsidence profiles have been prepared along cross lines XLs 5b, 7 and 9 in **Figures 11a, 12a and 13a** (the location of the cross lines is shown in **Figure 1**).

**Table 9 - Predicted Maximum Subsidence for Multiple Pillar Extraction Panels**

Panel #	XL #	Cover Depth H (m)	Panel Width W (m)	Average Mining Height T (m)	W/H (m/m)	Final TG Barrier Pillar Subsidence S <sub>p</sub> (m)		First Panel S <sub>max</sub> (m)		Final Panel S <sub>max</sub> (m)	
						mean	U95 % CL	mean	U95 % CL	mean	U95 % CL
Pillar Extraction Panels 14 to 26											
14	9	110	96	2.8	0.87	0.13	0.14	0.75	0.93	0.76	0.95
15	9	110	160.5	2.8	1.46	0.13	0.14	1.19	1.38	1.23	1.41
15	10	120	160.5	2.8	1.34	0.14	0.15	1.12	1.31	1.17	1.36
16	9	105	160.5	2.8	1.53	0.13	0.14	1.23	1.41	1.26	1.45
16	10	115	160.5	2.8	1.40	0.14	0.15	1.16	1.34	1.21	1.39
17	9	107	160.5	2.8	1.50	0.13	0.14	1.21	1.40	1.25	1.43
17	10	120	160.5	2.8	1.34	0.15	0.17	1.12	1.31	1.18	1.37
18	9	110	160.5	2.8	1.46	0.13	0.14	1.19	1.38	1.23	1.42
18	10	120	160.5	2.8	1.34	0.14	0.16	1.12	1.31	1.17	1.36
19	9	110	160.5	2.8	1.46	-	-	1.19	1.38	1.21	1.40
19	10	120	160.5	2.8	1.34	-	-	1.12	1.31	1.13	1.31
20	7	137	270.5	2.2	1.97	0.15	0.16	1.16	1.21	1.21	1.21
21	7	137	160.5	2.3	1.17	0.14	0.16	0.89	1.06	0.95	1.12
22	7	133	160.5	2.5	1.21	0.14	0.15	0.97	1.15	1.02	1.20
23	6	112	160.5	2.8	1.43	0.13	0.15	1.18	1.36	1.22	1.41
23	7	127	160.5	2.8	1.26	0.15	0.16	1.09	1.27	1.14	1.33
24	6	112	160.5	2.8	1.43	0.13	0.15	1.18	1.36	1.22	1.41
24	7	124	160.5	2.8	1.29	0.14	0.16	1.10	1.28	1.15	1.33
24	8	130	160.5	2.8	1.23	0.15	0.17	1.09	1.27	1.14	1.33
25	6	111	160.5	2.8	1.45	0.13	0.15	1.18	1.37	1.23	1.41
25	7	120	160.5	2.8	1.34	0.14	0.15	1.12	1.31	1.17	1.36
25	8	125	160.5	2.8	1.28	0.15	0.17	1.09	1.27	1.15	1.33
26	6	112	160.5	2.7	1.43	-	-	1.14	1.32	1.14	1.32
26	7	117	160.5	2.8	1.37	-	-	1.14	1.33	1.15	1.34
26	8	130	160.5	2.8	1.23	-	-	1.09	1.27	1.09	1.28

**Table 9 (Cont...) - Predicted Maximum Subsidence for Multiple Pillar Extraction Panels**

Panel #	XL #	Cover Depth H (m)	Panel Width W (m)	Average Mining Height T (m)	W/H (m/m)	Final TG Barrier Pillar Subsidence S <sub>p</sub> (m)		First Panel S <sub>max</sub> (m)		Final Panel S <sub>max</sub> (m)	
						mean	U95 % CL	mean	U95 % CL	mean	U95 % CL
Tailgate, South East Main and East Install Headings											
TG	5A	97	89	2.8	0.92	0.06	0.14	0.79	0.80	0.98	0.99
TG	5B	100	89	2.8	0.89	0.06	0.14	0.76	0.78	0.95	0.96
TG	5C	110	89	2.8	0.81	0.03	0.11	0.69	0.69	0.87	0.88
SEM	5A	105	140	2.8	1.33	0.07	0.14	1.12	1.16	1.27	1.31
SEM	5B	103	140	2.8	1.36	0.07	0.14	1.14	1.18	1.28	1.32
25	5A	110	160.5	2.8	1.46	0.05	0.12	1.19	1.21	1.34	1.36
23	5B	110	160.5	2.8	1.46	0.05	0.12	1.19	1.21	1.34	1.36
EI	5D	100	105	2.7	1.06	0.05	0.12	0.89	0.90	1.07	1.08

U95%CL Final  $S_{max}$  = Mean Final  $S_{max}$  + U95%CL error

Reference to the **Holla, 1987** curves for total pillar extraction mining indicates maximum subsidence above the production panels will range between 0.79 m and 1.46 m (38% and 55% the effective mining heights) for the given mining geometries, which are similar to the **ACARP, 2003** model predictions.

### 6.10.2 Maximum Panel Tilts and Horizontal Displacements

The maximum first and final tilt predictions for the proposed 160.5 m wide pillar extraction Panels 14 to 26 are summarised in **Table 10** for the range of cover depths and average panel mining heights of 2.2 to 2.8 m. An assumed maximum extraction ratio of 95% gives an effective mining height range from 2.09 m - 2.66 m.

Predictions of final maximum tilt values for the pillar extraction panels range from 14 mm/m to 36 mm/m. Maximum horizontal displacements are estimated to range from 140 to 360 mm for the predicted tilts and a 'K' factor of 10.

Predictions of final maximum tilt for the 89 m to 140 m wide mains panels range from 18 mm/m to 35 mm/m. Maximum horizontal displacements are estimated to range from 180 to 350 mm for the predicted tilts.

Representative first and final tilt and horizontal displacement profiles have been prepared along cross lines XLs 5b, 7 and 9 in **Figures 11b, 12b and 13b** (the location of the cross lines is shown in **Figure 1**).

Reference to the **Holla, 1987** curves suggests maximum tilt above the proposed pillar extraction panels will range between 17 mm/m and 30 mm/m, which are similar to the **ACARP, 2003** model predictions.

**Table 10 - Predicted Maximum Tilt and Horizontal Displacement for Multiple Pillar Extraction Panels**

Panel #	XL #	Cover Depth H (m)	Panel Width W (m)	Seam Thickness T (m)	Mean Final S <sub>max</sub> (m)	Final Panel T <sub>max</sub> (mm/m)		Final Panel HD <sub>max</sub> (mm)	
						Mean	U95% CL	Mean	U95% CL
Pillar Extraction Panels 14 to 26									
14	9	110	96	2.8	0.76	20	30	202	304
15	9	110	160.5	2.8	1.23	22	32	216	325
15	10	120	160.5	2.8	1.17	19	29	191	286
16	9	105	160.5	2.8	1.26	24	36	239	359
16	10	115	160.5	2.8	1.21	20	30	199	299
17	9	107	160.5	2.8	1.25	23	35	230	345
17	10	120	160.5	2.8	1.18	19	29	194	291
18	9	110	160.5	2.8	1.23	22	33	217	325
18	10	120	160.5	2.8	1.17	19	29	191	287
19	9	110	160.5	2.8	1.21	21	32	212	318
19	10	120	160.5	2.8	1.13	18	27	182	273
20	7	137	270.5	2.2	1.21	16	24	158	237
21	7	137	160.5	2.3	0.95	14	21	143	214
22	7	133	160.5	2.5	1.02	16	24	158	236
23	6	112	160.5	2.8	1.22	21	31	209	314
23	7	127	160.5	2.8	1.14	18	28	184	277
24	6	112	160.5	2.8	1.22	21	31	209	313
24	7	124	160.5	2.8	1.15	19	28	185	278
24	8	130	160.5	2.8	1.14	18	28	184	276
25	6	111	160.5	2.8	1.23	21	32	213	320
25	7	120	160.5	2.8	1.17	19	29	191	287
25	8	125	160.5	2.8	1.15	19	28	185	278
26	6	112	160.5	2.7	1.14	19	29	190	286
26	7	117	160.5	2.8	1.15	19	28	186	280
26	8	130	160.5	2.8	1.09	17	26	174	261
Tailgate, South East Main and East Install Headings									
TG	5A	97	89	2.8	0.80	22	33	218	327
TG	5B	100	89	2.8	0.78	21	31	208	313
TG	5C	110	89	2.8	0.69	18	27	178	267
SEM	5A	105	140	2.8	1.16	23	34	228	342
SEM	5B	103	140	2.8	1.18	23	35	233	349
25	5A	110	160.5	2.8	1.21	21	32	212	317
23	5B	110	160.5	2.8	1.21	21	32	212	317
EI	5F	100	105	2.7	0.90	24	35	237	354

Mean Final T<sub>max</sub> = 1.1925[(Mean Final S<sub>max</sub>)/(Effective Panel Width)]<sup>1.3955</sup>

U95%CL Final T<sub>max</sub> = Mean Final T<sub>max</sub> + U95%CL error (= 0.4\*mean value); HD<sub>max</sub> = 10 T<sub>max</sub>

### 6.10.3 Maximum Panel Curvature and Strains

The maximum first and final curvature and strain predictions for the proposed 160.5 m wide total extraction Panels 14 to 26 are summarised in **Tables 11A** and **11B** for the range of cover depths and average panel mining heights of 2.2 to 2.8 m. An assumed maximum extraction ratio of 95% gives an effective mining height range from 2.09 m to 2.66 m.

Predictions of final maximum hogging curvature values for the pillar extraction panels 14 to 26 range from  $0.51 \text{ km}^{-1}$  to  $1.37 \text{ km}^{-1}$ . Maximum tensile strains are estimated to range from 5 to 14 mm/m for the above curvatures.

Predictions of final maximum sagging curvatures for the pillar extraction panels 14 to 26 range from  $0.65 \text{ km}^{-1}$  to  $1.65 \text{ km}^{-1}$ . Maximum compressive strains are estimated to range from 7 to 17 mm/m for the above curvatures.

Predictions of final maximum hogging curvatures for the 89 m to 140 m wide TG, East Install Headings and SE Main Headings range from  $0.80 \text{ km}^{-1}$  to  $1.89 \text{ km}^{-1}$ . Maximum tensile strains are estimated to range from 8 to 19 mm/m for the above curvatures.

Predictions of final maximum sagging curvatures for the 89 m to 140 m wide TG, East Install Headings and SE Main Headings range from  $0.79 \text{ km}^{-1}$  to  $2.39 \text{ km}^{-1}$ . Maximum compressive strains are estimated to range from 8 to 24 mm/m for the above curvatures.

Representative first and final curvature and strain profiles have been prepared along cross lines XLs 5b, 7 and 9 in **Figures 11c, 12c and 13c** (the location of the cross lines is shown in **Figure 1**).

Reference to the **Holla, 1987** curves for high extraction pillar mining in the Newcastle Coalfield suggests maximum tensile strain above the pillar extraction panels will range between 4 mm/m and 10 mm/m with compressive strains ranging between 6 and 15 mm/m for the given mining geometries, which are generally 50 to 70 % of the **ACARP, 2003** model predictions.

As discussed previously, discontinuous displacements can result in secondary curvatures and strains, which exceed predicted 'smooth' profile values by 2 to 4 times occasionally. The discrepancy between the two models is therefore not surprising, as the data base will be strongly dependent on surface topography and near surface lithologies.

**Table 11A - Predicted Maximum Hogging Curvature and Tensile Strains for Multiple Pillar Extraction Panels**

Panel #	XL #	Cover Depth H (m)	Panel Width W (m)	Seam Thickness T (m)	Mean Final Panel $S_{\max}$ (m)	Final Panel Hogging Curvature $C_{\max}$ (km <sup>-1</sup> )		Final Panel Tensile Strain + $E_{\max}$ (mm/m)	
						Mean	U95% CL	Mean	U95% CL
Pillar Extraction Panels 14 to 26									
14	9	110	96	2.8	0.76	0.90	1.35	9	14
15	9	110	160.5	2.8	1.23	0.81	1.21	8	12
15	10	120	160.5	2.8	1.17	0.71	1.06	7	11
16	9	105	160.5	2.8	1.26	0.91	1.37	9	14
16	10	115	160.5	2.8	1.21	0.73	1.10	7	11
17	9	107	160.5	2.8	1.25	0.87	1.30	9	13
17	10	120	160.5	2.8	1.18	0.72	1.08	7	11
18	9	110	160.5	2.8	1.23	0.81	1.21	8	12
18	10	120	160.5	2.8	1.17	0.71	1.07	7	11
19	9	110	160.5	2.8	1.21	0.80	1.20	8	12
19	10	120	160.5	2.8	1.13	0.68	1.03	7	10
20	7	137	270.5	2.2	1.21	0.51	0.77	5	8
21	7	137	160.5	2.3	0.95	0.58	0.86	6	9
22	7	133	160.5	2.5	1.02	0.62	0.93	6	9
23	6	112	160.5	2.8	1.22	0.77	1.16	8	12
23	7	127	160.5	2.8	1.14	0.69	1.04	7	10
24	6	112	160.5	2.8	1.22	0.77	1.16	8	12
24	7	124	160.5	2.8	1.15	0.69	1.04	7	10
24	8	130	160.5	2.8	1.14	0.69	1.04	7	10
25	6	111	160.5	2.8	1.23	0.79	1.19	8	12
25	7	120	160.5	2.8	1.17	0.71	1.06	7	11
25	8	125	160.5	2.8	1.15	0.69	1.04	7	10
26	6	112	160.5	2.7	1.14	0.72	1.09	7	11
26	7	117	160.5	2.8	1.15	0.70	1.05	7	10
26	8	130	160.5	2.8	1.09	0.66	0.99	7	10

Mean Final Hogging  $C_{max} = 15.603(\text{Mean Final } S_{max})/(\text{Effective Panel Width})^2]$

U95%CL Final  $C_{max} = \text{Mean Final } C_{max} + \text{U95\%CL error } (= 0.5 * \text{mean value})$

+ $E_{max}$  = Maximum Tensile Strain = 10  $C_{max}$  (applies to mean and U95%CL values).

**Table 11A (Cont...) - Predicted Maximum Hogging Curvature and Tensile Strains for Multiple Pillar Extraction Panels**

Panel #	XL #	Cover Depth H (m)	Panel Width W (m)	Seam Thickness T (m)	Mean Final Panel $S_{\max}$ (m)	Final Panel Hogging Curvature + $C_{\max}$ (km <sup>-1</sup> )		Final Panel Tensile Strain + $E_{\max}$ (mm/m)	
						Mean	U95 % CL	Mean	U95 % CL
Tailgate, South East Main and East Install Headings									
TG	5A	97	89	2.8	0.80	0.95	1.42	9	14
TG	5B	100	89	2.8	0.78	0.92	1.37	9	14
TG	5C	110	89	2.8	0.69	0.82	1.23	8	12
SEM	5A	105	140	2.8	1.16	0.92	1.39	9	14
SEM	5B	103	140	2.8	1.18	0.94	1.41	9	14
25	5A	110	160.5	2.8	1.21	0.80	1.19	8	12
23	5B	110	160.5	2.8	1.21	0.80	1.19	8	12
EI	5F	100	105	2.7	0.90	1.26	1.89	13	19

Mean Final Hogging  $C_{max} = 15.603(\text{Mean Final } S_{max})/(\text{Effective Panel Width})^2]$

U95%CL Final  $C_{max} = \text{Mean Final } C_{max} + \text{U95\%CL error } (= 0.5 * \text{mean value})$

$+E_{max}$  = Maximum Tensile Strain =  $10 C_{max}$  (applies to mean and U95%CL values).

**Table 11B - Predicted Maximum Sagging Curvature and Compressive Strains for Multiple Pillar Extraction Panels**

Panel #	XL #	Cover Depth H (m)	Panel Width W (m)	Seam Thickness T (m)	Mean Final Panel $S_{\max}$ (m)	Final Panel Sagging Curvature $-C_{\max}$ (km <sup>-1</sup> )	Final Panel Sagging Curvature $-C_{\max}$ (km <sup>-1</sup> )	Final Panel Compressive Strain $-E_{\max}$ (mm/m)	Final Panel Compressive Strain $-E_{\max}$ (mm/m)
						Mean	U95% CL	Mean	U95% CL
Pillar Extraction Panels 14 to 26									
14	9	110	96	2.8	0.76	0.86	1.29	9	13
15	9	110	160.5	2.8	1.23	1.03	1.54	10	15
15	10	120	160.5	2.8	1.17	0.90	1.35	9	13
16	9	105	160.5	2.8	1.26	1.15	1.73	12	17
16	10	115	160.5	2.8	1.21	0.93	1.39	9	14
17	9	107	160.5	2.8	1.25	1.10	1.65	11	17
17	10	120	160.5	2.8	1.18	0.91	1.36	9	14
18	9	110	160.5	2.8	1.23	1.03	1.54	10	15
18	10	120	160.5	2.8	1.17	0.90	1.35	9	14
19	9	110	160.5	2.8	1.21	1.01	1.52	10	15
19	10	120	160.5	2.8	1.13	0.87	1.30	9	13
20	7	137	270.5	2.2	1.21	0.65	0.98	7	10
21	7	137	160.5	2.3	0.95	0.73	1.10	7	11
22	7	133	160.5	2.5	1.02	0.78	1.18	8	12
23	6	112	160.5	2.8	1.22	0.98	1.47	10	15
23	7	127	160.5	2.8	1.14	0.88	1.32	9	13
24	6	112	160.5	2.8	1.22	0.98	1.47	10	15
24	7	124	160.5	2.8	1.15	0.88	1.32	9	13
24	8	130	160.5	2.8	1.14	0.88	1.32	9	13
25	6	111	160.5	2.8	1.23	1.00	1.51	10	15
25	7	120	160.5	2.8	1.17	0.90	1.35	9	14
25	8	125	160.5	2.8	1.15	0.88	1.32	9	13
26	6	112	160.5	2.7	1.14	0.92	1.38	9	14
26	7	117	160.5	2.8	1.15	0.88	1.33	9	13
26	8	130	160.5	2.8	1.09	0.84	1.26	8	13

Mean Final Sagging  $C_{max} = 19.79(\text{Mean Final } S_{max})/(\text{Effective Panel Width})^2]$

U95%CL Final  $C_{max} = \text{Mean Final } C_{max} + \text{U95\%CL error } (= 0.5 * \text{mean value})$

$-E_{max}$  = Maximum Compressive Strain =  $10 C_{max}$  (applies to mean and U95%CL values).



**Table 11B (Cont...) - Predicted Maximum Sagging Curvature and Compressive Strains  
for Multiple Pillar Extraction Panels**

Panel #	XL #	Cover Depth H (m)	Panel Width W (m)	Seam Thickness T (m)	Mean Final Panel $S_{max}$ (m)	Mean Final Panel Sagging Curvature $-C_{max}$ ( $km^{-1}$ )	U95 % CL Final Panel Sagging Curvature $-C_{max}$ ( $km^{-1}$ )	Mean Final Panel Compressive Strain $-E_{max}$ (mm/m)	U95 % CL Final Panel Compressive Strain $-E_{max}$ (mm/m)
<b>Tailgate, South East Main and East Install Headings</b>									
TG	5A	97	89	2.8	0.80	0.91	1.36	9	14
TG	5B	100	89	2.8	0.78	0.88	1.32	9	13
TG	5C	110	89	2.8	0.69	0.79	1.18	8	12
SEM	5A	105	140	2.8	1.16	1.17	1.76	12	18
SEM	5B	103	140	2.8	1.18	1.19	1.78	12	18
25	5A	110	160.5	2.8	1.21	1.01	1.51	10	15
23	5B	110	160.5	2.8	1.21	1.01	1.51	10	15
EI	5F	100	105	2.7	0.90	1.60	2.39	16	24

Mean Final Sagging  $C_{max} = 19.79(\text{Mean Final } S_{max})/(\text{Effective Panel Width})^2]$

U95%CL Final  $C_{max} = \text{Mean Final } C_{max} + \text{U95\%CL error } (= 0.5 * \text{mean value})$

$-E_{max}$  = Maximum Compressive Strain =  $10 C_{max}$  (applies to mean and U95%CL values).

## 6.11 Prediction of Subsidence Impact Parameter Contours

### 6.11.1 Calibration of the SDPS<sup>®</sup> Model

Credible worst-case Subsidence contours for the proposed pillar extraction panels have been generated using SDPS<sup>®</sup> influence function-based subsidence prediction software.

As there is no readily available subsidence data yet available for Abel, the SDPS<sup>®</sup> model was calibrated to the credible worst-case (U95%CL) profiles predicted by the **ACARP, 2003** empirical model.

The outcome of the model calibration exercise is summarised in **Table 12**

**Table 12 - SDPS<sup>®</sup> Model Calibration Summary for the Proposed Pillar Extraction Panels**

Input Parameters from Modified ACARP, 2003	Value
Panel No.s below XL s 5 - 10 shown in <b>Figure 1</b>	P14-P26, TG,SE,EI Mains
Panel Void Widths, W (m)	160.5, 89, 140,105
Cover Depth, H (m)	100 - 150
Maximum Panel Extraction Ratio Assumed, e (%)	95
Actual Mining Height, T (m)	2.2 - 2.8
Effective Mining Height, h (m)	2.09 - 2.66
W/H range	0.9 - 1.97
SRP for Mining Area	Low
Maximum Final Panel Subsidence*, $S_{max}$ (m)	0.76 - 1.45
Effective $S_{max}/T_e$ Range	0.36 - 0.58
Barrier Pillar Width, $w_{cp}$ (m)	16.3 - 23.5
Roadway width (m)	5.5
Pillar Height, h(m)	2.4 - 2.6
Barrier Pillar Subsidence* $S_p$ (m)	0.03 - 0.17
$S_p/h$ Range	0.01 - 0.07
Distance to Influence Inflexion Point from Rib-Side (m) (d/H)	18 - 44 (0.19 - 0.34)
<b>SDPS Calibration Results for 'Best Fit' Solution to the Modified ACARP, 2003 Model Predictions<sup>^</sup></b>	<b>Optimum Values</b>
Influence Angle (Tan(beta))	2.3
Influence Angle (beta)	63.5°
Supercritical Subsidence Factors ( $S_{max}/T$ )	0.36 - 0.58
Distance to Influence Inflexion Point from Rib-Side (m) (d/H)	20 - 36 (0.20 - 0.26)

Notes:

\* - Upper 95% Confidence Limits predicted from modified version of ACARP, 2003

<sup>^</sup> - See SDPS manual extract in Appendix B for explanation of methodology and terms used.

The predicted **ACARP, 2003** and **SDPS<sup>®</sup>** model subsidence impact parameter profiles for Panels 14 - 19 along XL 9 have been compared in **Figures 14a to 14c**. The profiles for Panels 20 - 26 along XL 7 are presented in **Figures 15a to 15c**.

The predicted **SDPS**<sup>®</sup> subsidence and tilt profiles were generally located within +/- 10 to 20% of the predicted modified **ACARP, 2003** models Upper 95% Confidence Limits. This outcome is considered a reasonable fit considering that the **ACARP, 2003** profiles represent measured tilt profiles that are invariably affected by 'skewed' or kinked subsidence profiles.

The results of the analysis indicate that the majority of the predicted convex curvature (and tensile strain) and concave curvature (and compressive strains) predicted by the **SDPS**<sup>®</sup> model would fall within +/- 50% of the modified **ACARP, 2003** model predictions. This result is also considered reasonable in the context that the **ACARP, 2003** model represents measured profile data that includes strain concentration effects such as cracking and shearing. As mentioned earlier, this 'discontinuous' type of overburden behaviour can increase 'smooth' profile strains by 2 to 4 times occasionally.

### **6.11.2 Predicted Subsidence Contours**

Based on the calibrated **SDPS**<sup>®</sup> model, predictions of final worst-case subsidence contours for the pillar extraction panels in Areas 1 and 2 are presented in **Figures 16a** and **16b** (south and north areas).

Associated subsidence impact parameter contours of final Principal tilt, curvature, strain and horizontal displacements have been subsequently derived and are presented in **Figures 17a,b** to **20a,b** respectively. Pre and post mining surface levels are shown in **Figure 21**.

## **7.0 Subsidence Impacts and Management Strategies**

### **7.1 General**

Based on the predicted maximum panel subsidence, tilt and strain values for the total extraction panel layouts, the potential for the following subsidence related impacts and their likely affect on natural and man-made features have been assessed:

- surface cracking;
- height of sub-surface fracturing above the panels (direct and in-direct hydraulic connection zones);
- surface gradient changes;
- ponding;
- general slope stability and erosion;
- valley uplift and closure;
- scarp or surface step development;
- far-field horizontal displacements and strains;

Based on numerous field observations that a range of measured subsidence impact parameter magnitudes can occur at a given location for a given mining geometry and geology etc, it is therefore considered appropriate that a range of prediction values, based on statistics and probability of occurrence, be provided to allow specialist consultants and stakeholders to apply risk management principles in a practical way.

Discussions of likelihood of impact occurrence in the following sections generally refer to the qualitative measures of likelihood described in **Table 13**, and are based on terms used in **AGS, 2007** and **Vick, 2002**.

As explained in **Appendix A**, the terms ‘mean’ and ‘Upper 95% Confidence Limit’ used in these predictions consider that the predicted maximum subsidence effect values may be exceeded by 50% and 5% respectively for the panels mined. Therefore on a small number of occasions, the predicted values and impacts may be exceeded (as has been the case with the panels extracted to date in SMP Area 1). These are generally found to be related to the presence of adverse or anomalous geological or topographical conditions.

The selection of an appropriate ‘credible worst-case’ is normally inferred by the U95%CL value, but the reliability of current survey technology, available mitigation techniques, likely response action times, and the potential for uneconomic or marginal mining layouts should also be considered.

**Table 13 - Qualitative Measures of Likelihood**

<b>Likelihood of Occurrence</b>	<b>Event implication</b>	<b>Indicative relative probability of a single event</b>
Almost Certain	The event is expected to occur.	90-99%
Very Likely	The event is expected to occur, although not completely certain.	75-90%
Likely <sup>+</sup>	The event will probably occur under normal conditions.	50-75%
Possible	The event may occur under normal conditions.	10-50%
Unlikely <sup>*</sup>	The event is conceivable, but only if adverse conditions are present.	5-10%
Very Unlikely	The event probably will not occur, even if adverse conditions are present.	1-5%
Not Credible	The event is inconceivable or practically impossible, regardless of the conditions.	<1%

Notes:

+ - Equivalent to the mean or line-of-best fit regression lines for a given impact parameter presented in **ACARP, 2003**.

\* - Equivalent to the credible worst-case or U95%CL subsidence impact parameter in **ACARP, 2003**.

The predicted impacts and suggested management strategies for the natural and man-made features in the SMP area are presented in the following sections.

## **7.2 Surface Cracking**

### **7.2.1 Predicted Impacts**

The development of surface subsidence above a total pillar extraction panels is caused by the bending of the overburden strata as it sags down into the newly created void in the workings. The sagging strata are supported in turn by the collapsed immediate roof, which then slowly compresses to a maximum subsidence limit.

The predicted panel subsidence magnitudes of 0.75 m to 1.45 m are likely to result in surface cracks developing within the limits of the extracted panels. It is very unlikely that surface cracks will develop above first workings pillars, where subsidence magnitudes of < 20 mm are expected.

Cracks are likely to develop in the tensile strain zones that will typically occur from 18 m to 44 m in from the rib-sides of each total extraction panel. Crack widths of up to 10 mm may start to develop at the surface where tensile strains exceed 1 mm/m over a distance of 10 m. The cracks generally develop where maximum tensile strains occur. The tensile cracks will probably be tapered and extend to depths ranging from 5 to 10 m, and possibly deeper if near surface bedrock exposures are present.

Compressive strains > 2 to 3 mm/m can also cause cracking and upward 'buckling' of near surface rock beds due to low-angle shear failures. The compressive strains generally peak at one or two locations in the middle third area of the panels.

Based on the predicted range of maximum transverse tensile strains (i.e. 5 to 19 mm/m), surface crack widths of between 50 mm and 190 mm (based on the Upper 95% Confidence limit) could occur above Panels 14 to 26 and within the limits of extraction (i.e. goaf) beneath the SMP Area 2. The Upper 95% Confidence Limit used in these predictions considers that these values may be exceeded 5% of the time.

Therefore on a small number of occasions, the predicted crack widths may be exceeded (as has been the case with the panels extracted to date in SMP Area 1). These are generally found to be related to the presence of adverse or anomalous geological or topographical conditions. Strain concentration in near surface rock could also double the above crack widths locally to 100 mm and 380 mm respectively.

The predicted tensile strains above the extracted Tailgate, South East Mains and East Install headings are estimated to range between 9 mm/m and 16 mm/m, indicating crack widths of between 90 mm and 160 mm. Strain concentrations in near surface rock could also double the above crack widths locally to 180 mm and 320 mm respectively.

The predicted range of maximum transverse compressive strains (i.e. 7 to 24 mm/m) may result in shear displacements or 'shoving' of between 70 mm and 210 mm within the central limits of proposed production and extracted main headings panels.

Based on the strain contour figures, the location of the tensile cracking and total shear displacements for the proposed mining layout are shown in **Figure 22a**.

In addition, tensile cracks of similar magnitudes to those mentioned above will probably develop up to 30 m behind the advancing goaf edge of the total pillar extraction panels. The majority of these cracks are transient however, and likely to close in the central areas of the panels where permanent compressive strains develop after mining is completed. The typical crack pattern development behind a retreating pillar extraction face is presented in **Figure 22b**.

The previous Area 1 SMP report indicated that the transient cracks widths would be < final crack widths on average. However, based on the similarity in width observed between the transient and final cracks to-date, and the measured average retreat rates for Panels 1 to 4 of 23 m/week to 37 m/week, it is assessed that the extraction face does not move fast enough for the transient crack width reduction to occur generally. The face retreat rates can also vary significantly from < 10 m/week to 50 m/week, depending on mine roof conditions and operational factors, so it is possible that transient cracking will vary between dynamic and final static magnitudes.

It has therefore been assumed in this study that the transient crack widths will be similar in width to final subsidence crack width predictions above the proposed Area 2 Panels.

### **7.2.2 Impact Management Strategies**

Surface crack repair works may need to be implemented around the affected areas of the site, and in particular, where public roads and ephemeral watercourses are present. Crack repairs may involve ripping, backfilling and top dressing works or the pouring of cement-based grout, crushed rock into the wider, deeper cracks.

In regards to Viney Creek, surface cracking will be limited by the panel geometries and proposed first working buffer zones. It is considered 'very unlikely' that surface cracks will develop along the creek bed, however, if they do occur, the following remediation strategies may be adopted:

- Undertake pre-mining and post-mining inspections along the creek, with the results of these inspections communicated to the respective stakeholders. Should a significant impact be identified during these inspections, an appropriate remediation strategy will be developed.
- Consultation with DECCW has suggested that natural regeneration may be the favoured management strategy in most scenarios, due to the likely level of disturbance caused by other remediation strategies such as back filling with imported materials from haulage trucks.

## **7.3 Sub-Surface Cracking**

### **7.3.1 Sub-Surface Fracturing Zones**

The caving and subsidence development processes above a longwall or pillar extraction panel usually results in sub-surface fracturing and shearing of sedimentary strata in the overburden, see **Figure 23**. The extent of fracturing and shearing is dependent on mining geometry and overburden geology.

International and Australian research on longwall mining interaction with groundwater systems indicates that the overburden may be divided into essentially three or four zones of surface and subsurface fracturing. The zones are generally defined (in descending order) as:

- Surface Zone
- Continuous or Constrained Zone
- Fractured Zone
- Caved Zone

Starting from the seam level, the Caved Zone refers to the immediate mine workings roof above the extracted panel, which has collapsed into the void left after the coal seam has been extracted. The Caved Zone usually extends for 3 to 5 times the mining height above the roof of the mine workings.

The Fractured Zone has been affected by a high degree of bending deformation, resulting in significant fracturing and bedding parting separation and shearing. The Fractured Zone is supported by the collapsed material in The Caved Zone, which usually has a bulked volume equal to 1.2 to 1.5 times its undisturbed volume.

The Continuous or Constrained Zones refer to the section of overburden which has also been deformed by bending action, but to a lesser degree than the Fractured Zone below it.

The Surface Zone includes the tensile and compressive surface cracking caused by mine subsidence and is assumed to extend to depths of 5 to 10 m in the Newcastle Coalfield.

Based on reference to **Whittaker and Reddish, 1990** and **ACARP, 2003**, the impact of mining on the sub-surface aquifers and surface waters, requires an estimate of the 'Continuous' and 'Discontinuous' heights of fracturing or the A and B Zones - shown schematically in **Figure 24**.

*Continuous sub-surface fracturing* (A-Zone) refers to the zone of cracking above a longwall or pillar extraction panel that is likely to result in a direct flow-path or hydraulic connection to the workings, if a sub-surface (or shallow surface) aquifer was intersected.

*Discontinuous sub-surface fracturing* (B-Zone) refers to the zone above the A-Zone where there could be a general increase in horizontal and vertical rock mass permeability, due to bending or curvature deformation of the overburden. This type of fracturing does not usually provide a direct flow path or connection to the mine workings like the A-Zone; however, it is possible that B-Zone fracturing may interact with surface cracks, joints, or faults. This type of fracturing can therefore result in an adjustment to surface and sub-surface flow paths, but may not result in a significant change to the groundwater or surface water resource in the long-term.

In regards to the general zones of fracturing mentioned earlier, the A-Zone may be assumed to include the Caved and Fractured Zones, and the B-Zone will develop in the Constrained Zone. Both A and B-Zones can extend to the Surface Zone and will depend on the mining height, cover depth, geology and panel width.

Two empirically-based models (**Forster, 1995** and **ACARP, 2003**) and have been used in this study to predict the A and B-Zone heights of sub-surface fracturing within the study area.

The **Forster, 1995** model was developed from deep multi-piezometer data from subsided overburden in the Central-Coast area of the Newcastle Coalfield and indirectly defines the A- and B-Zones as a function of the mining height (the model refers to the A and B-Zones as the tops of the Fractured and Confined Zones respectively - see **Figure 24** for the model fracture zone definitions).

The **Forster, 1995** model predicts that the height of the Fractured or A-Zone will generally range between 21 and 33 times the mining height (T). The predicted extent or height of the Confined or B-Zone and its thickness will be dependent on the cover depth and height of A-Zone fracturing. A similar US version of the **Forster, 1995** model indicates that the height of



continuous fracturing could range between 10T and 24T with discontinuous fracturing from 24 T to 60T. A comment is made in a paper by **Mark, 2007**, that the “variation is also probably due to differences in geology and panel geometry”.

The **ACARP, 2003** model was derived from the **Forster, 1995** Model data, and supplemented with drilling fluid loss records from surface to seam drilling logs in subsided, fractured overburden from the NSW Southern Coalfield and Oaky Creek Mine in the Bowen Basin (**Colwell, 1993**).

The **ACARP, 2003** model includes several of the key parameters defined by **Whittaker and Reddish, 1989** and referred to in **Mark, 2007**. The additional parameters include the panel width, cover depth, maximum single panel subsidence and geological conditions (i.e. Subsidence Reduction Potential). The mining height is not applied directly, but indirectly through the subsidence prediction (further model development details may be found in **Appendix A**).

The measured data in **ACARP, 2003** has been plotted as the height of A or B-Zone fracturing /cover depth v.  $S_{\max}/\text{Effective Panel Width}^2$ . A log-normal regression line has subsequently been derived to give predictions of mean and U95%CL values for both fracture zones.

### 7.3.2 Sub-Surface Fracture Height Predictions

The predicted values for the **ACARP, 2003** model’s continuous and discontinuous sub-surface fracturing heights above the proposed pillar extraction panels 14 to 26 are summarised in **Table 14A** and presented in **Figures 25a** and **25b**.

**Table 14A - Summary of Predicted Sub-Surface Fracturing Heights above the Proposed Area2 Pillar Extraction Panels**

Panel No.	Cover Depth, H (m)	Panel Width, W (m)	Effective Mining Height, Te (m)	First Panel S <sub>max</sub> (mean) (m')	Panel S <sub>max</sub> /W <sup>,2</sup> (mean) (mm/m <sup>2</sup> or km <sup>-1</sup> )	Predicted Fracture Heights (m)					
						Continuous Fracture Zone (A Horizon)				Discontinuous Fracture Zone (B Horizon)	
						ACARP, 2003 Model (mean - U95%CL)		Forster, 1995) (21-33Te)		ACARP, 2003 Model (mean - U95%CL)	
Pillar Extraction Panels 14 to 26											
14	110	96	2.66	0.75	0.075	59	89	56	88	104	123
15	110	160.5	2.66	1.19	0.050	49	79	56	88	96	115
15	120	160.5	2.66	1.12	0.044	50	82	56	88	102	123
16	105	160.5	2.66	1.23	0.057	50	78	56	88	94	112
16	115	160.5	2.66	1.16	0.045	48	79	56	88	98	119
17	107	160.5	2.66	1.21	0.054	49	78	56	88	95	114
17	120	160.5	2.66	1.12	0.044	50	82	56	88	102	123
18	110	160.5	2.66	1.19	0.050	49	79	56	88	96	115
18	120	160.5	2.66	1.12	0.044	50	82	56	88	102	123
19	110	160.5	2.66	1.19	0.050	49	79	56	88	96	115
19	120	160.5	2.66	1.12	0.044	50	82	56	88	102	123

**Table 14A (cont...) - Summary of Predicted Sub-Surface Fracturing Heights above the Proposed Area2 Pillar Extraction Panels**

Panel No.	Cover Depth, H (m)	Panel Width, W (m)	Effective Mining Height, Te (m)	First Panel S <sub>max</sub> (mean) (m)	Panel S <sub>max</sub> /W <sup>2</sup> (mean) (mm/m <sup>2</sup> or km <sup>-1</sup> )	Predicted Fracture Heights (m)					
						Continuous Fracture Zone (A Horizon)				Discontinuous Fracture Zone (B Horizon)	
						ACARP, 2003 Model (mean - U95%CL)		Forster, 1995) (21-33Te)		ACARP, 2003 Model (mean - U95%CL)	
Pillar Extraction Panels 14 to 26											
20	137	270.5	2.09	1.16	0.031	46	83	44	69	109	133
21	137	160.5	2.19	0.89	0.035	49	86	46	72	111	135
22	133	160.5	2.38	0.97	0.038	51	86	50	78	110	133
23	112	160.5	2.66	1.18	0.048	49	79	56	88	97	117
23	127	160.5	2.66	1.09	0.042	52	86	56	88	107	130
24	112	160.5	2.66	1.18	0.048	49	79	56	88	97	117
24	124	160.5	2.66	1.10	0.043	51	84	56	88	105	127
24	130	160.5	2.66	1.09	0.042	53	88	56	88	110	133
25	111	160.5	2.66	1.18	0.049	49	79	56	88	97	116
25	120	160.5	2.66	1.12	0.044	50	82	56	88	102	123
25	125	160.5	2.66	1.09	0.042	51	84	56	88	106	127
26	112	160.5	2.57	1.14	0.046	48	78	54	85	96	116
26	117	160.5	2.66	1.14	0.044	49	80	56	88	100	120
26	130	160.5	2.66	1.09	0.042	53	88	56	88	110	133
23	110	160.5	2.66	1.19	0.050	49	79	56	88	96	115
25	110	160.5	2.66	1.19	0.050	49	79	56	88	96	115
Tailgate, South East Main and East Install Headings											
SE	105	140	2.66	1.03	0.066	53	82	56	88	97	115
SE	103	140	2.66	1.04	0.067	53	80	56	88	95	113
TG	97	89	2.66	0.89	0.089	56	82	56	88	94	111
TG	100	89	2.38	0.77	0.077	54	81	50	79	95	112
TG	110	89	2.66	0.77	0.077	60	89	56	88	104	123
EI	100	105	2.57	0.89	0.081	55	82	54	85	95	113

Heights of fracturing based on effective mining heights Te= 0.95T.

Effective Panel Width = lesser of actual width and 1.4H (i.e. the super-critical width).

**Bold** - Mean or U95%CL A-Horizon prediction is within 10 m of the surface.

*Italics* - Mean or U95%CL B-Horizon prediction is within 10 m of surface.

### 7.3.3 Discussion of A-Zone Horizon Model Predictions Above Pillar Extraction Panels

The **ACARP, 2003** model's predictions for the mean A-Zone horizon above the proposed pillar extraction panels (see **Figure 25b**) are likely to be within 10 m of the surface if mining occurred at cover depths of < 50 m, regardless of any adverse conditions (such as a fault) being present.

For panel cover depths of between 50 m and 80 m, the predicted U95%CL A-Zone horizon values are within 10 m of the surface, and it is considered that the potential for connective cracking to within 10 m of the surface is 'possible'.

Connective cracking to the surface is considered 'unlikely' for depths of cover between 80 m and 100 m, as the U95%CL values for A-Zone Horizon are predicted to range between 10 m and 20 m from the surface.

Connective cracking is considered 'very unlikely' for depths of cover > 100 m, as the A-Zone Horizon is predicted to be > 20 m below the surface (range is 19 m to 89 m below the surface for cover depths from 100 m to 140 m).

The **Forster, 1995** model indicates a similar range of connective cracking heights 44 m to 88 m above the workings.

#### **7.3.4 Discussion of B-Zone Horizon Model Predictions Above Pillar Extraction Panels**

The **ACARP, 2003** model predicts that the mean B-Zone Horizon values will occur within 10 m of the surface for cover depths < 100 m above the pillar extraction panels for the given mining geometries (see **Figures 25a** and **25b**). *Discontinuous sub-surface fracturing* for these panels is considered 'likely' to interact with surface cracks.

In areas of shallow or exposed surface rock, creek flows may be re-routed to below-surface pathways and re-surfacing down-stream of the mining extraction limits in these areas.

The predicted U95%CL B-Horizon values are all within 10 m of the surface for cover depths < 140 m. It is therefore assessed that surface water impacts from *Discontinuous sub-surface fracturing* interaction will be 'possible' where cover depths range between 100 m and 140 m.

**Mark, 2007** indicates that the height of *Discontinuous fracturing* could range between 48 m to 168 m above the workings.

#### **7.3.5 Impact on Rock Mass Permeability**

In regards to changes to rock mass permeability, **Forster, 1995** indicates that horizontal permeabilities in the fractured zones above longwall mines (see **Figure 24**) could increase by 2 to 4 orders of magnitude (e.g. pre-mining  $k_h = 10^{-9}$  to  $10^{-10}$  m/s; post-mining  $k_h = 10^{-7}$  to  $10^{-6}$  m/s).

Vertical permeability could not be measured directly from the boreholes but could be inferred by assuming complete pressure loss in the 'A-Zone', where direct hydraulic connection to the workings occurs. Only a slight increase in the 'B-Zone' or indirect / discontinuous fracturing develops (mainly due to increase in storage capacity) from bedding parting separation. It is possible however, that minor vertical flows will occur from B-Zone into the A-Zone (and workings) as well.

Discontinuous fracturing would be expected to increase rock mass storage capacity and horizontal permeability without direct hydraulic connection to the workings. Rock mass permeability is unlikely to increase significantly outside the limits of extraction.

### **7.3.6 Discussion of Prediction Model Uncertainties**

Due to the complexity of the problem, it is difficult to ascertain which of the two Newcastle Coalfield based models is likely to be the most accurate. It has therefore been considered necessary to review the assumptions made in each model.

Both models indicate that the height of continuous fracturing is fairly insensitive to depth of cover (see **Figure 25b**). However, it is apparent that the **Forster, 1995** model predicts a higher A-Zone horizon than the **ACARP, 2003** model and predicts surface connection could occur for cover depths up to 100 m.

The height of fracturing data presented in **Forster, 1995** and **ACARP, 2003** infers that the fracture height is not significantly influenced by the panel width alone (see **Figure 25c**). This seems to contradict arching theory, where the height of the ‘arch’ or fractured zone would be expected to increase as the panel width increases. However, as the effective width of the panel decreases with increasing height above the workings, the spanning capability of the rock ‘beams’ will also increase and effectively limit the height of continuous fracturing to the base of the spanning units.

What is clear from the above exercise is that there is a high degree of uncertainty in predicting the A and B-Zone horizons using any of the available models. The measurement of sub-surface fracturing and their impact on groundwater has therefore been undertaken over the first two panels at the Abel Mine for the purpose of validating the prediction models applied in this study; see **Section 7.3.7**.

### **7.3.7 Measured v. Predicted Heights of Fracturing above Panels 1 and 2**

The measured heights of fracturing zones (A and B Zones) above Panels 1 and 2 were based on deep borehole extensometer anchor displacements, vibrating wire piezometers and shallow slotted standpipe measurements. The locations of the monitoring bores are shown in **Figure 26**.

Pre and post mining piezometric head and extensometer measurements are summarised in **Tables 14B and 14C**. Plots of the data are presented in **Figures 27a to 27f**.

**Table 14B - Summary of Measured Deep and Shallow Piezometric Levels above Panels 1 and 2**

Piezo #	Panel No.	Depth of Cover H (m)	Piezometer Locations (m)		Pre-mining Piezometric Heads (m)		Post-mining Piezometric Heads (m)		Head Drop (m)	Fracture Zone*
			DBG	y	DBG	y	DBG	y		
Bore 1	1	99.3	30	69.3	17.2	82.1	>28.4	<70.9	>11.1	B
Piezo 1			35	64.3	19.6	79.7	34.9	64.4	15.3	B
			55	44.3	22.5	76.8	>50.5	<48.9	>27.9	A
			75	24.3	29.6	69.8	>70.4	<28.9	>40.9	A
Bore 2	2	73.2	30	45.2	16.7	56.5	21.2	54.8	4.5	B
Piezo 2			30	43.2	9.3	63.9	>29.0	<44.3	>19.7	A
			50	23.2	20.9	52.3	>47.6	<25.6	>26.7	A
			70	3.2	34.4	38.8	>59.8	<13.4	>25.4	A

DBG = depth below ground.

y = height above workings.

> or < indicates groundwater depth or level above workings has fallen below piezometer.

\* - see **Section 7.3.1** for definitions.

The deep piezometers (Piezo 1 and 2) in the boreholes to the south of Panel 1 and east of Panel 2 respectively, indicated that there are three distinct semi-confined aquifers of thinly interbedded bedded sandstone/siltstone overburden strata that are separated by claystone/mudstone aquitards. The aquifers are gravity fed by seepages into strata unit sub-crops to the north.

Pre-mining piezometric heads in Piezo 1 were 79.7 m, 76.8 m and 69.8 m above the workings. The shallow piezometer (Bore 1) in next to Panel 1 consists of a 30 m deep PVC standpipe with a 3 m to 6 m slotted screen, gravel packing and a bentonite seal. Groundwater level measurements in Bore 1 indicated an uppermost aquifer level of 82.1 m, which was similar to the piezometric head level indicated by the adjacent deep bore piezometer (Piezo 1).

Piezo 2 to the north east of Piezo 1 indicated that the three aquifers in the overburden had pre-mining piezometric heads above the workings of 63.9 m, 52.3 m and 32.8 m. The shallow standpipe piezometer (Bore 2) indicated a piezometric head above the workings of 56.5 m in the uppermost aquifer; however this was 7.4 m below the deep piezo cell water level reading at the same depth. On closer inspection of the borehole locations in **Figure 26** it would appear that the shallow piezometer is located east of a NW trending fault line and the deep piezometer is located to the west of it. It is considered possible that there is a disconnect between the groundwater levels on either side of the fault.

After extraction of Panel 1, the piezometric heads dropped 15.3 m in the uppermost aquifer and > 27.9 m and > 40.9 m in the lower aquifers (ie. the piezometric levels dropped below the cells at these depths). The deep borehole piezometric heads above Panel 2 dropped >19.74 m in the uppermost aquifer and > 25.6 m and > 13.4 m in the lower aquifers. The response of the groundwater levels in the standpipe piezometer to the east of the fault appears to be slower than the deep borehole piezometer, with a total head loss of only 4.5 m occurring to-date. Again, there appears to be a discrepancy in the groundwater level responses between the two instruments in the upper aquifer adjacent to Panel 2.

In general, the likely causes of the piezometric head drops above both panels is primarily linked to the development of A and B Zone Fracturing above each panel; see **Table 14C**.

**Table 14C - Summary of Measured Deep Borehole Extensometer Anchor Displacements above Panels 1 and 2**

Exto #	Panel No.	Depth of Cover H (m)	Anchor Location DBG (m)	Anchor Location y (m)	Maximum Anchor Displacement (mm)	Fracture Zone*
Exto 1	1	95	10	85	14	B
			20	75	13	B
			30	65	31	B
			40	55	27	B
			<b>50</b>	<b>45</b>	<b>33</b>	<b>B/A</b>
			60	35	1351	A
			70	25	868	A
			80	15	734	A
Exto 2	2	76	10	66	-13	B
			20	56	-19	B
			<b>30</b>	<b>46</b>	<b>-18</b>	<b>B/A</b>
			40	36	n.m.	A
			50	26	298	A
			60	16	78	A
			70	6	264	A

DBG = depth below ground

y = height above workings.

\* - see **Section 7.3.1** for definitions.

The maximum anchor displacements in **Table 14C** are relative displacements and indicate strata dilation or separation of sagging rock beds over extracted areas; see **Figures 27c** and **27f**. The extensometer data clearly defines the boundary between the Continuous or Constrained Zone of elastic bending above the workings, and the Fractured and Caved Zones below it.

The piezometric data generally show (i) complete head drop in the Fractured Zone where continuous fracturing to the workings has developed (ie. the A-Zone), and (ii) partial head loss or lowering of the ground water table in the Constrained Zone, where dilation of strata or bed separations have increased the available storage volumes for groundwater in the affected aquifers (ie. The B-Zone).

It should also be understood however, that some leakage of the upper aquifer in the B Zone may also be occurring into the A Zone, and this may therefore result in complete drainage of the upper aquifer in the short to medium term. The presence and characteristics of geological structure also appears to be affecting the response of the groundwater regime however, with the piezometer west of the NW fault line indicating drainage to the Continuous fracture zone with a slower, perched aquifer type response to the east of the fault.

Comparison between predicted v. measured heights of sub-surface fracturing zones above Panels 1 and 2 in SMP Area 1 have been assessed for model validation purposes.

The predicted values of A and B Zone Horizons are summarised in **Table 14D** and compared to measured values in **Table 4E**. Graphical comparisons are also presented in **Figures 27g** and **27h**.

**Table 14D - Summary of Predicted Sub-Surface Fracturing Heights above the Panels 1 and 2 in Area 1 Pillar Extraction Panels**

Panel No.	Cover Depth H (m)	Panel Width W (m)	Effective Mining Height Te (m)	First Panel S <sub>max</sub> (mean) (m)	Panel S <sub>max</sub> /W <sup>2</sup> (mean) (mm/m <sup>2</sup> or km <sup>-1</sup> )	Predicted Fracture Heights (m)					
						Continuous Fracture Zone (A Horizon)				Discontinuous Fracture Zone (B Horizon)	
						ACARP, 2003 Model (mean - U95%CL)		Forster, 1995 (21-33Te)		ACARP, 2003 Model (mean - U95%CL)	
1	95	120	2.55	1.03	0.071	50	76	54	84	89	105
2	76	150	1.88	1.02	0.045	44	64	39	62	74	87

**Table 14E - Summary of Predicted v Measured Sub-Surface Fracturing Heights above the Panels 1 and 2 in Area 1 Pillar Extraction Panels**

Panel No.	Panel Width W (m)	Cover Depth H (m)	Effective Mining Height Te (m)	First Panel S <sub>max</sub> (m)		Continuous Fracture Zone (A Horizon)		Discontinuous Fracture Zone (B Horizon)	
				P	M	P	M*	P	M
1	120	95	2.55	1.03	0.96	50 - 76	47	89 - 95	85- 95
2	150	76	1.88	1.02	1.02	44 - 64	45	74 - 76	66- 76

P - Predicted; M - Measured.

*italics* - strata dilation of <13 mm indicated at 10 m depth below surface suggests that interaction of B Zone with surface cracks is possible.

\* - Height of continuous fracturing may increase with time due to leakage from B-Zone.

The measurement of the A-Zone horizon above Panels 1 and 2 indicates the height of continuous sub-surface fracturing in the Fractured Zone has extended up to between 45 and 50 m above the 120 m and 150 m wide panels with cover depths of 73 m to 95 m. As mentioned earlier, it is apparent that there is some on-going leakage from the Constrained Zone into the Fractured Zone above Panel 1, which may cause that the effective A-Zone Horizon to increase over time.

The presence of a NW trending fault line east of Panel 2 however, appears to have disconnected the groundwater on either side of it and has lowered the near surface water table by approximately 4.5 m east of the fault and >15.3 m to the west of it. The effective height of Continuous fracturing may also increase with time at this location.

The results of the analysis demonstrates that the measured A and B Zones are located within the **ACARP, 2003** prediction model ranges. The height of continuous fracturing (A Horizon) is located within +/- 3 m of the predicted mean values and the discontinuous fracture zone extends to within 10 m of the surface. It is possible that the measured A Zone may increase over time, but should still be within the U95%CLs presented in **Table 14E**.

Overall, it is considered that the measured and predicted fracture zones are in good agreement for Panels 1 and 2 at this stage and indicates the predicted fracture zones for the Area 2 panels are likely to be within the mean and U95%CLs presented.

### 7.3.8 Impact Management Strategies

It is understood that there are no subsurface aquifers of potential resource significance within the overburden that could be affected by *continuous and/or discontinuous fracturing* above the extracted pillar panels. Subsequent groundwater and surface aquifer impact studies have considered the high level of uncertainty in regards to predicting the height of each zone of sub-surface fracturing.

Based on **Table 14A**, the **ACARP, 2003** model outcomes have been assessed in accordance with the Likelihood of Occurrence that continuous fracturing will intersect with surface cracks that extend to 10 m depth below the surface. The results are summarised in **Table 15** and **Figures 25a** and **25b**.

**Table 15 - Likelihood Assessment for Continuous Fracturing Extending from Mine Workings to Within 10 m of the Surface Above the Proposed Pillar Extraction Panels**

Likelihood of Occurrence*	Mining Height Range	Cover Depth Range (m)	Probability of a Single Hazardous Event
Likely	2.2 - 3.0	< 50	50 - 75%
Possible	2.2 - 3.0	50 - 80	5 - 50%
Unlikely	2.2 - 3.0	80 - 100	5 - 10%
Very Unlikely	2.2 - 3.0	>100	<5%

\* - refer to **Table 10** for definitions of likelihood of occurrence.

Based on discussions with the specialist surface and groundwater consultants for the project, the absence of significant surface alluvium and ephemeral nature of the creeks/gullies is unlikely to result in significant degradation of the creeks or inrush event into the underground workings should connective cracking to the surface occur. It is considered more likely that any redirected surface flows will be manageable underground and cracks able to be repaired at the surface.

It is therefore recommended that underground water make records for each of the extracted panels should be reviewed for the purpose of estimating the likely increases in mine water flow due to fracturing of the overlying aquifers. The presence of geological structure should also be viewed with caution and management strategies prepared to deal with disproportionate water inflows into the workings if aquifers become 'perched' behind adjacent faults.



Undermining faults may also result in higher continuous fracture connectivity and water makes also.

As the height of fracturing measurements are close to the predicted mean values derived from the **ACARP, 2003** model, it is not considered necessary to install too many more borehole extensometers above future panels in Areas 1 and 2. The installation of further deep extensometer and piezometers in other areas of the mine may however provide useful data where further faults exist between the panels (see **Section 8** for further monitoring suggestions).

## **7.4 Ponding**

### **7.4.1 Potential Impacts**

Ponding refers to the potential for closed-form depressions to develop at the surface after mining of total extraction panels beneath gentle slopes and relatively flat terrain. Ponding could affect drainage patterns, flora, fauna and groundwater dependent ecosystems.

The actual ponding depths will depend upon several other factors, such as rain duration, surface cracking and effective percolation and evapo-transpiration rates.

The potential pre and post mining ponding depths and volumes for the proposed mining layout have been estimated from the 1 m post-mining topographic contours shown in **Figure 28a**. The 1 m pre-mining topographic contours are shown in **Figure 28b** for comparison.

The potential worst-case pond depths, affected area and volume along each creek or flat areas above the middle of proposed panels, before and after mining, are summarised in **Table 16**.

Based on the results, it appears that approximately six closed form depressions with volumes ranging from 0.36 ML to 1 ML could develop along the Viney Creek tributaries or gullies above the central areas of Panels 23 to 26. The 'ponds' are estimated to have maximum potential pond depths of 0.8 to 1.0 m.

Two of the pond locations exist above Panels 24 and 25 and are already depressions, with one of the depressions above Panel 24 expected to be decrease (after mining) from 0.77 ML to 0.63 ML.

**Table 16 - Potential Worst-Case Ponding Assessment for the Area 2 Panels**

Location (see Figures 28a and 28b)	Pre-Mining Ponds				Post-Mining Ponds				Ponded Area Increase After Mining <sup>#</sup>
	Max Pond RL	Max. Depth (m)	Size L x B	Area (ha) [Vol] (ML)	Max Pond RL	Max. Depth (m)	Size L x B (m)	Area (ha) [Vol] (ML)	Area (ha) [Vol] (ML)
Panel 23 (south)	-	-	-	-	35.35	0.8	80x40	<b>0.25</b> [1.01]	<b>0.25</b> [1.01]
Panel 23 (north)	-	-	-	-	31.60	0.8	95x23	<b>0.17</b> [0.69]	<b>0.17</b> [0.69]
Panel 24 (north)	35.0	0.9	75x29	<b>0.17</b> [0.77]	34.1	1.0	64x25	<b>0.13</b> [0.63]	<b>-0.04</b> [-0.14]
Panel 25 (north1)	38.1	0.3	50x28	<b>0.11</b> [0.55]	37.50	0.9	84x39	<b>0.26</b> [1.16]	<b>0.15</b> [0.61]
Panel 25 (north2)	-	-	-	-	38.0	1.0	35x26	<b>0.07</b> [0.36]	<b>0.07</b> [0.36]
Panel 26 (north)	-	-	-	-	40.0	1.0	69x26	<b>0.14</b> [0.70]	<b>0.14</b> [0.70]

Pond Area =  $\pi$  x pond width x pond length/4;

Pond Volume = Area x Maximum Pond Depth/2.

# - Net increase = Post-mining pond - pre-mining pond.

## 7.4.2 Impact Management Strategies

An appropriate ponding management strategy may include:

- (i) The development of a suitable monitoring and mitigation response plan, based on consultation with the regulatory government authorities to ensure ponding impacts on existing vegetation do not result in long-term environmental degradation.
- (ii) The review and appraisal of changes to drainage paths and surface vegetation in areas of ponding development (if they occur), after each panel is extracted.

Overall, the impact of the increased ponding along the creek beds is likely to be 'in-channel' and therefore the potential effects on existing flora and fauna is likely to be minimal, however, further assessment on the ponding impacts may be needed by specialist ecological consultants to confirm this assessment. Local experience to-date suggests that if increased in-channel ponding occurs it can either remain as water source or remediated if required,

## **7.5 Flood Levels on Black Hill Land Pty Ltd Land**

### **7.5.1 Potential Impacts**

The pre-mining 1 in 100 Year ARI flood levels for the Black Hill Pty Ltd were provided by the stakeholder (see **Figure 28a**) to assess potential flooding impacts due to the proposed mining layout.

The post-mining 1 in 100 Year ARI flood levels will require a hydrological assessment based on the predicted surface levels prepared in this study. For indicative purposes, the worst-case flood levels have been estimated from the predicted post-mining contours, as shown in **Figure 28b**.

It is estimated that the areal extent of flooding in the subsided reaches of two Viney Creek tributaries above Panels 15, 17 and 18 may increase by up to 5% due to the 1 in 100 year event.

### **7.5.2 Impact Mitigation Strategies**

As mentioned above, a post-mining hydrological assessment of the Black Hill Land Pty Ltd site should be completed by the stakeholder for both the current site and redeveloped site conditions. The assessment should determine if any additional drainage system measures may be required as a result of mine subsidence.

## **7.6 Slope Instability and Erosion**

### **7.6.1 Potential Impacts**

To-date, local longwall mining experiences in undulating terrain with ground slopes up to 25° has not resulted in any large scale, *en-masse* sliding instability due to mine subsidence (or other natural weathering processes etc). In general, it is possible that localised instability could occur where ground slopes are > 15°, if the slopes are also affected by mining-induced cracking and increased erosion rates.

The rate of erosion is expected to increase significantly in areas with exposed dispersive / reactive alluvial or residual soils or tuffaceous claystone and slope gradients are increased by more than 2% (>20 mm/m).

Based on the difference between the post and pre-mining surfaces presented earlier, the predicted increase or decrease in surface slope gradients after mining are presented in **Figure 29**.

The above figures indicate that the maximum gradient changes will be located above Panels 14 to 26 and likely to range between 0.5% and 2.5%. It is assessed that some erosion / sedimentation adjustments may develop at these locations where exposed soils are present.

The predicted changes in surface gradients along Viney Creek are unlikely to exceed 0.5% and therefore unlikely to cause any degradation to the creek directly. Any sediment deposits from actively eroding areas upstream of the Schedule 2 sections of the creek will need to be monitored (and assessed) as mining progresses.

### **7.6.2 Impact Management Strategies**

To minimise the likelihood of slope instability and increased erosion potential due to cracking or changes to drainage patterns after mining, the following management strategies may be implemented:

- (i) Surface slope monitoring (combined with general subsidence monitoring along cross lines and centre lines);
- (ii) Placement of signs along public access ways warning of mine subsidence impacts.
- (iii) Infilling of surface cracking to prevent excessive ingress of run-off into the slopes as soon as practicable and preferably after each adjacent panel is completed.
- (iv) Slopes that are significantly affected by erosion after mining may need to be repaired and protected with mitigation works such as re-grading and re-vegetation of exposed areas, based on consultation with the relevant government agencies.
- (v) On-going review and appraisal of any significant changes to surface slopes such as cracking, increased erosion, seepages and drainage path adjustments observed after each panel is extracted.

## **7.7 Valley Uplift and Closure**

### **7.7.1 Potential Impacts**

Valley uplift and closure movements may occur along the drainage gullies present above the proposed mining area, based on reference to **ACARP, 2002** and Southern Coalfield experience.

High horizontal stresses have been measured and uplift movements of about 230 mm have occurred along the F3 Freeway cuttings in ridges about 10 km to the south-east of the mine, where massive conglomerate strata existed at the surface.

However, due to the suspected (and observed) low horizontal stress regime in the Abel mine workings roof to-date (i.e. the Upper Donaldson Seam at this location is in relatively flat area with shallow cover), it is considered unlikely that similar magnitude movements will occur in the gullies / broad crested valleys above the proposed panels.

The lack of thick, massive beds of conglomerate and sandstone units along the creeks / valleys at the surface will also mean the development of these phenomena are likely to be

limited to < 150 mm. Minor cracking in creek beds may cause some shallow sub-surface re-routing of surface flows due to the valley closure mechanism.

Uplift movements of between 100 mm and 150 mm have occurred in compressive strain zones above Area 1 panels to-date. Uplift movements of between 10 mm and 35 mm have also occurred just outside the limits of mining above the Area 1 panels. These movements are not due to the valley closure mechanism, but related to systematic subsidence development of compressive strains and cantilevering of the bending rock mass.

### **7.7.2 Impact Management Strategy**

The impact of valley uplift closure effects due to mine subsidence may be managed as follows:

- (i) Install and monitor survey lines along representative drainage gullies, where it is considered appropriate, and along gully crests during and after undermining. Combine with visual inspections to locate damage (cracking, uplift).
- (ii) Review predictions of upsidence and valley crest movements after each panel is extracted.
- (iii) Assess whether repairs to cracking, as a result of upsidence or gully slope stabilisation works are required to minimise the likelihood of long-term degradation to the environment or risk to personnel and the general public.

## **7.8 Far-Field Horizontal Displacements and Strains**

### **7.8.1 Background to Prediction Model Development**

Far-field displacements (FFDs) generally only have the potential to damage long, linear features such as pipelines, bridges and dam walls.

Horizontal movements due to longwall mining have been recorded at distances well outside of the angle of draw in the Newcastle, Southern and Western Coalfields (**Reid, 1998, Seedsman and Watson, 2001**). Horizontal movements recorded beyond the angle of draw are referred to as far-field horizontal displacements.

For example, at Cataract Dam in the Southern NSW Coalfield, **Reid, 1998**, reported horizontal movements of up to 25 mm when underground coal mining was about 1.5 km away. Seedsman reported movements in the Newcastle Coalfield of around 20 mm at distances of approximately 220 m, for a cover depth ranging from 70 to 100 m and a panel width of 193 m. However, the results may have been affected by GPS baseline accuracy limitations.

Based on a review of the above information, it is apparent that this phenomenon is dependent on (i) cover depth, (ii) distance from the goaf edges, (iii) maximum subsidence over the extracted area, (iv) topographic relief and (v) horizontal stress field characteristics.

An empirical model for predicting far-field displacement (FFDs) in the Newcastle Coalfield is presented in **Figure 30**. The model indicates that measurable FFD movements (i.e. 20 mm) generally occur in relatively flat terrain for distances up to 3 to 4 times the cover depth.

The direction of the FFD movement is generally towards the extracted area, but can vary due to the degree of regional horizontal stress adjustment around extracted area and the surface topography. The movements also appear to decrease around the corners of longwall panels.

An empirical model for predicting far-field strains (FFSs) in the Newcastle Coalfield is presented in **Figure 31a** and **31b**. The model indicates that measureable (but diminishing) strains can also occur outside the limits of longwall extraction for distances up to one cover depth (based on the Upper 95% Confidence limit curve). It is assessed that strains will be <0.5 mm/m at a distance equal to 0.5 x cover depth.

It should be noted that the model was based on steel tape measurements which did not extend further than a distance equal to the 1.5 times the cover depth from the extraction limits. Any FFE predictions that are >1.5 times the cover depth from the panels in this report are therefore an extrapolation of the regression lines for the database and likely to be conservative.

### 7.8.2 Potential Impacts

The surface features that have been assessed in this study for potential FFD and FFS impacts due to mining of the proposed pillar extraction panels include:

- Transgrid suspension towers 25B and 26B.
- F3 Freeway

As previously discussed, an SCZ setback distance has been applied to the above items that will minimise the potential for significant FFD or FFS impact. The SCZ setbacks are not the same for each feature and have been determined based on conservative tolerance strain limit estimates (shown in brackets below)

The design SCZ setback distances adopted in this study are summarised below in terms of 'angle of draw' from the pillar extraction limits to the surface feature:

**Transgrid Tower No.s 25B and 26B** (tensile strain < 2.5 mm/m) - 0.5 x cover depth (26.5° angle of draw), which gives a minimum set-back distance of 74 m for a cover depth of 147 m at the centre of the tower. The proposed panels P20 - P26 are 117 m and 390 m to the south east of the towers respectively (or 0.79 and 2.29 times the cover depth from the tower centres to give angles of draw of 38° and 66°).

**F3 Freeway** (tensile strain < 0.5 mm/m and lateral curvature radii > 200 km) - 1 x cover depth (45° angle of draw), which gives a minimum set-back distance range of 132 m to 137 m from the freeway. The proposed panels P14 to P19 are approximately 609 m to 1252 m west of the freeway or 4.61 to 9.13 times the cover depth (i.e. 78° to 84° angle of draw).

The suspension towers within the SMP area all have cruciform footings installed and will therefore tolerate significantly higher ground strains (e.g. > 10 mm/m).

Predictions of worst-case FFDs and FFSs are summarised in **Table 17**.

**Table 17 - Summary of Far-Field Displacement and Strain Predictions for the Proposed Pillar Extraction Panels**

Panel #	Feature	z (m)	H (m)	z/H	AoD (°)	Final S <sub>max</sub> (m)	FFD (mm)	FFS (mm/m)	Principal Movement Direction
15	F3 Freeway	609	132	4.61	78	1.45	0	0.0	W
19	F3 Freeway	1252	137	9.14	84	1.45	0	0.0	W
20	B26	110	145	0.76	37	1.2	24	0.6	N-NNW
20	B25	406	170	2.39	67	1.2	3	0.0	N-NNW

z = normal distance to feature from panel centreline.

H = Cover depth at panel end.

AoD = effective angle of draw.

Final S<sub>max</sub> = Final maximum panel subsidence (mean values).

FFD = Predicted far-field displacement (mean value).

FFS = Predicted far-field strain (U99%CL value).

The results of the analysis indicate that the Transgrid suspension towers B25 and B26 may be displaced north to north north west by 3 mm and 24 mm respectively after Panels 20 to 26 are extracted. Tensile ground strains at the towers range from 0.0 to 0.6 mm/m at an AoD of 72° and 37°.

The F3 Freeway is assessed to be well outside the limits of measureable displacement and strain (i.e. +/- 10 mm and +/- 0.3 mm/m) and will not require any further management plans to be implemented for Area 2.

It is considered that the impact of the predicted FFD and FFS values are within the tolerable limits of the features assessed.

### 7.8.3 Impact Management Strategies

The proposed set-back distances of high extraction mining to the sensitive features will reduce the potential for damage occurring to very low likelihoods (ie < 1% probability of occurrence). Monitoring of ground and feature movements as subsidence develops will still be necessary however at the Transgrid tower 26B.

It should also be understood that the predicted displacements and strains are likely to be less than currently available survey accuracy limits and will therefore be practically immeasurable. The monitoring may therefore be limited to visual inspections during mining only.

## **7.9 Transgrid Towers**

### **7.9.1 Predicted Subsidence and Potential Impacts**

Due to the decision of the mine to extract coal from Areas 1 and 2 simultaneously, it has been necessary to re-assess the predicted tower subsidence values presented in **DgS, 2009** for the Area 1 panels. A total of eleven Transgrid towers (26B to 36B) are potentially within the zone of vertical and/or horizontal displacement due to the Area 1 and 2 panels (six towers in Area 1 and five towers in Area 2).

Predictions of worst-case final subsidence, tilt and strain at each of the Transgrid Towers inside Area 2 have been made based on **Figures 16a,b to 20a,b**. Transient or dynamic affects have also been assessed using the measured subsidence development rates for Panels 1 and 2 in Area 1 and the prediction methodology provided in **SDPS, 2007**.

Detailed descriptions and predictions of the worst-case transient and final subsidence related movements at Transgrid Towers (26B to 36B) are provided in a separate report (**DgS, 2010**)

A summary of the subsidence prediction results for each tower (in logistical order of subsidence development) are re-presented in **Tables 18 to 20**.

The location of the towers and graphical representation of the analysis results for each tower are given in the abovementioned report for the predicted subsidence, tilt, strain and horizontal displacement respectively. The results are associated with 'smooth' subsidence profile development and do not include discontinuous strata behaviour effects.



**Table 18 - Transgrid Tower Locations and Mining Geometry**

Tower #	Panel #	Panel Width W (m)	Cover Depth Above Panel Rib H (m)	Average Mining Height (m)	Panel $S_{max}$ (m)	Panel Length L (m)	Inflexion Point Distance from Panel Side d(m)	Tower Distance From Start $y^+$ (m)	Tower Distance from Panel Side $x^*$ (m)
28B	18	160.5	127	2.8	1.36	390	36	11	42
29B	17	160.5	112	2.8	1.43	415	32	281	74
31B	7	160.5	85	2.2	1.31	604	33	552	67
32B	8	160.5	74	2.2	1.25	600	34	346	67
33B	8	160.5	70(54)	2.4	1.34	600	34	70	-165
	9	160.5	70(54)	2.4	1.34	394	26	-102	60
34B	10	160.5	67	2.4	1.34	440	26	31	27
36B	11	160.5	100	1.9	1.04	225	29	63	-149
35B	East Mains	125	91	2.1	1.00	281	33	-5	0
30B	East Mains	125	99	2.5	1.32	1265	33	605	15
27B	20	182	136	2.2	1.21	225	35	49	42
26B	20	182	147	2.2	1.21	225	35	-117	77

+ - positive distance measured from starting end of panel and within panel limits.

\* - positive distance measured from nearest side of panel and within panel limits.

Negative values indicate tower is located outside of panel limits.

(54) - cover depth at Tower 33B

**Table 19 - Transient\* Subsidence Impact Parameter Development at the Transgrid Towers**

Tower #	Final Tower Subsidence $S_{max}$ (m)	Maximum Tilt $T_{max}$ (mm/m)		Maximum Horizontal Displacement $HD_{max}$ (mm)		Initial Tower Movement Direction (grid bearing( $^{\circ}$ ))	Maximum Tensile Strain <sup>^</sup> $+E_{max}$ (mm/m)		Maximum Compressive Strain <sup>^</sup> $-E_{max}$ (mm/m)	
		30 m/wk	<10 m/wk	30 m/wk	<10 m/wk		30 m/wk	<10 m/wk	30 m/wk	<10 m/wk
28B	0.21	16	16	158	158	341	7	7	0	0
29B	1.45	0	1	3	10	144	0	2	0	3
31B	0.88	17	33	170	330	324	5	13	9	12
32B	1.27	21	38	210	380	144	8	15	12	17
33B	0.00	0	0	2	5	144	0	0	0	0
34B	0.58	43	43	430	430	172	6	19	8	16
36B	0.00	0	0	0	0	268	0	0	0	0
35B	0.02	2	2	20	20	185	1	1	0	0
30B	0.31	25	25	250	250	054	10	10	0	0
27B	0.52	19	19	190	190	196	2	2	2	2
26B	0.00	0	0	3	6	324	0.1	0.1	0	0

\* - Refers to subsidence movements directly associated with the retreating extraction face.

<sup>^</sup> - Maximum strains refer to major principal strains. Minor principle strains = 0.25 x major principle strains.

**Table 20 - Final\* Subsidence Impact Parameter Development at the Transgrid Towers**

<b>Tower #</b>	<b>Final Tower Subsidence <math>S_{max}</math> (m)</b>	<b>Tilt <math>T_{max}</math> (mm/m)</b>	<b>Horizontal Displacement <math>HD_{max}</math> (mm)</b>	<b>Final Tower Movement Direction grid bearing (°)</b>	<b>Total Tower Rotation<sup>#</sup> (°)</b>	<b>Major Principle Strain <math>E_{max}</math> (mm/m)</b>	<b>Minor<sup>^</sup> Principle Strain <math>e_{max}</math> (mm/m)</b>
28B	0.21	16	158	341	0	7	2
29B	1.45	1	10	199	55	-2	0
31B	0.88	33	334	327	3	-9	-3
32B	1.27	2	22	099	-45	-2	-1
33B	0.00	0	5	144	0	0.1	0.0
34B	0.58	43	425	144	0	-16/19	-4/5
35B	0.02	2	18	188	0	1.5	0.2
36B	0.00	0	28	268	0	1	0.2
30B	0.31	25	249	324	-90	3.5	1
27B	0.52	19	188	196	0	-2/2	-0.5/0.5
26B	0.00	0	6	324	0	0.1	0.0
25B	0.00	0	1	324	0	0.0	0.0

\* - Refers to subsidence movements after mining of panel has stopped.

# - Clockwise rotation is positive.

^ - minor principle strains = 0.25 x major principle strains; tension is positive.

*Italics* - Far-field displacements and strains are Upper 99%CL values.

## 7.9.2 Towers above the Proposed Pillar Extraction Panels

In summary, nine of eleven towers are within the proposed limits of the pillar extraction panels for Areas 1 (five out of six towers) and Area 2 (four out of five towers) and are likely to be subjected to subsidence ranging from 0.02 m to 1.45 m at the tower centres.

Transient tilts above the pillar extraction panels are estimated to range from 4 to 43 mm/m for the possible range of retreat rates (30 m/week or less). Transient tensile and compressive strains are expected to range from 1mm/m to 19 mm/m, depending on face retreat rates.

Final tower tilts will range between 2 mm/m and 43 mm/m. Horizontal displacements are estimated to range between 20 mm and 430 mm. Four or five of the tower locations are expected to have residual compressive strains ranging from 2 mm/m to 16 mm/m, with the other towers expected to have residual tensile strains ranging from 1 to 19 mm/m.

Surface cracking may increase the estimated 'smooth' profile values by 2 to 4 times occasionally if shallow bedrock exists beneath the towers. Local tilts may exceed the smooth profile tilts by 1.5 times due to secondary surface 'hump' development.

Predicted subsidence impact parameter development profiles for the first two towers likely to be effected by Area 2 Panels 18 and 17 (i.e. Towers 28 and 29) are presented in **Figures 32a-d** and **Figures 33a-d** respectively.

### **7.9.3 Towers outside of the Proposed Mining Limits**

The suspension tower 26B is very unlikely to be directly affected by subsidence or tilt, but may experience far-field horizontal movements, which are unlikely to exceed 24 mm horizontal displacement and 0.6 mm/m tensile strain. Tower 25B is assessed to be located outside the practical limits of measurable displacement and strain.

### **7.9.4 Impact Management Strategies**

Based on the predicted subsidence profiles for the eight transmission towers, it is assessed that cruciform footings or subsidence protection pillars would have been necessary above the proposed mining areas to mitigate subsidence impacts on the towers to tolerable limits.

While the towers already have cruciform footings installed, the design limits for the footings (and towers) to resist the predicted movements are uncertain and should be checked by a structural engineer before mine subsidence occurs. Advice from Transgrid is that their preliminary engineering analysis indicates that the cruciform footings are adequate for the predicted levels of subsidence.

Once the tower footings assessment and any necessary mitigation works have been completed, the following monitoring program may be implemented in accordance with a Transgrid Management Plan that will be prepared in consultation with Transgrid:

- (i) Install a minimum of four stable survey pegs or stations in the ground adjacent to each tower leg and on the structure itself (including Tower 33B).
- (ii) Determine 3-D coordinates (E, N, RL), levels and in-line strains between the pegs (perimeter distances only) with a minimum of two base-line surveys prior to mining. Survey accuracy should be within the limits discussed below.
- (iii) Conduct visual inspections and measurement of subsidence, total horizontal displacements and in-line distances between ground and tower stations during mine subsidence development. Record and photograph details of any changes to the towers and adjacent ground (i.e. cracking).
- (iv) Measure the vertical distance from the ground to the conductor catenaries between each tower before, during and after subsidence development.
- (v) Prepare and distribute results of each survey to relevant stakeholders.
- (vi) Review and implement any Trigger Action Response Plans.

Subsidence should be determined using precise levelling and terrestrial total station traverse techniques to determine 3-D coordinates (see **Section 8** for survey accuracy requirements).

## 7.10 Black Hill Road and Drainage Infrastructure

### 7.10.1 Details and Potential Impacts

Black Hill Road will be undermined by the proposed Area 2 Panels 23 to 26. The road is bitumen sealed, dual carriageway within the Cessnock City Council (CCC) district.

The road is 7 m wide with 1m wide unsealed shoulders. The road formation is generally on-grade with two filled embankments up to 3 m high with culverts placed where the road crosses ephemeral drainage gullies associated with Viney Creek.

A 900 mm diameter reinforced concrete pipe (RCP) culvert and headwalls provide drainage through the fill above the barrier pillar between Panels 25 and 26. The downstream headwall for this culvert (Culvert No. 1) consists of a 1.8 m high by 2.5 m long gabion basket retaining wall. The second culvert (Culvert No. 2) consists of two 1200 mm diameter RCP and headwalls in the fill above Panel 23.

A summary of the predicted subsidence effects acting on the road, fill embankments and culverts due to Panels 23 to 26 are presented in **Table 21**.

**Table 21 - Summary of Worst-Case Subsidence Predictions for Black Hill and Taylors Road due to Panels 23 to 26**

Location	Panels	Cover Depth (m)	Final Maximum Subsidence $S_{max}$ (m)	Final Maximum Tilt $T_{max}$ (mm/m)	Final Maximum Tensile Strain* (mm/m)	Final Maximum Compressive Strain* (mm/m)	Final Horizontal Displacement (mm)
Black Hill Road	23	135	0.60	27	10	5	270
	24	125	0.57	27	10	5	270
	25	120	1.39	30	12	8	300
	26	110	1.34	30	12	10	300
Fill & Culvert 1	25/26	115	0.10	6.5	12	-	65
Fill & Culvert 2	23	135	0.77	23	4	5	230
Taylors Road	26	130	1.34	23	8	8	270

\* - Tensile and compressive strains may increase 2 to 4 times occasionally due to crack development.

Graphical representation of the final subsidence, tilt, curvature, horizontal displacement and strain profiles along Black Hill Road are presented in **Figures 34a to 34e**.

The impacts due to the predicted subsidence effects may include:

- Tensile crack widths of between 40 mm to 120 mm.
- Compressive shearing or shoving between 50 mm to 100 mm

- Loss or increase of super-elevation at bends in the road of +/- 1% to 2.5%.
- Cracking of culverts and fill embankments.
- Erosion and slope instability of fill embankments.

Similar cracking and shearing impacts are also expected along Taylors Road.

### **7.10.2 Impact Management Strategies**

Impact management strategies for the Black Hill and Taylors Road may require the following:

- (i) Pre-mining condition survey of road and drainage infrastructure prior to commencement of second workings.
- (ii) Installation of subsidence monitoring lines along one side of road to review measured impacts and predictions.
- (iii) On-going consultation with Cessnock City Council in regards to preparation of a Public Roads Management Plan for managing mine subsidence impacts within the road corridors.

The stakeholder should be notified of mine subsidence survey results and mining activities in advance of subsidence development adjacent to the mine. The Public Roads Management Plan will also include an emergency response plan to unanticipated mining related impacts.

## **7.11 Energy Australia Power Line Easements**

### **7.11.1 Potential Impacts to 132 kV Line**

There are seven pairs of timber power poles (EA1 to EA7) in Area 1 and seven pole pairs (EA8 to EA14) in the Area 2. The pole pairs are approximately 15 m high and 5 m apart and are connected by a galvanised steel brace between the tops of the poles. The pole pairs are spaced from 161 m to 269 m along the easement, as shown in **Figure 1**.

The conductors are supported by relatively flexible vertical 'stringers' that will be able to tolerate some adjustment due to pole movements.

Worst-case predictions of final subsidence, tilt, strain and final tilt direction at each pole are presented in **Tables 22A** and **22B** for Area 1 and 2 panels respectively. The predictions have been determined from the contour predictions presented in **Figures 16a,b** to **20a,b**. The clearances of the conductors have also been assessed based on the predicted final subsidence profile for the easement (see **Figure 35**) and presented in the tables below.

**Table 22A - Worst Case Final Subsidence Predictions for Energy Australia 132 kV  
Power Poles EA1 to EA7 (Area 1)**

Pole Pair and Pole No.	Panel No.	Final Subs $S_{max}$ (m)	Final Tilt $T_{max}$ (mm/m)	Final Tilt Direction (grid bearing) (o)	Final Ground Strain (mm/m)	Final HD* Base (mm)	Final HD^ Top (mm)	Final Pole Pair Closure (mm)	Conductor Clearance Loss (m)
1.1	8	0.00	0	234	0.1	0	0	0	0.62
1.2	8	0.00	0	234	0.1	0	0		0.62
2.1	8	1.24	-7	56	-13	75	187	53	1.37
2.2	8	1.25	-5	57	-9	54	134		1.38
3.1	7	1.52	-5	57	-10	55	137	34	1.51
3.2	7	1.53	-4	57	-8	41	103		1.51
4.1	6	1.54	0	58	0	0	1	1	1.37
4.2	6	1.54	0	58	0	0	0		1.36
5.1	5	1.30	-4	238	-6	43	108	79	0.78
5.2	5	1.29	-7	237	-9	75	187		0.72
6.1	4	0.36	-31	260	12	307	768	120	0.87
6.2	4	0.27	-26	263	13	259	647		0.82
7.1	EM	1.43	-7	258	-19	72	180	78	0.70
7.2	EM	1.41	-10	306	-19	103	258		0.70

**Table 22B - Worst Case Final Subsidence Predictions for Energy Australia 132 kV  
Power Poles EA8 to EA14 (Area 2)**

Pole Pair and Pole No.	Panel No.	Final Subs $S_{max}$ (m)	Final Tilt $T_{max}$ (mm/m)	Final Tilt Direction (grid bearing) (o)	Final Ground Strain (mm/m)	Final HD* Base (mm)	Final HD^ Top (mm)	Final Pole Pair Closure (mm)	Conductor Clearance Loss (m)
8.1	19/EM	0.04	-5	101	6	53	133	66	0.01
8.2	19/EM	0.06	-8	104	7	80	199		0.03
9.1	TG	0.00	0	171	0	3	7	8	0.04
9.2	TG	0.00	-1	169	1	6	15		0.03
10.1	TG	-0.07	8	346	7	84	211	39	0.03
10.2	TG	-0.05	7	346	6	69	172		0.03
11.1	SCZ	0.00	0	0	0	0	0	0	0.54
11.2	SCZ	0.00	0	0	0	0	0		0.50
12.1	23	-1.08	22	253	-9	224	561	62	0.00
12.2	23	-1.01	25	252	-8	249	623		0.00
13.1	23	-0.23	15	75	10	148	370	69	0.11
13.2	23	-0.27	18	75	9	175	438		0.01
14.1	24	-0.01	1	46	1	9	21	1	0.00
14.2	24	-0.01	1	40	1	9	22		0.00

Pole pair are numbered from west to east (i.e. Pole 1.1 is west of Pole 1.2).

\* - HD Base = Absolute horizontal displacement of pole at ground level.

^ - HD top = Absolute horizontal displacement of pole at conductor level (assumed to be 15 m above the ground)

*Italics* - Far-field displacements and strains.

Each of the power pole pairs will be subject to transient movements towards the retreating pillar extraction face. In Area 1, the poles will generally start moving towards the north and then 'swing' around (up to 90 degrees in bearing) to their final positions after subsidence is fully developed. In Area 2, the poles will move south initially before 'swinging' around to their final positions.

The poles will also be subject to tensile and compressive strains associated with the subsidence 'wave' as it passes underneath the poles. The transient tilts and strains are expected to range from 50% to 100% of the final values, depending on panel geometry and face retreat rates.

During subsidence development the distance between the pole pairs will tend to close by between 0 mm and 120 mm in Area 1 and from 0 mm to 69 mm in Area 2 (see **Tables 22A and 22B**). These movements are primarily due to the differential tilt between the poles that may be exacerbated or reduced by the ground strains.

Conductor clearances are estimated to be decreased by between 0.02 m and 1.17 m along the easement as shown in **Tables 22A and 22B**.

#### **7.11.2 Potential Impacts to 11 kV and 415 V Line**

There are forty-nine timber power poles (1 to 49) in Areas 1 and 2 that will be within or just outside the zone of mine subsidence (twenty six in Area 1 and twenty three in Area 2). The poles are approximately 15 m high and 85 m apart on average (distances vary from 31 m to 132 m) as shown in **Figure 1**.

The conductors are supported by relatively inflexible ceramic insulators that will probably not be able to tolerate the predicted pole movements.

Worst-case predictions of final subsidence, tilt, strain and final tilt direction at each pole are presented in **Table 23**. The predictions have been determined from the contour predictions presented in **Figures 16a,b to 20a,b**. The clearances of the conductors have been assessed from the easement subsidence profiles presented in **Figure 36**.

**Table 23 - Worst-Case Final Subsidence Predictions for Energy Australia 11 kV Power Poles in Areas 1 and 2**

Pole No.	E	N	Maximum Subsidence $S_{\max}$ (m)	Final Tilt <sup>+</sup> $T_{\max}$ (mm/m)	Final Tilt Direction (grid) (o)	Final Ground Strain <sup>&amp;</sup> (mm/m)	Final HD* Base (mm)	HD <sup>^</sup> Top (mm)	Conductor Clearance Loss (m)
1	370798	6368197	0.00	0	0	0	0	0	0.02
2	370820	6368126	0.04	11	151	19	114	284	0.03
3	370777	6368016	0.06	17	236	24	166	416	0.68
4	370753	6367997	1.30	40	235	-34	397	992	1.41
5	370724	6367918	1.52	7	58	-13	67	168	1.36
6	370674	6367809	1.24	43	235	-30	432	1080	1.14
7	370631	6367696	1.03	53	53	-18	526	1315	1.11
8	370584	6367577	1.28	1	250	-2	8	21	1.12
9	370553	6367510	1.10	27	54	-21	268	670	0.63
10	370526	6367446	0.16	23	233	20	228	571	0.68
11	370495	6367377	1.41	2	150	-2	23	58	1.36
12	370479	6367313	1.31	20	54	-18	196	490	0.77
13	370445	6367229	0.57	43	234	9	431	1077	0.43
14	370405	6367131	0.29	31	328	17	305	763	0.13
15	370348	6367019	0.17	21	151	13	207	518	0.15
16	370295	6366898	0.12	15	341	11	149	371	0.50
17	370255	6366800	1.05	31	202	-9	306	764	0.96
18	370217	6366726	0.87	35	344	-2	352	880	0.49
<b>19</b>	<b>370193</b>	<b>6366664</b>	<b>0.62</b>	<b>25</b>	<b>164</b>	<b>-1</b>	<b>250</b>	<b>625</b>	<b>0.24</b>
20	370143	6366685	0.34	19	345	19	189	474	0.00
21	370102	6366700	1.03	35	344	-9	351	877	0.00
22	370083	6366663	0.26	9	306	22	86	214	0.37
<b>23</b>	<b>370057</b>	<b>6366600</b>	<b>1.00</b>	<b>2</b>	<b>287</b>	<b>-17</b>	<b>24</b>	<b>61</b>	<b>0.64</b>
<b>24</b>	<b>370009</b>	<b>6366499</b>	<b>0.47</b>	<b>31</b>	<b>164</b>	<b>7</b>	<b>306</b>	<b>765</b>	<b>0.00</b>
<b>25</b>	<b>369944</b>	<b>6366485</b>	<b>0.40</b>	<b>28</b>	<b>164</b>	<b>9</b>	<b>280</b>	<b>700</b>	<b>0.00</b>
<b>26</b>	<b>369833</b>	<b>6366446</b>	<b>0.63</b>	<b>32</b>	<b>164</b>	<b>1</b>	<b>324</b>	<b>811</b>	<b>0.00</b>
<b>27</b>	<b>369779</b>	<b>6366425</b>	<b>0.79</b>	<b>31</b>	<b>164</b>	<b>-5</b>	<b>315</b>	<b>787</b>	<b>0.00</b>
<b>28</b>	<b>369713</b>	<b>6366398</b>	<b>1.00</b>	<b>26</b>	<b>164</b>	<b>-11</b>	<b>258</b>	<b>646</b>	<b>0.00</b>
<b>29</b>	<b>369650</b>	<b>6366377</b>	<b>1.08</b>	<b>22</b>	<b>165</b>	<b>-12</b>	<b>218</b>	<b>545</b>	<b>1.01</b>
<b>30</b>	<b>369662</b>	<b>6366193</b>	<b>1.14</b>	<b>23</b>	<b>80</b>	<b>-11</b>	<b>232</b>	<b>581</b>	<b>0.52</b>
<b>31</b>	<b>369616</b>	<b>6366134</b>	<b>0.10</b>	<b>6</b>	<b>248</b>	<b>12</b>	<b>61</b>	<b>153</b>	<b>0.00</b>
<b>32</b>	<b>369582</b>	<b>6366080</b>	<b>1.02</b>	<b>21</b>	<b>251</b>	<b>-10</b>	<b>206</b>	<b>516</b>	<b>0.00</b>
<b>33</b>	<b>369460</b>	<b>6365995</b>	<b>0.01</b>	<b>2</b>	<b>78</b>	<b>2</b>	<b>17</b>	<b>42</b>	<b>0.00</b>
<b>34</b>	<b>369332</b>	<b>6365906</b>	<b>0.00</b>	<b>0</b>	<b>0</b>	<b>0</b>	<b>0</b>	<b>0</b>	<b>0.00</b>
<b>35</b>	<b>369965</b>	<b>6366377</b>	<b>0.25</b>	<b>22</b>	<b>345</b>	<b>11</b>	<b>221</b>	<b>553</b>	<b>0.73</b>
<b>36</b>	<b>369913</b>	<b>6366233</b>	<b>1.27</b>	<b>15</b>	<b>255</b>	<b>-10</b>	<b>155</b>	<b>386</b>	<b>0.00</b>
<b>37</b>	<b>369899</b>	<b>6366136</b>	<b>1.38</b>	<b>3</b>	<b>56</b>	<b>-3</b>	<b>28</b>	<b>71</b>	<b>0.00</b>
<b>38</b>	<b>369885</b>	<b>6366040</b>	<b>0.88</b>	<b>28</b>	<b>74</b>	<b>-5</b>	<b>279</b>	<b>698</b>	<b>0.00</b>
<b>39</b>	<b>369872</b>	<b>6365791</b>	<b>0.07</b>	<b>1</b>	<b>260</b>	<b>-1</b>	<b>7</b>	<b>17</b>	<b>0.00</b>
<b>40</b>	<b>369792</b>	<b>6365825</b>	<b>0.00</b>	<b>0</b>	<b>102</b>	<b>0</b>	<b>2</b>	<b>4</b>	<b>0.00</b>
<b>41</b>	<b>369834</b>	<b>6365744</b>	<b>0.02</b>	<b>1</b>	<b>34</b>	<b>0</b>	<b>14</b>	<b>34</b>	<b>0.00</b>
<b>42</b>	<b>369685</b>	<b>6365712</b>	<b>0.52</b>	<b>22</b>	<b>271</b>	<b>1</b>	<b>225</b>	<b>561</b>	<b>0.00</b>
<b>43</b>	<b>369788</b>	<b>6365689</b>	<b>0.00</b>	<b>0</b>	<b>0</b>	<b>0</b>	<b>0</b>	<b>0</b>	<b>0.00</b>



**Table 23 (Cont...) - Worst-Case Final Subsidence Predictions for Energy Australia 11 kV Power Poles in the Areas 1 and 2**

Pole No.	E	N	Maximum Subsidence $S_{max}$ (m)	Final Tilt <sup>+</sup> $T_{max}$ (mm/m)	Final Tilt Direction (grid) (o)	Final Ground Strain <sup>&amp;</sup> (mm/m)	Final HD* Base (mm)	HD <sup>^</sup> Top (mm)	Conductor Clearance Loss (m)
44	369929	6365860	0.00	0	268	0	2	4	0.00
45	370402	6366188	0.39	22	73	6	221	552	0.00
46	370399	6366144	0.15	9	70	8	93	232	0.00
47	370396	6366109	0.10	3	146	8	33	84	0.00
48	370393	6366072	0.08	5	302	4	46	114	0.00
49	370395	6366030	0.02	1	176	1	13	33	0.00

+ - Transient tilts due to travelling subsidence wave may be assumed to equal the final tilt magnitudes at a given location.

Further analysis may be required if marginal conditions indicated.

& - Transient strains may be assumed to range from +/- Final Values.

\* - HD Base = Absolute horizontal displacement of pole at ground level.

^ - HD top = Absolute horizontal displacement of pole at conductor level (assumed to be 15 m above the ground)

**Bold** - Area 2 poles.

The power poles will be subject to transient movements towards the retreating pillar extraction face. The poles will generally start moving towards the north and then 'swing' around (up to 90 degrees in bearing) to their final positions after subsidence is fully developed. The poles will also be subject to tensile and compressive strains associated with the subsidence 'wave' as it passes underneath the poles. The transient tilts and strains are expected to range from 50% to 100% of the final values, and will be dependent on face retreat rates.

Conductor clearances are estimated to be decreased by between 0.00 m and 1.21 m along the easement as shown in **Table 23**.

### 7.11.3 Impact Management Strategies

Appropriate impact management strategies for the Energy Australia power line easements may include:

- (i) Development of a management plan for Area 2 based on consultation with Energy Australia to ensure the predicted subsidence effects on the poles and powerlines do not result in unsafe conditions or loss of serviceability during and after mining.
- (ii) Replacement of any damaged poles and/or mitigation works to conductors as mine subsidence develops.

Suitable responses to predicted subsidence impacts may be to provide flexible/roller-type conductor sheathing on the poles to control the tension during/after mining impacts. It is noted that shortening of several conductors (to reduce catenary sag) and adjustment to sheathing was necessary above Panel 1.

- (iii) Damage from subsidence (i.e. cracking and tilting) can manifest quickly after mining (i.e. within hours). The appropriate management plan will therefore need to consider

the time required to respond to an impact exceedence if it occurs. The erection of temporary fencing in critical areas before subsidence develops may also need to be considered.

The Management Plan may include the following actions:

- (i) Visual inspections of powerlines in actively subsiding areas
- (ii) Measurement of the vertical distance from the ground to the conductor catenaries between each pole pair before, during and after subsidence development.
- (iii) Preparation and distribution of survey results of each survey to relevant stakeholders.
- (iv) Review and implement Trigger Action Responses as necessary.

## 7.12 Optus Fibre Optic Cable

### 7.12.1 Potential Impacts

The Optus Fibre Optic cable is buried within a shallow trench that is located within the Transgrid Powerline easement (see **Figure 1**).

The worst-case final subsidence predictions along the easement after mining are presented in **Table 24**.

**Table 24 - Worst-Case Subsidence Predictions for the Optus Fibre Optic Cable Easement**

Panel	Cover Depth (m)	Mining Height (m)	Final Subsidence $S_{max}$ (m)	Final Tilt $T_{max}$ (mm/m)	Final In-Line Ground Strain* (mm/m)		Final Principle Ground Strain+ (mm/m)	
20	140	2.2	1.09	16	-2	1	-5.5	5
18	125	2.8	1.31	19	-3	4	-9	12.5
17	110	2.8	1.45	21	-3	4	-12	13
16	105	2.8	0.08	2	-1	1	-	3.5
East Mains	95	2.5	1.17	20	-4	3	-14	13.5
7	85	2.2	1.19	22	-7	5	-16.5	20
8	75	2.2	1.29	25	-5	5	-22	21
10	67	2.35	1.13	25	-7	6	-24	26
East Mains	92	2.10	0.01	1	-0.2	0.2	-	3

\* - Predicted in-line strains are based on 'smooth' subsidence profiles and may increase locally by 2 to 4 times occasionally due to surface cracking.

+ - Predicted principle strains are U95%CL values and include an allowance for surface cracking effects.

Graphical representation of the final subsidence, tilt and strain profiles along the Optus FOC easement are presented in **Figures 37a to 37c**.

### **7.12.2 Impact Management Strategies**

Based on discussions with Optus engineers, the following strategies are available to mitigate against cable impacts if horizontal strains exceed 2 mm/m:

- Uncover and relocate the cable prior to mine subsidence impacts
- Reroute and replace the FOC after mine subsidence impact occurs
- Limit subsidence impacts to within tolerable limits (details have been requested and yet to be supplied)

Optus have advised that the predicted subsidence levels exceed the safe characteristics of the fibre optic cable and Optus is of the view that the most appropriate method to manage the possible subsidence impacts is to relocate the cable to a route outside the predicted subsidence area. Following further consultation, Optus and Donaldson Coal have written to the Mine Subsidence Board, outlining the proposed relocation of the fibre optic cable and requesting acceptance and approval of the works.

## **7.13 Hunter Water Pipeline**

### **7.13.1 Potential Impacts**

The Hunter Water pipeline is buried within a trench that traverses the site above the proposed East Mains and Panel 2 pillar extraction panels in Area 1 and the Tailgate headings, Panel 20 and 21 in Area 2 (see **Figure 1**).

The worst-case subsidence predictions along the pipeline easement after mining is complete are presented in **Table 25**.

**Table 25 - Worst-Case Subsidence Predictions for the Hunter Water Pipeline Easement**

Panel	Cover Depth (m)	Mining Height (m)	Final Subsidence $S_{max}$ (m)	Final Tilt $T_{max}$ (mm/m)	Final Curvature $C_{max}$ (km <sup>-1</sup> )		Final Horiz. Displacement (mm)		Final Ground Strain* (mm/m)	
					In-line	Lateral	In-Line	Lateral	In-Line	Lateral
2	70	2.5	0.58	14	-0.8 to 0.6	-0.35 to 0.5	136	370	-8 to 6	-3.5 to 5
East Mains	90	2.8	1.19	29	-0.9 to 1.0	-0.1 to 0.2	290	73	-9 to 10	-1 to 2
1	105	2.8	1.27	28	-1.0 to 1.3	-0.3 to 0.2	280	49	-10 to 13	-3 to 2
TG Mains	105	2.8	0.96	21	-1.2 to 0.6	-0.1 to 0.1	210	205	-12 to 6	-1 to 1
21	135	2.8	0.20	4	-0.2 to 0.1	-0.1 to 0.15	40	157	-2 to 1	-1 to 1.5
20	140	2.2	0.25	4	-0.2 to 0.1	-0.1 to 0.05	40	153	-2 to 1	-1 to 0.5

\* - tensile strain is positive.

Graphical representation of the final subsidence, tilt, curvature, horizontal displacement and strain profiles along the Hunter Water pipeline easement are presented in **Figures 38a to 38e**.

Based on reference to **Ho and Dominish, 2004**, the impact of the predicted subsidence movements will be dependent on the tolerable limits of the UPVC pipeline walls and rubberised ring joints to the induced bi-lateral curvatures and tensile/compressive strains acting along the pipeline. Both parameters are likely to increase or decrease the normal and shear stresses in the pipeline wall.

The generation of stress in the pipeline walls due to curvature in both the vertical and horizontal planes will be function of the pipe wall thickness, pipe diameter and Young's Modulus of the pipe material and internal operating pressures.

The transfer of strain (and stress) into the pipe wall will also be dependent on the depth of backfill over the pipe and the coefficient of friction between the trench backfill and the pipe wall.

The deformed shape of the pipeline after mining should therefore be assessed by Hunter Water Engineers in order to determine whether mitigation works will be required during subsidence development.

### **7.13.2 Impact Management Strategies**

The proposed management strategies required to minimise impact on the pipeline due to subsidence are:

- Develop a Hunter Water Pipeline Management Plan for Area 2.
- Confirm tolerable in-line and lateral pipeline deformation limits to be used for trigger action responses, based on consultation with Hunter Water engineers.
- Install survey pegs and monitor the deformation of the ground surface along and across representative sections of the pipeline.
- Uncover the pipeline sections where deformations and strains have exceeded the tolerable or agreed trigger action response limits.
- Re-align the pipeline, replace damaged sections and backfill prior to re-commissioning.

## **7.14 Telstra Copper Cables**

### **7.14.1 Potential Impacts**

The Telstra copper cables are buried within shallow trenches located throughout the SMP Area (see **SMP Plan 2**).

These cables will be subject to various levels of subsidence effect.

### **7.14.2 Impact Management Strategies**

A Management plan will be developed in consultation with Telstra to maintain the serviceability of the currently in service cables. Consultation with Telstra as to the design tolerances, location and Management Plan has already commenced.

## **7.15 Farm Dams**

### **7.15.1 Potential Impacts**

Non-engineered farm dams and water storages will be susceptible to surface cracking and tilting (i.e. storage level changes) due to mine subsidence. The tolerable tilt and strain values for the dams would depend upon the materials used, construction techniques, foundation type and likely repair costs to re-establish the dam's function and pre-mining storage capacity.

The predicted worst-case subsidence deformations (subsidence, tilt and horizontal strain) at the known dam sites in Area 2 are presented in **Table 26** and based on **Figures 16a to 19a**.

**Table 26 - Summary of Worst-Case Subsidence Predictions for Existing Farm Dams**

Location	Panels	Cover Depth (m)	Final Maximum Subsidence $S_{max}$ (m)	Final Maximum Tilt $T_{max}$ (mm/m)	Final Maximum Tensile Strain* (mm/m)	Final Maximum Compressive Strain* (mm/m)
Catholic Diocese	23	115	0.4 - 1.2	10 - 30	7	2
House 2 Lot	25	122	0.4	21	5	5
House 3 Lot	26	131	0.8	22	10	10

\* - Tensile and compressive strains may increase 2 to 4 times occasionally due to crack development.

The expected phases of tensile and compressive strain development may result in breaching of the dam walls or water losses through the floor of the dam storage area. Loss or increase of storage areas may also occur due to the predicted tilting. Damage to fences around the dams may also occur and require repairing.

It should be noted that dams similar to those in SMP Area 2 have been subsided by underground coal mines elsewhere in NSW and any damage has been effectively managed. The dams were reinstated in a timely manner and an alternative supply of water was provided by the mine during the interim period.

### 7.15.2 Impact Management Strategies

In accordance with the Project Approval and Statement of Commitments a Dam Monitoring and Management Strategy (DMMS) will be formulated for each dam prior to any mining occurring which will impact on the dams. The DMMS will provide for:

- (i) The individual inspection of each dam by a qualified engineer for:
  - current water storage level;
  - current water quality (EC and pH);
  - wall orientation relative to the potential cracking;
  - wall size (length, width and thickness);
  - construction method and soil / fill materials;
  - wall status (presence of rilling / piping / erosion / vegetation cover);
  - potential for safety risk to people or animals;
  - downstream receptors, such as minor or major streams, roads, tracks or other farm infrastructure; and
  - potential outwash effects.
- (ii) Photographs of each dam will be taken prior to and after undermining, when the majority of predicted subsidence has occurred.

- (iii) Dam water levels, pH and EC will be monitored prior to and after undermining to assess the baseline and post mining dam water level and water quality in order to determine whether rehabilitation is required.
- (iv) In the event that subsidence / crack development monitoring indicates a significant potential for dam wall failure, dam water will be managed in one of the following manners:
  - pumped to an adjacent dam to lower the water level to a manageable height that reduces the risk of dam wall failure,
  - discharged to a lower dam via existing channels if the water cannot be transferred, or not transferred if the dam water level is sufficiently low to pose a minor risk.
  - An alternate water supply will be provided to the dam owner until the dam can be reinstated.
- (v) In the event of subsidence damage to any dams the Company shall remediate the damage and reinstate the dam in conjunction with the Mine Subsidence Board.

## 7.16 Stock Watering System on the Catholic Diocese Land

### 7.16.1 Potential Impacts

The cattle grazing on the Catholic Diocese land are watered by a series of buried pipelines which supply several watering troughs.

There are four 75 mm diameter PVC pipelines (Lines 1 to 4) that provide stock water to 8 troughs around the Catholic Diocese Land, see **Figure 1**. Two of the lines (Lines 3 and 4) provide water to two non-principal residences in the south of the Area 2.

The pipelines are connected to the 200 mm diameter Hunter Water pipeline at different locations above the East Mains Panels and Panel 1. It will be necessary to ensure that the water supply will not be disrupted by mine subsidence effects.

The worst-case subsidence parameter predictions along the pipeline easements and Hunter Water mains connections after mining is complete are presented in **Table 27** and have been derived from the subsidence contours in **Figure 16a**.

Graphical representation of the final subsidence, tilt, and strain profiles along the three stock watering lines are presented in **Figures 39a to 39c** (Line 1), **Figures 40a to 40c** (Line 2), **Figures 41a to 41c** (Line 3) and **Figures 42a to 42c** (Line 4).

Based on reference to the comments on the Hunter Water pipeline in **Section 7.13.1**, it is estimated that the smaller diameter pipeline in shallower trenches will have higher tolerable ground movement impact limits than the Hunter Water Pipeline. However, it is assessed that damage to joints/couplings along the pipelines and at connections between troughs and the mains should be anticipated during mining.

**Table 27 - Worst-Case Subsidence Predictions for the Stock Watering System on the Catholic Diocese Land**

Line	Panel	Location	Final Subsidence $S_{max}$ (m)	Final Tilt $T_{max}$ (mm/m)	Final Ground Strain $E_{max}$ (mm/m)	Final Curvature $C_{max}$ ( $km^{-1}$ )	Final Horiz. Displacement (mm)
1	<b>TG</b>	<b>HW</b>	<b>0.95</b>	<b>0.9</b>	<b>-0.01</b>	<b>-0.001</b>	<b>9</b>
	EM	-	-	-	-	-	-
	4	T1.3	0.29	23	2.2	0.22	230
	5	T1.2	1.32	0	-1.0	-0.10	0
	7	T1.1	0.01	3	5.5	0.55	30
2	EM	T2.3	0.014	0	0	0.0	0
	2	HW	0.22	0	0	0.0	0
	2	kink	0.02	2	2.6	0.26	20
	2/3	T2.2	0.0	18	5.8	0.58	180
	2/3	T2.1	0.0	3	2.6	0.26	30
3	1	HW	1.19	2	-3.5	-0.35	20
	<b>TG</b>	<b>T3.1</b>	<b>0.93</b>	<b>7</b>	<b>-7.6</b>	<b>-0.76</b>	<b>70</b>
	<b>SE</b>	<b>Junction</b>	<b>0.41</b>	<b>16</b>	<b>2.3</b>	<b>0.23</b>	<b>160</b>
	<b>23</b>	-	-	-	-	-	-
	<b>24</b>	<b>NPR</b>	<b>1.31</b>	<b>3</b>	<b>-0.1</b>	<b>-0.01</b>	<b>30</b>
4	<b>SE</b>	<b>Junction</b>	<b>0.46</b>	<b>2</b>	<b>-0.2</b>	<b>-0.02</b>	<b>20</b>
	<b>SE</b>	<b>T4.1</b>	<b>0.45</b>	<b>-1</b>	<b>0.1</b>	<b>0.01</b>	<b>10</b>
	<b>26</b>	<b>NPR</b>	<b>0.84</b>	<b>17</b>	<b>-3.1</b>	<b>-0.31</b>	<b>170</b>

Notes:

EM = East Mains.

HW = Hunter water pipeline.

T1.3 = Trough #3 on Line # 1.

Kink = High angle change in pipeline direction.

NPR = Non-principal residence

**Bold** - Area 2 Panels

### 7.16.2 Impact Management Strategies

The proposed management strategies may be required to minimise impact on the stock watering system due to subsidence are:

- Review the existing Draft Property Subsidence Management Plan for the Catholic Diocese Land and assess the daily water supply requirements for the stock and non-principal residences and range of impact management options.
- Determine whether it is possible to isolate sections of line that may be actively subsided in the future through existing valves or installation of additional ones.
- Install flexible couplings at the troughs, Hunter Water mains and residences prior to subsidence development.
- Consider either duplication of the line to allow a temporary by-pass system to operate during mining or isolate and repair damage to the line at short notice.



As noted in the Statement of Commitments, in the event of interruptions to water supplies due to subsidence impacts on farm dams, water tank pipelines, water mains and irrigation systems within the application area, the Company commits to providing water supplies of equivalent quality and quantity to locations convenient to those affected until such time that the affected farm dams, water tanks, pipelines, water mains and irrigation systems are restored.

## **7.17 Principal Residences**

### **7.17.1 Details and Potential Impacts**

The four Principal residences and other ancillaries/outbuildings within Area 2 include the following:

#### House No. 1 above Panel 25

- single storey masonry veneer house with strip/pad footings (main residence)
- four 4.5m diameter above ground water tanks
- septic tank and on-site effluent disposal field
- weather board clad cottage on raft slab with two PVC water tanks and outhouse
- corrugated iron clad shed
- earth dam 4-5 m high with existing piping failures (due to dispersive clay soils)
- slab on ground driveway
- timber post and wire boundary fences
- gently undulating terrain with 4°-5° ground slopes near the house, and increasing to between 5°-10° towards the north west of the property
- the property has been cleared of trees and partly used for grazing livestock
- Unsealed gravel access road to Black Hill Road

#### House No. 2 above Panel 24

- single storey, 'Forever board' clad house with pad footings (main residence)
- 5m diameter above ground concrete water tank
- septic tank and on-site effluent disposal field
- corrugated iron clad shed on slab footings
- gravel driveway
- vegetable garden with rockwork walls
- yard fencing and concrete pathways
- timber post and wire boundary fences
- gently undulating terrain with 3°-5° ground slopes near the house
- unsealed gravel access road to Black Hill Road

#### House No. 3 outside limits of Panel 25 and 26

- single storey, weatherboard clad house on pad/strip footings (main residence)
- 4.5m diameter above ground water tank

- hardi-plank garage with slab footings
- septic tank and drainage field
- corrugated iron clad shed on slab
- small bird aviary (metal frame on concrete slab)
- vegetable garden (under construction)
- a large fig tree approximately 10 m west of the house
- gently undulating terrain with 3°-5° ground slopes near the house
- unsealed gravel access road to Black Hill Road
- 3m high earth embankment dams for watering livestock (cattle). The dam was full and in good condition

House No 4 - Catholic Diocese site of proposed high school and outside limits of Panel 22

- single storey, timber framed, weatherboard clad house on pad/strip footings with adjoining garage
- mains water supply
- septic tank and drainage field
- yard fencing
- unsealed gravel access driveway to Black Hill Road

Additional buildings within the proposed high school site

- small single storey, full-Masonry Office Building on raft slab (currently used as an office/amenities facility by the Catholic Diocese)
- large single storey shed on raft slab (currently used as a storage facility by Catholic Diocese)

Residence outside limits of Area 2 and east of Panel 20

- double storey timber clad building on deep stump footings
- above ground 4.5 mm diameter water tank
- steel framed and sheet metal clad garage, machinery shed and horse stables on concrete slab footings
- in-ground concrete swimming pool with 'stencilcrete' paving (uncracked) and timber framed outdoor shelter
- 'Biocycle' tank and onsite effluent disposal area
- small chicken pen
- two 'tanked' dams to 3 m depth and 10 m diameter in dispersive clay soils
- one earth embankment dam 3m deep by 5 m diameter with 1 m high dam wall (a small piping failure with minor seepage was noted). *Note: The dam is above Panel 20*
- timber post and wire boundary fences (north-western boundary fence posts severely termite damaged) with a galvanised iron gate at the northern end of the property
- gently undulating terrain with 3°-5° ground slopes near the house and increasing to 10° to 15° along Viney Creek
- unsealed gravel access driveway to Black Hill Road

- two reinforced concrete pipe culverts (300 mm diameter) and headwalls in fill across Viney Creek. The culvert was in a generally poor condition with some open cracks and piping failures.
- sandstone and siltstone bedrock exposures were observed in the northwest of the property.
- the property has been partially cleared and has several uncleared eucalypt forest areas.
- very dense stands of melaleucas (paper bark trees) were observed amongst the native eucalypts along the edges of the Transgrid 330 kV powerline corridor.

*Note: The above property is located within Area 2, however the Principal Residence and ancillary structures/features are located outside the limits of the application area. A description of the properties assets has been provided for completeness. It is assessed that some of the property fences and a small stock watering dam however will be affected by mine subsidence due to Panel 20.*

The internal condition of the Principal Residences is generally good with only some minor hairline cracking in internal plasterboard walls and ceiling cornices (considered to be caused moderately reactive clay movements during seasonal soil moisture content changes).

No geotechnical site classifications in accordance with **AS2870, 1996** of the clay soils have been completed at the properties. Observation of piping failures in several earth dams on the properties indicates the clay soils are highly dispersive and susceptible to erosion and moisture reactivity.

As described in **Sections 3.2** and **5.3** it is intended to leave sufficient first workings only barriers below and around the Principal residences only to minimise the potential for subsidence impact. Based on reference to **Table 3** and the conditions at each house site above the Area 2 panels, it is recommended that a minimum set-back distance to second workings limits be set at 26.5° angle of draw (i.e. 0.5 times the cover depth) from the corners of each Principal Residence.

The predicted subsidence effect contours around the Principal Residences are presented in **Figures 43a** to **43e**. The contours indicate that the maximum subsidence at the Principal Residences within the SCZ is likely to be < 20 mm, with tilts < 2 mm/m, curvature < 0.1 km<sup>-1</sup>, and tensile strains < 2 mm/m.

The above Subsidence Control Zones will also limit impacts to the existing water tanks and on-site effluent disposal areas adjacent to the Principal Residences, with subsidence also likely to be < 20 mm after completion of the panels. To-date the angle of draw to 20 mm subsidence contour has ranged between 1° and 23° around Panels 1 to 4.

Some of the property fences, dams and access road from Black Hill Road that are outside the SCZs may be moderately impacted by mine subsidence. Management of impact to these features will be included in the appropriate property management plan.

### **7.17.2 Impact Management Strategies**

As previously discussed, all residences and associated machinery sheds, in-ground tanks and pipes within the SMP Area will be protected from significant damage by the SCZs. The maximum subsidence is estimated to be < 20mm for minimum set back distances of 26.5 degrees for the proposed SCZ beneath the Principal Residences. Any damage to Principal residences should not be greater than Category 0 to 2 Damage Classification categories (i.e. "Negligible" to "Slight" in accordance with **AS2870, 1996**).

The proposed management strategies required to minimise impact to the Principal Residences due to subsidence are:

- Installation of monitoring pins or pegs around each structure and conduct base line subsidence, peg location and strain measurements prior to undermining.
- In addition to the pre-mining inspections of the properties by representatives of Abel Mine, an inspection of the above properties to be made by the MSB before and after second workings in the vicinity of the site are undertaken.
- Structure surveys and visual inspections should be completed not before one month after second workings of a panel has been completed.
- Any minor repair works to internal/externals cracking or re-levelling of Principal and non-Principal structures should be implemented as soon as mining related movements have ceased.
- If impacts to Principal Residences exceed a Category 2 damage classification in accordance with AS2870, 1996 or "Moderate" damage, then it will necessary to review the SCZ set back distance in regards to applying them to other Principal Residences.

## **7.18 Non-Principal Residences (All Other Surface Structures)**

### **7.18.1 Details and Potential Impacts**

The two non- principal residences (Houses No. 5 and 6) and ancillaries/outbuildings within Area 2 include the following features:

#### House No. 5 (Panel 24):

- single storey, 'Forever board' clad house with pad footings
- mains water supply
- septic tank and on-site effluent disposal field
- corrugated iron clad shed on slab footings
- timber post and wire boundary fences
- gently undulating terrain with 3°-5° ground slopes near the house

- unsealed gravel access driveway to Black Hill Road

#### House No. 6 (Panel 26):

- single storey, masonry house with slab footings.
- mains water supply.
- septic tank and on-site effluent disposal field.
- double storey timber framed and weatherboard clad storage building on slab footings.
- timber post and wire boundary fences.
- gently undulating terrain with 5°-8° ground slopes near the house.
- unsealed gravel access driveway to Black Hill Road
- single storey, full-masonry office building (No.1) on raft slab (currently used as a storage facility by Catholic Diocese) with no power connection.
- single storey, external timber framed, corrugated iron clad building (No. 2) with internal masonry walls on slab footings (currently used as a storage facility by Catholic Diocese), with no power connection. This structure is located above Panel 25.

The subsidence effects estimated for the above structures are based on **Figures 36a to 36e** and summarised in **Table 28**.

**Table 28 - Worst-Case Final Subsidence Effect Predictions for the Non-Principal Residences and Structures on the Catholic Diocese Land**

Panel	Location	Subsidence $S_{\max}$ (m)	Tilt $T_{\max}$ (mm/m)	Ground Strain* $E_{\max}$ (mm/m)	Curvature $C_{\max}$ ( $\text{km}^{-1}$ )	Horiz. Displacement (mm)
24	Residence No. 5	1.12 - 1.30	6 - 19	-8 to 4	-0.5 to 0.8	60 - 190
	Garage	1.17 - 1.28	9 - 17	-9 to 5	-0.7 to -0.9	90 - 170
25	Storage Building No. 2	0.55 - 1.08	26 - 33	-10 to 5	-1.0 to 0.50	260 - 330
26	Residence No. 6	0.23 - 0.73	21 - 30	-10 to 5	-1.0 to 0.5	210 - 300
	Garage/ Storage Building	0.60 - 1.00	18 - 29	-10 to 5	-1.0 to 0.5	60 - 190
	Storage Building No. 1	0.43 - 0.95	25 - 31	-9 to 7	-0.9 to 0.7	250 - 310
Tailgate Headings	Storage building on Central Road	0.46 - 0.81	17 - 26	-15 to 3	-1.5 to 0.3	170 - 260
South East Mains	Building Farm 15	0.07 - 0.27	9 - 23	8 to 11	0.8 to 1.1	90 - 230

\* - Predictions include transient strains.

Based on the predicted subsidence effects, the existing non-principal residences and buildings on Catholic Diocese Land may be subject to subsidence ranging from 0.07 m to 1.3 m, tilting from 6 to 33 mm/m, sagging and hogging curvatures of 1.5 and 1.1 km<sup>-1</sup>, horizontal compressive/tensile strains of 15 and 11 mm/m and horizontal displacements from 60 mm to 330 mm.

It is assessed that the buildings will sustain 'moderate' to 'severe' damage (or Category 3 to 4 damage as defined in **AS2870, 1996**) by the associated tilts, strains and curvatures.

### **7.18.2 Impact Management Strategies**

Appropriate management strategies for the existing non-principal residences that may be impacted by mine subsidence should include and address the following issues in consultation between the stakeholders and the MSB and in accordance with the Subsidence Specific Commitments by the Company Section E (from the Abel Project Approval).

- A plan of management shall be prepared and implemented for the mitigation and remediation of any damage in conjunction with the Mine Subsidence Board to include:
- A pre and post mining condition survey and/or inspection of all structures within the mining lease should be made by the MSB.
- Determine when mining impacts will occur to the buildings and vacate premises prior to any impact. Install temporary fencing to prevent site personal or general public access to any potentially unstable structures.
- A monitoring plan for the property during and post mining and safety/hazard management plan.
- The timing of disconnection of power and water supply etc if required.
- An inspection of mine subsidence damaged properties should be made by registered building inspectors and any repair / mitigation / remediation works to be undertaken will be related to the extent of damage experienced (see Schedule 1 of Project Approval).

Mine subsidence is expected to develop soon after the face retreats beneath a property and would be expected to continue until the face is 1 to 2 times the cover depth past the property (see **Section 8** for more details). Subsidence movements would also be expected to 'start again' soon after the passing of subsequent panels, albeit at decreasing rates and magnitudes. It is considered likely that subsidence movements will affect undermined properties for periods of at least 6 to 8 weeks after each panel is extracted.

## **7.19 Property Fences and Livestock Grazing on Catholic Diocese Land**

### **7.19.1 Potential Impacts**

The impact of 1.0 m to 1.45 m of subsidence on the grazing of livestock and fencing could include the disruption of the buried water supply pipelines (see **Section 7.15**), the development of surface cracks and erosion, breakage of wire fencing strands and the possible failure of strainer posts.

Failure of fencing could allow livestock to get out of paddocks within the Catholic Land, but not from the site itself. Ponding may affect grazing or pasture areas temporarily until remediation works are completed.

It is noted that several fence posts have termite damage and therefore less resistant to mine subsidence effects.

### **7.19.2 Impact Management Strategies**

The above impacts may be managed with the rapid repair of surface cracking, damaged water supply pipes and fences. Relocation of livestock before mining impacts occur may also be undertaken in anticipation of fence failure or loss of water supply. The current Draft Property Subsidence Management Plan (PSMP) will be reviewed in consultation with the landowner to address these potential issues.

## **7.20 Disused Buildings on Catholic Diocese Land**

### **7.20.1 Potential Impacts**

The previous land user buildings on the Catholic Diocese Land are either in various stages of disrepair or have been demolished.

Mine subsidence is likely to impact existing disused residences and structures above the proposed pillar extraction panels significantly (based on damage criteria presented in **AS2870, 1996**).

### **7.20.2 Impact Management Strategies**

An “in principle” agreement has been reached relating to the demolition of four of these structures.

Quotations have been received for demolition and these are currently being assessed by an appropriately qualified and agreed consultant.

## **7.21 Proposed Re-Development of Black Hill Land Pty Ltd Land**

### **7.21.1 Predicted Impacts**

It is understood that there is to be no residual subsidence risk remaining beneath the site after mining has ceased.

The impacts to the Black Hill Land Pty Ltd land after the mining of pillar extraction panels 14 to 18 may include the following:

- Maximum surface subsidence ranging from 0.75 m to 1.45 m.
- Surface cracking from 50 mm to 190 mm wide.
- Negligible surface ponding.
- Changes to surface gradients of +/- 3.5% above pillar extraction panels.

Approximately 90% to 95% of mine subsidence development will occur within 4 to 6 weeks after undermining occurs. On-going residual settlements of up to 50 mm due to goaf reconsolidation may continue for a period of up to 1 year, however, these movements are unlikely to result in further impact occurring to the surface.

### **7.21.2 Impact Management Strategies**

The predicted impact management strategies for the Black Hill Land Pty Ltd are likely to be adequately addressed by the proposed strategies presented in earlier sections of this report for the management of surface cracking, ponding and slope instability if they occur.

The barrier pillars that will be left between the extracted panels do not represent a future subsidence potential risk to future land re-development and ultimately the users for the following reasons:

- The factor of safety of the barrier pillars after mining of Panels 14 to 19 will be > 2.23 under double abutment loading conditions. Reference to **ACARP, 2005** suggests that the pillars will have a probability of failure of < 1 in 10 million.
- The proposed barrier pillars left between the panels will be strain-hardening and very unlikely to cause further increases in subsidence after the initial subsidence development period. It is unlikely that future pillar rib instability will result in any significant decrease in pillar strength or stiffness. The heights of the pillars are also unlikely to increase above 2.6 m in this area of the mine due to practical mining height constraints.
- The goaf adjacent to the pillars will provide support to overburden between the barrier pillars.



Based on the above, it is not considered necessary to remove or extract the pillars to minimise future subsidence potential or demonstrate long-term stability criteria have been satisfied for subsequent re-development. It is an option that may be discussed with the DPI, however there are ventilation and underground safety risks involved with removing the pillars during mining.

A Property Subsidence Management Plan (PSMP) is being developed in consultation with the landowner to address these potential issues.

## **7.22 Aboriginal Heritage Sites**

### **7.22.1 Potential Impacts**

Two scattered artefact sites exist within Area 2, with one in the Area 1. All are outside the zone of subsidence (within the Viney Creek SCZ) due to the proposed mining layout (see **Figure 1**). It is therefore very unlikely that the sites above the pillar extraction panels will be affected or damaged by surface cracking and increased erosion rates.

Further artefact sites may be present along Viney Creek which have yet to be identified (**ERM, 2008**) but will also be contained within the Viney Creek SCZ.

### **7.22.2 Impact Management Strategies**

The Department of Environment, Climate Change and Water (DECCW) require that an archaeological record of the artefact scatters be developed before recommending that mining activities be approved. The record for the SMP Area is understood to have now been completed.

As the archaeological surveys to-date have not identified any sites that are likely to be affected by mine subsidence, formal management plans will not need to be established prior to mining of Panels 14 to 26.

## **7.23 F3 Freeway and John Renshaw Drive**

### **7.23.1 Potential Impacts**

John Renshaw Drive and the F3 Freeway are located 750 m to 2100 m from the proposed mining areas. Based on cover depths of 100 m to 150 m, the roads are well outside the angle of draw around the proposed Area 2 panels (with distances ranging from 5 to 15 times the cover depth). Far-field horizontal displacements towards the mining area are very unlikely to occur along some sections of both roads closest to extracted panels P14 to P26. Horizontal strains associated with FFDs are also very unlikely to occur.

It is therefore assessed that it is very unlikely that the proposed Area 2 Panels will result in impacts to the abovementioned roads.

### **7.23.2 Impact Management Strategies**

It is not considered necessary to monitor far-field movements along these roads as any movements that occur will probably be less than survey accuracy limits for horizontal displacement (i.e. <10 to 20 mm).

It is however, considered reasonable to conduct visual inspections along the roads during subsidence development and prepare an impact management response strategy to deal with mining impacts if they do occur.

A series of far-field monitoring stations that monitor total horizontal displacement and strain may be established at strategic points around the mining lease to further define appropriate set-back distances from sensitive items of infrastructure that may exist elsewhere within the mining lease.

## **7.24 Comparison of Subsidence Profile Predictions to the Environmental Assessment**

For completeness the proposed SMP mining layout and impact predictions have been compared to the Environmental Assessment (see **Figure 44a**).

A representative predicted subsidence profile (XL B) across EA Panels (UD 15 to UD 6) with similar geometry to the SMP Panels P14 to P26, are presented **Figure 44b** and has been compared to the predicted profiles for XL 7 (see **Figure 16a**) in **Figure 44c**. The differences between the profiles are primarily due to the seam thickness differences along each cross line that were assumed.

It is considered that the predicted subsidence and associated impacts to the natural and man-made features will be similar in magnitude and location to the EA study outcomes.

## 8.0 Monitoring Requirements

### 8.1 Subsidence Development

The development of subsidence above a pillar extraction panel generally consists of two phases that are defined as 'primary' and 'residual' subsidence.

Primary subsidence is referred to the subsidence that is directly related to the retreating pillar extraction face.

Residual subsidence, due to re-consolidation of goaf, represents approximately 5 to 10% of maximum final subsidence and will be on-going for several months after primary subsidence ceases.

Maximum subsidence above a panel generally does not start to occur until the retreating extraction face has moved at least a distance equal to the width of the panel, and is referred to as the 'square' position.

Reference to **ACARP, 2003** and local data for the Area 1 panels indicate that primary subsidence is likely to commence at a given location above the panel centreline when the pillar extraction face is a distance of about 0.5 times the cover depth ahead of the point. The subsidence will then start to accelerate up to rates from 50 to 100 mm/day when the face is 0.5 to 1 times the cover depth past of the point, and then decrease to < 2 mm/day when the face is > 2 times the cover depth past it (see **Figure 45a**).

A summary of the subsidence magnitude and rate of development at several locations above the first two pillar extraction panels at Abel is presented in **Tables 29A** and **29B**.

**Table 29A - Summary of Maximum Subsidence Development above Panels 1 and 2 Centrelines**

Panel (Peg#)	Cover Depth H (m)	Panel Width W (m)	W/H	Start of Subsidence, d (distance to face)			End of Subsidence*, d (distance to face)		
				d <sub>start</sub> (m)	d <sub>start</sub> /H (m/m)	time (weeks)	d <sub>finish</sub> (m)	d <sub>finish</sub> /H (m/m)	time (weeks)
1 (47)	97	120	1.24	-50	-0.5	-1.1	175	1.8	3.7
2 (231)	70	160	2.29	-16	-0.2	-0.5	175	2.5	5.7

*italics* - Negative distances indicate face has not reached point on centreline.

\* - d<sub>finish</sub> = face distance past point where subsidence development rate has decreased to < 2mm/day.

**Table 29B - Summary of Maximum Subsidence Rate Development above Panels 1 and 2 at the Abel Mine**

Panel (Peg#)	Cover Depth H (m)	Panel Width W (m)	Face Retreat Rate [mean] (m/week)	Peak Subsidence Development Rate (mm/day)	Location of Peak Subsidence, d (distance to face)		
					$d_{peak}$ (m)	$d_{peak}/H$ (m/m)	time to peak (weeks)
1 (47)	97	120	30 - 59 [37]	77	74	0.8	1.9
2 (231)	70	150	25 - 50 [32]	101	101	49	1.9

The development of subsidence is also affected by the velocity of the retreating extraction face. The measured rates of retreat for the first four Abel Mine panels (Panels 1 to 4) have ranged between <10 m/week to 50 m/week with an average of approximately 30 m/week (see Panel 1 and 2 retreat rates in **Figures 45b** and **45c**).

The development of subsidence along the centreline of the Area 1 and 2 panels has been predicted using the final worst-case subsidence, tilt and strain contours presented in **Section 6.11** and the dynamic subsidence prediction module provided in the SDPS software package. An extract from the SDPS User Manual on the theory behind the dynamic calculations is presented in **Appendix B**.

Predictions of subsidence development curves for 10 m/week, 30 m/week and 50m/week have been derived using the dynamic subsidence analysis module provided in the SDPS program, and are presented in **Figures 45a** to **45c**. The predicted curves are consistent with the measured curves for the Area 1 panels in regards to subsidence development, and indicate that 90% to 95% of maximum panel subsidence will occur within 4 to 6 weeks, depending on the inevitable variation in retreat rates that will occur during second workings.

The default value of the time coefficient in the SDPS model has been adopted to provide a conservative estimate of effective rate of residual subsidence development after the primary subsidence phase has finished.

Further subsidence is also expected to develop when adjacent panels are subsequently extracted and will be due to the compression of barrier pillars when subject to increasing abutment loads. The development and magnitude of these movements will be similar to the residual subsidence movements.

## 8.2 Surface Monitoring Plans

Based on the surface topography and surface infrastructure present above the proposed pillar extraction panels, the following subsidence and strain-monitoring program is suggested to provide adequate information to monitor and implement appropriate subsidence impact management plans and provide pillar stability and performance data.

The following general monitoring program activities are suggested:

- (i) A minimum of one transverse subsidence line across the pillar extraction panels. The lines should be installed to at least the middle of the next adjacent panel before undermining occurs. The final transverse surveys for each panel should include the previous panels to capture chain pillar subsidence as it develops.
- (ii) A longitudinal line extending in-by and out-by from each panels starting and finishing points, for a minimum distance equal to the cover depth (i.e. to an AoD of 45°).
- (iii) A survey line along and across the banks of Viney Creek (refer to surface water consultants).
- (iv) Depending on location of a principal residence, either one or two survey lines to measure angle of draw over the proposed first workings areas running parallel and transverse to the panel centreline.
- (v) A minimum of 4 pegs spaced 10 m apart adjacent to or around any feature of interest (i.e. transgrid tower, archaeological sites) to measure subsidence, tilt and strain.
- (vi) The panel survey pegs should be spaced at a minimum of 10 m and a maximum of 20 m apart. For the first two or three panels it is recommended that the pegs are spaced 10 m apart along full crosslines and centrelines.

As more survey data is obtained it is envisaged that the peg spacing may be widened at non-critical locations (eg the central sections of the panel centrelines) or deleted altogether.

- (vii) A minimum of two baseline surveys of subsidence and strain is recommended before mine subsidence occurs to establish survey accuracy.
- (viii) Survey frequency will be dependent upon mine management requirements for subsidence development data in order to implement subsidence and mine operation management plans.
- (ix) Visual inspections and mapping of damage to be conducted before, during, and after mining.
- (x) The location of the extraction face should be recorded with each survey.

Further site or stakeholder specific monitoring may also be required. The suggested locations of the key monitoring program survey lines are shown in **Figure 46**.

### **8.3 Survey Accuracy**

Subsidence and strains may be determined using total station or spirit levelling and steel tape techniques, depending on the survey accuracy requirements.

The accuracy of total station traverse techniques from a terrestrial base line is normally expected to be within  $\pm 10$  mm for level and  $\pm 10$  to  $20$  mm for horizontal displacement (i.e. a strain measurement accuracy of  $\pm 1$  to  $2$  mm/m over a  $10$  m bay-length).

The accuracy of level measurements using spirit level should give subsidence to within  $\pm 3$  mm. Strain measurements using the steel tape techniques would be expected to have an accuracy of  $\pm 2$  mm (or  $0.2$  mm/m strain over  $10$  m).

It is recommended that total station techniques are used only for locating and monitoring of absolute X and Y displacements were possible and spirit levelling be used to measure all vertical movements. Steel tape measurements would be the preferred method for measuring strain.

### **8.4 Sub-Surface Monitoring**

Monitoring of sub-surface fracture heights above pillar extraction panels may be necessary within the mining lease to confirm the predictions of potential areas of connective surface cracking.

Two deep borehole extensometers have been installed in the middle of Area 1 and 2 panels to monitor heights of sub-surface fracturing due to the caving or goafing process during mining. Two deep boreholes above the barrier pillars between the panels have been instrumented with vibrating wire piezometers to monitor groundwater impacts.

The details and results of the monitoring have now been successfully collated and indicate that the height of continuous fracturing is within the predicted ranges. The installation of further deep boreholes will be dependent on the outcomes of the SMP submission to the DPI.

Inspections and monitoring of underground workings stability, groundwater makes and goaf air entry should continue to be recorded and included with subsidence monitoring data. In particular, the presence of faults between panels has the potential to create perched water tables and delayed inflow responses into extracted panels.

## **9.0 Conclusions**

It is concluded that the assessed range of potential subsidence and far-field displacement impacts after the mining of the proposed pillar extraction panels will be manageable for the majority of the site features, based on the analysis outcomes and discussions with the stakeholders to-date.

It is considered that the predicted subsidence and associated impacts to the natural and man-made features will be similar in magnitude and location to the EA study outcomes.

The measurement of the A-Zone horizon above Panels 1 and 2 indicates the height of continuous sub-surface fracturing in the Fractured Zone has occurred to between 45 and 50 m above the 120 m and 150 m wide panels with cover depths of 73 m to 95 m. The discontinuous subsurface fracturing in the Constrained Zone has lowered the near surface water table by approximately 15.3 m above Panel 1, however it is anticipated that it will recover in the medium to long term after mining is completed. The near surface water table above Panel 2 appears to have dropped below the piezo to a depth  $> 19.7$  m on the western side of a NW striking fault but fell only 4.5 m on the eastern side of the fault.

No practically measureable mine subsidence or far-field displacement movements or impacts are expected along John Renshaw Drive or the F3 Freeway due to the proposed mining layout.

Subsidence Control Zones (SCZ) have been proposed to limit impacts to within tolerable levels from the proposed mining layout at Abel for Viney Creek and four Principal Residences plus other structures on the proposed Catholic Diocese High School Site. The proposed setback distances applied at this stage are considered conservative, however, they will still need to be confirmed as adequate by subsidence monitoring as mining progresses.

The above subsidence impact limit criteria will be achieved in the SCZ with first workings only proposed at this stage. The potential exists however to implement a partial pillar extraction layout provided the long-term stability of remnant pillars and tolerable impacts to surface features can be demonstrated.

Provided the proposed impact management strategies are acceptable to the relevant stakeholders, the proposed mining layout is considered satisfactory at this stage.

If the estimated worst-case impacts cannot be reasonably managed in the event that exceedences occur through mitigation or amelioration strategies, then it will be necessary to adjust to the mining layout further to provide a more acceptable risk to the stakeholders.

The extent of mining layout adjustment will also require further discussions (and review of monitoring data) after the completion of a given panel with stakeholder and government agencies.

## 10.0 References

ACARP, 1993. **Improved Methods of Subsidence Engineering**, NERDDP Project No. 1311. Willey, P., Hornby P., Ditton S., Puckett, G. & McNally, P.

ACARP, 1998a. **Chain Pillar Design (Calibration of ALPS)**. Colwell, M., Mark, C. ACARP Report No. C6036 (October).

ACARP, 1998b. **ACARP Project No. C5024, Establishing the Strength of Rectangular and Irregular Pillars**. Galvin, J.M., Hebblewhite, B.K., Salamon, M.D.G., Lin, B.B.

ACARP, 2002. **Subsidence Impacts on River Valleys, Cliffs, Gorges and River Systems**. Project No. C9067, Waddington Kay & Associates, Report WKA110.

ACARP, 2003. **ACARP Project No. C10023, Review of Industry Subsidence Data in Relation to the Impact of Significant Variations in Overburden Lithology and Initial Assessment of Sub-Surface Fracturing on Groundwater**, Ditton, S. and Frith, R.C. Strata Engineering Report No. 00-181-ACR/1 (Sep).

ACARP, 2005. **Systems Approach to Pillar Design**. Strata Control Technologies Pty Ltd, UNSW School of Mining, Coffey Geosciences Pty Ltd. ACARP Project No. C9018. (May).

AGS, 2007. **Commentary on Practice Note Guidelines for Landslide Risk Management 2007**. Australian Geomechanics Society Journal Vol 42 No.1.

Appleyard, 2001. **A Review of the Formulation and Implementation of Graduated Design Guidelines for Residential Construction in Mine Subsidence Areas of NSW**. Appleyard, L. D. Published in Mine Subsidence Technical Society (MSTS) 5<sup>th</sup> Triennial Conference Proceedings, Coal Mine Subsidence 2001 - Current Practice and Issues (August).

AS2870, 1996. **Australian Standard - Residential Slabs and Footings**.

Colwell, 1993. **Water Inflow Investigation for a Longwall Operation**. M. Colwell. Published in Queensland Coal Geology Groups Conference Proceedings, New Developments in Coal Geology, Brisbane.

DgS, 2010. **Subsidence Impact Parameter Predictions at the Transgrid Towers 25B to 36B due to the Proposed Area 1 and 2 SMP Pillar Extraction Panels at the Abel Mine**. DgS Report No. ABL-002/2 (14 Dec).

DIPNR, 2005. **Management of Stream/Aquifer Systems in Coal Mining Developments - Implementation Manual**. NSW Department of Infrastructure, Planning and Natural Resources.

DMR, 1995. **The Newcastle Coalfield**. Geological Sheet Series. NSW Department of Minerals Resources.



ERM, 2008. **Lower Hunter Estates Development Report**. ERM Report No. 0073083 (April).

Fell et al, 1992. **Geotechnical Engineering of Embankment Dams**. Fell, R., MacGregor, P., Stapledon, D. Balkema.

Forster, 1995. **Impact of Underground Coal Mining on the Hydrogeological Regime, Central Coast, NSW**. Forster, I. Published in Australian Geomechanics Society (AGS) Conference Proceedings (February), Engineering Geology of Newcastle – Gosford Region, University of Newcastle.

Hawley and Brunton, 1995. **The Newcastle Coalfield, Notes to Accompany the Newcastle Coldfield Geology Map**. Hawley, S.P. and Brunton, J.S., Coal and Petroleum Geology Branch, Department of Mineral Resources.

Ho and Dominish, 2004. **Buried Pipelines Subjected to Mining Induced Ground Movements: Numerical Analysis of Impact and Development of Mitigation Concepts**. D.K.. Ho and P.G. Dominish, Worley Pty Ltd. Published in 6th Triennial Conference Proceedings of the Mine Subsidence Technological Society, Maitland (November).

Holla, 1987. **Mining Subsidence in NSW. 2. Surface Subsidence Prediction in the Newcastle Coalfield**. L. Holla. Department of Mineral Resources (January)

ISRM, 1985. **Suggested Method for Determining Point Load Strength (Revised Version)**. International Society of Rock Mechanics Commission on Testing Methods. Intl. J. Rock Mech. Min. Sci. and Geomech. Abstr. 22 pp51-60.

Levanthal and Stone, 1995. **Geotechnical Design Features - Deep cuttings and High Embankments on the western Margin of the Newcastle Coal Measures (F3-Sydney/Newcastle Freeway)**. Levanthal, A.R. and Stone, P.C. Published in Australian

Mark, 2007. **Multi-Seam Mining in the United States: Background**. Mark, C.M. NIOSH Information Circular 9495.

Mark & Molinda, 1996. **Rating Coal Mine Roof Strength from Exploratory Drill Core**. C. Mark, GM Molinda. Proc. of 15th Int'l Conf. On Ground Control in Mining, Morgantown, WV.

Parsons Brinkerhoff, 2003. **Black Hill Master Plan and Site Re-development Report**. Parsons Brinkerhoff Pty Ltd (16/12/03).

Pells *et al*, 1998. **Foundations on Sandstone and Shale in the Sydney Region**, Pells, P.J.N., Mostyn, G. and Walker, B.F.. Australian Geomechanics Journal.

Reid, 1998. **Horizontal Movements around Cataract Dam, Southern Coalfields**. Reid, P. Mine Subsidence Technological Society 4<sup>th</sup> Triennial Conference Proceedings. Newcastle, July 1998.

Seedsman and Watson, 2001. **Sensitive Infrastructure and Horizontal Ground Movement at Newstan Colliery**. Seedsman, R. W. and Watson, G. Mine Subsidence Technological Society 5<sup>th</sup> Triennial Conference Proceedings, Maitland, August 2001.

SDPS, 2007. **Subsidence Deformation Prediction System - Quick Reference Guide and Working Examples**. Agioutantis, Z., Karmis, M. Department of Mining and Minerals Engineering, Virginia Polytechnic Institute and State University, Virginia.

South East Archaeology (2006). **Aboriginal Archaeology Study for the Abel Underground Mine project**. Kuskie P.

Van de Merwe and Madden, 2002. **Rock Engineering for Underground Coal Mining**. J. Van de Merwe and B.J. Madden, SIMRAC, Camera Press, Johannesburg.

Vick, 2002. **Degrees of Belief: Subjective Probability and Engineering Judgement**. Vick, S.G. ASCE Press.

Whittaker and Reddish, 1989. **Subsidence Occurrence, Prediction and Control**. B.N. Whittaker and D.J. Reddish. Developments in Geotechnical Engineering, 56, Elsevier.



## **APPENDIX A – Summary of ACARP, 2003 and Updates**

## **ACARP, 2003 EMPIRICAL SUBSIDENCE PREDICTION MODEL**

### **A1 Introduction**

This appendix provides a description of how subsidence develops above longwall panels and provides a summary of the empirical subsidence prediction models used in this study: **ACARP, 2003** and SDPS (Surface Deformation Prediction System).

The **ACARP, 2003** model was originally developed by Strata Engineering (Australia) Pty Ltd under ACARP funding with the goal of providing the industry with a robust and reliable technique to utilise the significant amount of geological and testing information already gathered by mining companies.

Over the past six years the **ACARP, 2003** model has been used successfully by the model's author, Steven Ditton, at several longwall mines in the Newcastle, Hunter Valley, Western and Southern Coalfields of NSW and the Bowen Basin, Queensland.

Subsidence prediction work for Stage 1 of the Moolarben Coal Project in 2006 resulted in further external scrutinization of the model and the robustness of the methodology by an Independent Hearing and Assessment Panel (IHAP), which was set up to assess Environmental Impact Assessments for new coal mining projects by NSW Department of Planning (DoP).

The outcomes of the IHAP for Moolarben resulted in several refinements to the model, as requested by the independent subsidence expert, Emeritus Professor J M Galvin, UNSW School of Mining and Director of Galvin and Associates Pty Ltd.

The refinements generally included several technical adjustments and clarification of the terminology used, to enable a better understanding of the model by the wider technical community.

Over the past two years, Ditton Geotechnical Services Pty Ltd (DgS) has modified the **ACARP, 2003** model to be able to use it to calibrate an influence function model (SDPS<sup>®</sup>) that was developed by the Polytechnical Institute for the US Coalfields. The SDPS<sup>®</sup> program allows a wider range of topographic and complex mining layouts (including longwall and pillar extraction panels) to be assessed.

This appendix summarises the **ACARP, 2003** model in its current format and explains the refinements made to the original model. Details of the **SDPS<sup>®</sup>** model itself are provided at the back of this appendix and discussed further in the main body of the report.

## **A2 Description of Subsidence Development Mechanisms Above Longwalls**

After the extraction of a single longwall panel, the immediate mine roof usually collapses into the void left in the seam. The overlying strata or overburden then sags down onto the collapsed material, resulting in settlement of the surface.

The maximum subsidence occurs in the middle of the extracted panel and is dependent on the mining height, panel width, cover depth, overburden strata strength and stiffness and bulking characteristics of the collapsed strata. For the case of single seam mining, maximum panel subsidence has not exceeded 60% of the mining height (T) in over 95% of the published cases for the Newcastle, and Southern Coalfields (refer ACARP, 2003 and Holla and Barclay, 2000). For the 5% of cases, which did exceed 60%T, the maximum subsidence did not exceed 65%T (i.e. 2.7 m for a 4.2m mining height). The actual subsidence may also be lower than this value due to the spanning or bridging capability of the strata above the collapsed ground (or the goaf).

The combination of the above factors determines whether a single longwall panel will be sub-critical, critical, or supercritical in terms of maximum subsidence.

Sub-critical subsidence refers to panels that are narrow and deep enough for the overburden to bridge or 'arch' across the extracted panel regardless of geology. It is therefore termed 'geometrical' or 'deep beam arching'.

Beyond the sub-critical range, the overburden becomes Critical, and is unable to arch without the presence of massive, competent strata. Failure of the strata starts to develop and it sags down onto the collapsed or caved roof strata immediately above the extracted seam. Critical panels refer to panels with widths where maximum possible subsidence starts to develop.

If relatively thick and strong massive strata exist, then 'critical arching' or 'shallow Voussoir beam' behaviour can occur for panel W/H ratios up to 1.8 (e.g. massive Wollar Sandstone strata > 33 m thick, has spanned across 250 m wide and 140 m deep longwall panels at Ulan Mine in the Western Coalfield. Panel sag subsidence was 1.2 m for a mining height of 3.2 m).

Supercritical panels refer to panels with widths that cause complete collapse of the overburden. In the case of super-critical panels, maximum panel subsidence does not usually continue to increase significantly with increasing panel width.

In the Australian coalfields, sub-critical or (geometrical arching) behaviour generally occurs when the panel width (W) is <0.6 times the cover depth (H) and supercritical when W/H > 1.4. Critical behaviour usually occurs between W/H ratios of 0.6 and 1.4 and represents the transition between 'geometrical arching' to 'shallow beam bending' to 'complete failure' of the overburden.

The maximum subsidence for sub-critical and critical panel widths is < 60% of the longwall extraction height and could range between 10% and 40% (of the extraction height).

The surface effect of extracting several adjacent longwall panels is dependent on the stiffness of the overburden and the chain pillars left between the panels. Invariably, 'extra' subsidence occurs above a previously extracted panel and is caused primarily by the compression of the chain pillars and adjacent strata between the extracted longwall panels.

A longwall chain pillar undergoes the majority of life-cycle compression when subject to double abutment loading (i.e. the formation of goaf on both sides of it, after two adjacent panels have been extracted). Surface survey data indicates that an extracted panel can affect the chain pillars between three or four previously extracted panels. The stiffness of the overburden and chain pillar system will determine the extent of load transfer to the preceding chain pillars. If the chain pillars go into yield, the load on the pillars will be mitigated to some extent by load transfer to adjacent fallen roof material or goaf.

The surface subsidence usually extends outside the limits of extraction for a certain distance (i.e. the angle of draw). The angle of draw distance is usually less than or equal to 0.5 to 0.7 times the depth of cover (or angles of draw to the vertical of 26.5° to 35°) in the NSW and QLD Coalfields.

The effect of extracting several adjacent longwall panels is dependent on the stiffness of the overburden and the chain pillars left between the panels. Invariably, 'extra' subsidence occurs above a previously extracted panel and is caused primarily by the compression of the chain pillars and adjacent strata between the extracted longwall panels.

A longwall chain pillar undergoes the majority of life-cycle compression when subject to double abutment loading (i.e. the formation of goaf on both sides of it, after two adjacent panels have been extracted). Surface survey data indicates that an extracted panel can affect the chain pillars between three or four previously extracted panels. The stiffness of the overburden and chain pillar system will determine the extent of load transfer to the preceding chain pillars. If the chain pillars go into yield, the load on the pillars will be mitigated to some extent by load transfer to adjacent fallen roof material or goaf.

The surface subsidence usually extends outside the limits of extraction for a certain distance (i.e. the angle of draw). The angle of draw distance is usually less than or equal to 0.5 to 0.7 times the depth of cover (or angles of draw to the vertical of 26.5° to 35°) in the NSW and QLD Coalfields.

### **A3 ACARP Project Overview**

The original **ACARP, 2003** model was originally developed for the Newcastle Coalfield to deal with the issue of making reliable subsidence predictions over longwall panels by using both geometrical and geological information.

The project was initially focused on the behaviour of massive sandstone and conglomerate strata in the Newcastle Coalfield, but has now been successfully used in other coalfields since development over the past six years. This has occurred naturally due to the expansion of the

model's database with data from other coalfields and has resulted in generic refinements to the model to deal with the wider range of geometrical and geological conditions.

In regards to geometry, the subsidence above a series of longwalls is strongly influenced by the panel width, the cover depth, the extraction height and the stiffness of the interpanel pillars (i.e. the chain pillars) and immediate roof and floor strata.

In regards to geology, the presence of massive strata units, such as conglomerate and sandstone channels above longwall panels, has resulted in reduced subsidence compared to that measured over longwall panels with similar geometry and thinner strata units.

Geological structure, such as faults and dykes, can cause increases in subsidence due to their potential to adversely affect the spanning capability of the overburden.

During the original development of the model, a database of maximum single and multi longwall panel subsidence and associated massive strata units was compiled for the Newcastle Coalfield. The database draws on subsidence data from over fifty longwall panels and covers a panel width to cover depth (W/H) ratio from 0.2 to 2.0 (cover depth ranges between 70 m and 351 m), as shown in **Figure A1**.

The original project database includes single seam longwall mining data from eleven collieries within the Newcastle Coalfield, as presented in **Table A1**.

**Table A1 - Empirical Database Sources from Newcastle Coalfield**

Colliery	Colliery	Colliery
Cooranbong	Lambton	Wyee
New Wallsend No. 2 (Gretley)	Teralba	
Moonee	Burwood	
Stockton Borehole	West Wallsend	
Newstan	John Darling	

The wide range of single longwall panel W/H ratios in the database was considered unique compared to the other Australian coalfields and enabled the study to focus on overburden and chain pillar behaviour effects separately.

Pillar extraction or multiple seam data was not used to produce the subsidence prediction curves, as it invariably makes the assessment of geological influences more difficult. Other NSW and QLD longwall and high pillar extraction mine data that have been added to the model database over the past 6 years are shown in **Table A2**.

**Table A2 - Empirical Longwall Database Sources from Other Coalfields**

<b>Coalfield</b>	<b>Colliery</b>	<b>Colliery</b>
Newcastle	West Wallsend	Newstan
	Tasman	
Hunter Valley	United	Wollemi
	Austar	
Southern	Berrima	Appin
	Elouera	Dendrobium
Western	Springvale	Angus Place
	Ulan	
Queensland	Cook	Oaky Creek
	Moranbah North	

In summary, the key features of the **ACARP, 2003** model are that it:

- Is derived from a comprehensive database of measured subsidence, strain, tilt and curvature above longwalls in the Newcastle, Hunter Valley, Western and Southern Coalfields.
- Has been validated with measured subsidence profile data over the past 6 years.
- Adds to the **DMR, 1987** model for the Newcastle Coalfield, as it addresses multiple panels and contains significantly more longwall data.
- Includes the effects of massive sandstone/conglomerate lithology on subsidence, based on the linking of borehole and subsidence data.
- Allows reliable predictions of maximum single panel subsidence, chain pillar subsidence, tilt, curvature, strain and the angle of draw within a 90% Confidence Interval.
- Enables ‘greenfield’ sites (i.e. where there is no subsidence data) to be assessed rapidly and accurately.
- Provides maximum subsidence predictions based on Upper 95% Confidence Limits (or 5% Probability of Exceedence limits), which in practice have rarely been exceeded.

The confidence limits have been derived by the application of central limit theory and the likely normal distribution of residuals about lines of best fit or regression lines determined for the model database.

- Utilises historical information directly - predictions are based on actual data.



- Enables prediction of secondary tilt, curvature and strain magnitudes. Effects such as ‘skewing’ due to rapid surface terrain variations, surface ‘hump’ or step development and cracking can result in tilt, curvature and strain magnitudes significantly greater than predicted ‘smooth’ profile values.

This issue has been addressed empirically by linking measured impact parameters with key mining geometry variables. Strain concentration factors and database confidence limits have been developed to estimate the likely range of subsidence impact parameters.

- Is amenable to subsidence contouring and allows the impacts on surface features to be assessed, including post-mining topography levels for watercourse impact assessment.
- Predictions of subsidence at specific locations can be done to provide an indication of likely subsidence magnitude; however, depending on the sensitivity of the feature, it may be prudent to adopt maximum predicted subsidence for a given panel.
- Incorporates an empirical model of sub-surface fracturing and far-field displacements.

Recent far-field horizontal displacement model work in the Newcastle Coalfield suggests the empirical model is conservative.

The following key input parameters are required to make subsidence predictions using the model:

- Panel Width (W)
- Cover Depth (H)
- Seam Working Height (T)
- Overburden lithology details, specifically the thickness and location of massive strata units (t, y).
- Chain Pillar Height (h), Width ( $w_{cp}$ ) and Length (l) [solid dimensions]
- Roadway width
- Number of panels to be extracted

The statistical inferences and estimates of the model uncertainty associated with the prediction methodology are presented in the following sections.

## A4 Single Panel Subsidence Predictions

### A4.1 Geometrical Factors

The major finding of the **ACARP, 2003** project in regards to mining geometry was that the historical relationship between subsidence and panel width to cover depth ratio ( $W/H$ ) is not a constant for the range of cover depths ( $H$ ) involved.

**Figure A2** shows the range of maximum subsidence that can occur above longwall panels with similar mining geometries and a range of cover depths. The apparent differences between the DMR's Southern NSW and Newcastle Coalfield curves and laminated overburden theory (**Heasley, 2000**) also support the above finding.

For an overburden consisting of sedimentary rock layers, **Heasley, 2000** applied laminated beam theory by **Salamon, 1989** to form the basis of the pseudo-numerical subsidence prediction program LAMODEL ("LAyered MODEL" of overburden) that has been found to have reasonable success in the US Coalfields.

According to Lamodel theory, the maximum seam roof convergence ( $C_{\max}$ ) above a longwall panel of mining height ( $T$ ), width ( $W$ ) and cover depth ( $H$ ), with an idealised overburden of uniform lamination thickness ( $t$ ), Young's Modulus ( $E$ ), unit weight ( $\gamma$ ) and Poisson's Ratio ( $\nu$ ) is:

$$C_{\max} = \sqrt{(12(1-\nu^2)/t) (\gamma H/E) (W^2/4)} \text{ or } T \text{ (whichever is the lower value)}$$

In terms of traditional empirical models of estimating subsidence, the above equation indicates that the maximum single panel subsidence is a function of  $(W^2/t^{0.5})$ ,  $(\gamma H/E)$  and  $T$ .

The **ACARP, 2003** model surmised that single panel subsidence was a function of  $W/H$ ,  $\gamma H/E$  or  $H$ ,  $T$ ,  $W/t$  and  $y/H$ . The first three parameters are related to panel geometry (Width, Cover Depth and Mining Height, whilst the last two parameters (strata unit thickness,  $t$ , and distance  $y$ , to the unit above the workings) infer geological influences of massive strata units (*Note: that the  $W/t$  parameter was incorrectly inversed in ACARP, 2003*).

Based on the above, surface subsidence increases with increasing cover depth ( $H$ ) for the same  $W/H$  ratio, and is primarily a function of the increasing panel width ( $W$ ). For constant single panel width ( $W$ ), subsidence will therefore decrease with increasing cover depth ( $H$ ).

The subsidence data was subsequently separated into three cover depth categories of  $H = 100, 200$  and  $300 \text{ m} \pm 50 \text{ m}$  and is presented in **Figures A3 to A5**.

The influence of overburden lithology was found to be readily apparent, once the database was filtered using the above cover depth ranges.

## A4.2 Geological Factors

Once the first stage in the development of the subsidence prediction model had addressed the influence of cover depth the effect of “significant” overburden lithology above single longwall / miniwall panels could be addressed.

**Figure A6** illustrates a physical model, showing the subsidence reducing effects of a massive strata unit.

Borehole data was used to derive the thickness and location of massive strata units considered to be critically important for surface subsidence prediction, for a given panel width and depth. The methodology takes into account the maximum massive strata unit thickness ( $t$ ) at each location and the height to the base of the unit above the longwall panel ( $y$ ).

The subsidence above a panel, given cover depth ( $H$ ) and panel width ( $W$ ) decreases significantly when a massive strata unit is thicker than a certain minimum limit value. The thickness is also reduced when the unit is closer to the surface. The strata unit is considered to have a 'high' subsidence reduction potential (SRP) when it exceeds a minimum thickness for a given  $y/H$  ratio, as shown in **Figures A7.1 to A7.3** for each cover depth category.

For a thin strata unit located relatively close to a panel, the 'Subsidence Reduction Potential (SRP)' will be 'low'. However, there is also an intermediate zone, where a single strata unit (or several thinner units) below the 'high' subsidence reduction thickness can result in a 'moderate' reduction in subsidence. A second limit line can therefore be drawn, which represents the threshold between 'moderate' and 'low' SRP.

It is considered that the 'high' SRP limit line represents the point between elastic and yielding behaviour of a spanning beam. The 'moderate' SRP limit line represents the point between yielding behaviour and collapse or failure of a spanning beam (which has been yielding).

The limit lines have been determined for the strata units located at various heights ( $y$ ) above the workings in each depth category, as shown in **Figures A8 to A10**.

## A4.3 Summary of Model Concepts

The **ACARP, 2003** model introduces several new parameters, to improve the definition of various types of overburden behaviour and the associated mechanics.

As outlined in **Section A4.2**, the 'Subsidence Reduction Potential' (SRP) of massive or thickly bedded geological units above single longwall panels for the Newcastle Coalfield has been introduced to describe the influence that a geological unit may have on subsidence magnitudes. The massive geological units are defined in terms of 'high', 'moderate' or 'low' SRP.

Massive unit thickness, panel width, depth of cover and height of unit above the workings are considered to be key parameters for assessing overburden stiffness and spanning capability over a given panel width, controlling surface subsidence. A conceptual model for overburden behaviour is illustrated in **Figure A11**.

Variation in subsidence along the length of a panel may therefore be due to the geometry and / or SRP variation of geological units within the overburden.

The database also indicates the presence of a 'Geometrical Transition Zone', whereby subsidence increases significantly regardless of the SRP of the geological units, as shown in **Figure A12**. This behaviour occurs when panel width to cover height ratio (W/H) ranges from 0.6 to 0.8. This phenomenon can be simply explained as a point of significant shift in structural behaviour and the commencement of overburden breakdown.

The model allows the user to determine the range of expected subsidence magnitudes and the location of geology related SRP and/or 'geometrical transition zones' along a panel. Identification of the transition zones is an important factor in assessing potential damage risks of differential subsidence to important infrastructure, buildings and natural surface features, such as rivers, lakes and cliff lines etc.

For W/H ratios  $<0.7$ , the overburden spans across the extracted panel like a 'deep' beam or linear arch, whereby the mechanics of load transfer to the abutments is governed by axial compression along an approximately parabolic shaped line of thrust, see **Figure A13**.

For W/H ratios  $>0.7$  the overburden geometry no longer allows axially compressive structural behaviour to dominate, as the natural line of thrust now lies outside of the overburden. Bending action due to subsequent block rotation occurs. Provided that the abutments are able to resist this rotation, flatter lines of thrust still develop within the overburden, but the structural action is now dominated by bending action. This type of overburden behaviour has been defined as 'shallow' beam behaviour, which in structural terms is fundamentally less stiff than 'deep' beam behaviour. This results in a significant increase in subsidence or sag across an extracted longwall panel (all other factors being equal), as shown **Figure A13**.

"Voussoir beam" or "fractured linear arch" theory can be used to explain both types of overburden behaviour, as deep seated or flatter arches develop in the strata in an attempt to balance the disturbing forces.

The 'strata unit location factor' ( $y/H$ ) was developed to assist in assessing the behaviour of massive strata units above the workings. The  $y/H$  factor is a simple way to include the influence of the unit location above the workings in terms of the effective span of the unit and the stresses acting upon it.

The key elements of this factor and their influence on the behaviour of the strata unit are:

- $y$ , the height of the beam above the workings, which determines the effective span of the beam, and
- $H$ , cover depth over the workings, which exerts a strong influence on the stress environment and, hence, the propensity for buckling or compressive failure of the beam.

Essentially beam failure due to the action of increasing horizontal stress (i.e. crushing or buckling) appears more likely as  $y$  decreases and  $H$  increases. The ratio of  $y/H$  may therefore be used to differentiate between the SRP of a beam of similar thickness, but at varying heights above the workings. The model also demonstrates that as the depth of cover increases, a thicker beam is required to produce the same SRP above a given panel width.

## A5 Multiple Longwall Panel Subsidence Prediction

### A5.1 General

The effect of extracting several adjacent longwall panels is governed by the stiffness of the overburden and the chain pillars left between the panels. Invariably, 'extra' subsidence occurs above a previously extracted panel and is caused primarily by cracking of the overburden and the compression of the chain pillars and adjacent strata between the extracted longwall panels.

A conceptual model of subsidence mechanisms above adjacent longwall panels in a single seam is shown in **Figure A14**.

### A5.2 Predicting Subsidence above Chain Pillars (ACARP, 2003 Model)

A chain pillar undergoes the majority of life-cycle compression when subject to double abutment loading (i.e. the formation of goaf on either side, after two adjacent panels have been extracted). Surface survey data indicates that an extracted panel can affect the chain pillars of up to three or four previously extracted panels. The stiffness of the overburden and chain pillar system will determine the extent of load transfer to preceding chain pillars.

Multiple-panel effects have therefore been included in the model by adding empirical estimates of surface subsidence over chain pillars to the maximum subsidence predictions for single panels.

The empirical model presented in **ACARP, 2003** for estimating the subsidence above a chain pillar, was based on the regression equation presented in **Figure A15**. The model compares the ratio of chain pillar subsidence ( $S_p$ ) over the extraction height ( $T$ ), to the width of the chain pillar divided by the cover depth multiplied by the total extracted width ( $1000w/W'H$ ).

A regression analysis on the data indicates a strong exponential relationship for  $1000wcp/W'H$  values up to 0.543. For values  $> 0.543$ , the relationship becomes constant.

$$S_p/T = 7.4044e^{-10.329F} \quad (R^2 = 0.92) \text{ for } F < 0.543, \text{ and}$$

$$S_p/T = 0.023 \text{ for } F > 0.543$$

where

$$F = 1000w/W'H$$

$W'$  = The total extracted width which includes the width of the panels extracted on both sides of the subject chain pillar, and the width of the chain pillar itself (i.e.  $W' = W_i + w(i) + W_{i+1}$ ).

*Note that the final subsidence for a longwall panel with several subsequent extracted panels was then determined empirically by adding 50% of the predicted chain pillar subsidence ( $S_p$ ) to the single panel  $S_{max}$  estimate.*

*This approach however, did not include an abutment angle to estimate pillar loads, which are likely to vary significantly between sub-critical and supercritical panel layouts.*

*The chain pillar model has now been amended to include better predictions of chain pillar load that are consistent with ALTS methodology (refer **ACARP, 1998a**) and has resulted in the modified version presented in Section A5.2.*

## **A5.2 Predicting Subsidence above Chain Pillars (DgS, 2008 Model)**

After the **ACARP, 2003** model was published; further studies on chain pillar subsidence measurements were undertaken at several mine sites in the Western (Springvale, Angus Place and Ulan) and Southern Coalfields (Appin and Elouera). The measured subsidence above the chain pillars was significantly greater than the Newcastle Coalfield pillars and considered to be linked to the stress acting on the pillars and the longwall mining height.

Maximum subsidence above the chain pillars invariably occurred after the pillars were subject to double abutment loading conditions (i.e. goaf on both sides).

The **ACARP, 2003** model for estimating chain pillar subsidence was subsequently superseded by the pillar stress v. strain type approach presented in **Figure A16**. The chain pillar stress was estimated by assuming a design abutment angle of  $21^\circ$  for the pillar load, according to the methodology presented in **ACARP, 1998a**.

Prediction of subsidence above the chain pillars ( $S_p$ ) was determined based on the following regression equation using the mining height,  $T$  and pillar stress,  $\sigma$ :

$$S_p/T = 0.238469/(1+e^{-(\sigma-25.5107)/7.74168}) \quad (R^2 = 0.833)$$

The uncertainty of the predictions was estimated by calculating the variance of the residuals about the regression lines and calculating 90% Confidence Limits for the database as follows:

$$90\% \text{ CL } S_p \text{ error} = 0.048T$$

It was also considered necessary to test if the above stress v. strain type approach was adequate for reliable predictions, by comparing the subsidence outcomes with the pillar Factor of Safety; see **Figure A17**.

The strength of the chain pillars was estimated using the rectangular pillar strength formulae presented in **ACARP, 1998b**. The FoS was derived by dividing the pillar strength by the pillar load (i.e. stress).

Generally it has been found that significant surface subsidence above the chain pillar (i.e. 10 - 30% of pillar height) starts to occur when the pillar FoS is  $< 2$ . For FoS values greater than 2, subsidence above the pillars is virtually independent of FoS and the pillars generally perform elastically under load.

The database indicates that when the FoS is  $< 2$ , the stiffness of the pillar starts to decrease, due to the development of load induced fracturing within the pillar. FoS values of  $< 2$  represent pillar stresses that exceed 50% of the pillar strength. Laboratory testing of coal and sandstone samples also show sample ‘softening’ as the ultimate load carrying capacity of the sample is approached.

For pillars with FoS values  $< 1$ , the subsidence above the chain pillars tend to a maximum limit of approximately 25 to 30% of the mining height. This type of behaviour is expected for chain pillars that have width to height ratios  $w/h > 5$ , which is the point where ‘strain hardening’ deformation starts to develop with increased confinement of the ‘pillar core’.

### A5.3 Calculation of First and Final Subsidence for Multiple Longwall Panels

Multiple panel predictions can be made by adding the predicted single panel subsidence to a proportion of the chain pillar subsidence (including the residual subsidence) to estimate first and final subsidence above a given longwall panel.

The definition of first and final  $S_{\max}$  is as follows:

First  $S_{\max}$  = the total subsidence after the extraction of a longwall panel, including the effects of previously extracted longwall panels adjacent to the subject panel.

Final  $S_{\max}$  = the total subsidence over an extracted longwall panel, after at least three more panels have been extracted, or when mining is completed.

First and final  $S_{\max}$  values for a panel are predicted by adding 50% and 100% of the predicted subsidence over the chain pillars (i.e. between the previous and current panel) less the goaf edge subsidence (see **Section A5**).

Residual subsidence above chain pillars and longwall blocks tends to occur after extraction due to (i) increased overburden loading on pillars and (ii) on-going goaf consolidation or creep effects. Based on the final chain pillar subsidence measurements presented in **Figure A16**, the residual movements can increase subsidence by a further 10 to 30%.

An example of measured multiple longwall subsidence behaviour is presented in **Figure A18**.

Final subsidence is normally estimated by assuming a further 20% of the chain pillar subsidence will occur. However, this may be increased or decreased, depending on local experience.

The prediction of first and final subsidence originally presented in **ACARP, 2003** involved the use of several empirical coefficients, which have proven to be difficult to apply in practice. The interested may refer to this methodology, however, the above method is considered easier to apply and likely to result in a similar outcome.



In summary, the mean values of the first  $S_{\max}$  and final  $S_{\max}$  are calculated as:

$$\text{First } S_{\max} = \text{Single } S_{\max} + 0.5(S_{p(i-1)} - S_{\text{goe}})$$

$$\text{Final } S_{\max} = \text{First } S_{\max} + 1.2(\text{Final } S_{p(i)} - \text{First } S_{\text{goe}})$$

The U95% Confidence Limits or Credible Worst Case Values are then:

$$\text{U95\% First } S_{\max} = \text{mean First } S_{\max} + 1.64 (\text{U95\% } S_{\max} \text{ error} + \text{U95\% } S_p \text{ error})^{1/2}.$$

$$\text{U95\% Final } S_{\max} = \text{mean Final } S_{\max} + 1.64 (\text{U95\% } S_{\max} \text{ error} + \text{U95\% } S_p \text{ error})^{1/2}.$$

## **A6 Subsidence Profile and Impact Parameter Predictions**

Part of the **ACARP, 2003** project included the development of several models to predict the maximum panel deformation parameters and surface profiles associated with subsidence. The following models were developed:

- panel goaf edge or rib subsidence,
- angle of draw,
- maximum transverse and longitudinal tilt, curvature and strain,
- the locations of the above parameters over the longwall panel for the purposes of subsidence profile development, and
- heights of continuous and discontinuous fracturing above the longwall, based on measured surface tensile strains and fracture limit horizons over extracted panels (see **Section A7** for details).

A conceptual model of surface deformation profiles that develop above longwall panels is given in **Figure A19**.

All of the above subsidence parameters have been statistically linked to key geometrical parameters such as the cover depth (H), panel width (W), working height (T) and chain pillar width ( $w_{cp}$ ) and shown in **Figures A20 to A27**.

A summary of all the empirical model relationships between the key subsidence profile parameters that were developed in **ACARP, 2003** and DgS are presented in **Table A3**.

**Table A3 - Summary of Subsidence Impact Parameter Prediction Models Developed from ACARP, 2003**

Parameter	Regression Equation and +/- 90% Confidence Limits or Upper95% CL	Coefficient of Determination ( $R^2$ )	Figure No.
Subsidence Reduction Potential (SRP) of Strata Unit in Overburden with thickness t, panel width, W and location factor, y/H above workings for Cover Depth Category	<p><b>High</b> SRP t for a given panel W plots above line for given strata unit y/H.</p> <p><b>Moderate</b> SRP t plots between High SRP line and next y/H line below it.</p> <p><b>Low</b> SRP t plots below Moderate SRP limit line.</p>	N/A - curve location determined by successful re-prediction of >90% of cases I databases	<p><b>Figure A8</b> for H&lt;150m;</p> <p><b>Figure A9</b> for H&lt; 250m;</p> <p><b>Figure A10</b> for H&lt; 350m</p>
Single Maximum Longwall Panel Subsidence (Single $S_{max}$ ) for Assessed Strata Unit SRP of Low, Moderate or High	<p>Upper and Lower bound prediction lines for a given SRP are used to estimate range of <math>S_{max}/T</math> for a given Panel W/H.</p> <p>Average of limit lines value is mean Single <math>S_{max}</math> value +/- 0.03T for W/H &lt; 0.6; +/- 0.1T for 0.6&lt;W/H&lt;0.9; +/-0.05T for W/H&gt;0.9</p>	N/A - curve location determined by successful re-prediction of >90% of cases I databases	<p><b>Figure A3</b> for H&lt;150m;</p> <p><b>Figure A4</b> for H&lt; 250m;</p> <p><b>Figure A5</b> for H&lt; 350m</p>
Chain Pillar Subsidence, $S_p$ (m)	Mean $S_p/T = 0.238469/(1+e^{-(\frac{25.5107}{7.74168} \ln \frac{W}{H})})$ +/- 0.048T	$R^2 = 0.833$	<b>Figure A16</b>
Goaf Edge Subsidence	Mean $S_{goe}/S_{max} = 0.0722(W/H)^{-2.557}$ U95%CL $S_{goe}/S_{max} = 0.0719(W/H)^{-1.9465}$	$R^2 = 0.82$	<b>Figure A20</b>
Angle of Draw	Mean AoD = $7.646 \ln(S_{goe}) + 32.259$ U95%CL = Mean AoD + $8.7^\circ$	$R^2 = 0.56$	<b>Figure A21</b>
Maximum Tilt $T_{max}$ (mm/m)	$T_{max} = 1.1925(S_{max}/W')^{1.3955}$ +/- 0.4T <sub>max</sub> (W' = lesser of W and 1.4H)	$R^2 = 0.94$	<b>Figure A22</b>
Maximum Convex Curvature $C_{max}$ (km <sup>-1</sup> )	Mean $C_{max} = 15.60(S_{max}/W'^2)$ +/- 0.5Mean	$R^2 = 0.79$	<b>Figure A23</b>
Maximum Concave Curvature $C_{min}$ (km <sup>-1</sup> )	Mean $C_{min} = 19.79(S_{max}/W'^2)$ +/- 0.5Mean	$R^2 = 0.79$	<b>Figure A24</b>
Maximum Tensile Strain $E_{max}$ (mm/m)	Mean 'smooth' $E_{max} = 5.2C_{max}$ +/- 0.5 Mean Mean 'Cracked' $E_{max} = 14.4C_{max}$	$R^2 = 0.72$ $R^2 = 0.32$	<b>Figure A25</b>
Maximum Compressive $E_{min}$ (mm/m)	Mean $E_{min} = 5.2(C_{min})$ +/- 0.5 Mean Mean 'Cracked' $E_{min} = 14.4C_{min}$	$R^2 = 0.72$ $R^2 = 0.32$	<b>Figure A25</b>
Critical Panel Width	$W_{crit} = 1.4H$ where H = cover depth	N/A	<b>ACARP, 2003</b>

**Table A3 (Continued) - Summary of Subsidence Impact Parameter Prediction Models  
Developed from ACARP, 2003**

Subsidence at Inflexion Point or Maximum Tilt $S_{Tmax}$	Mean $S_{Tmax}/S_{max} = -0.0925(W/H) + 0.7356$ +/- 0.2	$R^2 = 0.5$	<b>ACARP, 2003</b>
Distance to Inflexion Point, $d/H$	$d/H = 0.2425 \ln(W/H) + 0.3097$	$R^2 = 0.73$	<b>Figure A27</b>
Distance to Peak Tensile Strain (mm/m)	$d_t/H = 0.1643 \ln(W/H) + 0.2203$ for $W/H > 0.6$ ; $d_t/H = 0.2425 \ln(W/H) + 0.2387$ for $W/H < 0.6$ ;	$R^2 = 0.28$	<b>Figure A27</b>
Distance to Peak Compressive Strain (mm/m)	$d_c/H = 0.3409 \ln(W/H) + 0.3996$ for $W/H > 0.6$ ; $d_c/H = 0.2425 \ln(W/H) + 0.3767$ for $W/H < 0.6$	$R^2 = 0.59$	<b>Figure A27</b>

\* - If  $H$  within 25 m of depth category boundary, then average result with overlying or underlying depth category value.

- Centreline profile parameters are not presented here (refer to **ACARP, 2003**).

## **A7      Subsidence Profile Predictions above Longwall Panels**

Predicted 'smooth' subsidence profiles above single and multiple longwall panels have been determined based on cubic spline curve interpolation through seven key points along the subsidence trough (i.e. maximum in-panel subsidence, inflexion point, maximum tensile and compressive strain, goaf edge subsidence, subsidence over chain pillars and 20 mm subsidence or angle of draw limit).

The locations of these points have been determined empirically, based on regression relationships between the variables and the geometry of the panels (see **Table A3**). Both transverse and longitudinal profiles have been derived in this manner.

First and second derivatives of the fitted spline curves provide 'smooth' or continuous subsidence profiles and values for tilt and curvature. Horizontal displacement and strain profiles were derived by multiplying the tilt and curvature profiles by an empirically derived constant associated with the bending surface beam thickness (based on the linear regression relationship between the variables, as discussed in **ACARP, 2003**).

An allowance for the possible horizontal shift in the location of the inflexion point (within the 95% Confidence Limits of the database) has also been considered, for predictions of subsidence at features located over the goaf or extracted area.

## A8 Subsidence Contour Predictions above Longwall Panels

Subsidence contours can be derived with geostatistical kriging techniques over a 10 m square grid using Surfer 8® software and the empirically derived subsidence profiles along cross lines, centre lines and corner lines around the ends of the longwall panels. Vertical ‘slices’ may taken through the contours to (i) determine subsidence profiles along creeks or infrastructure, and (ii) assess the likely impacts on the relevant surface features.

### A8.1 Subsidence Contours

Subsidence contour predictions have been made in this study using SPDS®, which is an influence function based model that firstly calculates seam convergence and pillar displacements empirically around the workings. The influence of an extracted element of coal is transmitted to the surface via a 3-D influence function, which also takes varying topography into account.

The model is usually calibrated to measured maximum subsidence values by adjusting key parameters such as influence angles and inflexion point location from extracted panel sides.

### A8.2 Tilt and Curvature Contours

The predicted principal tilt and curvature contours were derived using the calculus module of the Surfer8® program and the predicted subsidence contours from the SPDS® runs. The subsidence contours were based on a 10 m grid.

Principal tilts (i.e. surface gradient or slope) were calculated by taking the first derivative of the subsidence contours in x and y directions as follows:

$$T_p = [(\partial s / \partial x)^2 + (\partial s / \partial y)^2]^{0.5}$$

where  $\partial s$  = subsidence increment over distances  $\partial x$  and  $\partial y$   
along x and y axes.

Principal curvatures (i.e. rate of change in slope or surface bending) were calculated by taking the second derivative of the subsidence contours in x and y directions as follows:

$$C_p = [(\partial^2 s / \partial x^2)(\partial s / \partial x)^2 + 2(\partial^2 s / \partial x \partial y)(\partial s / \partial x)(\partial s / \partial y) + (\partial^2 s / \partial y^2)(\partial s / \partial y)^2] / pq^{2/3}$$

where  $p = (\partial s / \partial x)^2 + (\partial s / \partial y)^2$  and  $q = 1 + p$

### A8.3 Strain

Before predictions of strain can be made, the relationship between the measured curvatures and strain must be understood. As discussed in **NERDDP, 1993b** and **ACARP, 2003**, structural and geometrical analysis theories indicate that strain is linearly proportional to the curvature of an elastic, isotropic bending ‘beam’; see **Figure A28**. This proportionality

actually represents the depth to the neutral axis of the beam, or in other words, half the beam thickness. **NERDDP, 1993b** studies returned strain over curvature ratios ranging between 6 and 11 m for NSW and Queensland Coalfields. Near surface lithology strata unit thickness and jointing therefore dictate the magnitude of the proportionality constant between curvature and strain.

**ACARP, 2003** continued with this approach and introduced the concept of secondary curvature and strain concentration factors due to cracking. The peak strain / curvature ratio for 'smooth' subsidence profiles in the Newcastle Coalfield was assessed to equal 5.2 m (mean) and 7.8 m (U95%CL) with the possibility that surface cracking could increase the 'smooth-profile' strains to 10 or 15 times the curvature. The above values may also be affected by the thickness of near surface geology.

Reference to **DMR, 1987** also suggests a curvature to strain multiplier of 10 for high pillar extraction and longwall panels in the Newcastle Coalfield.

Attempts by others to reduce the variability in strain and curvature data by introducing additional parameters, such as the radius of influence,  $r$ , by **Karmis et al, 1987** and cover depth,  $H$ , by **Holla and Barclay, 2000**, appear to have achieved moderate success in the coalfields in which they were applied. However, when these models were applied to the Newcastle Coalfield data presented in **ACARP, 2003**, the results did not appear to improve things unfortunately; see **Figures A29.1** and **A29.2**.

It is therefore considered that the variability in behaviour is probably due to other parameters, which are very difficult to measure (such as the thickness and flexural, buckling and shear strengths of the near surface strata).

Provided that the likelihood of cracking can be ascertained from the strain predictions, then appropriate subsidence management plans can still be implemented.

## **A9 Prediction Of Subsidence Impact Parameters And Uncertainty Using Regression Analysis Techniques**

### **A9.1 Regression Analysis**

Key impact parameters have been predicted using normalised longwall subsidence data from the Newcastle Coalfield. This approach allows a reasonable assessment of the uncertainty involved using statistical regression techniques. A linear or non-linear regression line has been fitted to the database for each impact parameter, normalised to easily measured parameters, such as maximum subsidence, panel width and cover depth. The quality or significance of the regression line is influenced by the following parameters:

- (i) the size of the database,
- (ii) the presence of outliers, and
- (iii) the physical relationship between the key parameters.

The regression curves were reviewed carefully, as such curves can be (i) affected by outliers, and (ii) misleading, in that by adopting a mathematical relationship which gives the best fit (i.e.  $R^2$ ) the curves are controlled by the database and may not reflect the true underlying physical dependencies or mechanisms that the data represents.

These issues are inherent in all prediction modelling techniques because, for example, all models must be calibrated to field observations to validate their use for prediction or back analysis purposes.

The regression techniques presented in the **ACARP, 2003** was done by firstly assessing conceptual models of the mechanics and key parameter dependencies (based on established solid mechanics and structural analysis theories), before generating the regression equations.

Several outliers in the model databases were excluded in the final regression equations, but only when a reasonable explanation could be given for each anomaly (i.e. multiple seam subsidence, geological faults and surface cracking effects).

The regression equations in **ACARP, 2003** have  $R^2$  (i.e. Coefficients of Determination) values generally greater than 50%; indicating that the relationships between the variables are significant. For cases where the  $R^2$  values are < 50%, the regression lines are almost horizontal (i.e. the parameter doesn't change significantly over the range of the database), and the use of the regression line will be close to the mean of the database anyway.

### **A9.2 Prediction Model Uncertainty**

The level of uncertainty in the model predictions has been assessed using statistical analysis of the residuals or differences between the measured data and regression lines (i.e. lines of best fit). The *Standard Error* of the prediction has been derived from the



residuals, which has then been multiplied by the appropriate 'z' or 't' statistic for the assumed normal probability distribution, to define Upper (and Lower) Confidence Limits.

The residual population errors for single panel subsidence are shown in **Figure A30**.

The empirical database therefore allows an assessment of variance and standard error such that the required subsidence parameter's mean and upper 95% Confidence Limit (Credible Worst Case) values can be determined for a given mining geometry and geology.

Provided there are (i) more than 10 data points in the data sets covering the range of the prediction cases, and (ii) the impact parameter and independent variables have an established physical relationship based on solid or structural mechanics theories, then it is considered unlikely that the regression lines will be significantly biased away from the underlying physical relationship between the variables by any limitations of the data set.

On-going review of each of the regression equations over the past six years by DgS has not required significant adjustment of the equations to include new measured data points. The regression equations derived are also amenable to spreadsheet calculation and program automation.

It is also important to make the distinction between the terms confidence *limit* and confidence *interval*. The Credible Worst Case terminology used in the model is **not** the upper limit of the 95% Confidence **Interval** - which would encompass 95% of the data. Since the lower 95% Confidence Limit is rarely used in practice, it was considered appropriate to adopt the 5% Probability of Exceedence values instead (this by definition represents the upper limit of the **90% Confidence Interval**).

Further, the term *Upper 95% Confidence Limit* used in the **ACARP, 2003** model is considered acceptable in the context of 'one-tailed' probability distribution limits (i.e. the Lower 95% Confidence Limit is generally of little practical interest).

## **A10 Subsidence Model Validation Studies**

### **A10.1 Model Development**

The **ACARP, 2003** model was developed such that the outcomes would re-predict > 90% of the database. Validation studies also included comparison of measured and predicted subsidence, tilt and strain profiles above several longwall panel crosslines and centrelines. Examples of predicted and measured profiles above multiple panels for the Newcastle Coalfield are shown in **Figures A31 to A34** using the **ACARP, 2003** model. Subsequent predictions v. measured subsidence profiles are presented in **Figures A35 to A38** using the updated version of the model discussed herein.

DgS is usually required to review predicted v. measured subsidence profiles after the completion of a longwall panel and report the results to DPI. Over the past six years, the model has generally over predicted measured subsidence, with the data falling somewhere between the mean and U95%CL values.

The predictions of curvature and strain, however, are generally problematic due to the common effects of discontinuous or cracking behaviour (i.e. lithological variation and cracking), resulting in measured strains that can be two to four times greater than predicted 'smooth' profile strains. This issue is discussed further in **Section A10.2**.

### **A10.2 Field Testing of Strain Predictions**

Strain and curvature concentrations can increase 'smooth' profile strains by 2 to 4 times in the Newcastle Coalfield, when the panel width to cover depth ratio (W/H) exceeds 0.8 or radius of curvature is less than 2 km, see **ACARP, 2003**.

In the context of subsidence surveys, the definition of strain is the change in length (extension or compression) of a bay-length, divided by the original value of the bay length.

Where cracking occurs, measured strains will be highly dependent on the bay-length, and where rock exposures exist with widely spaced or adversely orientated jointing exist, much larger crack widths (than for the deep soil profile case) can occur.

For example, for a measured strain of 3 to 6 mm/m along a recently observed cross line above a longwall panel in the Newcastle area, several cracks developed in the soil surface, which ranged in width between 10 and 30 mm, whilst within 10 m of the area, a single 100 mm wide crack developed in a sandstone rock exposure of medium strength and with widely spaced jointing, see **Figure A39**.

At the moment, it is not possible to predict the magnitude of strains accurately, however, it is possible to make reasonable predictions that strains > 2 mm/m will cause cracking within the tensile strain zones and shearing, buckling within the compressive zones above a longwall with shallow surface rock. The strains and cracking can therefore be managed effectively by assuming cracks will occur and may need to be repaired after each longwall is completed.

## **A11 Sub-Surface Fracturing Model Development Outcomes**

### **A11.1 Whittaker and Reddish Physical Model**

It is considered that the published physical modelling work in **Whittaker and Reddish, 1989** provides valuable insight into the mechanics of sub-surface fracturing over longwall panels. The outcomes included specific guidelines (over and above such work as the Wardell Guidelines) for the prevention of inundation of mine workings beneath surface and sub-surface water bodies.

Their model was developed in response to the water ingress problems associated with early longwall extraction at the Wistow Mine in Selby, UK. The longwall panel was located at 350 m depth and experienced groundwater inflows of 121 to 136 litres/sec when sub-surface fracturing intersected a limestone aquifer 77 m above the seam.

The model identifies two distinct zones of fracturing above super-critical width extractions (continuous and discontinuous fracturing) and relates the height of each to “measured maximum tensile strain at the surface”. As such, its use is also based upon being able to make credible subsidence predictions. The basis of the model is summarised in **Figure A40**.

The definition of the extent of ‘continuous’ fracturing refers to the height at which a direct connection of the fractures occurs within the overburden and the workings; it represents a ‘direct’ hydraulic connection for groundwater inflows.

The definition of the extent of ‘discontinuous’ fracturing refers to the height at which the horizontal permeability increases as a result of strata de-lamination and fracturing. Direct connection of fractures within the overburden and workings is still considered possible, but will depend on the geology (e.g. massive units and / or the presence of persistent vertical structure, such as faults and joints).

A review of the methodology applied to develop the model and its key features are summarised below:

- The model was based on laboratory experiments of longwall extraction physical models.
- The physical model was constructed from multiple layers of coloured sand and plaster fixtures, with sawdust bond breakers placed between each successive layer. The model was initially devoid of vertical joints.
- The scale and mechanical properties of the model satisfied dimensional analysis and similtude laws.

The model was used to simulate the overburden behaviour of a panel with a W/H ratio of 1.31 and a progressively increasing working height range that commenced at 1.2 m and finished at 10.8 m. The advancing longwall face was simulated by removing timber blocks at the base of the model in 1.2 m to 2.0 m lift stages.

The extent or heights of ‘continuous’ and ‘discontinuous’ fracturing above the longwall ‘face’ was measured and plotted with the associated peak tensile strain predictions at the surface.

The fracturing path progressed up at an angle from the solid rib and inwardly towards the centre of the panel; see **Figure A40**.

The fracturing in question occurred close to the rib-side only, as fracturing in the overburden above the middle portion of the panel tended to ‘close’ and did not appear to represent an area in which groundwater inflows into the workings would be generated.

Any inflow conditions were therefore considered to be “mainly associated with the longwall rib-side fracture zone [or tensile strain zone]”.

A case study at Oaky Creek Colliery in the Bowen Basin was presented in Colwell, 1993; this attempted to calibrate the Whittaker and Reddish model with actual drilling and strain measurement data. Three fully cored boreholes were drilled over previously extracted longwall panels with a W/H ratio of 2.11 and strain measurement data was obtained from a nearby operating panel with a W/H of 1.37. The results of the study were very positive and have been subsequently collated with further case histories in **Section A8.2**.

#### **A11.2 Preliminary Sub-Surface Fracturing Prediction Model For Australian Coalfields**

The database of drilling data from previously published documents is summarised ACARP, 2003. Australian data was initially plotted with the UK Model results and a regression analysis was used to define a convenient relationship between the parameters and assessing whether other parameters of significance could be identified.

The results are presented in **Figure A41** and summarised below:

$$\{ \text{A-Line} \} \quad A = a/H = 0.2077 \ln(E_{\max}) + 0.150, \quad R^2 = 0.44$$

$$\{ \text{B-Line} \} \quad B = b/H = 0.1582 \ln(E_{\max}) + 0.651, \quad R^2 = 0.49$$

where

a, b = height above workings to A and B Horizons,

H = cover depth,

$E_{\max}$  = the maximum predicted tensile strain for a ‘smooth’ profile,

The Australian database appears to be similar to the Whittaker and Reddish model, however the predicted surface strains are much lower for a given height of ‘continuous’ and ‘discontinuous’ fracturing above the workings. It is also apparent that the model relies on the measured surface strain data, which has been noted previously for its high variability.

To overcome this issue it was decided to re-plot the database using the previously derived  $S_{\max}/W'^2$ , term to provide a readily measurable field parameter that would not be compromised by surface strain concentration effects. The revised regression results are shown in **Figure A42** and summarised below:

$$\{\text{A-Line}\} A = a/H = 0.2295 \ln(S_{\max}/W'^2) + 1.132, R^2 = 0.44;$$

$$\{\text{B-Line}\} B = b/H = 0.1694 \ln(S_{\max}/W'^2) + 1.381, R^2 = 0.46;$$

where

a, b = height above workings to A and B Horizons,  
 H = cover depth (m).  
 $S_{\max}/W'^2$  = Overburden Curvature Index,  
 W' = lesser of W and 1.4H

Based on the alternative approach, the same apparent differences still remain between the Australian height of fracturing database and the UK physical modelling results. The apparent discrepancies between the model and measured values indicate that there are fundamental differences present (i.e. in particular the physical model had no preexisting subsurface fracturing present).

The A and B horizons in the sub-surface fracturing model presented in **Whittaker and Reddish, 1989** also appear to be the similar in regards to definition to the heights to the top of the 'Fractured Zone' and 'Constrained Zone' above an extracted longwall panel defined in **Forster, 1993**. There is also a departure in this model from assessing heights of fracturing based on the extraction height only, although the predicted tensile strain or  $S_{\max}$  is directly related to the extraction height. It is considered that sub-surface fracture heights are a function of overburden bending and therefore primarily a function of the significant geometrical parameters  $S_{\max}$ , W, H and T. The influence of massive lithology is included in the  $S_{\max}$  prediction.

Overall, the **ACARP, 2003** sub-surface fracturing model was considered preliminary, more drilling data was required. The heights of fracturing derived, however, did appear to be conservative based on reference to several NSW and Queensland case studies.

It was also noted in **ACARP, 2003** that future calibration work on the model would be required to improve confidence in its use.

### A11.3 Influence of Geology on Sub-Surface Fracture Heights

For the purposes of study completeness, an assessment was made on whether the geology had the potential to control or limit the height of fracturing above a longwall panel. Reference to the database presented in **ACARP, 2003**, indicates that two of the case studies were assessed to have High SRP and had A Horizons that coincided with the base of the massive strata units. The other data points had low SRP with no massive units present.

The massive strata unit affected data, however, did not appear to plot at lower than predicted levels compared to the low SRP cases, although this observation was based on a small sample of data. At this stage, the potential for a spanning strata unit to mitigate the height of continuous fracturing above the workings cannot be ignored.

Overall, the results suggest that the presence of massive sandstone or conglomerate lithology could control the height of direct hydraulic fracturing. Due to the complex nature of this problem, it is usually recommended that a mine undertake a sub-surface fracture-monitoring program, which includes a combination of borehole extensometer and piezometer measurements during extraction in non-sensitive areas of the mining lease. Mitigation strategies for longwall mining are generally limited to (i) reducing the extraction height and (ii) decreasing the panel width.

## A12 Far-Field Displacements and Strain Predictions

### A12.1 Background

The term far-field displacements (FFD) generally refer to the horizontal surface movements that occur outside the vertical subsidence limit or angle of draw to an extracted pillar panel or longwall block. It is currently understood that FFDs are a phenomenon caused by the reduction of horizontal stress when collapse of overburden rock (i.e. goafing) occurs above an extracted area. There also appears to be a strong correlation between the FFDs and the surface subsidence magnitude (which is also an indicator of horizontal stress relief). A conceptual model of the mechanics of FFDs is presented in **Figure A43**.

Horizontal stress in rock is normally greater than the vertical stress at a given depth of cover; it has been 'locked' into the strata by tectonic movements and over-consolidation pressures (i.e. stress). Over-consolidation stresses occur in sedimentary rock after uplift and erosion over millennia has gradually removed the overlying material since the time of formation. Tectonic induced stress usually results in strong directional bias between the major and minor principal stress magnitudes, with variation due to stiffness of the lithological units as well (refer to **Nemcik et al, 2005, Pells, 2004, McQueen, 2004, Enever, 1999 and Walker, 2004**).

It is considered that both of the abovementioned horizontal stress development mechanisms are likely to be present in the near surface rocks in the western area of the Newcastle Coalfield.

FFD's have only recently become an issue in the Newcastle Coalfield because of adverse surface impact experiences in the Southern Coalfield (e.g. horizontal movements of around 25 mm have been measured over 1.5 km away from extracted longwall panels on a concrete dam wall. No cracking damage occurred to the dam wall because of these movements however).

The strains associated with FFDs are usually very low, however, there is one case in the Southern Coalfield where a bridge was subject to lateral shearing of approximately 50 mm along the river bed axis.

To-date, it is understood that there are no precedents in the Newcastle Coalfield where similar FFD effects (measured or inferred via damage) have occurred around longwalls or total extraction panels. Horizontal movements have been measured outside the angle of draw limits from mine workings however, albeit at smaller distances and magnitudes (eg. 20 mm of horizontal movement has been measured in undulating terrain at 250 m from one longwall block where the cover depth was 135 m).

The horizontal stress in the Newcastle Coal Measures has been measured at several locations along the F3 Freeway to the west of Wyong and Newcastle (**Lohe and Dean-Jones, 1995**). The magnitude of the measured horizontal stress indicates that it is relatively high, with magnitudes that are 1.5 to >5 times the vertical stress, in relatively flat or moderately undulated terrain.

The major principal horizontal stress is usually orientated N to NE in the Western Newcastle Coalfield, but it can be re-orientated parallel to the axis of a ridge due to natural weathering processes near the surface (which cause lateral unloading towards the gullies); refer to **Lohe and Dean Jones, 1995**.

## A12.2 Insitu Stress Field

Reference to stress measurement data in **Lohe and Dean-Jones, 1995** indicates that the 'shallow' (ie < 100 m below the surface) regional stress field in the undulating terrain along the eastern and eastern sides of Lake Macquarie is likely to have it's major principal horizontal stress > 5 x vertical stress (and assuming horizontal stress is zero at the surface). Deeper strata at depths > 150 m is likely to have it's major principal horizontal stress <2 x vertical stress.

The stress data from the above reference was measured using over-coring / HI-Cell techniques and is presented in Table A4.

**Table A4 - Horizontal Stress Field Measurements in Newcastle Coalfield Relevant to Tasman**

Location	Depth (m)	In-situ Stress Measurements*			
		Major Sigma 1 (MPa)	Minor Sigma 2 (MPa)	Vertical Sigma 3 (MPa)	Sigma1+/ Sigma 3
Wakefield	24	10.4	0.42	0.6	17.3
Wallsend Borehole	100	13.3	9.7	2.5	5.3
West Wallsend No. 2	190	27.4	20.3	4.75	5.8
Kangy Angy	70	11.8	4.2	1.75	6.7
Moonee	90	11.7	8.3	2.25	5.2
West Wallsend	170	6.4	n/a	4.25	1.5
Ellalong	320	6.5	4.6	8.0	0.8

\* - All measurements in medium strength sandstone.

+ - ratio assumes horizontal stress is zero at the surface (which is not always correct).

The shallow stress data is plotted in **Figure A44** and indicates that the major principal horizontal stress could be as high as 6 MPa at the surface (unless weathered rock and soil is present) with the Major and Minor Principal Horizontal stresses equal to approximately 4 times the vertical stress for depths up to 250 m.

This high Sigma 1 reading, however, may be associated with a sandstone / conglomerate ridgeline and not typical for the areas away from ridgelines (although a residual 'surface' horizontal stress range from 1.5 to 6.5 MPa has also been assessed for the Sydney Metropolitan area in **McQueen, 1999** and **Pells, 2002**).

Another commonly used assumption in the NSW Coalfields is that the major principal horizontal stress is approximately 2 x the vertical stress and the minor principal horizontal stress is 1.4 ~ 1.5 x the vertical stress (or the Major Principal Horizontal Stress is 1.33~1.4 x



the Minor Principal Horizontal Stress). It is also acknowledged that the horizontal stress in the Newcastle and Sydney areas can be 4 to 5 times the vertical stress, based on shallow rock mass data at depths < 50 m; refer to **Lohe and Dean Jones, 1995**. The sources of this stress field imbalance has been explained in **Enever, 1999**, **Pells, 2002** and **Fell *et al*, 1992** as being due to:

- (i) the 'overconsolidation' ratio; where the vertical pressure due to ancient surface at the time of consolidation has since been eroded away, leaving a 'locked' in horizontal stress component in today's sedimentary rock mass. The OCR can be shown to decrease exponentially with depth and is equal in all directions at a given point.
- (ii) Tectonic strain; where crustal plate movements apply a strain to the rock mass and the resultant stress is dependent on the stiffness of the individual beds and direction of movement.
- (iii) Geological structure (faults/dykes); where discontinuities can change the magnitude and orientations of the regional stress field significantly.
- (iv) Topographic relief (ridges/valleys/gorges); where the magnitude and direction of the regional stress field can vary due to geometric affects.

The influence of underground mining can also result in changes (both increases and decreases) in horizontal and vertical stress field magnitudes as the rock mass adjusts to a new equilibrium state.

Based on the measured stress conditions, the horizontal stress magnitudes may be estimated based on the equations presented in **Nemcik et al, 2005**:

$$\sigma_H = K\sigma_v + E\varepsilon = \sigma_v [(v/1-v)OCR] + E\varepsilon$$

$$\sigma_h = f(\sigma_H) \text{ and } \sigma_v = 0.025H \text{ (MPa)}$$

where,

$\sigma_H$  = Major Horizontal Principal Stress;

$\sigma_h$  = Minor Horizontal Principal Stress;

$\sigma_v$  = Vertical Stress;

$v$  = Poisson's Ratio (normally ranges between 0.15 and 0.4 in coal measure rocks);

$(v/1-v)$  = Horizontal to vertical stress ratio factor ( $K_o$ ) due to Poisson's Ratio effect on its own;

OCR = The over-consolidation ratio, which relates vertical pre-consolidation pressure ( $\sigma_{vo}$ ) with current vertical pressure ( $\sigma_v$ ) as follows,  $OCR = \sigma_{vo}/\sigma_v = H_o/H$ .

*(Note: This is an additional term that has been introduced by DgS, and has been mentioned (but not derived) in Pells, 2002 and calculated in Fell et al, 1992).*

E = Young's Modulus for rock-mass unit;

$\varepsilon$  = Tectonic Stress Factor (TSF) or Tectonic Strain.

Due to the wide range of horizontal stress values noted in the literature, it is recommended that the horizontal stress magnitudes be measured in-situ at several lithological horizons before high extraction mining commences.

Based on the apparent complexity and large variation between the interpretations of published stress field data, it was considered necessary to conduct a sensitivity analysis on the stress field profiles during the calibration of Map-3D<sup>®</sup> using the flat terrain data (see **Section A12.3** for details).

Total horizontal displacement measurements outside the ends and corners of several longwall panels in the Newcastle Coalfield (Newstan and West Wallsend Collieries), have been plotted against distance from the panel goaf edge / cover depth at the panel; refer to **Figure A45**.

Curves of best fit have been fitted to identify data trends from various locations from the ends and corners of the panels (note: the movements outside the corners of a longwall are typically smaller than the panel ends). The data has been obtained using GPS / EDM traverse techniques with quoted accuracy limits of +/- 7 to 10 mm.

The data in **Figure A45** has also been normalised to maximum measured subsidence ( $S_{\max}$ ) above a given panel and is presented in **Figure A46**. It is considered that presenting the data in this format allows all of the available data to be used appropriately to make subsequent FFD predictions.

The data presented in **Figures A47** was measured from the sides of several longwall panels using in-line, steel tape measurements. This method is considered more accurate than the EDM techniques, however, they do not capture all of the displacement. The measured values have subsequently been adjusted to absolute movements, based on the EDM measurements presented in **Figures A45** and **A46**.

A combined graph of normalised total displacement data from the ends and sides of the longwall panels is presented in **Figure A48** with worst-case design curves from ends, corners and sides of a longwall panel for flat terrain conditions.

The empirical models may be used for calibrating the numerical models input parameters when proposed mining layouts and topographical conditions are considered to be well outside the available database (see **DgS, 2007**).

### A12.3 Numerical Far-Field Displacement Modeling

The numerical modelling program Map-3D<sup>®</sup> has been applied at several mines in the Newcastle Coalfield to-date for the purposes of estimating FFD movements. The model was chosen mainly due to its suitability for modelling large-scale rock masses.

The program is a 3-dimensional elastic, isotropic, boundary-element model, which essentially starts with an infinite solid space and calculates the effects of excavations, geological structure, varying material types, and free-surfaces on the regional stresses and strains. Further details about the software can be found at the Map-3D<sup>®</sup> web site.

The model is firstly calibrated to measured displacement data for a given mining geometry, regional horizontal stress field and surface topography. The Young's Modulus or stiffness of the overburden is then adjusted above an extracted panel (or panels) and assumed caving zone until a reasonable match is achieved.

Although the empirical models indicate that subsidence is a key parameter for predicting FFDs, numerical modelling of horizontal stress relief effects does not require the subsidence above the panels to be matched (by the model) because the extraction of coal and subsequent goafing behaviour can be calibrated to measured far-field displacements instead. Therefore, the modelling outcomes are not linked to the modelled subsidence directly.

Non-linearity can be introduced into the model to analyse the effects of fault planes and bedding using displacement-discontinuity elements with normal and shear stiffness and Mohr-Coulomb friction and cohesive strength properties.

Multiple mining stages and irregular topography can also be defined to enable mechanistic extrapolation of existing empirical databases with a reasonable degree of confidence.

An example of a predicted far-field displacement pattern around a high extraction pillar panel mine is presented in **Figure A49**.

### A12.5 Empirical Strain Prediction Model

Strain measurements from the side of several longwall panels from West Wallsend and Newstan Collieries and were also normalised to maximum panel subsidence. The data are presented in **Figure A50**.

Several curves are shown with the data in the above figure, one is the best-fit or mean curve and two are upper limit confidence limit curves for the data (U95%CL and U99%CL). The confidence limit curves have been defined using weighted non-linear statistical techniques and the residual errors about the mean curve.

## A13 References

- ACARP, 1998a. **Chain Pillar Design (Calibration of ALPS)**. ACARP Project No. C6036, Colwell, M. Colwell Geotechnical Services.
- ACARP, 1998b, **Project No. C5024, Establishing the Strength of Rectangular and Irregular Pillars**. J.M.Galvin, B.K. Hebblewhite, M.D.G. Salamon and B.B.Lin. School of Mining, UNSW.
- ACARP, 2003. **Review of Industry Subsidence Data in Relation to the Impact of Significant Variations in Overburden Lithology and Initial Assessment of Sub-Surface Fracturing on Groundwater**. ACARP Project No. C10023. S. Ditton and R. Frith, Strata Engineering Report No. 00-181-ACR/1.
- Colwell, 1993. **Water Inflow Investigation for a Longwall Operation**. M. Colwell. Published in Queensland Coal Geology Groups Conference Proceedings, New Developments in Coal Geology, Brisbane.
- DgS, 2007. **Prediction of Far-Field Displacements Due to Pillar Extraction or Longwall Mining in Mountainous Terrain**. S. Ditton. Proceedings of the 7<sup>th</sup> Triennial MSTs Conference on Mine Subsidence, University of Wollongong (November 26-27)
- DMR, 1987. **Mining Subsidence in NSW: 2. Surface Subsidence Prediction in the Newcastle Coalfield**. L. Holla. Department of Minerals Resources (June).
- Enever, 1999. **Near Surface In-situ Stress and its Counterpart at Depth in the Sydney Metropolitan Area**. Enever, J.R. Published in Australian Geomechanics Society (AGS) Conference Proceedings of the 8<sup>th</sup> Annual Conference on Geomechanics, Hobart.
- Fell *et al*, 1992. **Geotechnical Engineering of Embankment Dams**. Fell, R., MacGregor, P. and Stapledon, D.A.A. Balkema.
- Forster, 1995. **Impact of Underground Coal Mining on the Hydrogeological Regime, Central Coast, NSW**. I.R. Forster. Published in Australian Geomechanics Society (AGS) Conference Proceedings (February), Engineering Geology of Newcastle – Gosford Region, University of Newcastle.
- Holla and Barclay, 2000. **Mine Subsidence in the Southern Coalfield**. L.Holla and E.Barclay. Department of Minerals Resources (June).
- Karmis, et al, 1987. **Surface Deformation Characteristics Above Undermined Areas: Experiences from the Eastern United States Coalfields**. M. Karmis, A. Jarosz, P. Schilizzi & Z. Agioutantis. Published in Civil Engineering Transactions Journal, Institution of Engineers, Australia.
- Lohe and Dean-Jones, 1995. **Structural Geology of the Newcastle-Gosford Region**. E.M. Lohe and G.L. Dean-Jones. Published in Australian Geomechanics Society (AGS)

Conference Proceedings (February), Engineering Geology of Newcastle – Gosford Region, University of Newcastle.

McQueen, 2004. **In-situ Rock Stress and Its Effect in Tunnels and Deep Excavations in Sydney**. McQueen, L.B. Article presented in Australian Geomechanics Journal Vol 39. No. 3 (September).

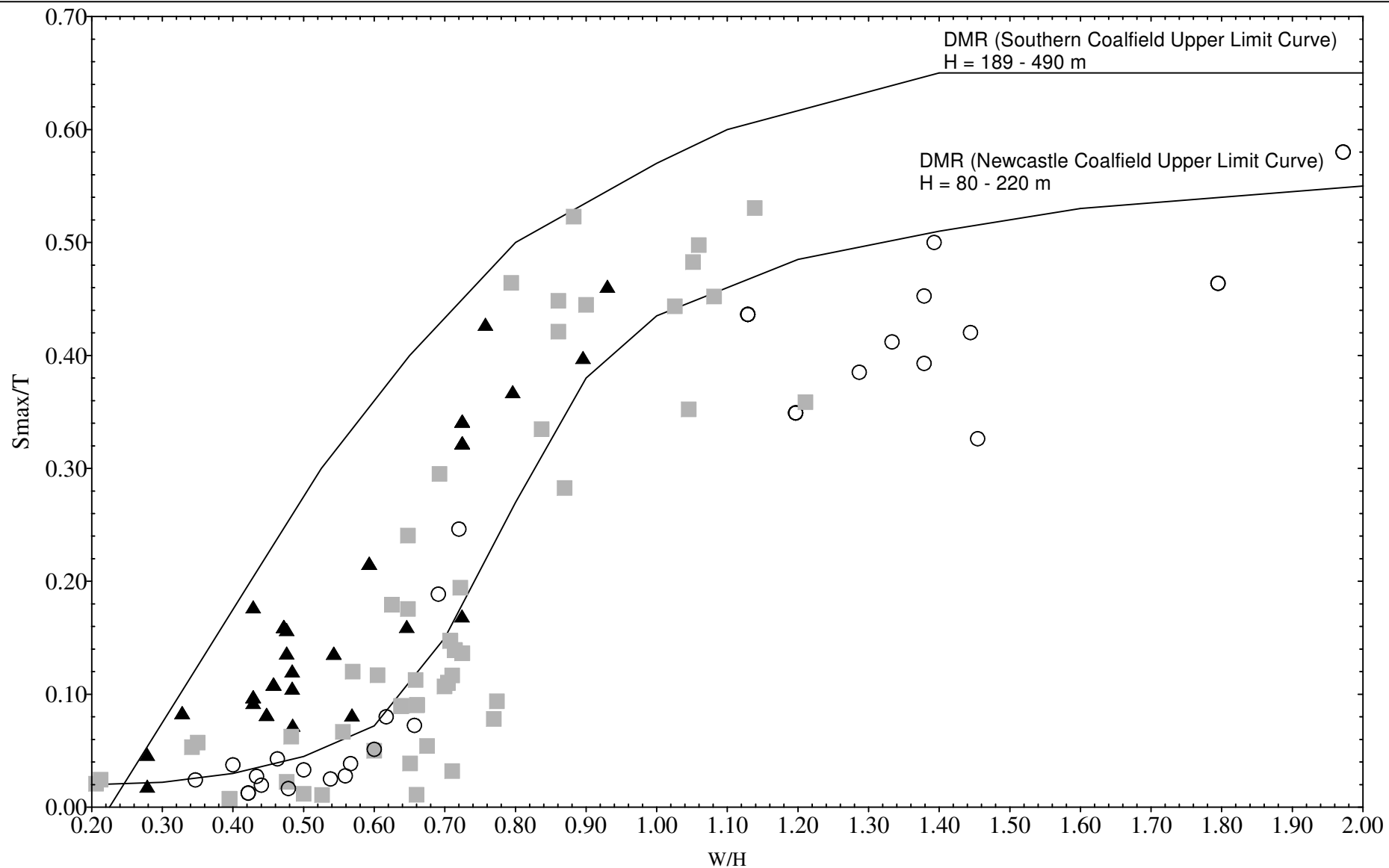
Nemcik et al, 2005. **Statistical Analysis of Underground Stress Measurements in Australian Coal Mines**. Nemcik, J., Gale, W. and Mills, K. Published in proceedings of the Bowen Basin Geology Symposium.

Pells, 2002. **Developments in the Design of Tunnels and Caverns in the Triassic Rocks of the Sydney Region**. International Journal of Rock Mechanics and Mining Sciences No. 39. Pells, P.J.N.


Pells, 2004. **Substance and Mass Properties for the Design of Engineering Structures in the Hawkesbury Sandstone**. Article presented in Australian Geomechanics Journal Vol 39. No. 3 (September).

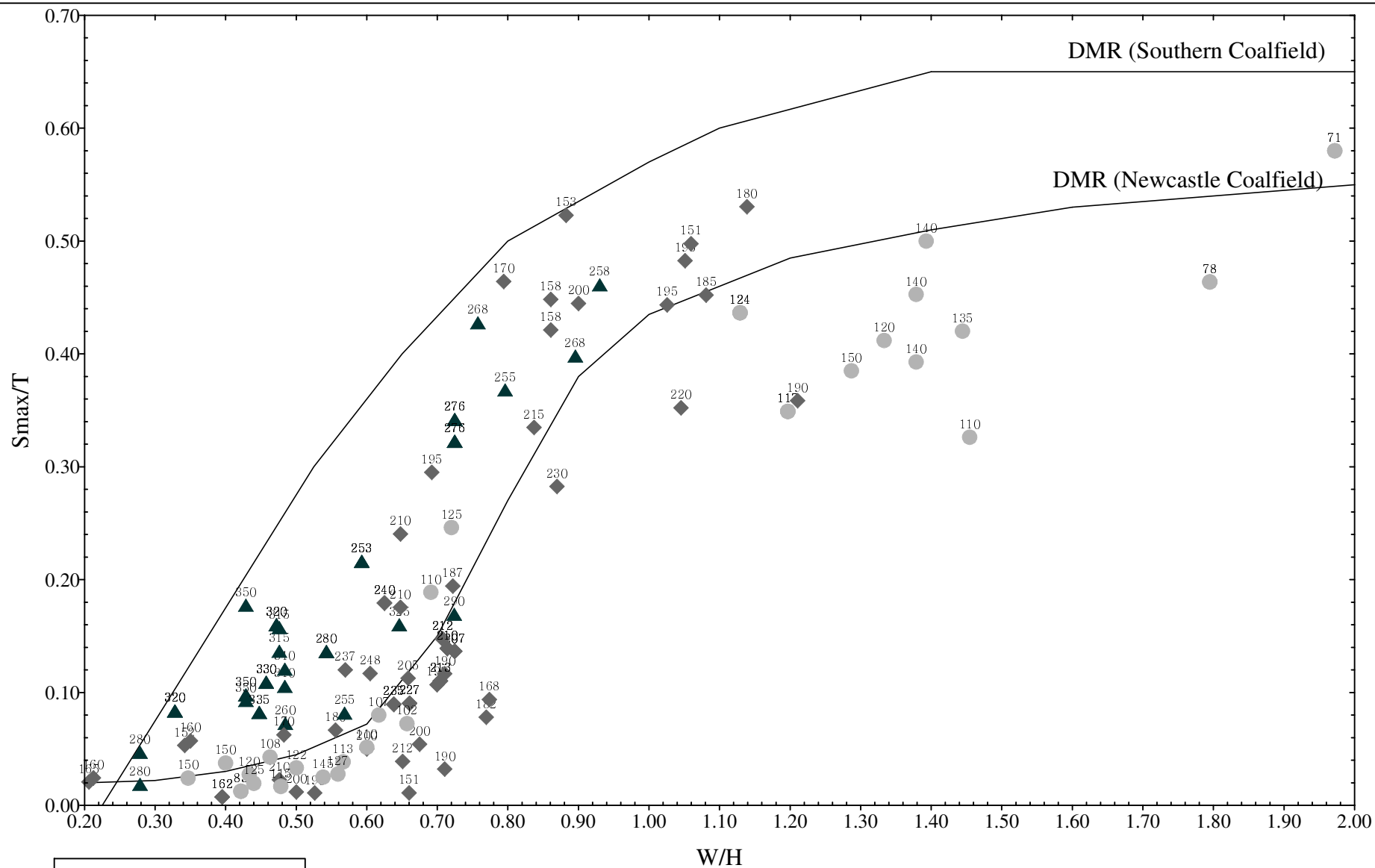
Walker, 2004. **Stress Relief on Hillsides and Hillside Excavations**. Walker, B.F. Article presented in Australian Geomechanics Journal Vol 39. No. 3 (September).

Whittaker & Reddish, 1989. **Subsidence, Occurrence, Prediction and Control**. B. N. Whittaker and D.J. Reddish. Department of Mining Engineering, University of Nottingham, UK.



LEGEND	
Cover Depth, H (m)	
○	H = 70m to H = 151m
■	H = 151m to H = 251m
▲	H = 251m to H = 350m

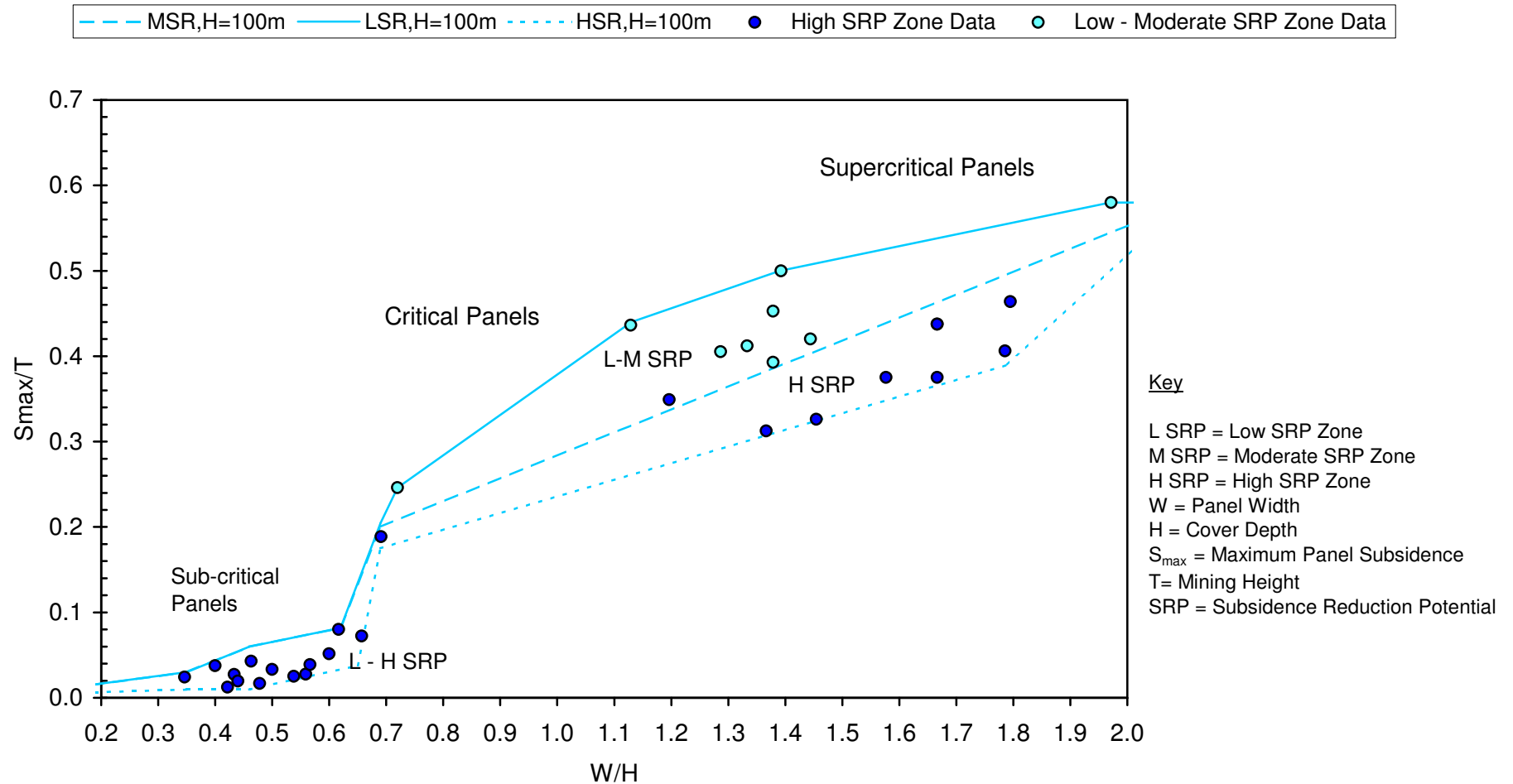
	Engineer:	S.Ditton	Client:	Adapted from ACARP, 2003			
	Drawn:	S.Ditton					
	Date:	08.06.08	Title:	Project Database and DMR Subsidence Prediction Curves for Single Longwall Panels in Newcastle Coalfield			
	Ditton Geotechnical Services Pty Ltd						
			Scale:	NTS		Figure No:	A1




LEGEND	
Data Point	
Cover Depth, H (m)	
	H = 70m to H = 151m
	H = 151m to H = 251m
	H = 251m to H = 350m



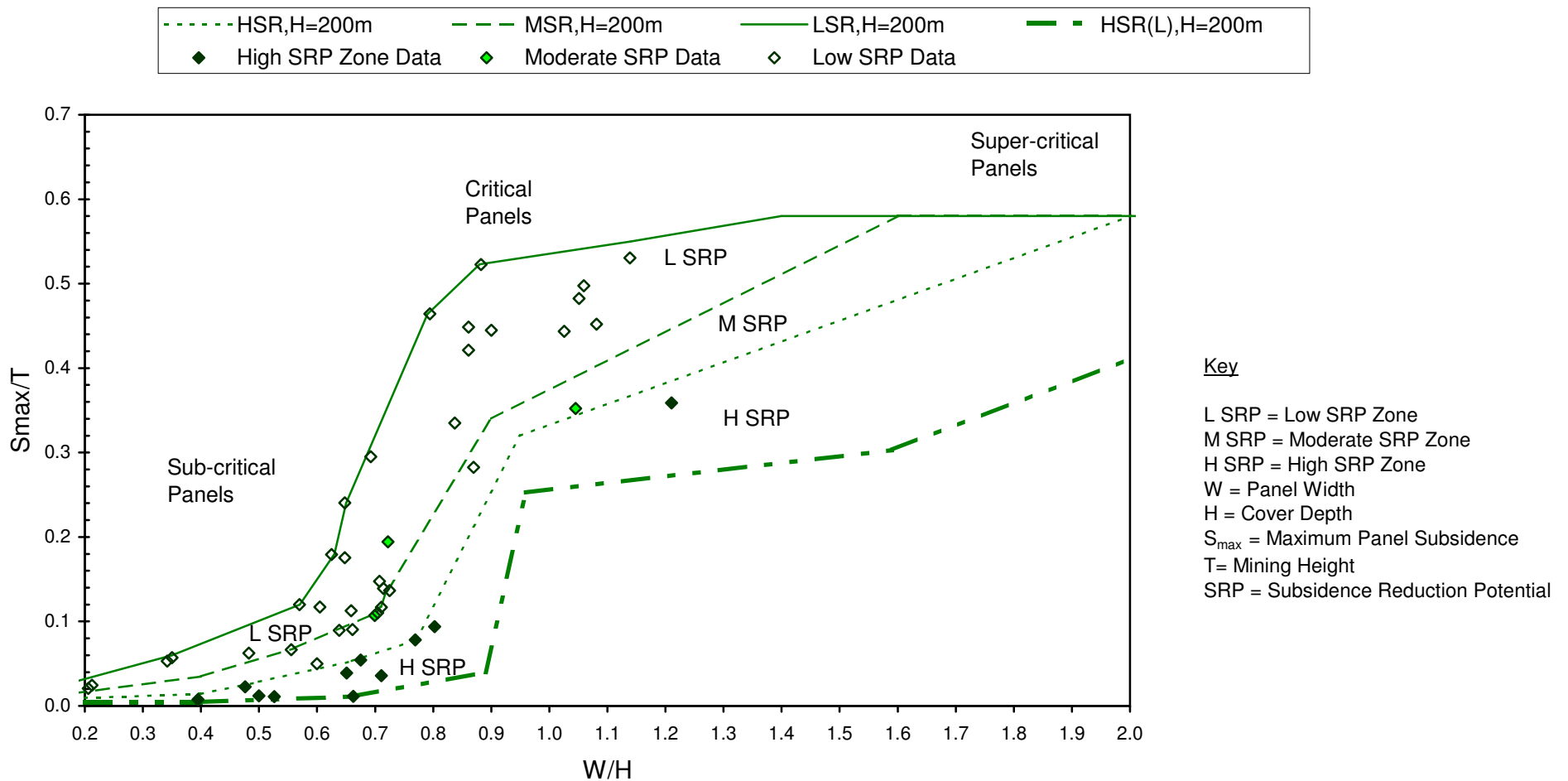
Engineer:	S.Ditton	Client:	Adapted from ACARP , 2003		
Drawn:	S.Ditton				
Date:	08.06.08				
Ditton Geotechnical Services Pty Ltd		Title:	Project Database for Single Longwall Panels in Newcastle Coalfield showing Cover Depth for Each Point		
		Scale:	NTS		Figure No:




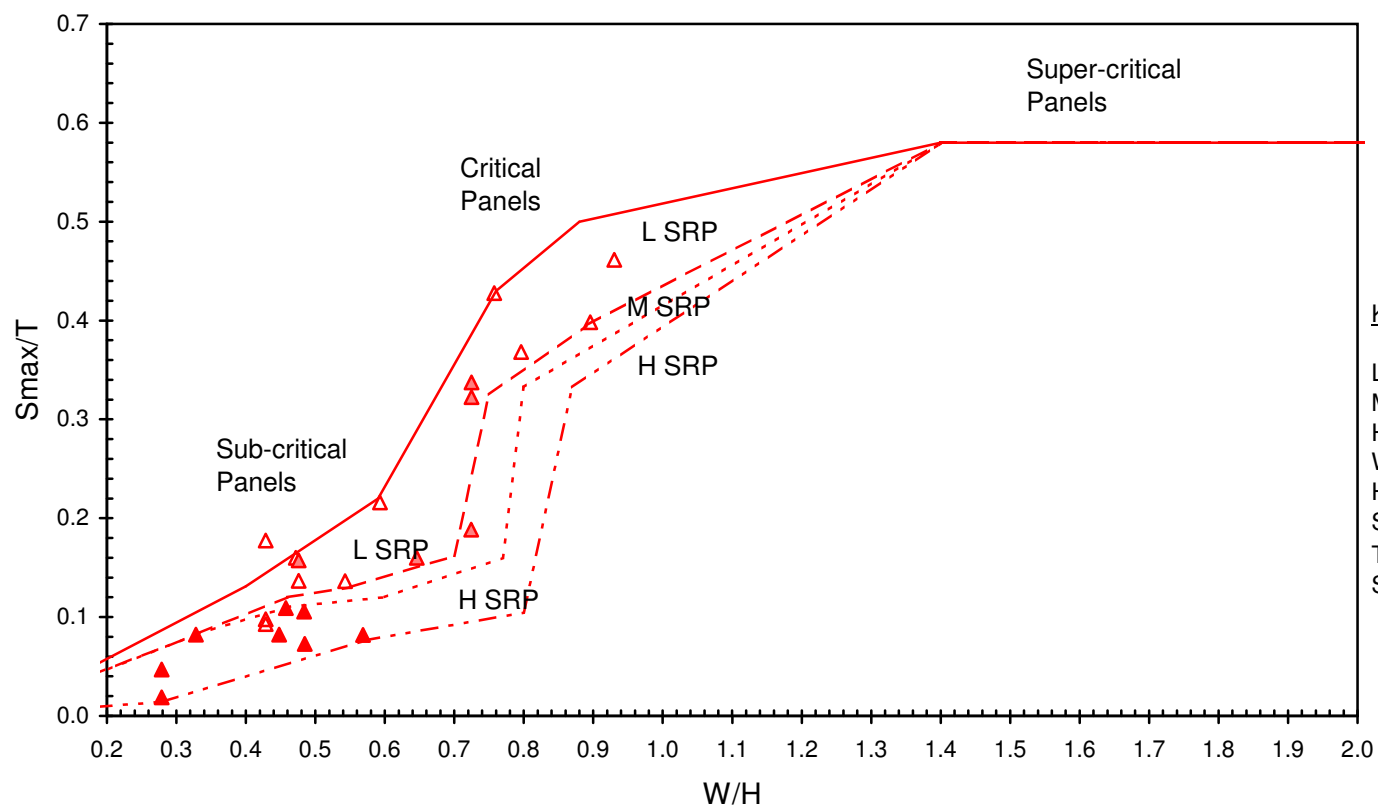
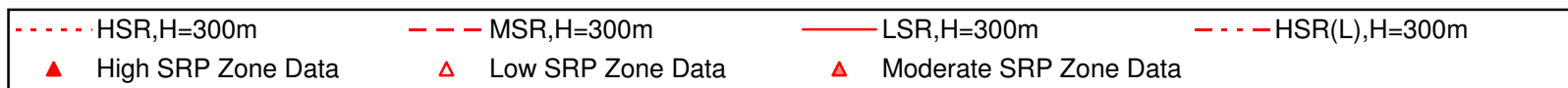
Note: No SRP distinguishment for panels with  $W/H < 0.65$

	Engineer:	S.Ditton	Client:	Adapted from ACARP, 2003			
	Drawn:	S.Ditton					
	Date:	08.08.08	Title:	Empirical Model for Predicting Subsidence Above Panels with Cover Depths Between 50 and 150 m and Low to High SRP Zones			
	Ditton Geotechnical Services Pty Ltd			Scale:	NTS		Figure No:






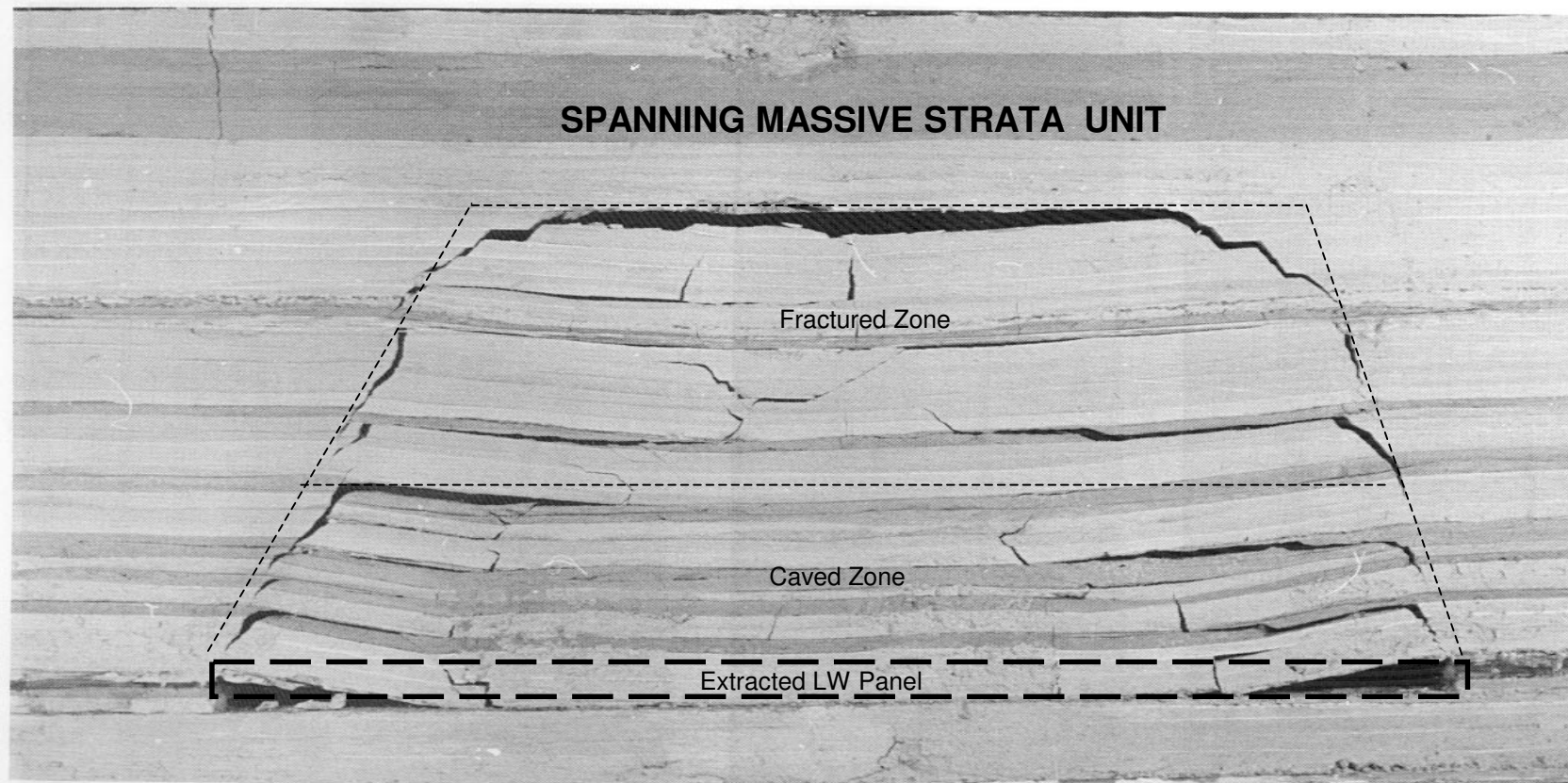
	Engineer:	S.Ditton	Client:	Adapted from ACARP, 2003			
	Drawn:	S.Ditton					
	Date:	08.08.08	Title:	Empirical Model for Predicting Subsidence Above Panels with Cover Depths Between 250 and 350 m and Low to High SRP Zones			
	Ditton Geotechnical Services Pty Ltd						
				Scale:	NTS		Figure No:



Key

L SRP = Low SRP Zone  
 M SRP = Moderate SRP Zone  
 H SRP = High SRP Zone  
 W = Panel Width  
 H = Cover Depth  
 $S_{max}$  = Maximum Panel Subsidence  
 T = Mining Height  
 SRP = Subsidence Reduction Potential

	Engineer:	S.Ditton	Client:	Adapted from ACARP, 2003		
	Drawn:	S.Ditton				
	Date:	08.08.08	Title:	Empirical Model for Predicting Subsidence Above Panels with Cover Depths Between 250 and 350 m and Low to High SRP Zones		
	Ditton Geotechnical Services Pty Ltd			Scale:	NTS	Figure No:



Physical model of caved strata above longwall extraction with strong overburden. Mining data:  $h = 84\text{m}$ ;  $w = 118\text{m}$ ;  $M = 4\text{m}$ .

DgS



Engineer: S.Ditton

Drawn: S.Ditton

Date: 08.08.08

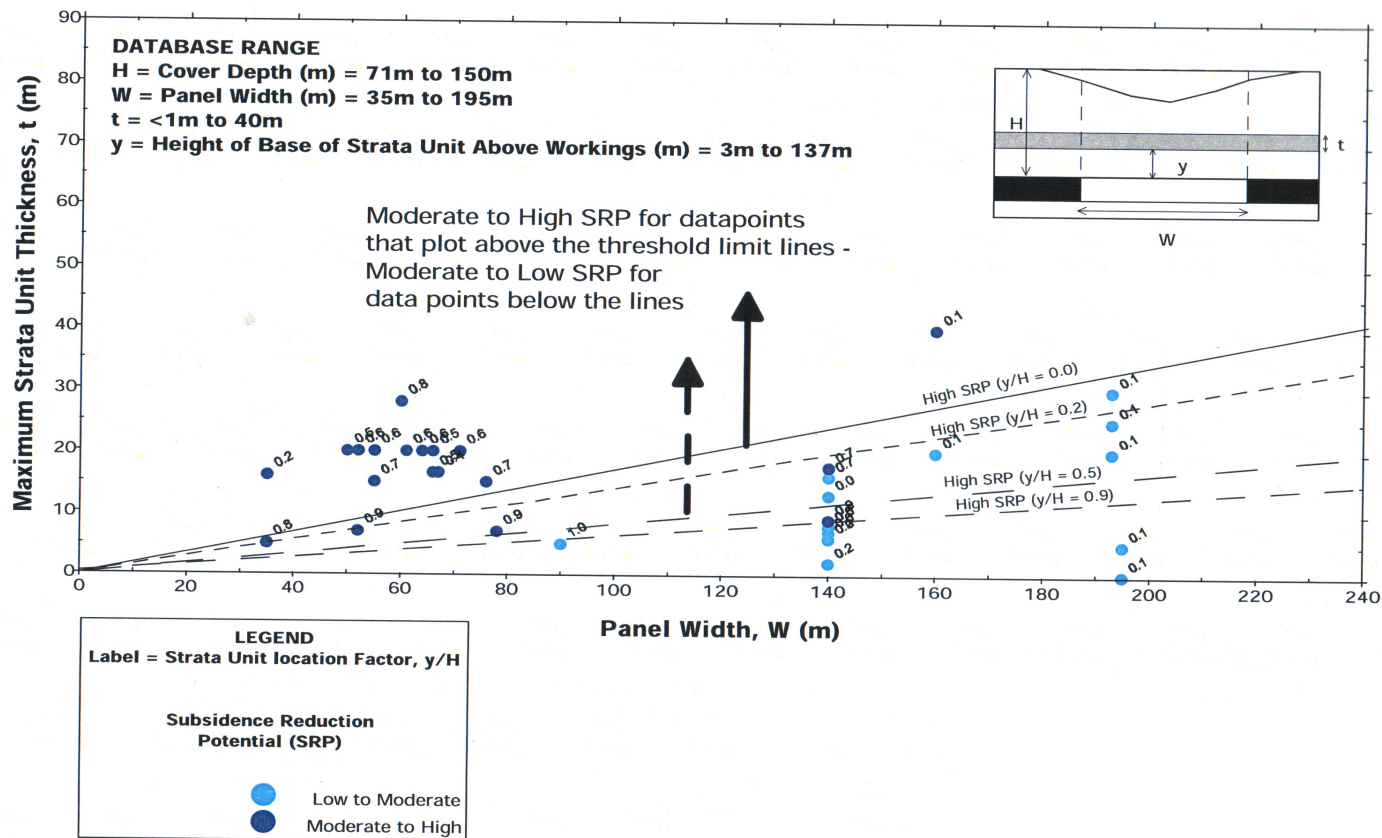
Ditton Geotechnical  
Services Pty Ltd

Client: Adapted from ACARP, 2003

Title: Physical Overburden Model Showing the Subsidence Reducing Effect of  
a Massive Strata Unit At the Surface

Scale: NTS

Figure No: A6



DgS



Engineer: S.Ditton

Drawn: S.Ditton

Date: 08.08.08

Ditton Geotechnical

Services Pty Ltd

Client:

Extract from ACARP, 2003

Title:

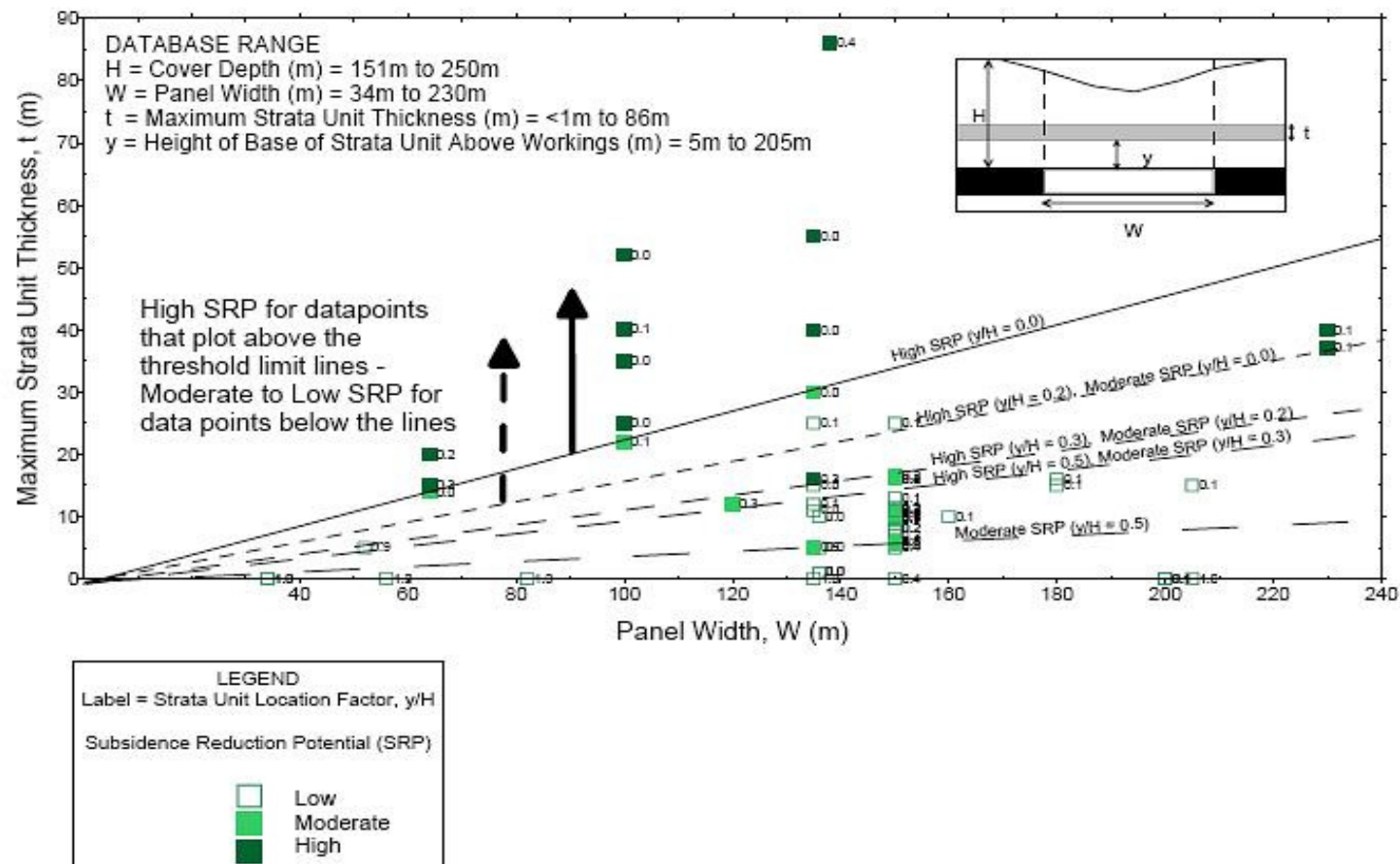
Project Database of Maximum Strata Unit Thickness and SRP Threshold Limit Lines for  
 H=50 m to 150 m

Scale:

NTS

Figure No:

A7.1



DgS



Engineer: S.Ditton

Drawn: S.Ditton

Date: 08.08.08

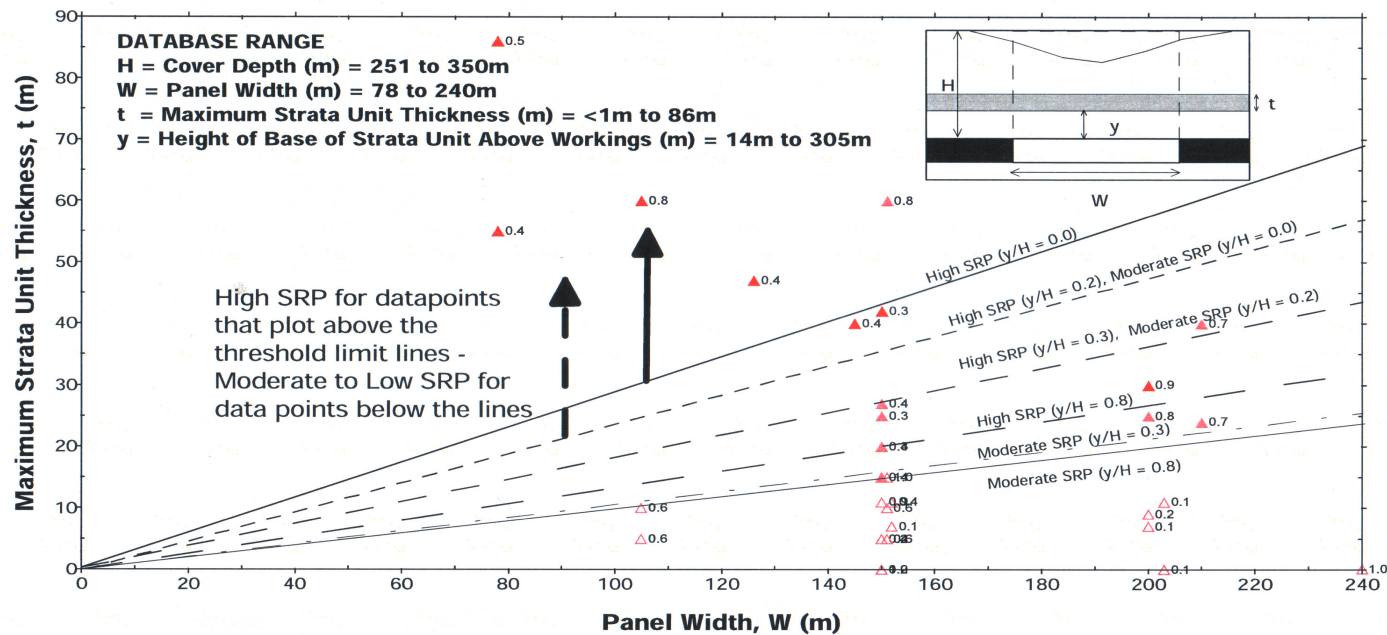
Ditton Geotechnical  
Services Pty Ltd

Client: Extract from ACARP, 2003

Title: Project Database of Maximum Strata Unit Thickness and SRP Threshold Limit Lines for  
H=150 m to 250 m

Scale: NTS

Figure No: A7.2



DgS



Engineer: S.Ditton

Drawn: S.Ditton

Date: 08.08.08

Ditton Geotechnical  
 Services Pty Ltd

Client:

Extract from ACARP, 2003

Title:

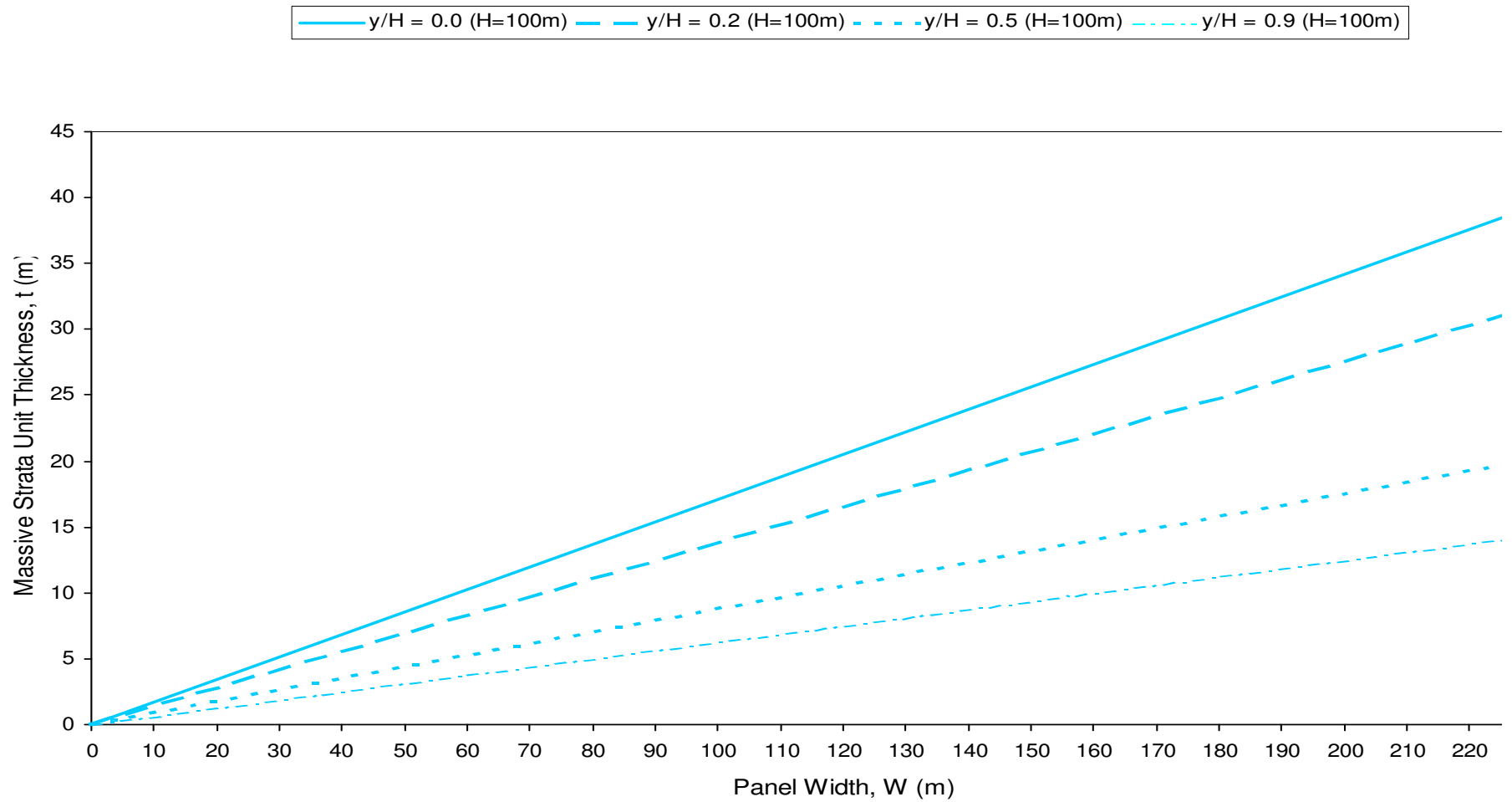
Project Database of Maximum Strata Unit Thickness and SRP Threshold Limit Lines for  
 H=250 m to 350 m

Scale:

NTS

Figure No:

A7.3



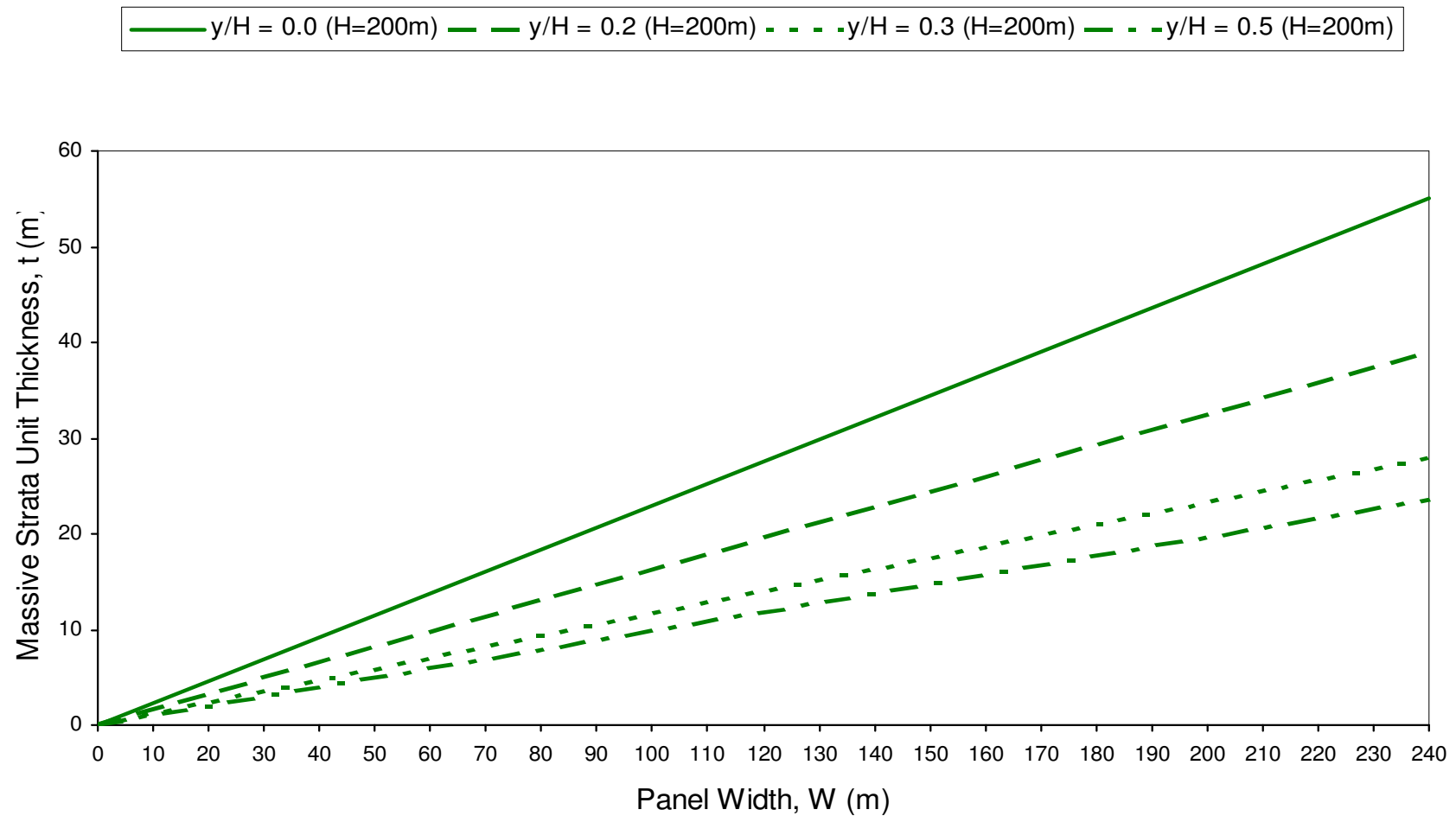
Engineer: S.Ditton  
 Drawn: S.Ditton  
 Date: 08.08.08  
 Ditton Geotechnical  
 Services Pty Ltd

Client: Adapted from ACARP, 2003

Title: Empirical Model for Predicting Subsidence Reduction Potential Above Panels with  
 Cover Depths Between 50 and 150 m

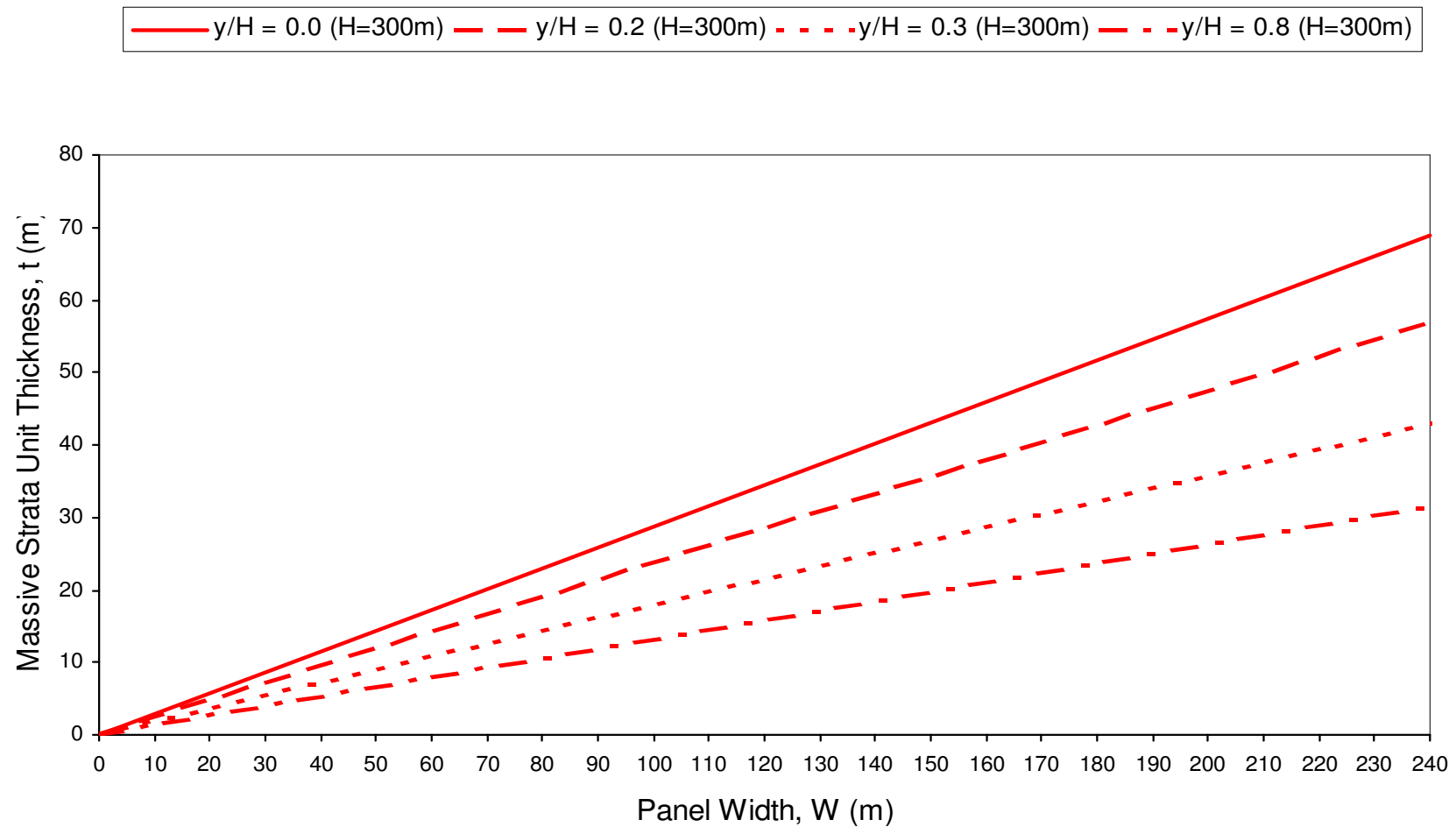
Scale: NTS


Figure No: A8

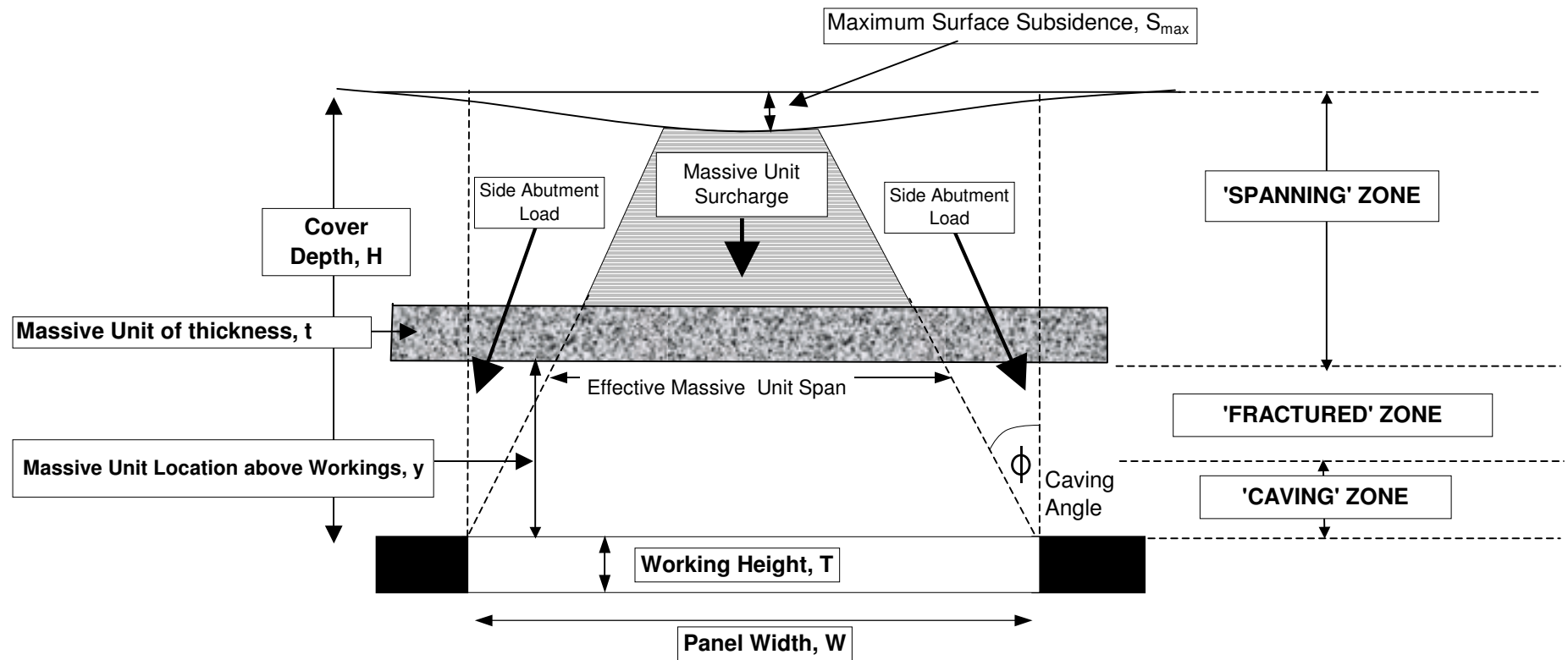



Engineer:	S.Ditton	Client:	Adapted from ACARP, 2003			
Drawn:	S.Ditton					
Date:	08.08.08	Title:	Empirical Model for Predicting Subsidence Reduction Potential Above Panels with Cover Depths Between 150 and 250 m			
Ditton Geotechnical Services Pty Ltd						
		Scale:	NTS		Figure No:	A9

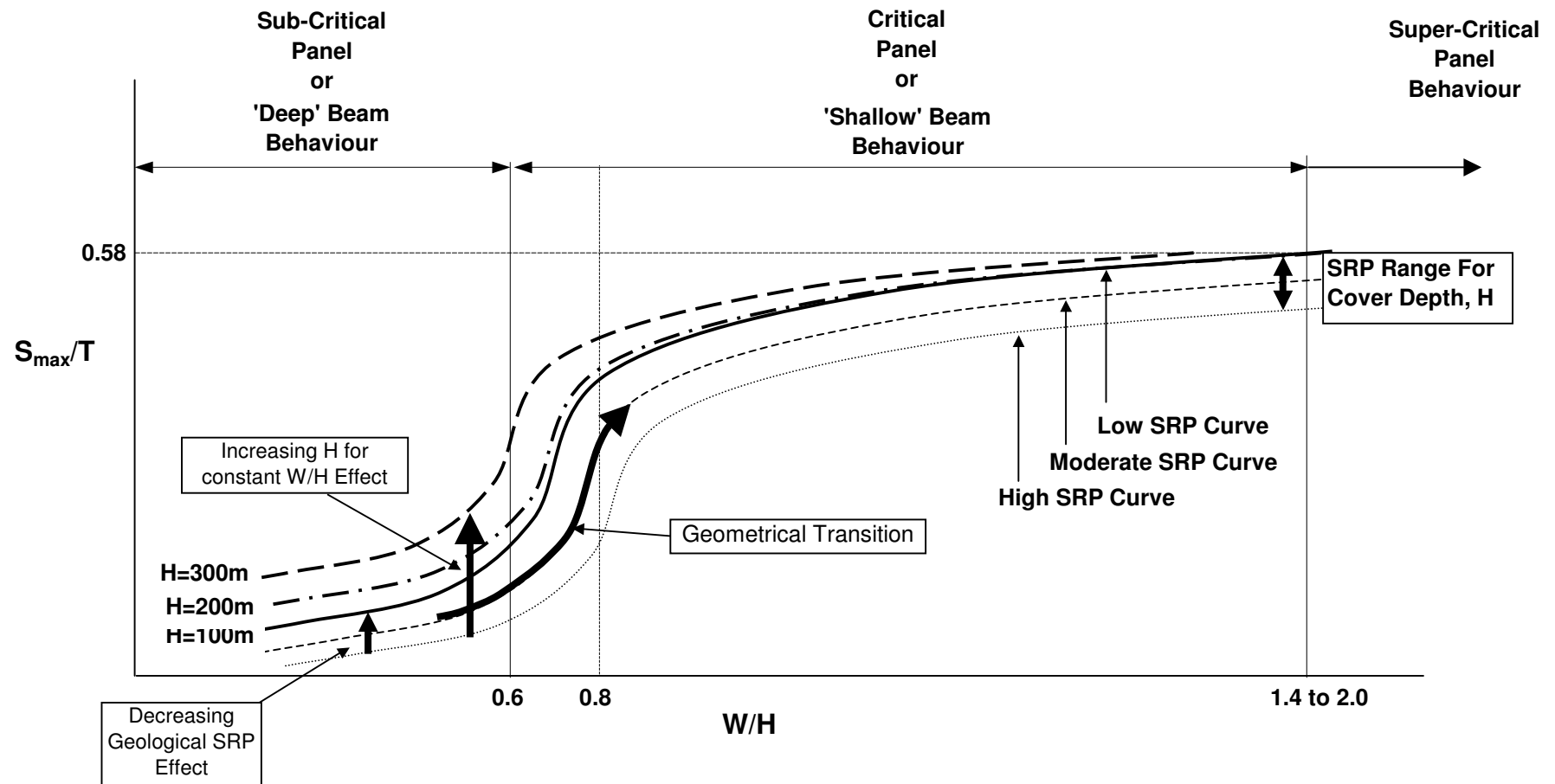





	Engineer:	S.Ditton	Client:	Adapted from ACARP, 2003			
	Drawn:	S.Ditton					
	Date:	08.08.08	Title:	Empirical Model for Predicting Subsidence Reduction Potential Above Panels with Cover Depths Between 250 and 350 m			
	Ditton Geotechnical Services Pty Ltd						
			Scale:	NTS		Figure No:	A10



	Engineer:	S.Ditton	Client:	Adapted from ACARP, 2003			
	Drawn:	S.Ditton					
	Date:	08.08.08	Title:	Overburden with Massive Strata Unit Behaviour Concept Model and Key Parameter Definitions			
	Ditton Geotechnical Services Pty Ltd						
			Scale:	NTS		Figure No:	A11



	Engineer:	S.Ditton	Client:	Adapted from ACARP, 2003		
	Drawn:	S.Ditton				
	Date:	08.08.08	Title:	Geomechanical and Geological Effects of Overburden Behaviour on Maimum Subsidence for Single Panels		
	Ditton Geotechnical					
	Services Pty Ltd		Scale:	NTS		Figure No: A12

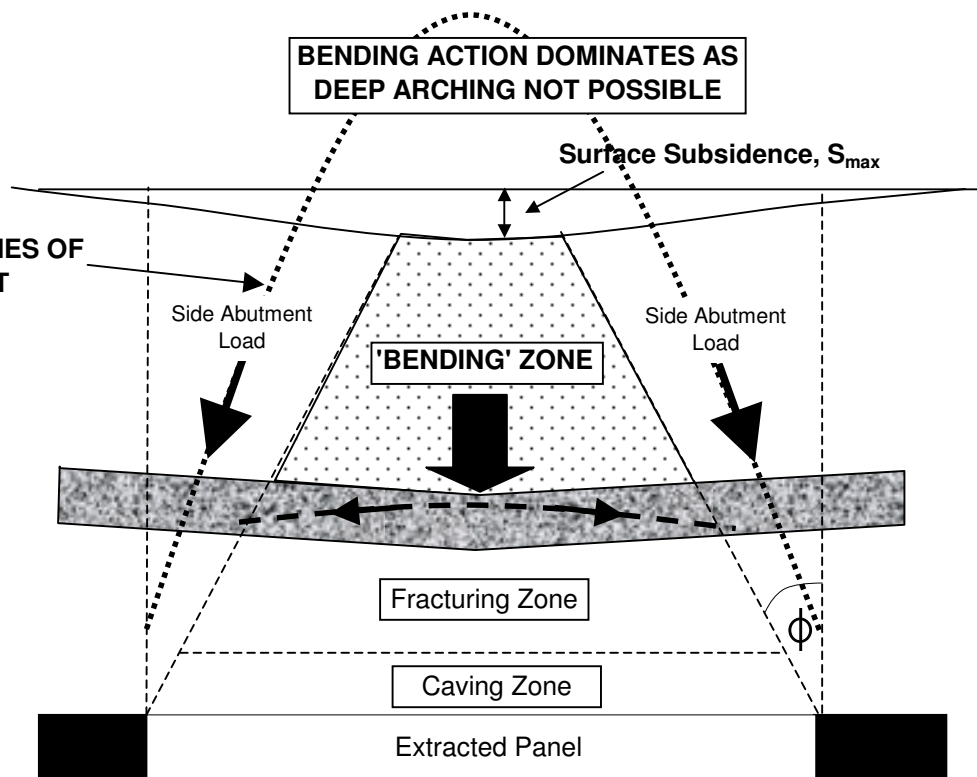
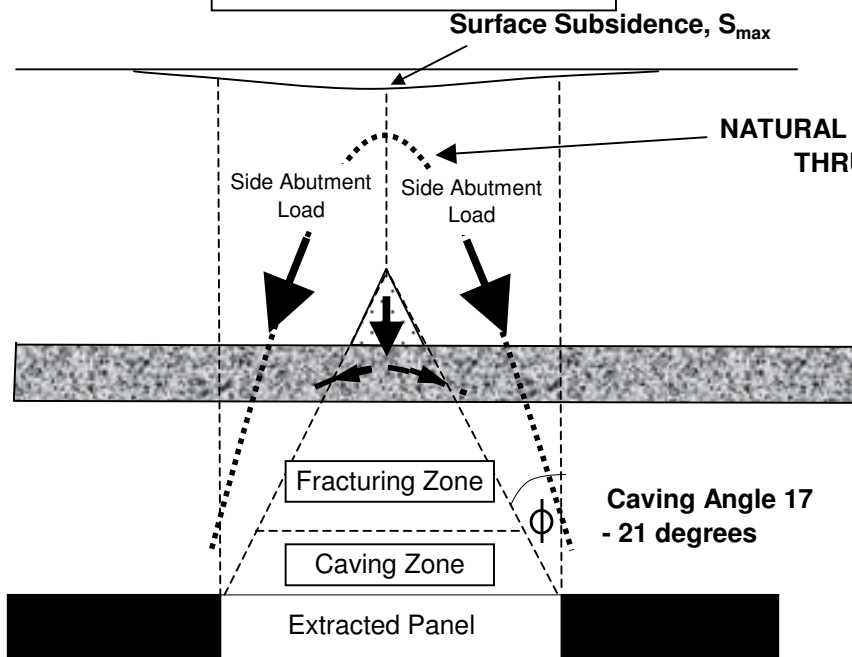
**DEEP 'BEAM' BEHAVIOUR**  
( $W/H < 0.7$ )

Geometrical  
Transition

**SHALLOW 'BEAM' BEHAVIOUR**  
( $W/H > 0.7$ )

**AXIAL ACTION OR  
DEEP 'ARCHING' DOMINATES  
SMALL BENDING ZONE**

**BENDING ACTION DOMINATES AS  
DEEP ARCHING NOT POSSIBLE**



**DgS**



Engineer: S.Ditton

Drawn: S.Ditton

Date: 08.08.08

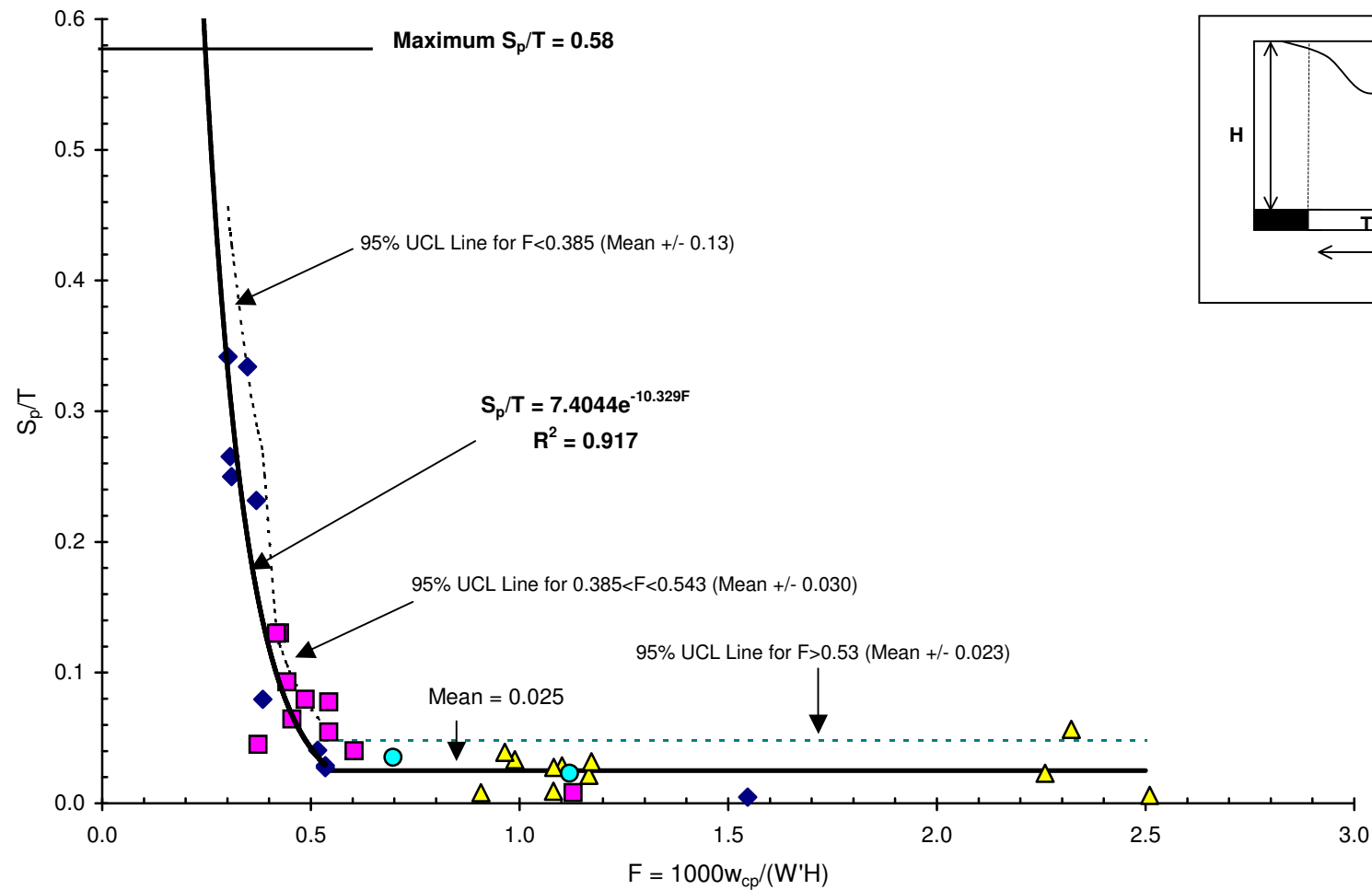
Ditton Geotechnical  
Services Pty Ltd

Client: Adapted from ACARP, 2003

Title: Overburden with Massive Strata Units Behaviour Concept Models of Beam Action Types  
for Subcritical and Supercritical Longwall Panels

Scale: NTS

Figure No: A13



Engineer: S.Ditton

Drawn: S.Ditton

Date: 08.08.08

Ditton Geotechnical  
Services Pty Ltd

Client:

Extract from ACARP, 2003

Title:

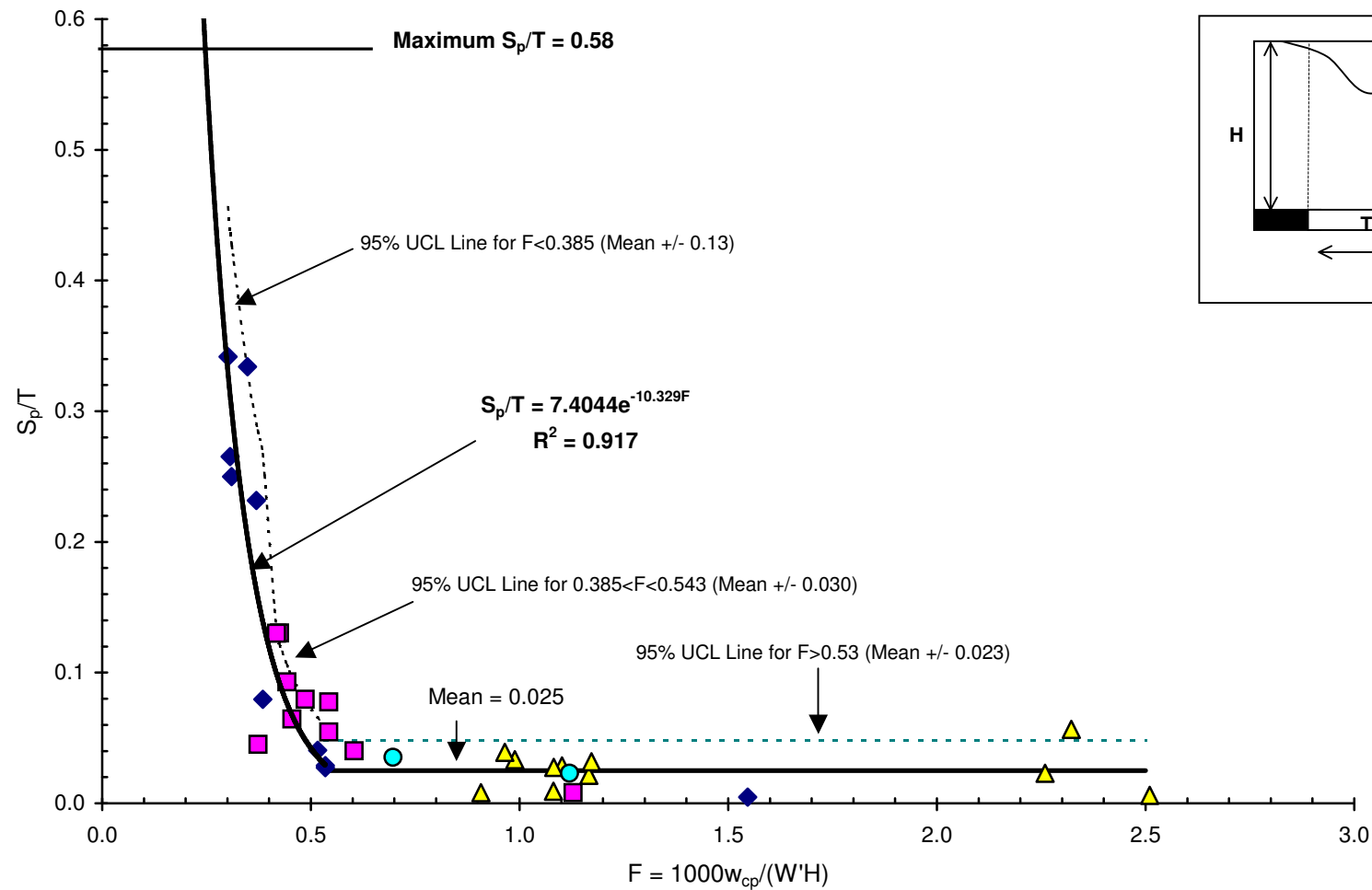
2003 Empirical Model for Predicting Subsidence above Chain Pillars Subject to Double  
Abutment Loading


Scale:

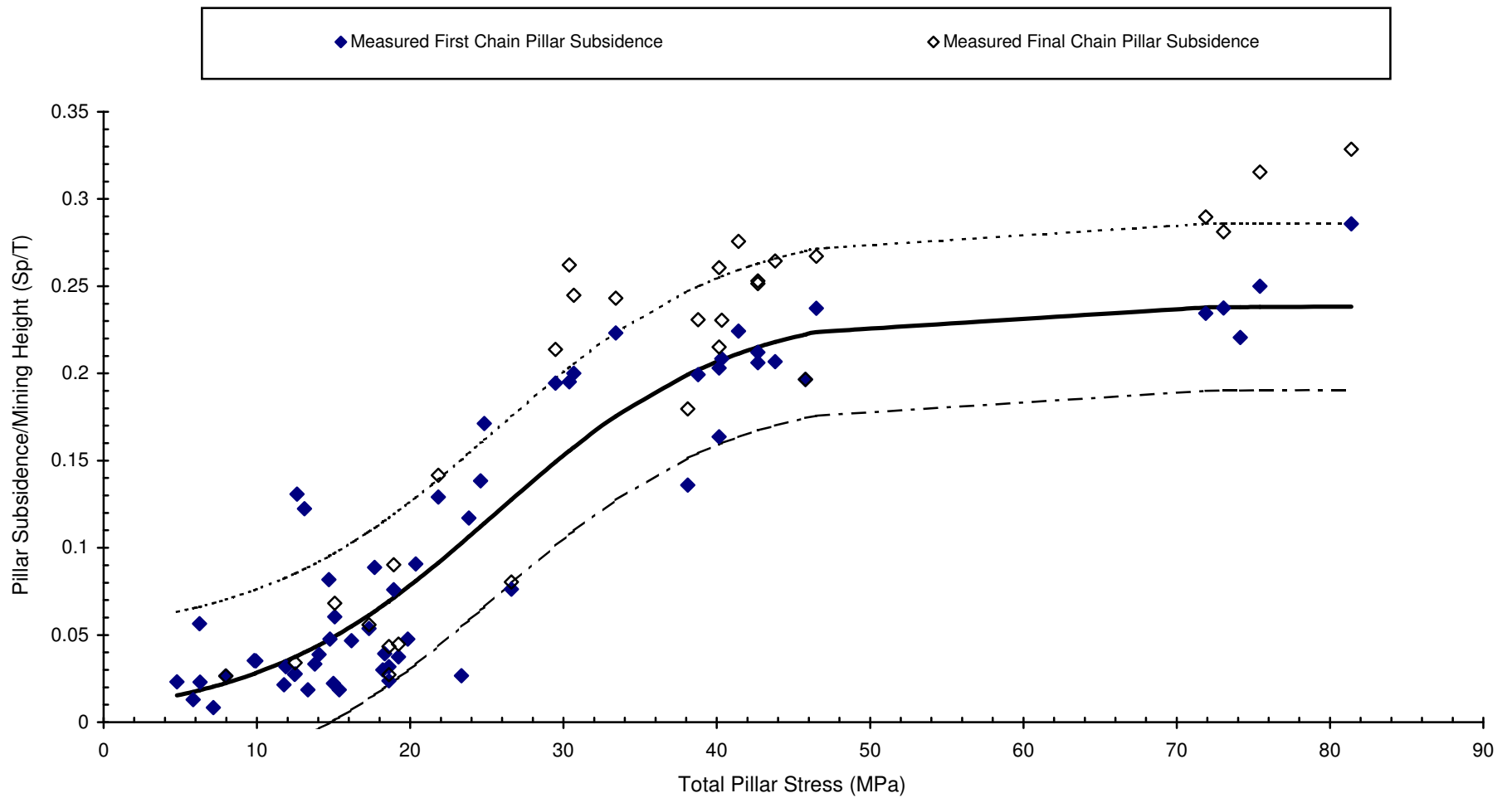
NTS


Figure No:

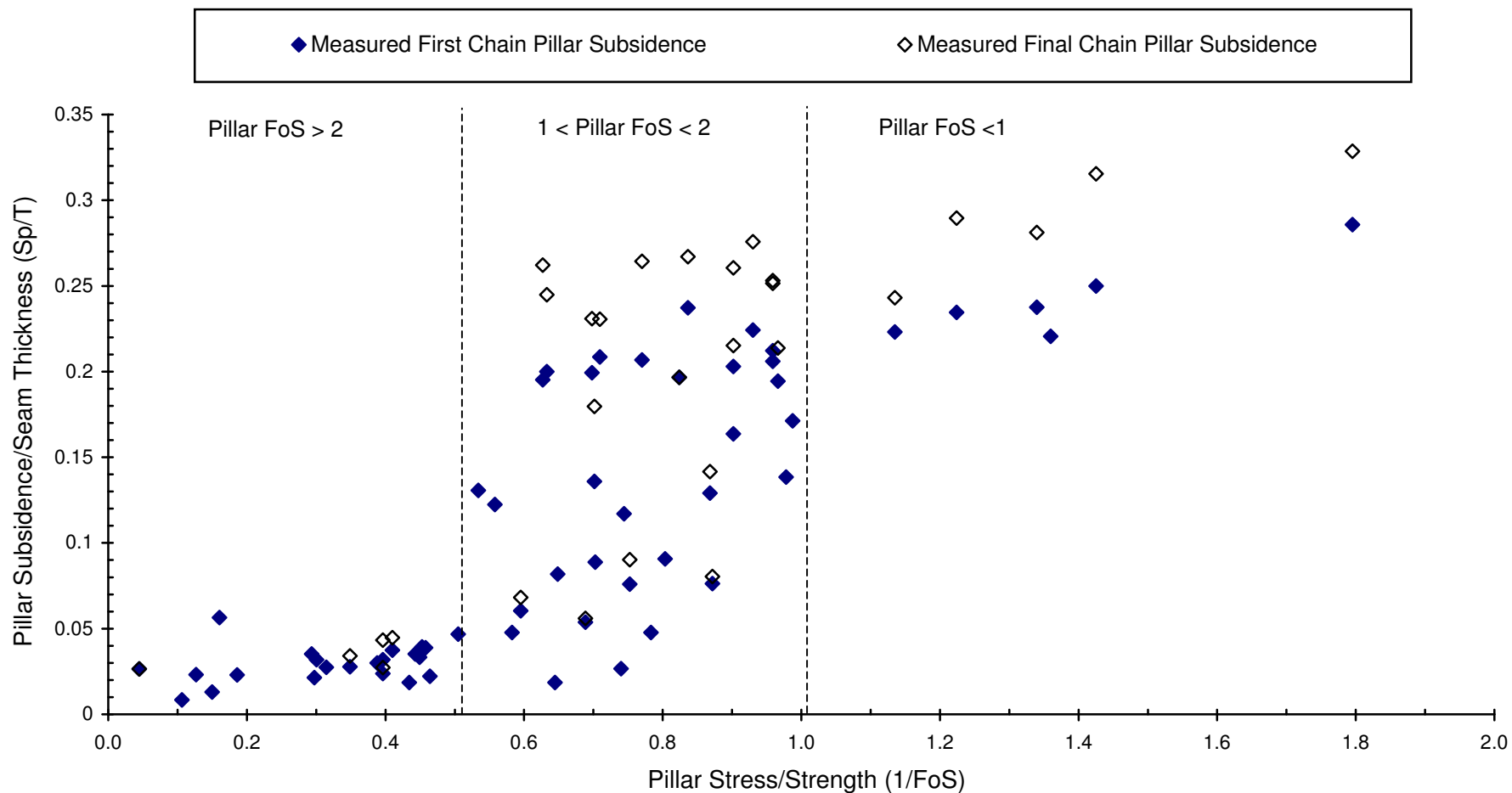
A14



	Engineer:	S.Ditton	Client:	Extract from ACARP, 2003			
	Drawn:	S.Ditton					
	Date:	08.08.08	Title:	2003 Empirical Model for Predicting Subsidence above Chain Pillars Subject to Double Abutment Loading			
	Ditton Geotechnical Services Pty Ltd						
			Scale:	NTS		Figure No:	A15

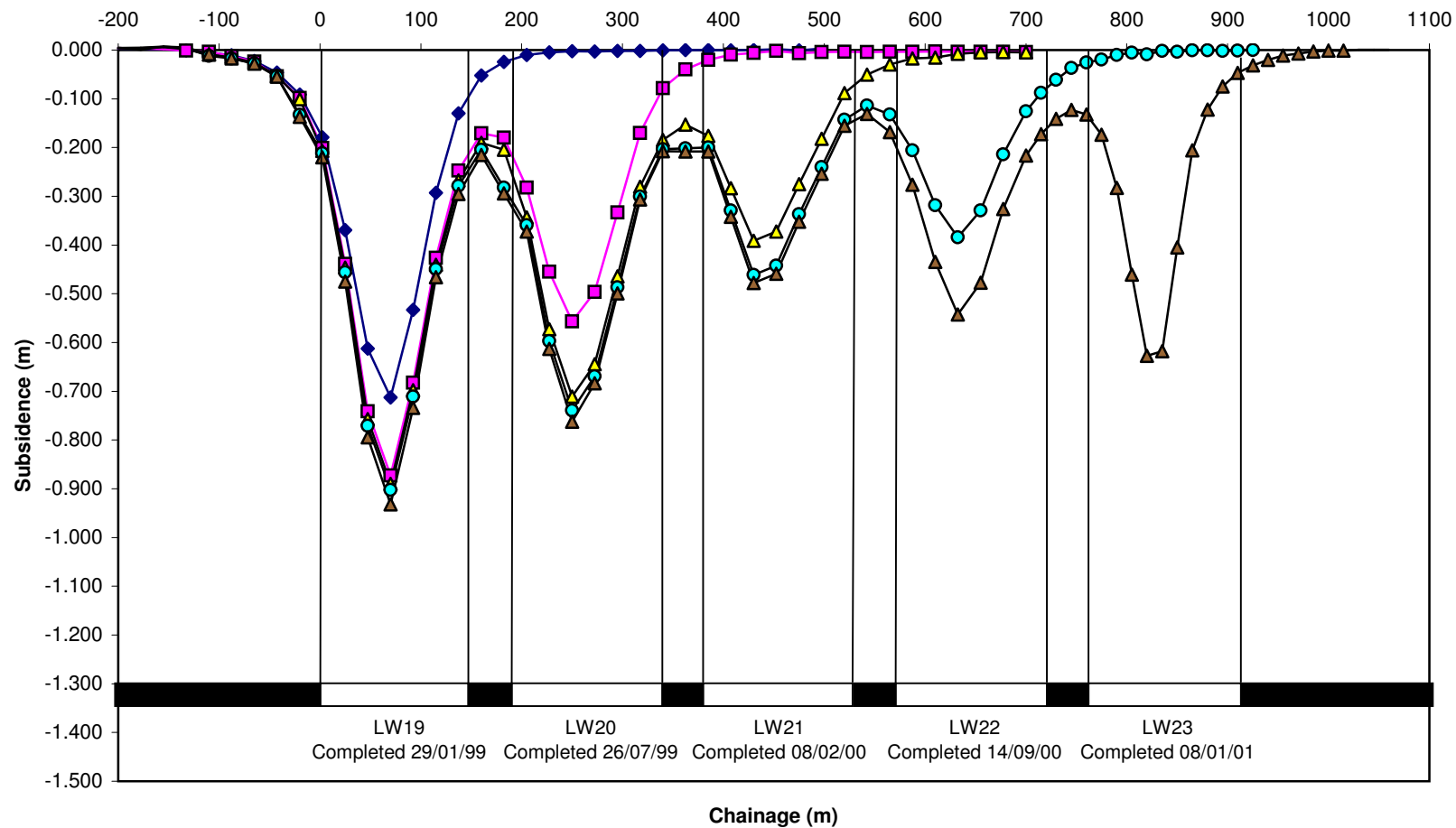



	Engineer:	S.Ditton	Client:	Adapted from ACARP, 2003			
	Drawn:	S.Ditton					
	Date:	08.08.08	Title:	2008 Empirical Model (DgS) for Predicting Subsidence above Chain Pillars Subject to Double Abutment Loading			
	Ditton Geotechnical Services Pty Ltd						
			Scale:	NTS		Figure No:	A16



Engineer:	S.Ditton	Client:	Adapted from ACARP, 2003	
Drawn:	S.Ditton			
Date:	08.08.08	Title:	Empirical DgS, 2008 Model Data of $1/FoS$ v. Subsidence above Chain Pillars Subject to Double Abutment Loading	
Ditton Geotechnical Services Pty Ltd		Scale:	NTS	Figure No: A17

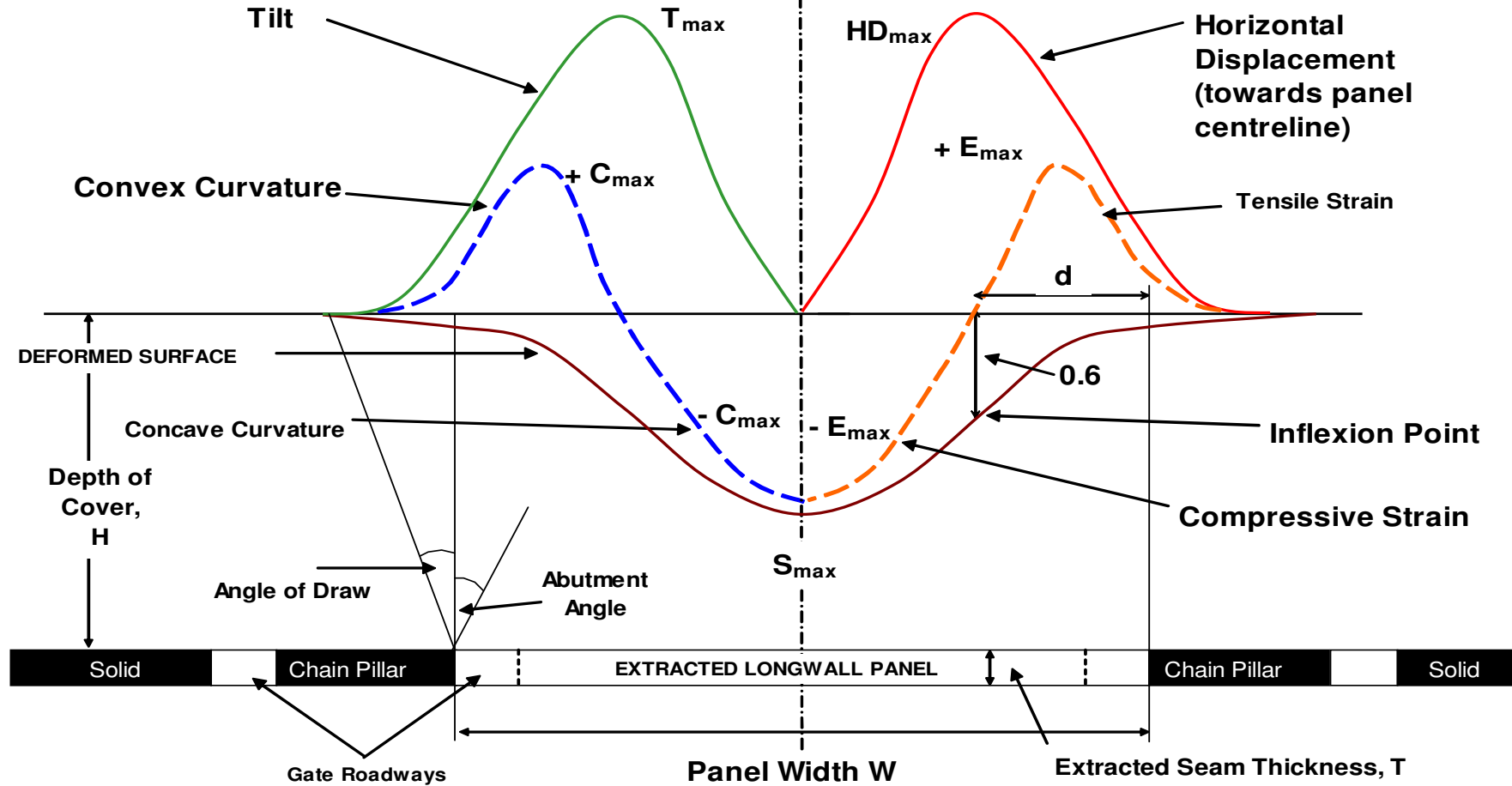




	Engineer:	S.Ditton	Client:	Adapted from ACARP, 2003			
	Drawn:	S.Ditton					
	Date:	08.08.08	Title:	Measured Multiple Longwall Panel Subsidence in Newcastle Coalfield			
	Ditton Geotechnical Services Pty Ltd						
			Scale:	NTS		Figure No:	A18

## VERTICAL DISPLACEMENT PARAMETER PROFILES

## HORIZONTAL DISPLACEMENT PARAMETER PROFILES



DgS



Engineer: S.Ditton

Drawn: S.Ditton

Date: 08.08.08

Ditton Geotechnical  
Services Pty Ltd

Client:

Extract from ACARP, 2003

Title:

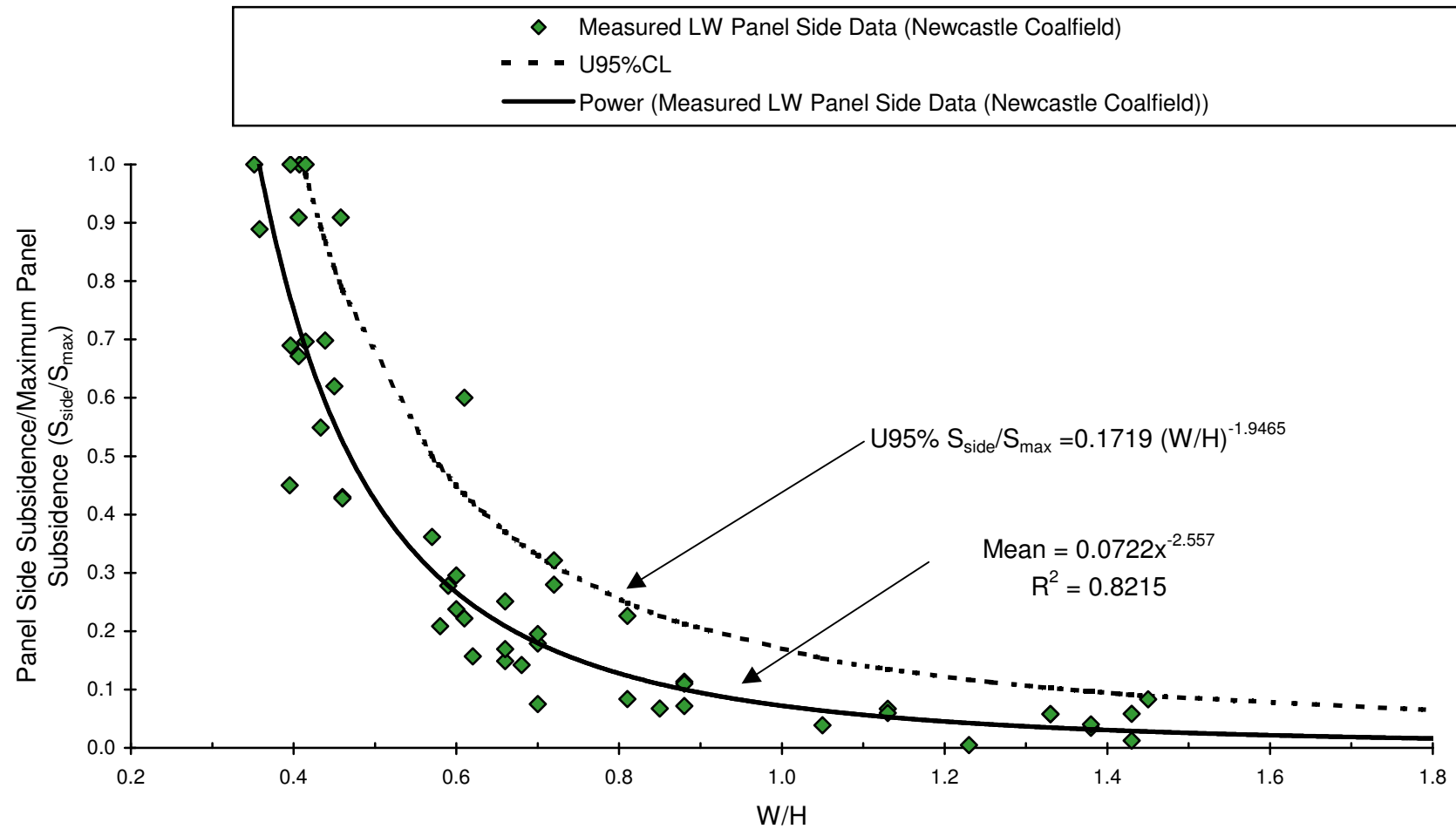
Mine Subsidence Trough Deformation Parameters  
(adapted from Holla, 1987)

Scale:

NTS

Figure No:

A19



DgS



Engineer: S.Ditton

Drawn: S.Ditton

Date: 08.08.08

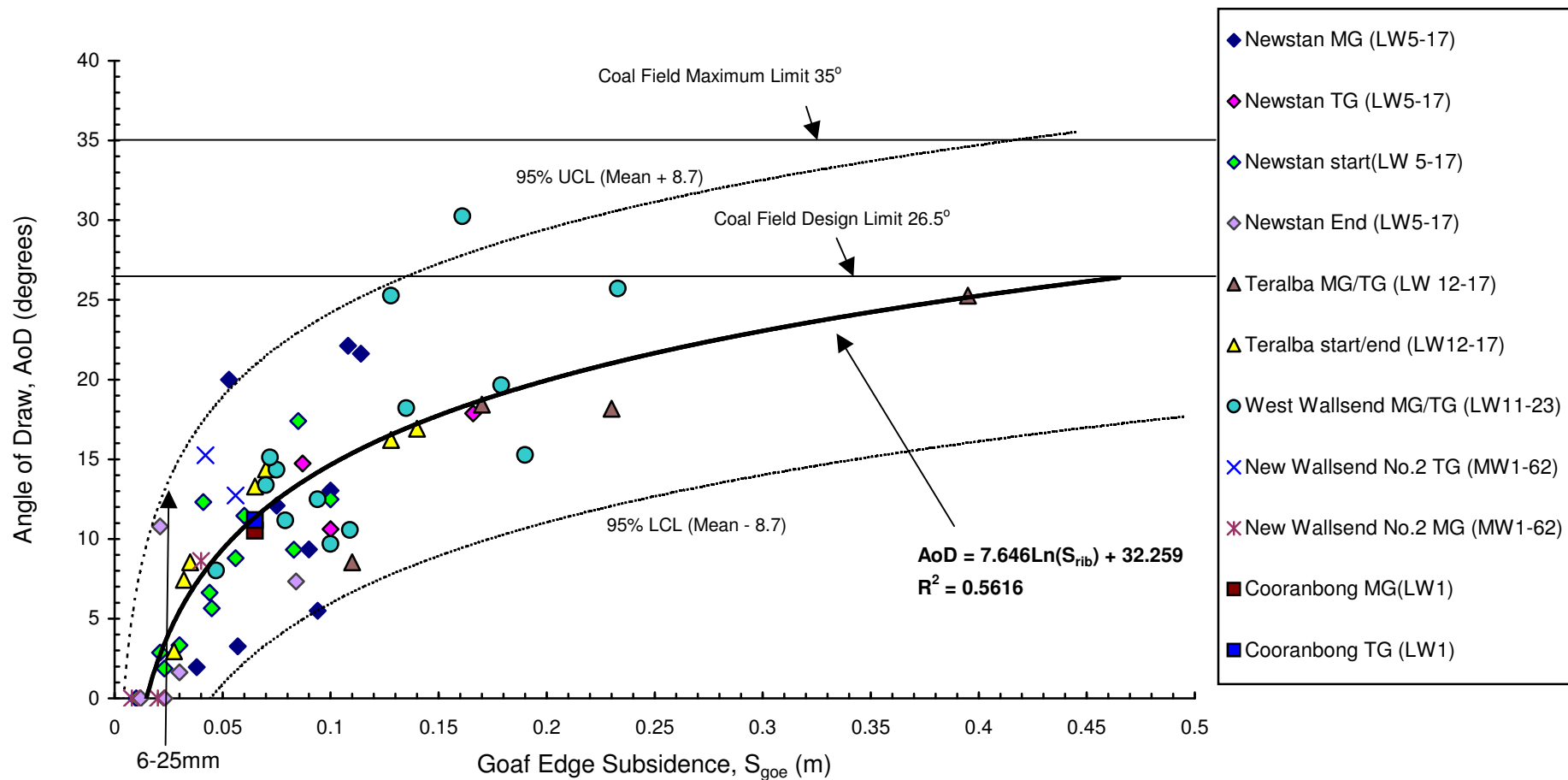
Ditton Geotechnical  
Services Pty Ltd

Client: Adapted from ACARP, 2003

Title: Empirical Model for Goaf Edge Subsidence Prediction Above Longwall Panels

Scale: NTS

Figure No: A20



DgS



Engineer: S.Ditton

Drawn: S.Ditton

Date: 08.08.08

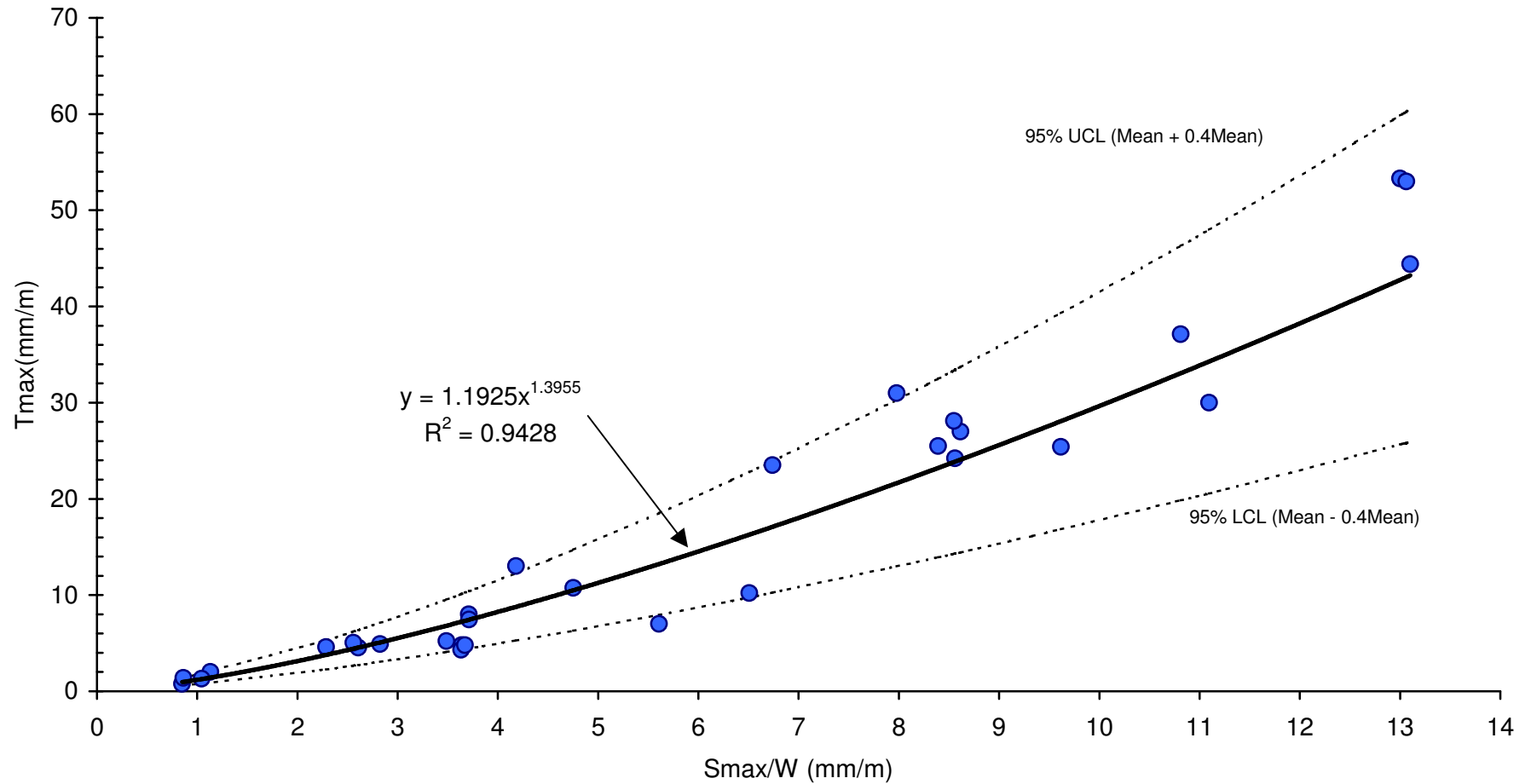
Ditton Geotechnical  
Services Pty Ltd


Client: Extracted from ACARP, 2003

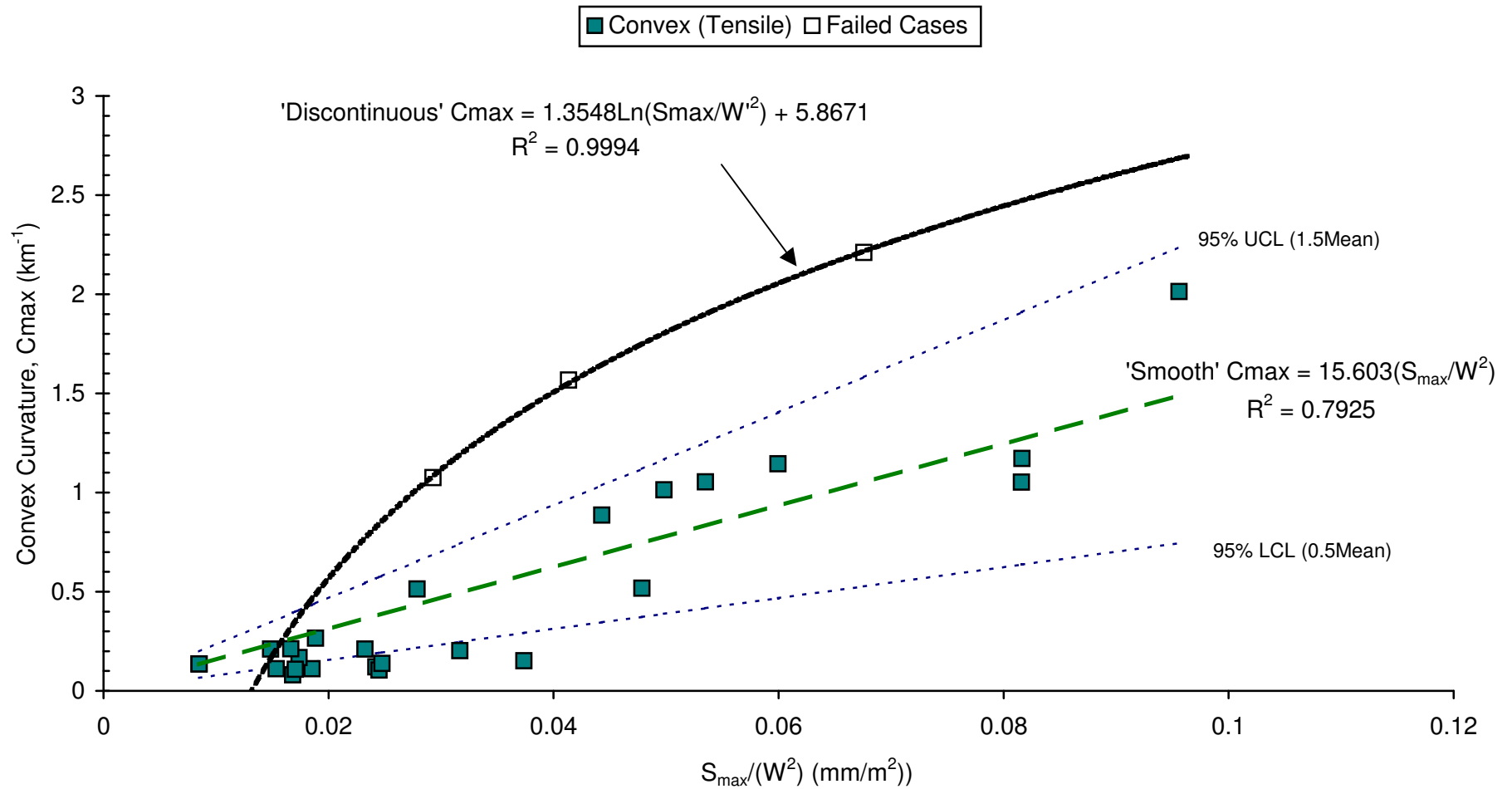
Title: Empirical Prediction Model for Longwall Panel Angle of Draw

Scale: NTS

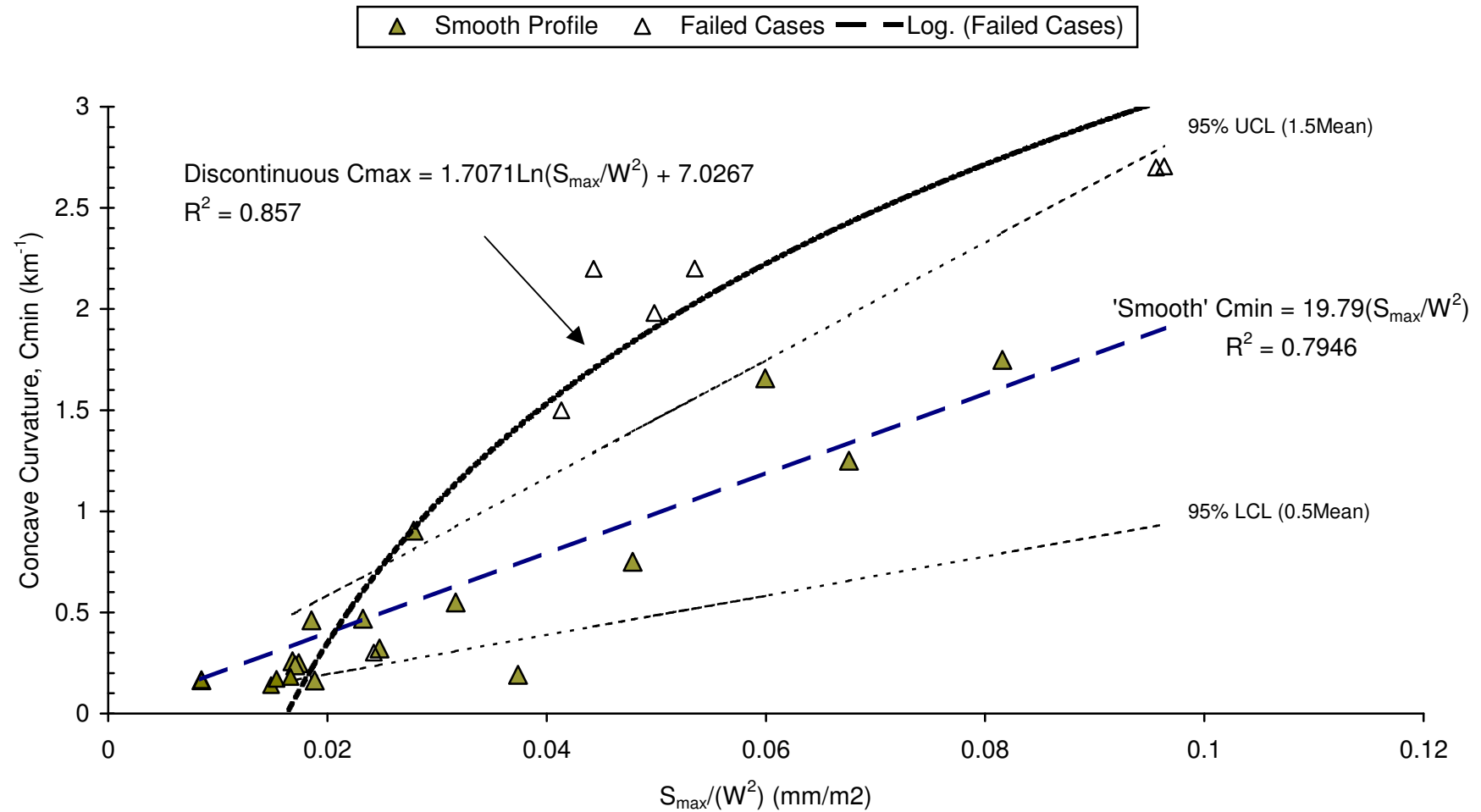
Figure No: A21



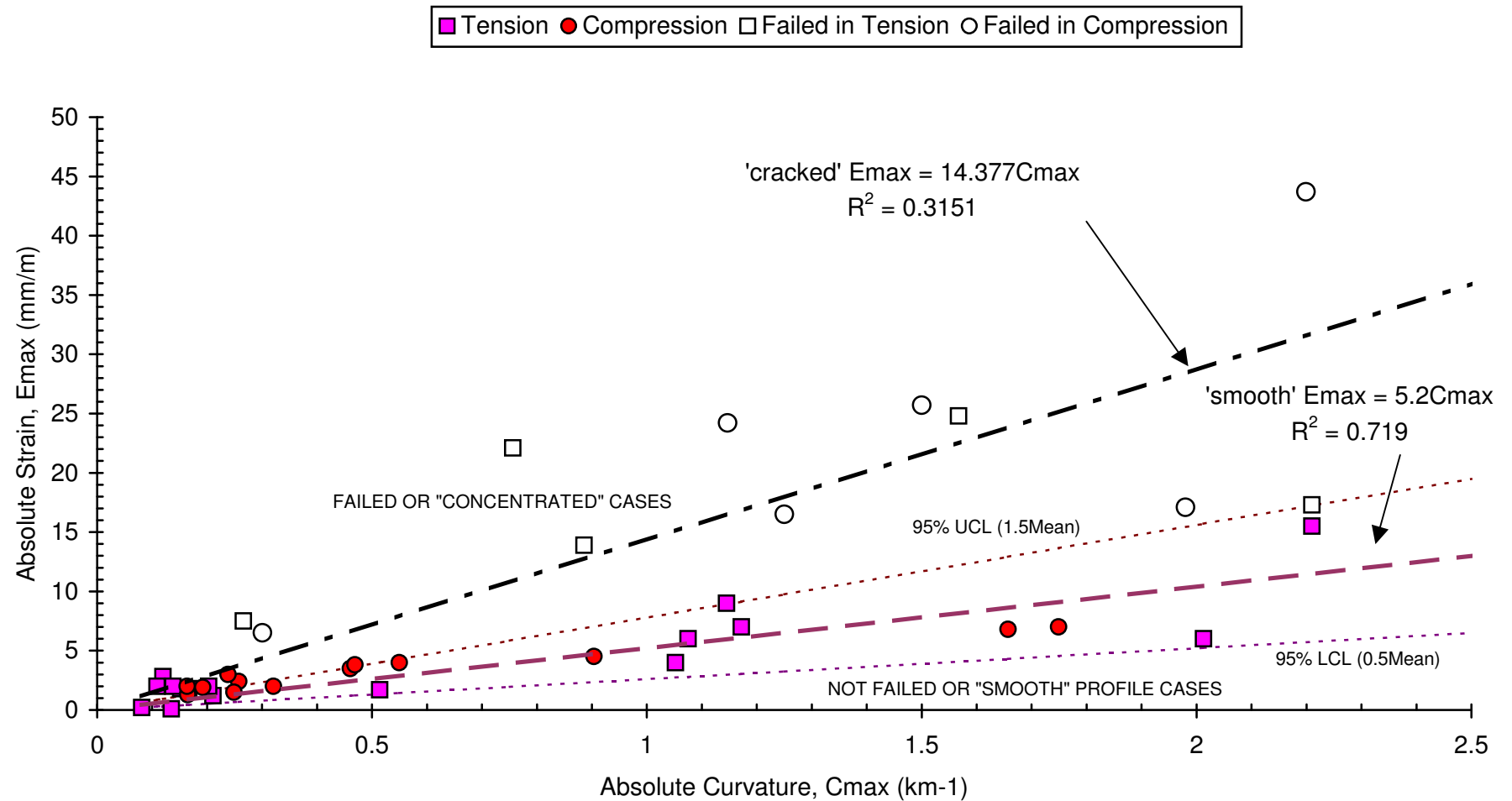
	Engineer:	S.Ditton	Client:	Extract from ACARP, 2003			
	Drawn:	S.Ditton					
	Date:	08.08.08	Title:	Empirical Model for Maximum Panel Tilt Prediction Above Longwall Panels			
	Ditton Geotechnical Services Pty Ltd						
			Scale:	NTS		Figure No:	A22



Engineer:	S.Ditton	Client:	Extract from ACARP, 2003	
Drawn:	S.Ditton			
Date:	08.08.08	Title:	Empirical Model for Maximum Panel Convex Curvature Prediction Above Longwall Panels for Smooth and Discontinuous Profiles	
Ditton Geotechnical Services Pty Ltd		Scale:	NTS	Figure No: A23



Engineer:	S.Ditton	Client:	Extract from ACARP, 2003	
Drawn:	S.Ditton			
Date:	08.08.08	Title:	Empirical Model for Maximum Panel Concave Curvature Prediction Above Longwall Panels for Smooth and Discontinuous Profiles	
Ditton Geotechnical Services Pty Ltd		Scale:	NTS	Figure No: A24



DgS



Engineer: S.Ditton

Drawn: S.Ditton

Date: 08.08.08

Ditton Geotechnical  
Services Pty Ltd

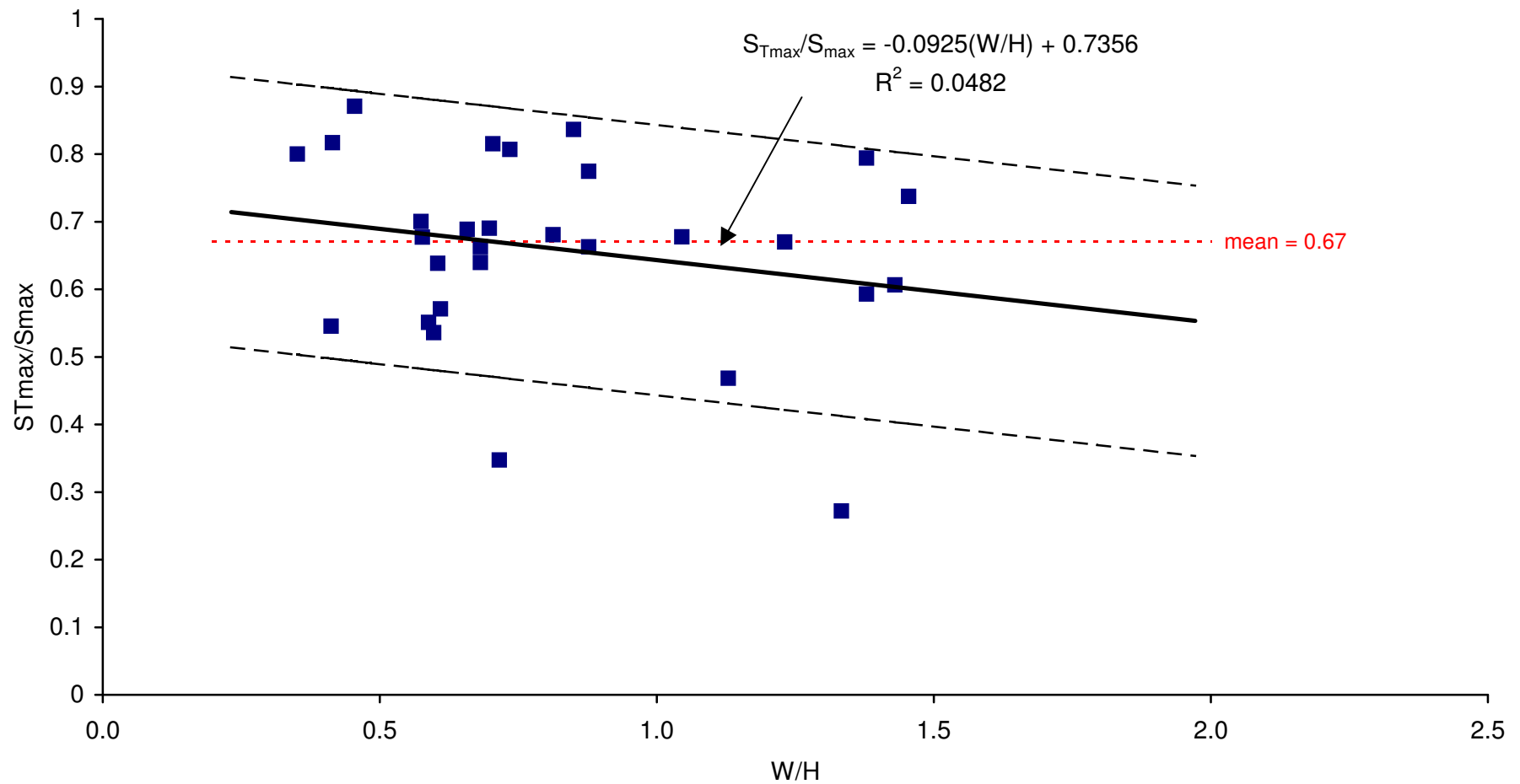
Client: Extract from ACARP, 2003


Title: Empirical Model for Maximum Panel Strain Prediction Above Longwall Panels  
for Smooth and Cracked Profiles

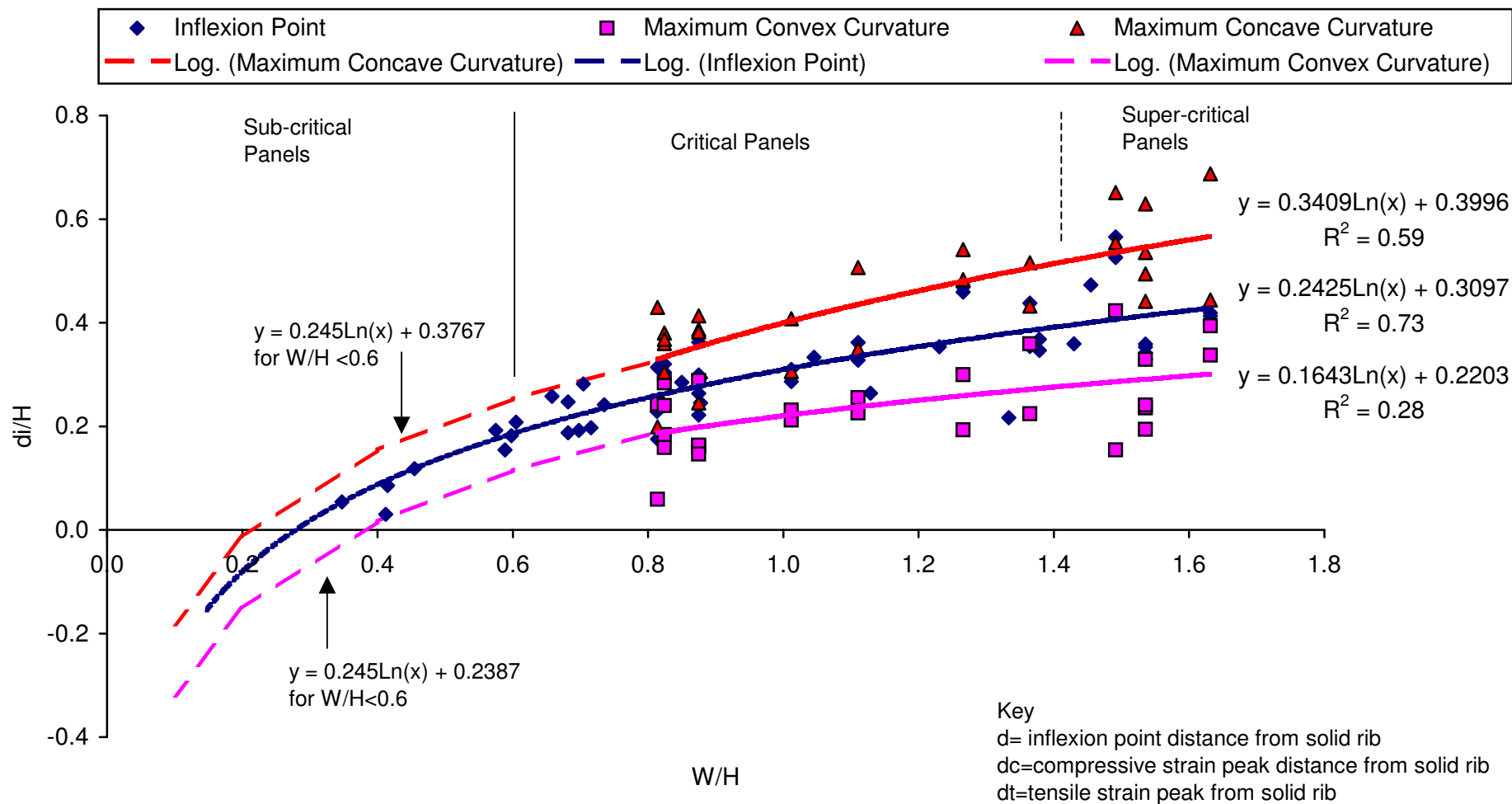
Scale: NTS

Figure No: A25





	Engineer:	S.Ditton	Client:	Extract from ACARP, 2003			
	Drawn:	S.Ditton					
	Date:	08.08.08	Title:	Empirical Model for Subsidence at Maximum Tilt Above Longwall Panels			
	Ditton Geotechnical Services Pty Ltd						
			Scale:	NTS		Figure No:	A26



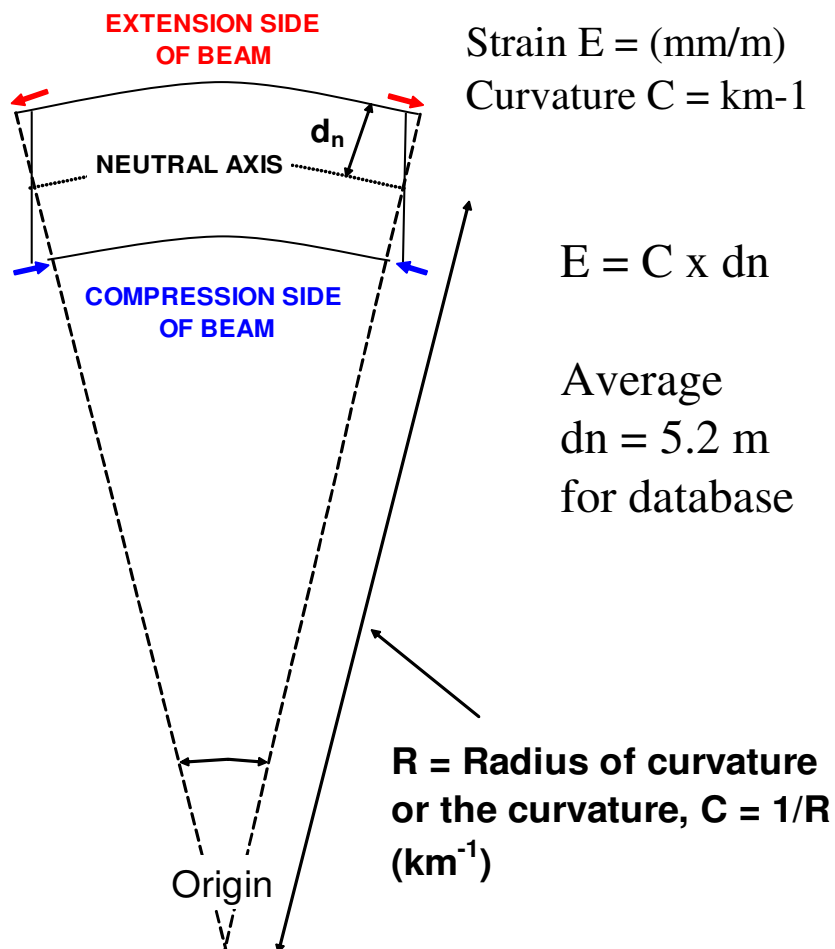
Engineer: S.Ditton  
 Drawn: S.Ditton  
 Date: 08.08.08  
 Ditton Geotechnical  
 Services Pty Ltd


Client: Adapted from ACARP, 2003

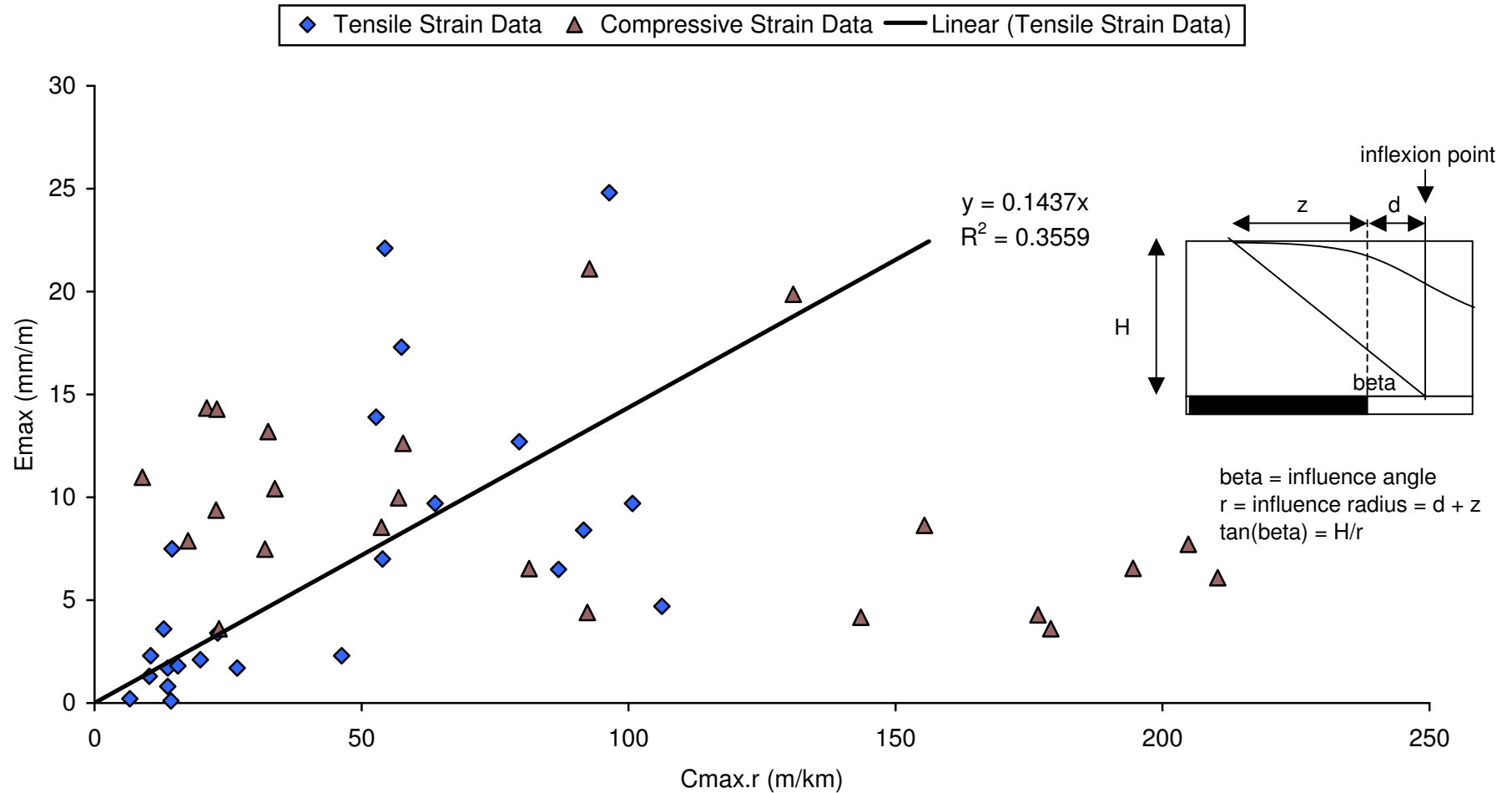
Title: Empirical Model for Predicting the Location of Inflexion Point, Maximum Tensile and Compressive Strain Peaks due to Longwall Panel Subsidence in the Newcastle Coalfield

Scale: NTS

Figure No: A27



	Engineer:	S.Ditton	Client:	Extract from ACARP, 2003	
	Drawn:	S.Ditton			
	Date:	08.08.08	Title:	Bending Beam Theory for Strain Prediction from Curvature Measurements	
	Ditton Geotechnical Services Pty Ltd		Scale:		Figure No: A28



DgS



Engineer: S.Ditton

Drawn: S.Ditton

Date: 08.08.08

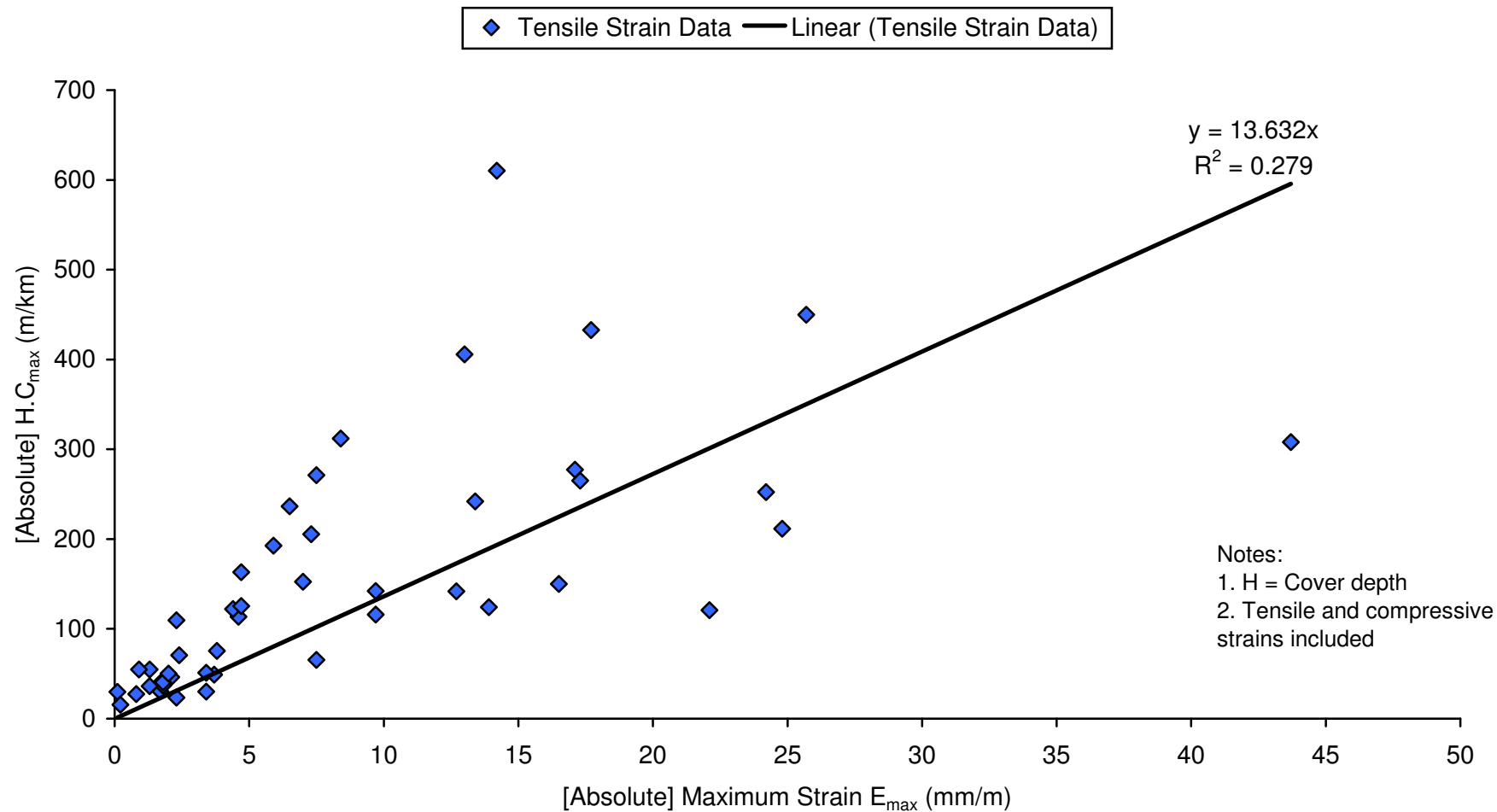
Ditton Geotechnical  
Services Pty Ltd


Client: Karmis, 1987 Adapted for ACARP, 2003

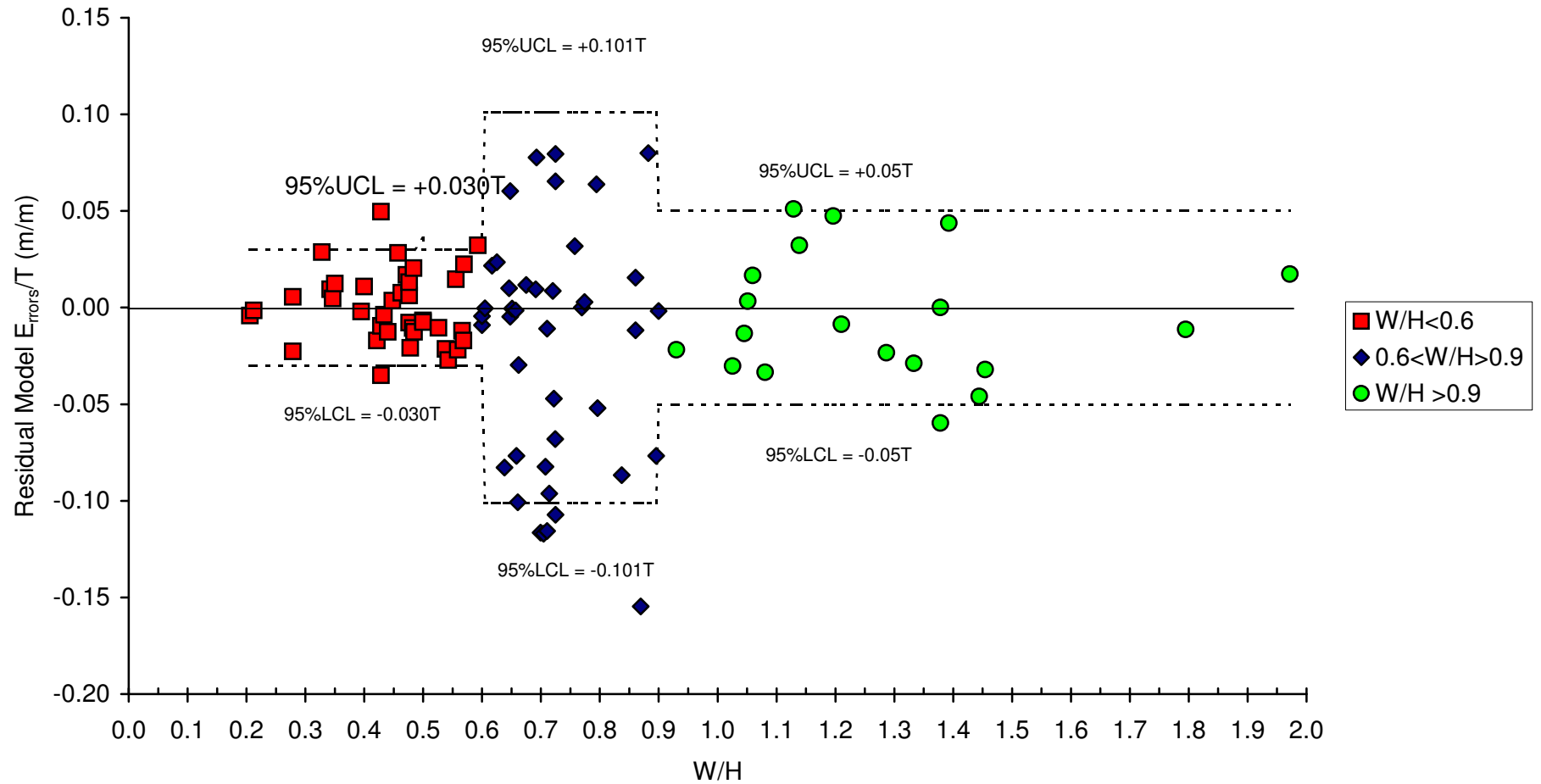
Title: Empirical Model Recommended by Karmis et al, 1987 for Predicting Strain from Curvature  
Above Longwall Panels in Newcastle Coalfield


Scale: NTS

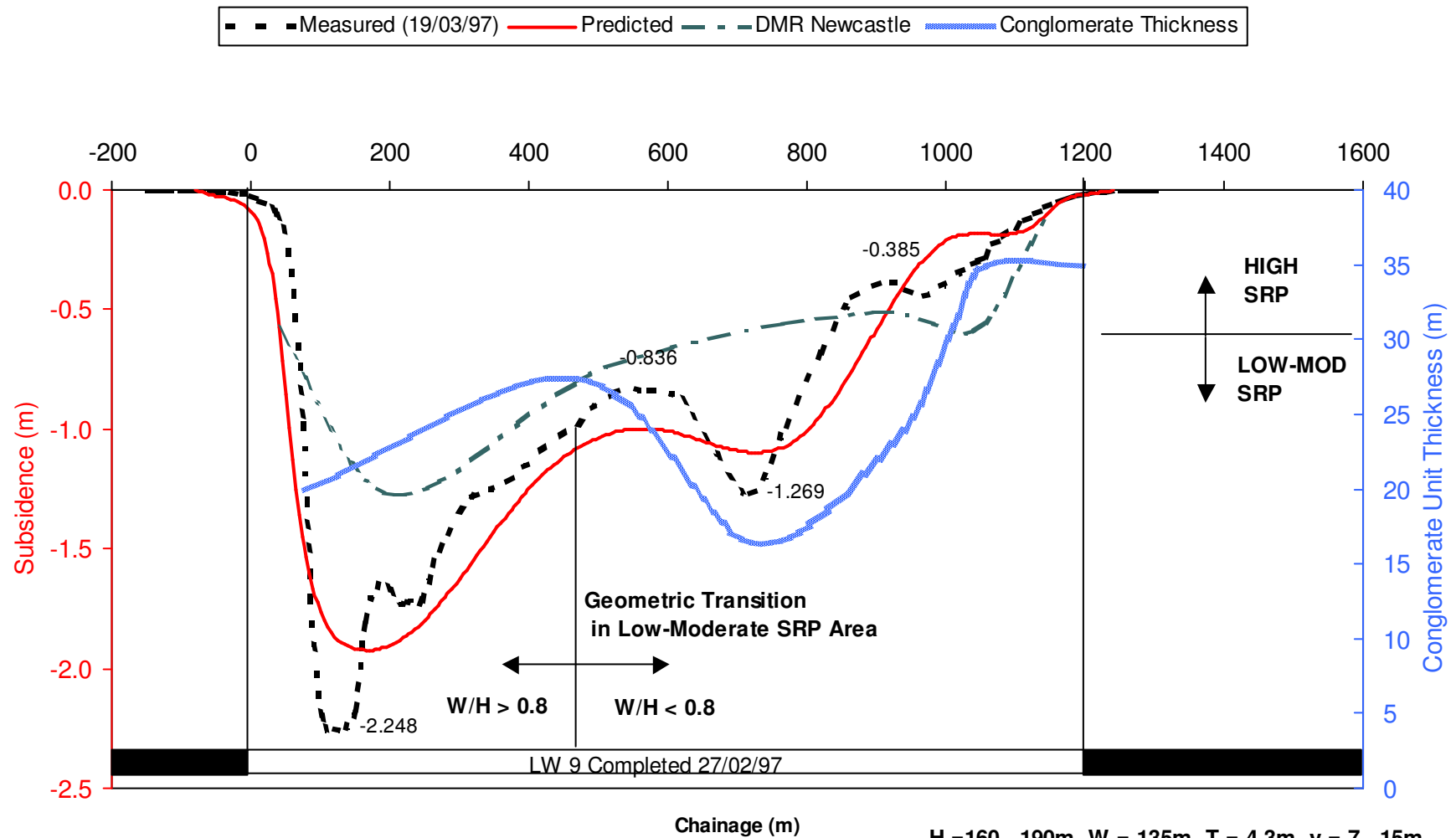
Figure No: A29.1




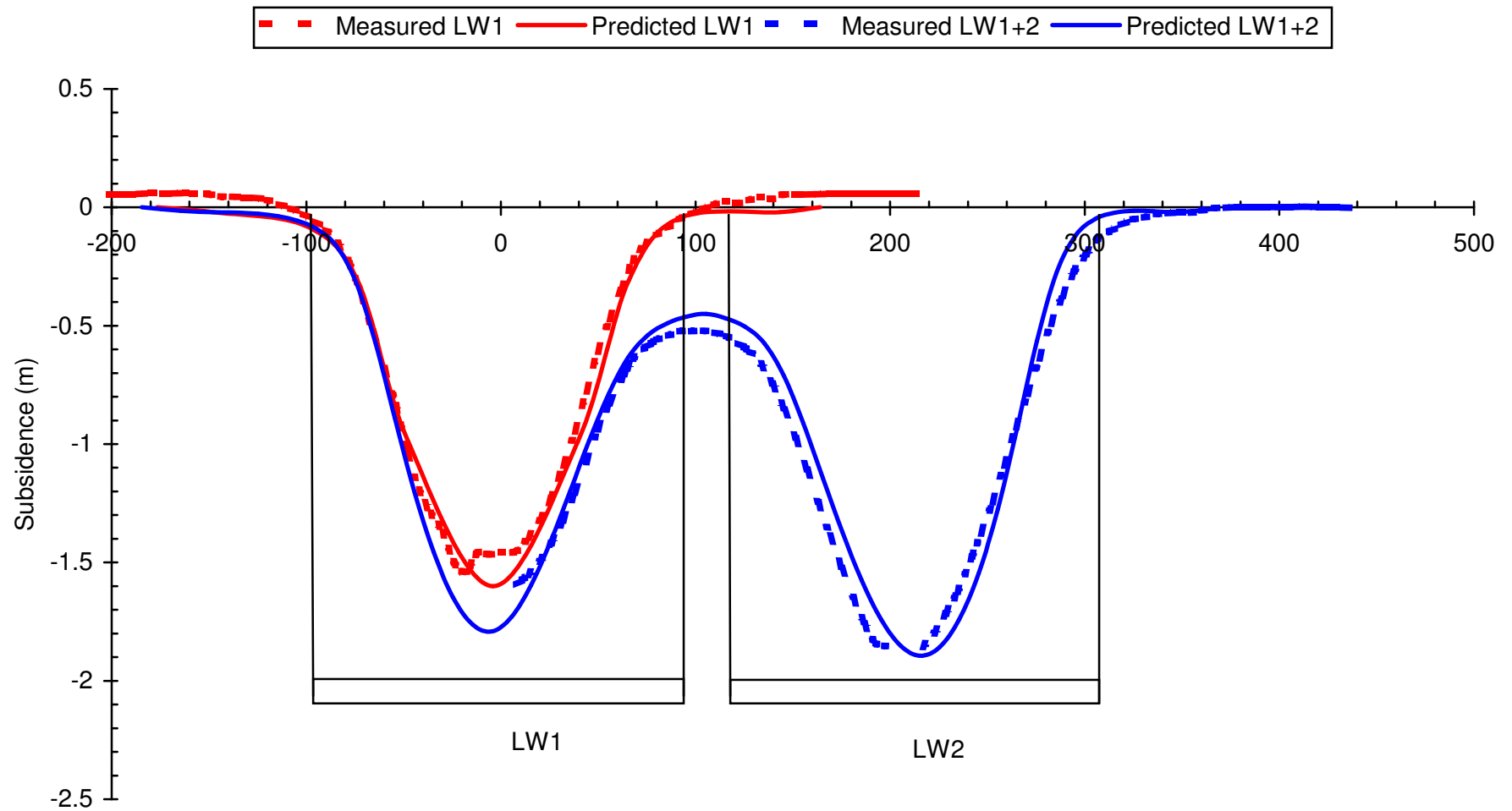
	Engineer:	S.Ditton	Client:	Holla and Barclay, 2000 Adapted for ACARP, 2003			
	Drawn:	S.Ditton					
	Date:	08.08.08	Title:	Empirical Model Recommended by Holla and Barclay, 2000 for Predicting Curvature from Maximum Strain Above Longwall Panels in the Newcastle Coalfield			
	Ditton Geotechnical Services Pty Ltd						
			Scale:	NTS		Figure No:	A29.2



	Engineer:	S.Ditton	Client:	Extract from ACARP, 2003			
	Drawn:	S.Ditton					
	Date:	08.08.08	Title:	Residual Errors of Database for Single Panel Prediction Model above Longwalls in the Newcastle Coalfield			
	Ditton Geotechnical Services Pty Ltd						
			Scale:	NTS		Figure No:	A30



	Engineer:	S.Ditton	Client:	Extract from ACARP, 2003		
	Drawn:	S.Ditton				
	Date:	08.08.08	Title:	Predicted v. Measured Centreline Subsidence Profiles for a Newcastle Coalfield Longwall with Massive Conglomerate Strata and Sub-Critical to Supercritical Transition		
	Ditton Geotechnical Services Pty Ltd			Scale:	NTS	Figure No:

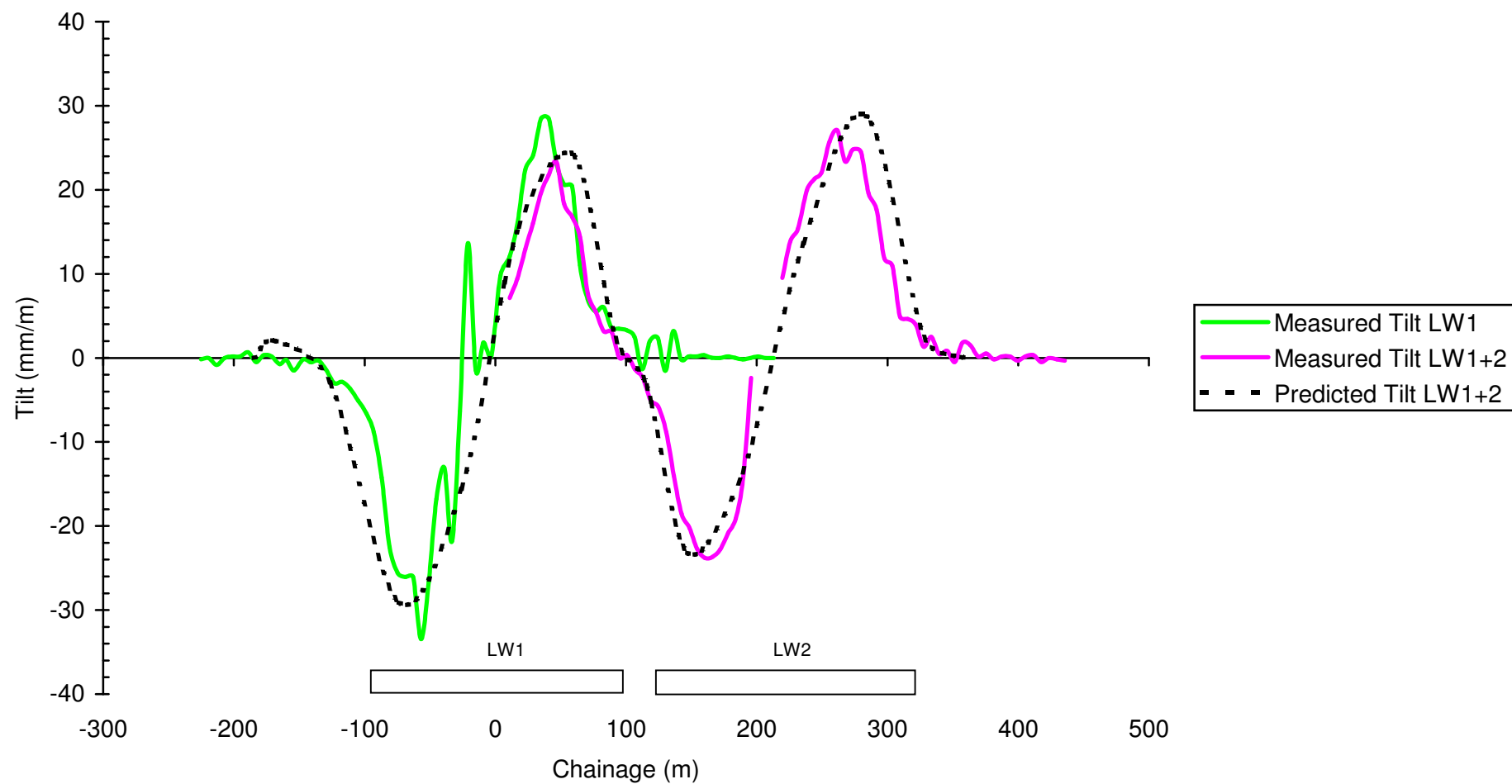



Engineer: S.Ditton  
 Drawn: S.Ditton  
 Date: 08.08.08  
 Ditton Geotechnical  
 Services Pty Ltd

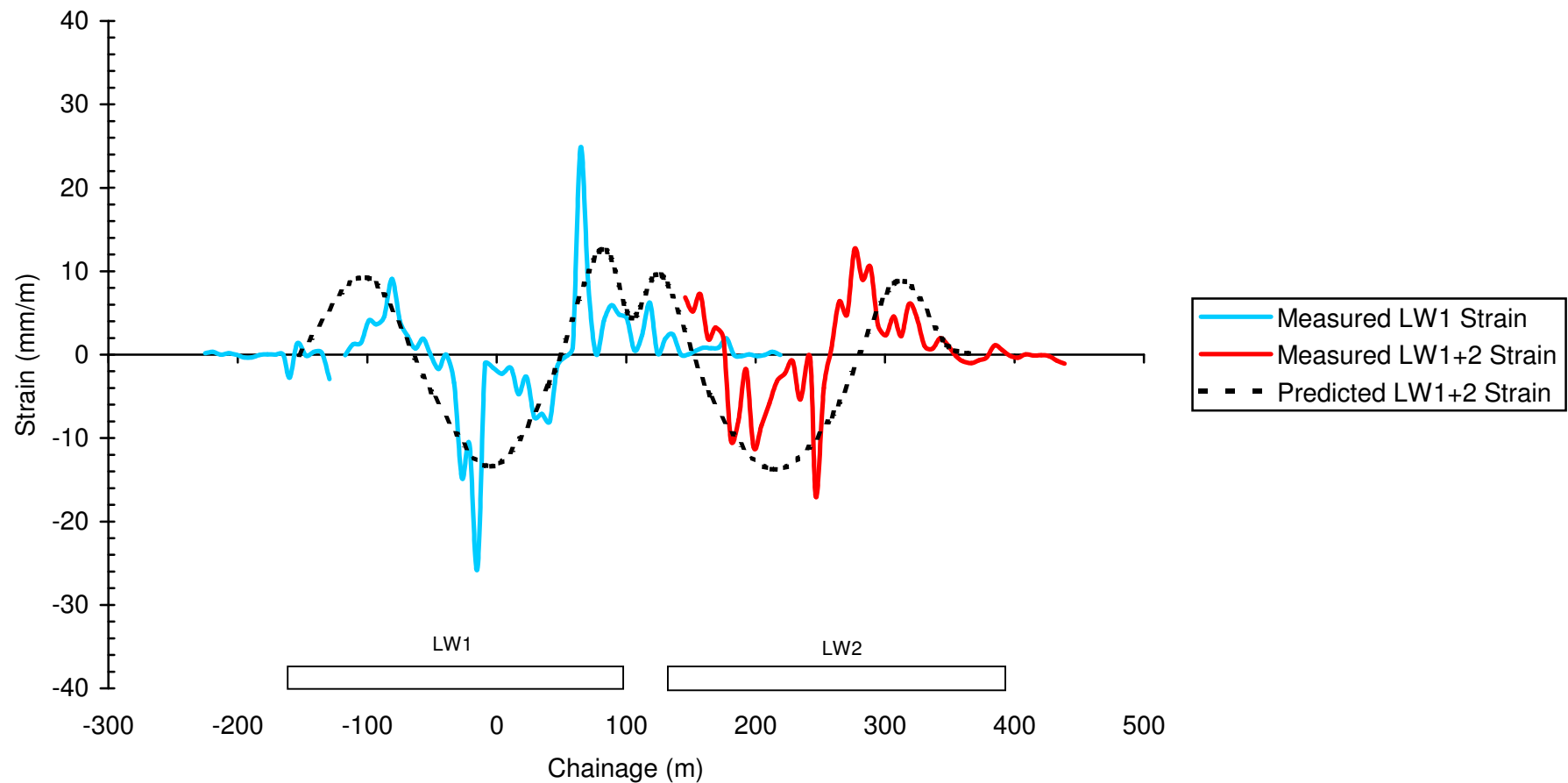
Client: Extract from ACARP, 2003  
 Title: Predicted v. Measured Crossline Subsidence Profiles for a Newcastle Coalfield Longwall Mine  
 Scale: NTS

Figure No: A32





	Engineer:	S.Ditton	Client:	Extract from ACARP, 2003		
	Drawn:	S.Ditton				
	Date:	08.08.08	Title:	Predicted v. Measured Crossline Tilt Profiles for a Newcastle Coalfield Longwall Mine		
	Ditton Geotechnical Services Pty Ltd					
			Scale:	NTS		Figure No:



DgS



Engineer: S.Ditton

Drawn: S.Ditton

Date: 08.08.08

Ditton Geotechnical  
Services Pty Ltd

Client:

Extract from ACARP, 2003

Title:

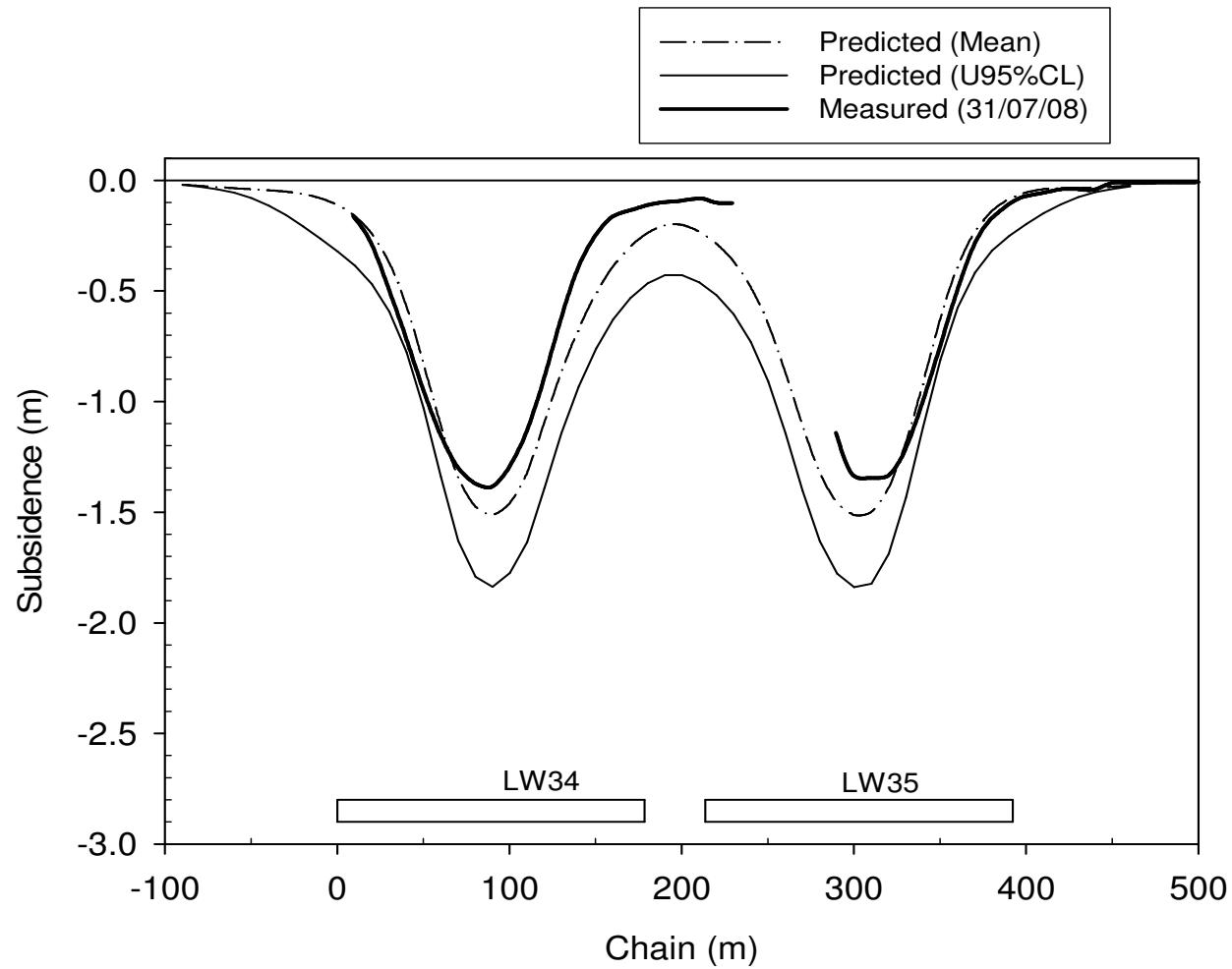
Predicted v. Measured Crossline Strain Profiles for a Newcastle Coalfield Longwall Mine


Scale:

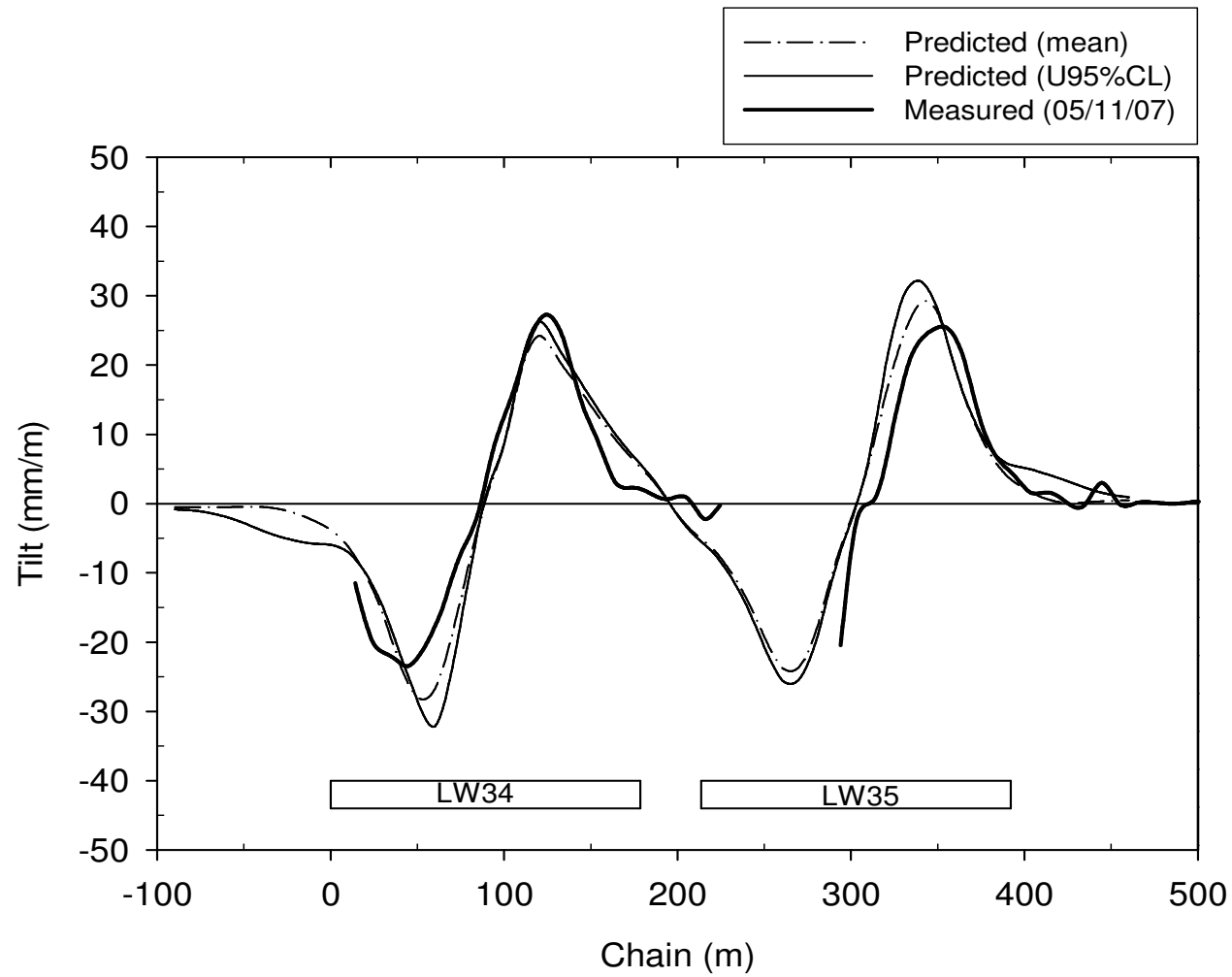
NTS


Figure No:

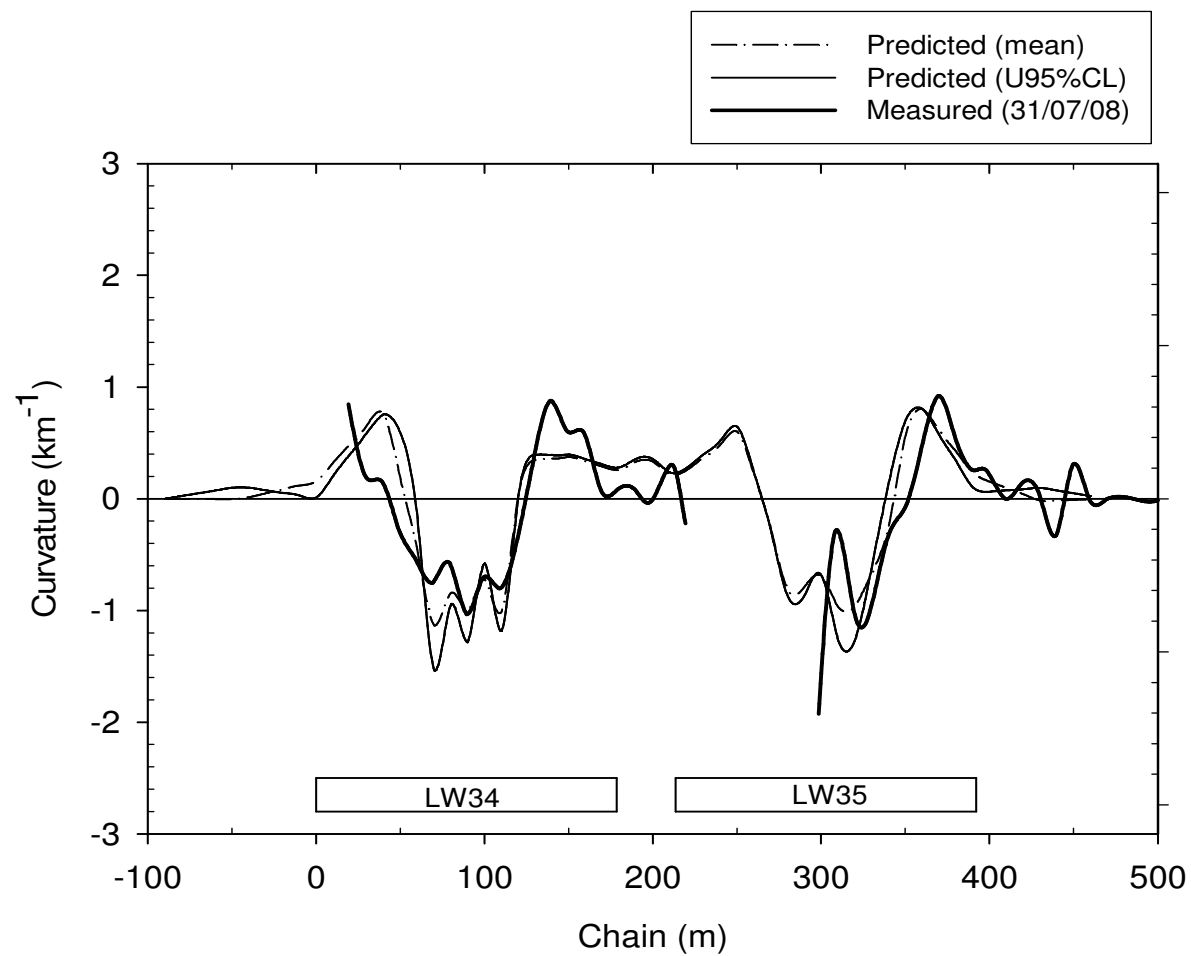
A34




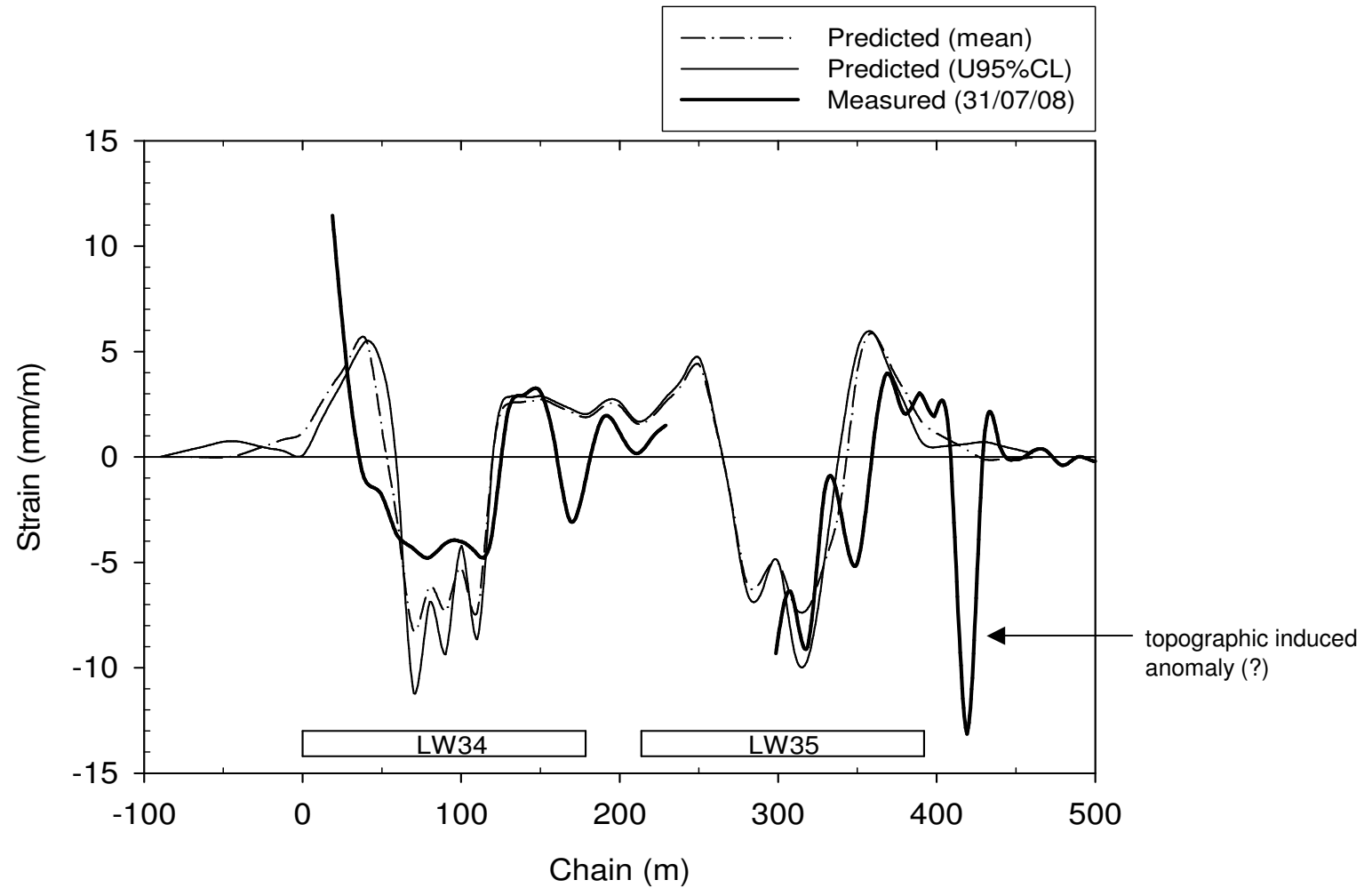
	Engineer:	S.Ditton	Client:	DgS, 2008 Modified ACARP, 2003 Model Outcomes			
	Drawn:	S.Ditton					
	Date:	07.09.08	Title:	Predicted v. Measured Crossline Subsidence Profiles for a Newcastle Coalfield Longwall Longwall Panel			
	Ditton Geotechnical Services Pty Ltd						
			Scale:	NTS		Figure No:	A35



	Engineer:	S.Ditton	Client:	DgS, 2008 Modified ACARP, 2003 Model Outcomes			
	Drawn:	S.Ditton					
	Date:	07.09.08	Title:	Predicted v. Measured Crossline Tilt Profiles for a Newcastle Coalfield Longwall Mine			
	Ditton Geotechnical						
	Services Pty Ltd		Scale:	NTS		Figure No:	A36



	Engineer:	S.Ditton	Client:	DgS, 2008 Modified ACARP, 2003 Model Outcomes			
	Drawn:	S.Ditton					
	Date:	07.09.08	Title:	Predicted v. Measured Crossline Curvature Profiles for a Newcastle Coalfield Longwall Mine			
	Ditton Geotechnical						
	Services Pty Ltd		Scale:	NTS		Figure No:	A37



DgS



Engineer: S.Ditton

Drawn: S.Ditton

Date: 08.09.08

Ditton Geotechnical  
Services Pty Ltd

Client: DgS, 2008 Modified ACARP, 2003 Model Outcomes

Title: Predicted v. Measured Crossline Strain Profiles for a Newcastle Coalfield Longwall Mine

Scale: NTS

Figure No: A38



#### Strain Concentration Factor Calculation for 10 m Baylength<sup>^</sup>

- Measured crack width = 100 mm.
- Measured crack depth >5 m
- Location = 27 m from solid rib.  
S<sub>max</sub> = 1.4 m.
- Cover depth, H = 180 m.
- LW panel width, W = 175 m.  
(W/H = 0.97)
- Measured curvature,  
C = 1.15 km<sup>-1</sup>  
(radius of 867 m)
- Measured strain over 10 m,  
E = 5.8 mm/m\*
- Concentrated strain = crack  
width/bay-length = 100/10 = 10  
mm/m.

Therefore, concentrated strain =  
10/5.8 = 1.7 x uniform strain.

\*- peak strains measured 10 m to  
south of crack at same distance from  
rib.

<sup>^</sup> - It is likely that strain concentration  
includes strain from adjacent 'bays'.

DgS



Engineer: S.Ditton

Drawn: S.Ditton

Date: 08.08.08

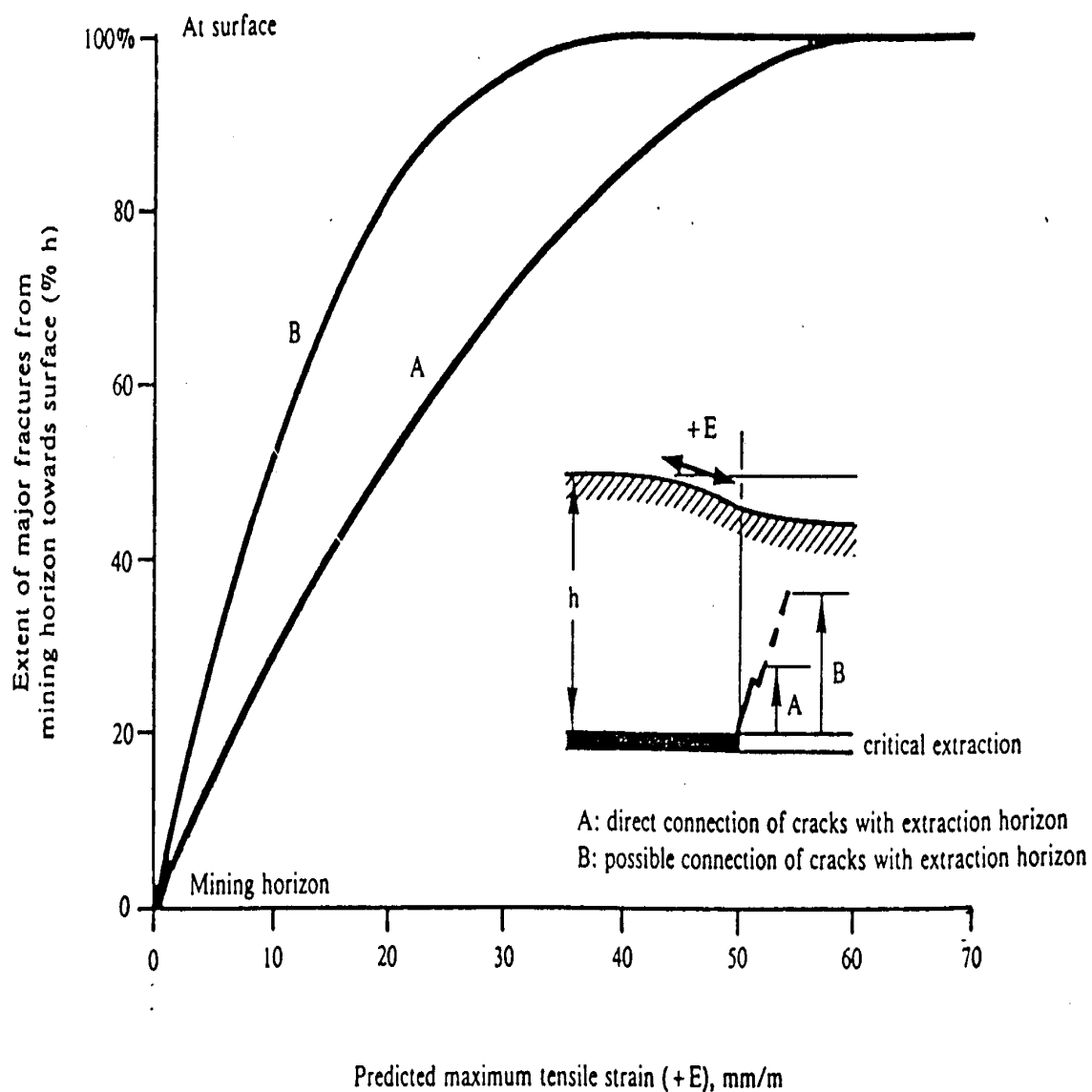
Ditton Geotechnical  
Services Pty Ltd

Client: Adapted from ACARP, 2003

Title: Example of Strain Concentration Effect Above Longwall with Shallow Surface Rock

Scale: NTS

Figure No: A39



Engineer: S.Ditton  
 Drawn: S.Ditton  
 Date: 30.04.07  
 Ditton Geotechnical  
 Services Pty Ltd

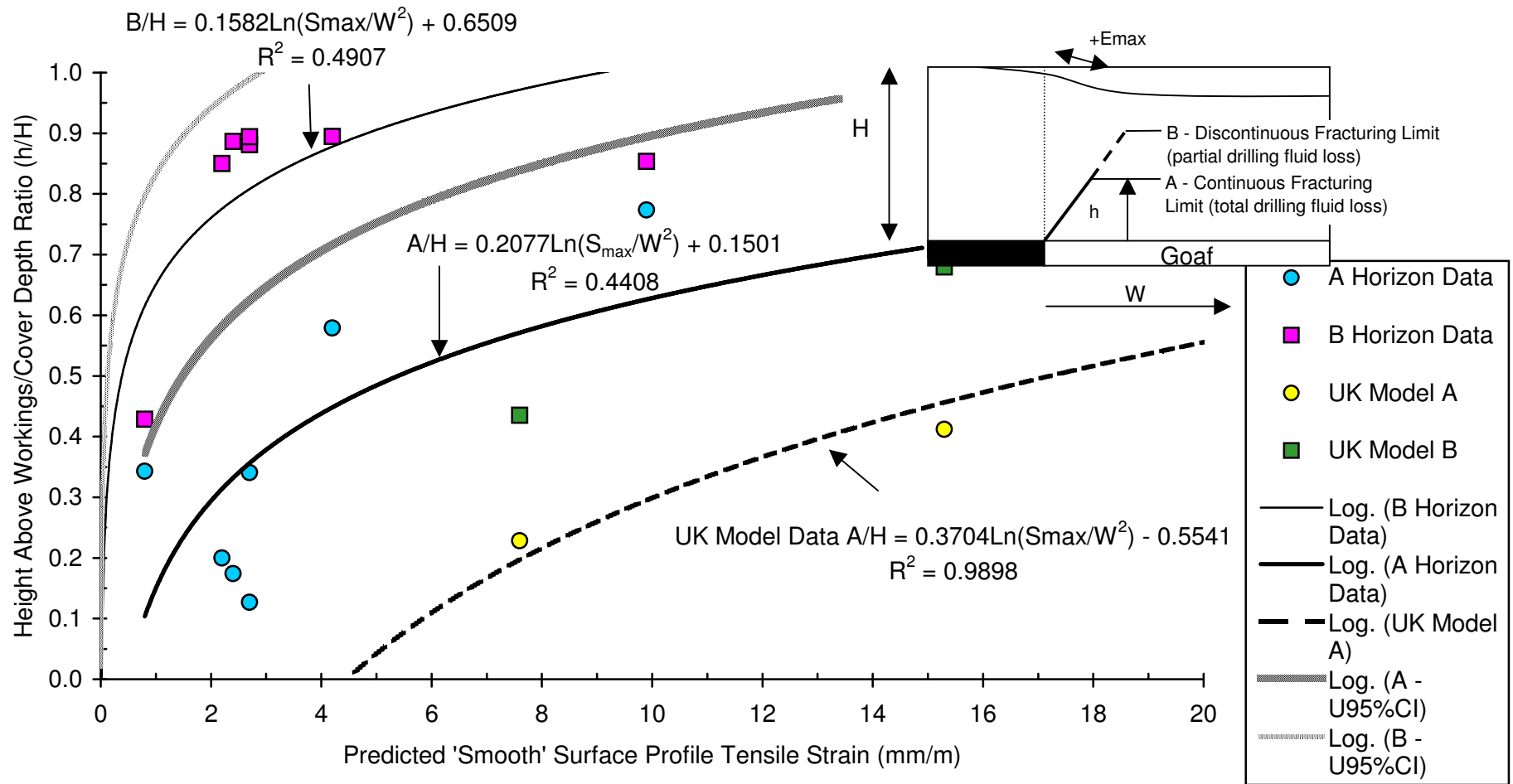
Client: Extract from ACARP, 2003

Title: Empirically Based Sub-Surface Fracturing Model  
 Presented in Whittaker & Reddish, 1989

Scale: NTS

Figure No: A40





DgS



Engineer: S.Ditton

Drawn: S.Ditton

Date: 12.08.08

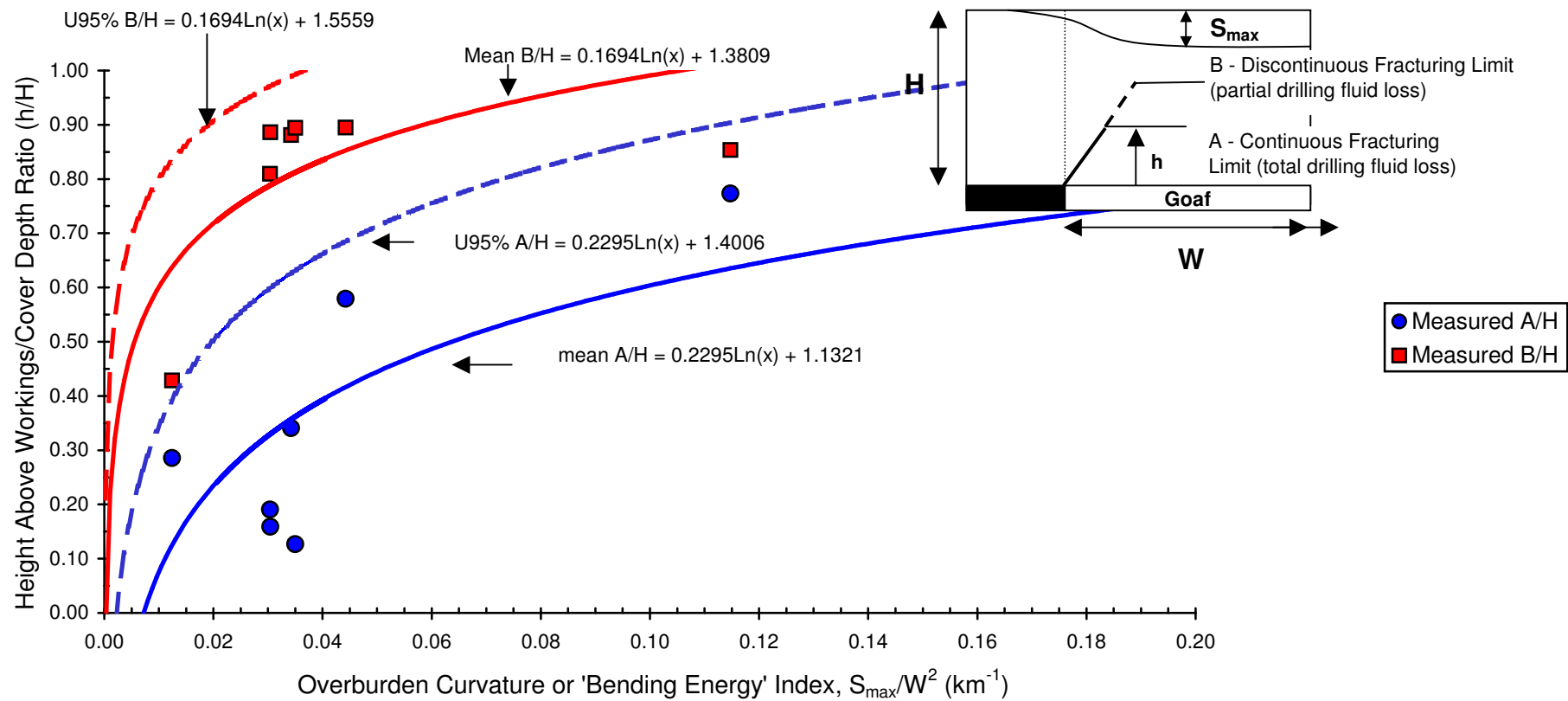
Ditton Geotechnical  
Services Pty Ltd

Client: Extract from ACARP, 2003

Title: Continuous and Discontinuous Sub-Surface Fracture Height Model above Longwalls  
using Surface Tensile Strains

Scale: NTS

Figure No: A41



DgS



Engineer: S.Ditton

Drawn: S.Ditton

Date: 12.08.08

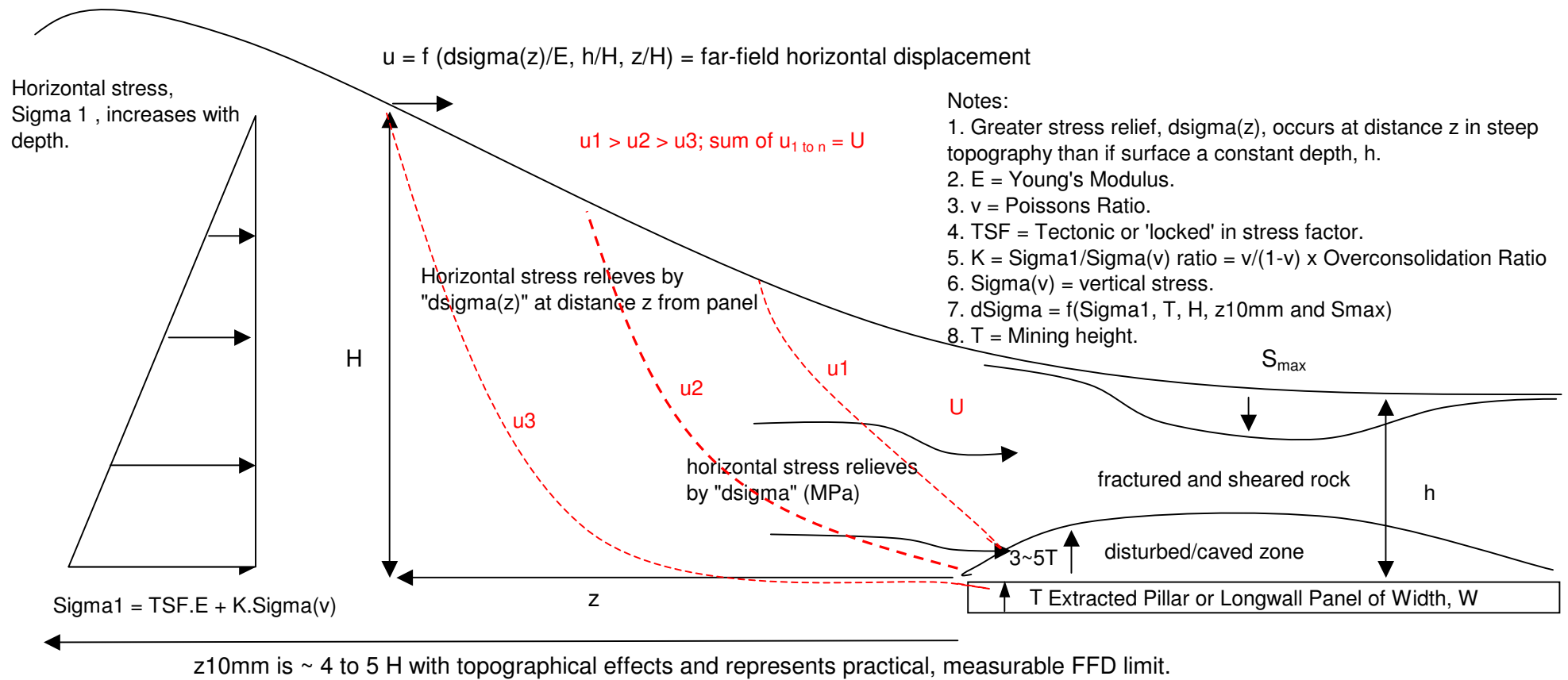
Ditton Geotechnical  
Services Pty Ltd

Client: Extract from ACARP, 2003

Title: Continuous and Discontinuous Sub-Surface Fracture Heights above Longwalls  
(based on ACARP, 2003)

Scale: NTS

Figure No: A42



Simple Analytical Model for Predicting Total FFD :  $U = 0.5(\sigma_1 \times 12.3/2)z_{10mm}/[E(H+h)/2] + \text{'tail' of 10mm} + S_{\max} \text{ component (refer to text)}$

DgS



Engineer: S.Ditton

Drawn: S.Ditton

Date: 22.05.07

Ditton Geotechnical  
Services Pty Ltd

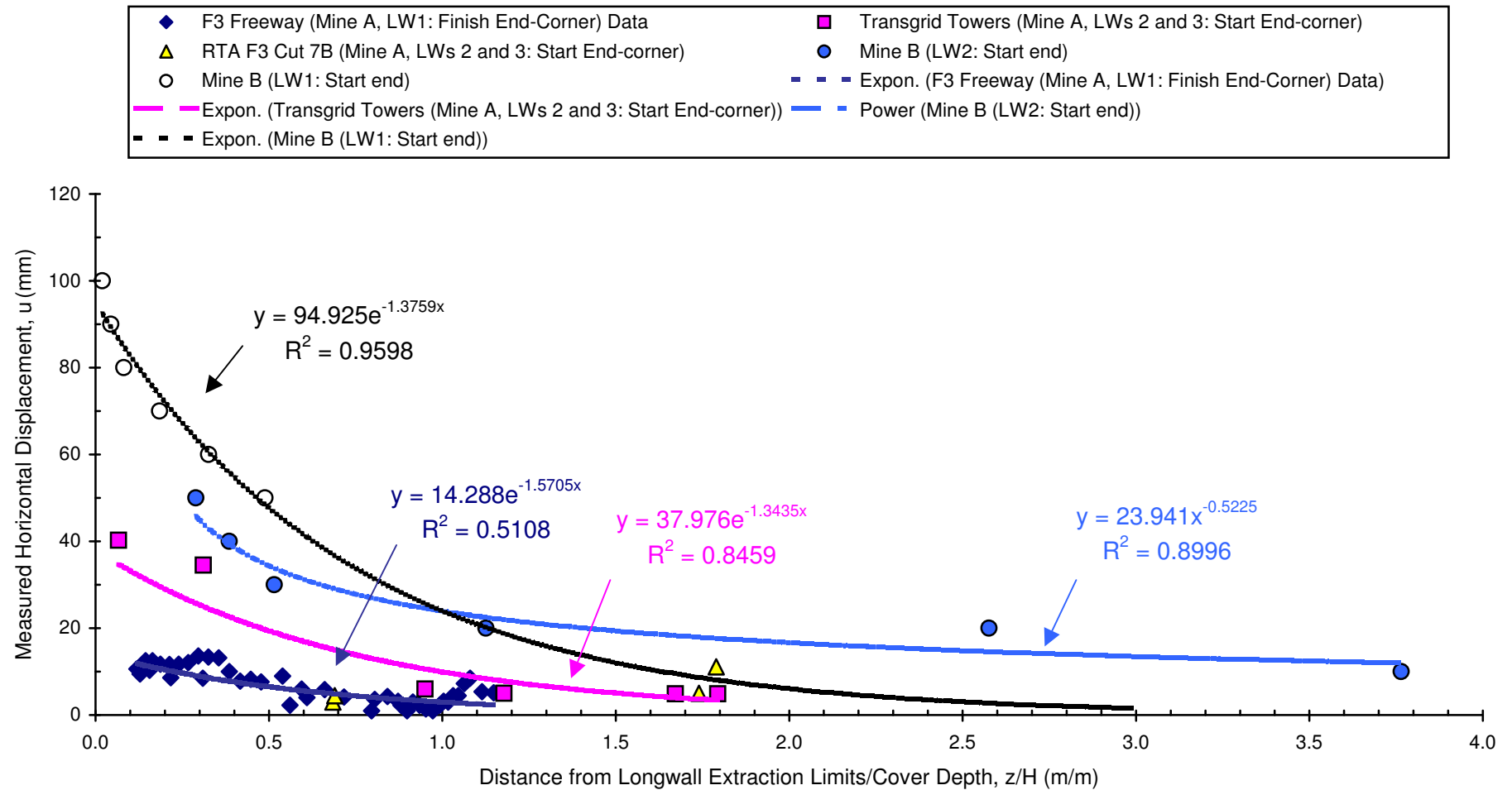
Client: DgS, 2007

Title: Conceptual Model of Far-Field Displacement Outside Angle of Draw Limits from Pillar  
Extraction or Longwall Panels

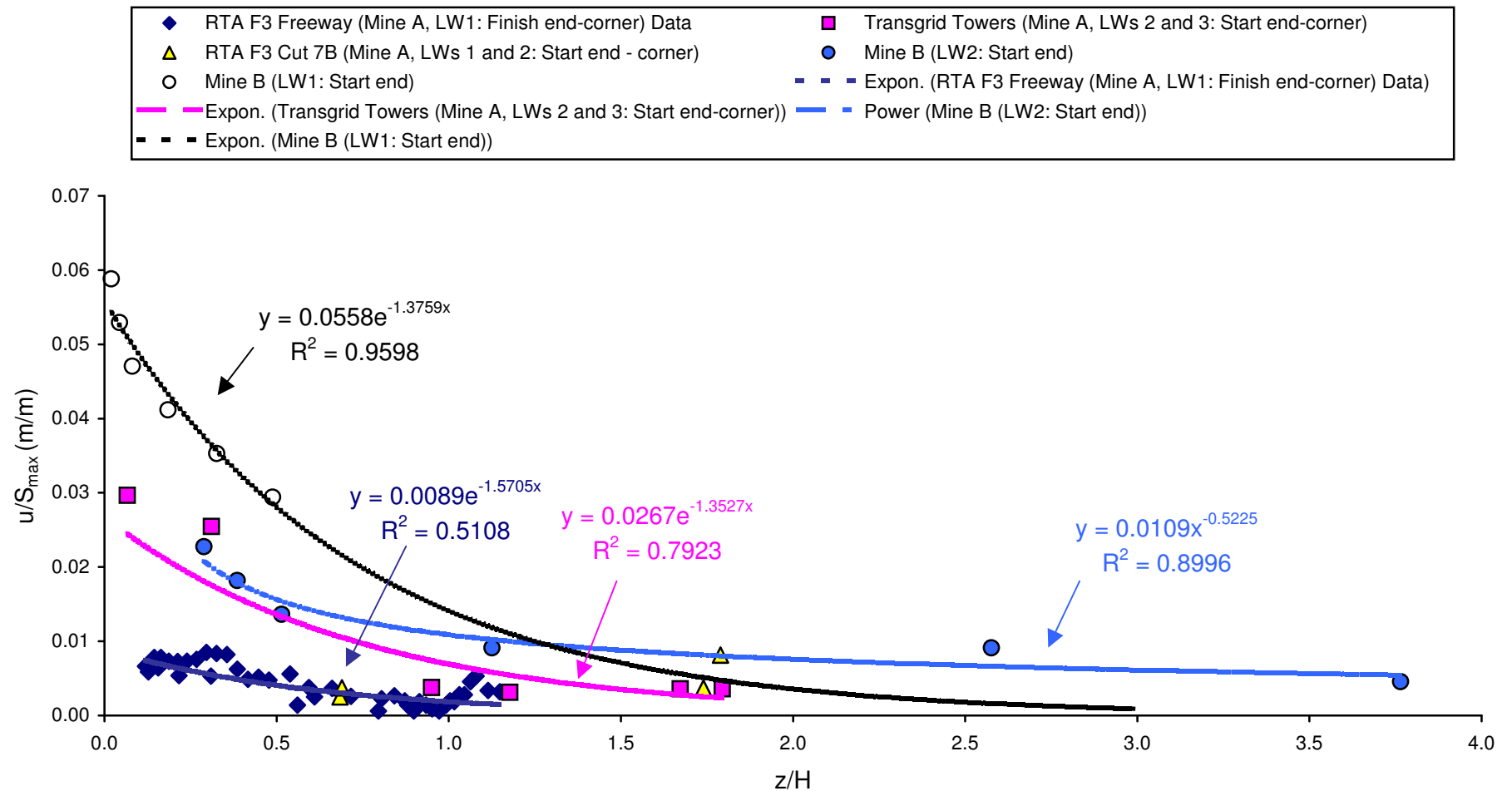
Scale: NTS

Figure No: A43

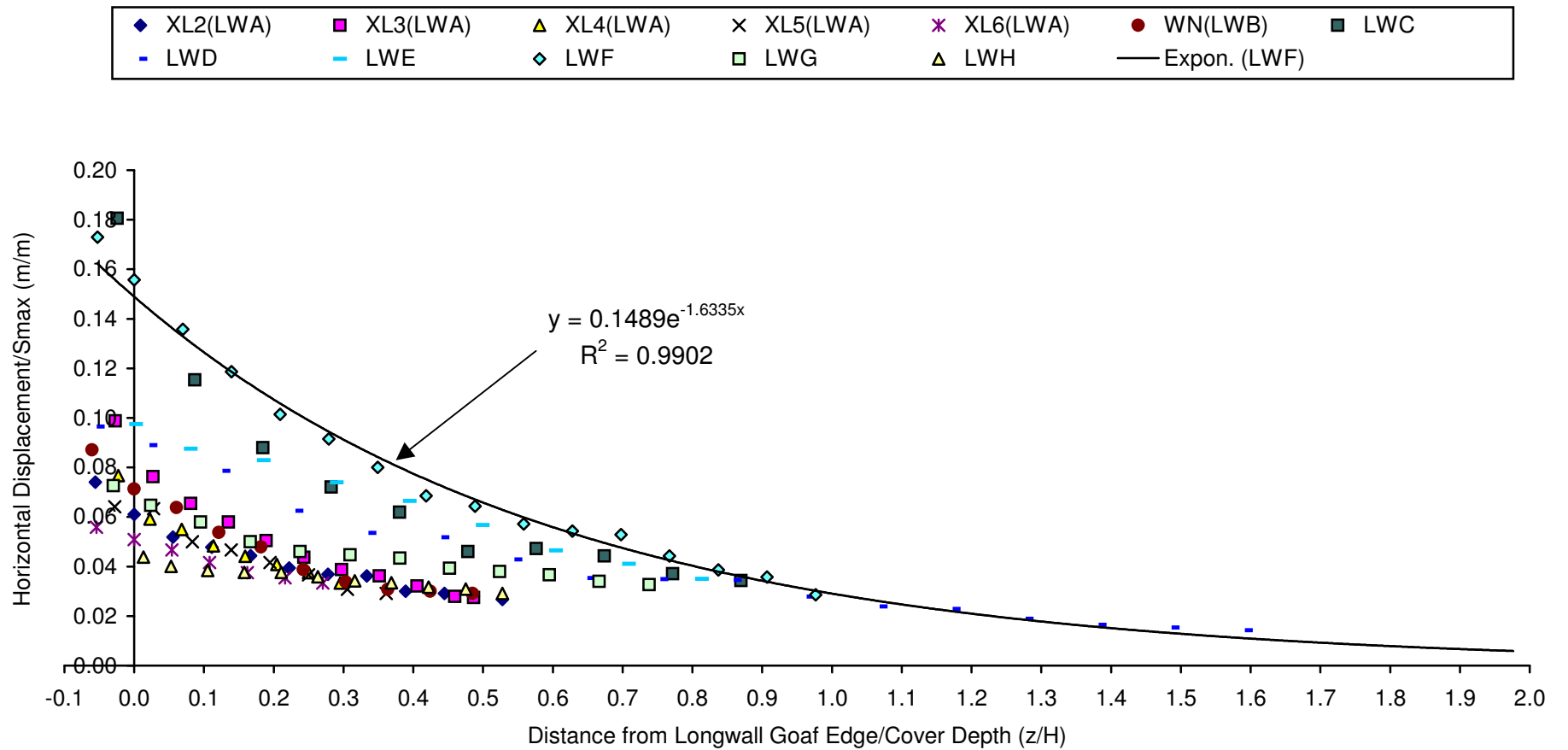





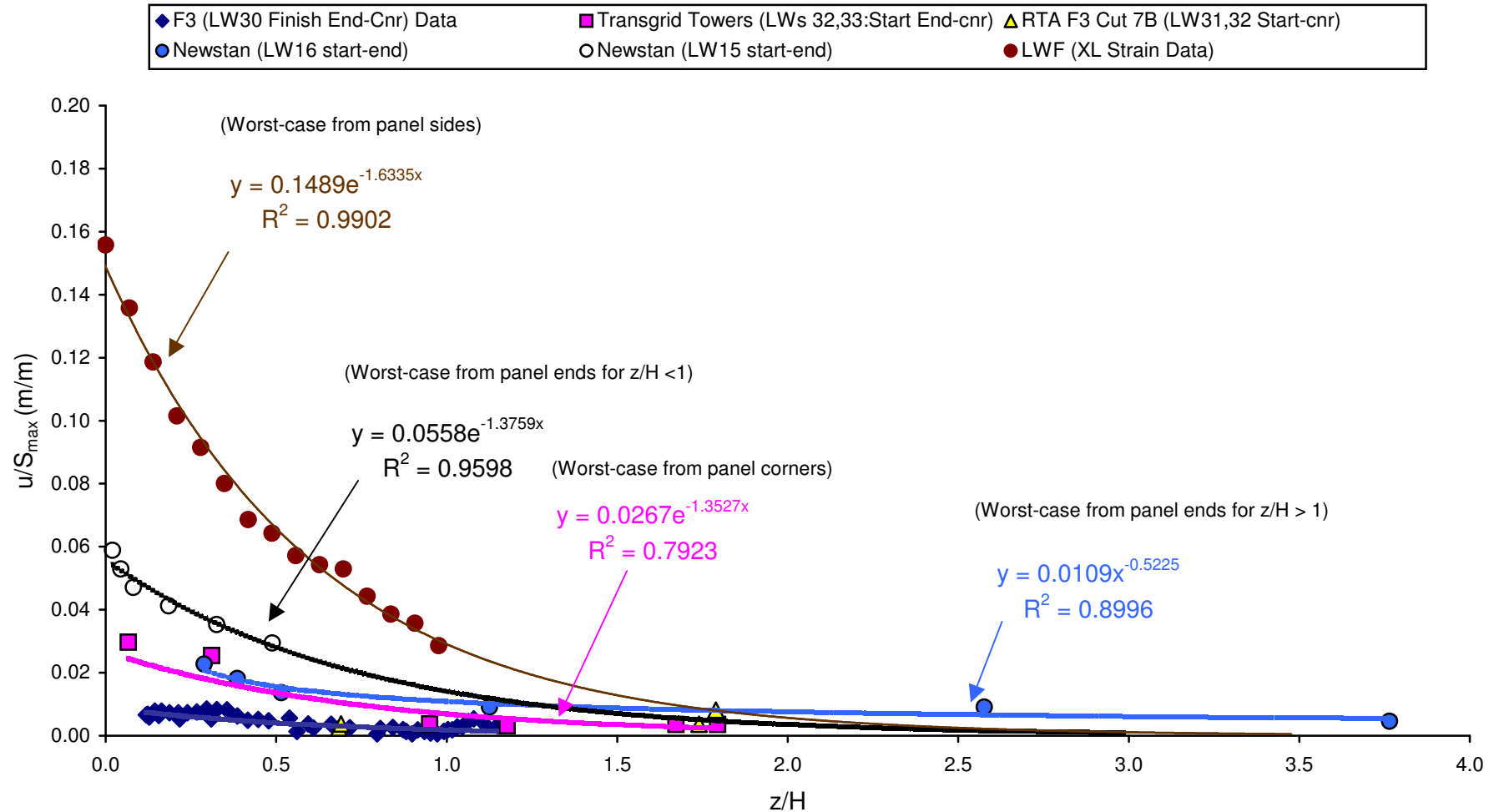
Engineer:	S.Ditton	Client:	DgS, 2007
Drawn:	S.Ditton		
Date:	22.05.07	Title:	Empirical far-field displacement prediction model using total station electronic distance measurements from longwall panel ends
Ditton Geotechnical Services Pty Ltd		Scale:	NTS
		Figure No:	A45



Engineer:	S.Ditton	Client:	DgS, 2007
Drawn:	S.Ditton		
Date:	22.05.07	Title:	Empirical far-field displacement prediction model using total station electronic distance measurements from longwall panel ends and normalised to maximum panel subsidence
Ditton Geotechnical Services Pty Ltd		Scale:	NTS
		Figure No:	A46



	Engineer:	S.Ditton	Client:	DgS, 2007			
	Drawn:	S.Ditton					
	Date:	22.05.07	Title:	Empirical far-field displacement prediction model using cummulative steel tape measurements from longwall sides and normalised to maximum panel subsidence			
	Ditton Geotechnical Services Pty Ltd						
			Scale:	NTS		Figure No:	A47



Engineer: S.Ditton  
 Drawn: S.Ditton  
 Date: 22.05.07  
 Ditton Geotechnical  
 Services Pty Ltd

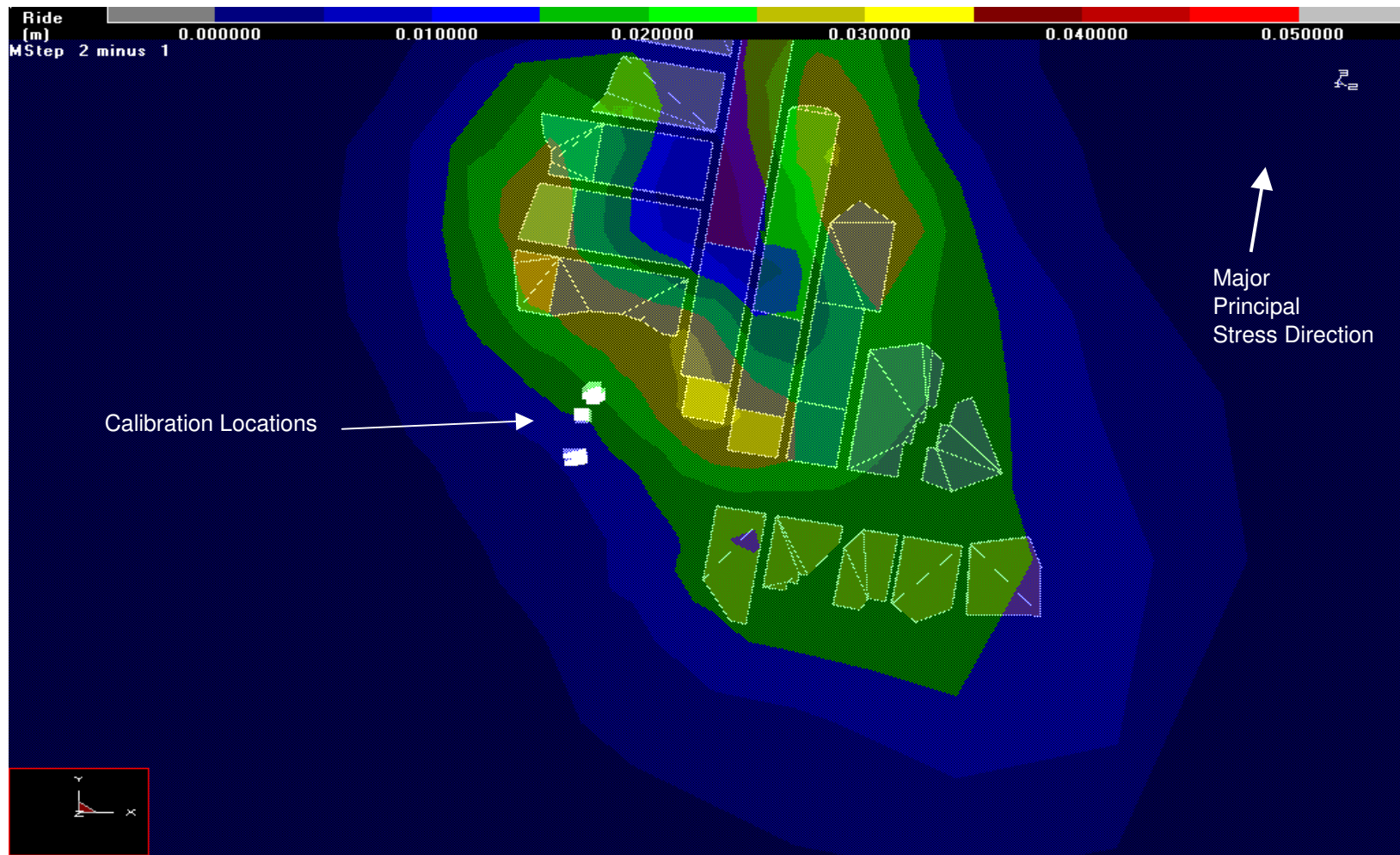
Client: DgS, 2007


Title: Combined empirical far-field displacement prediction models for longwall panel sides, ends and corners.

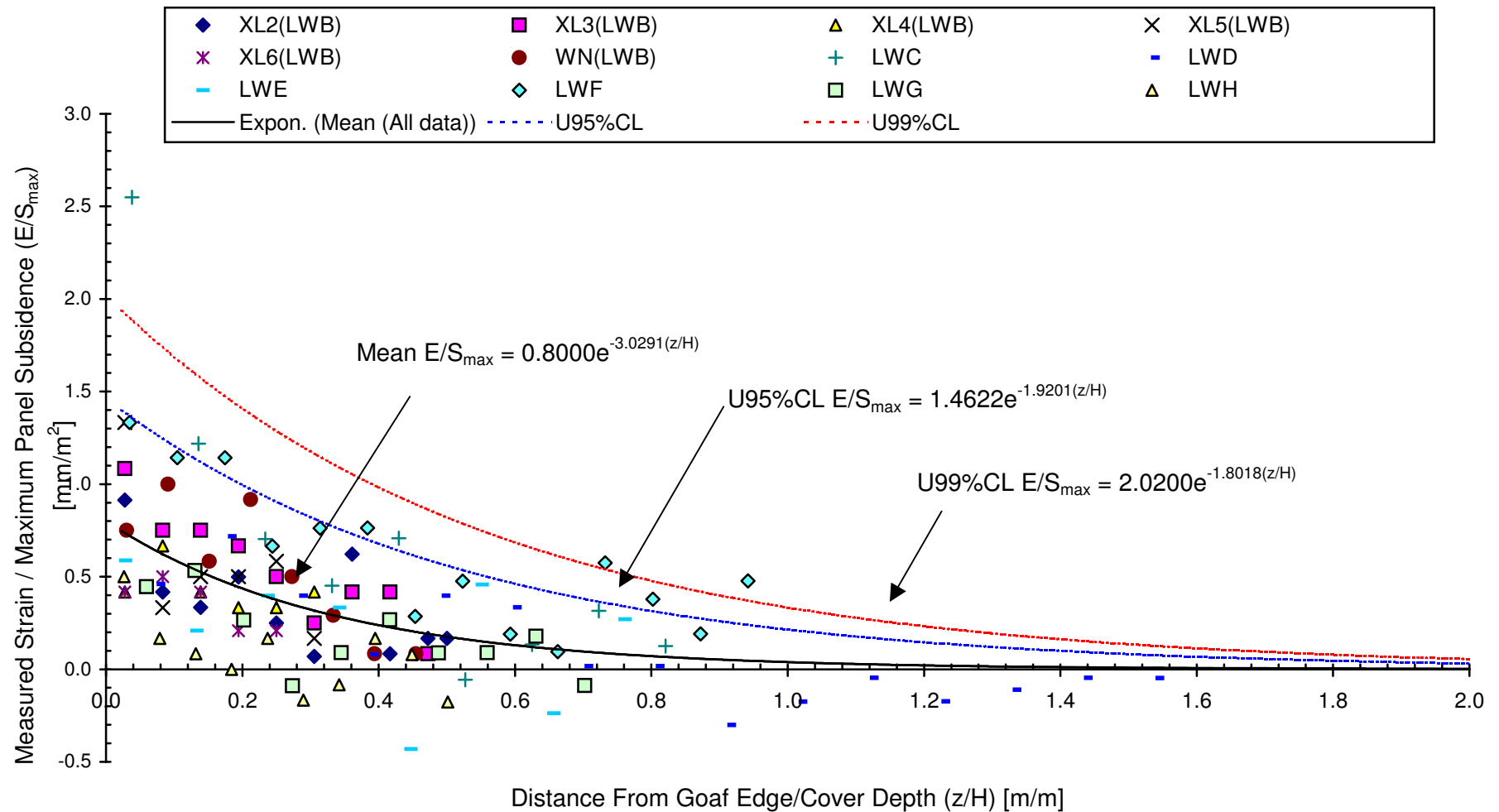
Scale: NTS


Figure No: A48





	Engineer:	S.Ditton	Client:	DgS, 2007				
	Drawn:	S.Ditton						
	Date:	22.05.07	Title:	Example of Map-3D Elastic Boundary Element Model Far-Field Displacement Contours Around a Complex Pillar Extraction Mining Layout				
	Ditton Geotechnical Services Pty Ltd							
	Scale:		NTS			Figure No:	A48	



	Engineer:	S.Ditton	Client:	DgS, 2007			
	Drawn:	S.Ditton					
	Date:	22.05.07	Title:	Empirical far-field strain prediction model using cummulative steel tape measurements from longwall sides and normalised to maximum panel subsidence			
	Ditton Geotechnical Services Pty Ltd			Scale:	NTS		Figure No:



## **APPENDIX B – Extracts from the SDPS<sup>®</sup> User Manual**

# SDPS

**Surface Deformation Prediction System**  
*for Windows*  
**version 5.2**

**Quick Reference Guide and Working Examples**

by

Dr. Zacharias Agioutantis and Dr. Michael Karmis  
Department of Mining and Minerals Engineering  
Virginia Polytechnic Institute and State University  
Blacksburg, Virginia 24061-0239

This software package is the property of the Department of Mining and Minerals Engineering, VPI & SU. It has been licensed and may be distributed only to O.S.M.R.E. and State Regulatory Agencies. The SDPS software can be purchased by individuals and/or companies through Carlson Software.

February 2002

## List of Symbols

w	the panel width; the minimum dimension of a panel
h	panel depth; the vertical distance between the mining horizon and the surface; also known as the overburden thickness
m	the seam thickness; the extraction thickness (note that the extraction thickness may be different than the seam thickness)
R	the extraction ratio
R*	the adjusted extraction ratio
d	the distance of the inflection point from the rib (a positive value indicates that the position of the inflectionpoint is inby); also referred to as the “edge effect”
$\beta$	the influence angle
r	the influence radius
Smax	the maximum subsidence
a	the maximum subsidence factor
Bs	the strain coefficient
%HR	the percent hardrock in the overburden
Wp	the pillar width
Hp	the pillar height
Wo	the opening width

# 1.7 Overview of Subsidence Parameters

## Maximum Subsidence Factor

The values of maximum subsidence factor, as function of the width-to-depth ratio and the percent hardrock in the overburden, are shown in the supercritical subsidence factor tables for longwall panels and for room-and-pillar panels respectively. When using the profile function method, the subsidence factor is calculated for the actual width-to-depth ratio of the panel. For example, for a panel with  $W/h = 0.8$  (subcritical) and  $\%HR = 50\%$  the subsidence factor is equal to 0.38.

When using the influence function method, the technique requires knowledge of the supercritical subsidence factor, which will subsequently be adjusted through the superposition concept by the program itself. For example, for a panel with  $W/h = 0.8$  (subcritical) and  $\%HR = 50\%$  the subsidence factor is found for  $W/h = 1.5$  (supercritical) and equal to 0.40.

### Notes:

A panel is considered supercritical for  $W/h$  greater than 1.2. Due to numerical approximations there may be slight variations to the supercritical subsidence factors presented in the supercritical subsidence factor tables.

## Inflection Point

The location of the inflection point from the rib, with respect to overburden depth ( $d/h$ ), can be estimated based on two empirical curves (see the Inflection Point Diagram). Both curves were statistically generated from the available field data. The first is an average curve based on a least squares estimator, while the second is considered an envelope or conservative curve in the sense that it tends to overpredict the surface impact of a given excavation area. In essence, this means that for average data the predicted subsidence profile could be either inside or outside of the measured subsidence line, whereas for conservative (envelope) data, an attempt is made to keep the prediction lines outside the measured ones, i.e. overestimate the influence of the mined area to the surface.

From experience and constant validation of the programs, the authors recommend that, for Appalachian predictions, improved accuracy is obtained by using the following rule: determine the  $d/h$  ratio using the conservative curve for subcritical panels ( $W/h < 1.2$ ) determine the  $d/h$  ratio using the average curve for supercritical panels ( $W/h \geq 1.2$ ).

### Notes:

Always use the actual width-to-depth ratio.

## Angle of Influence

The angle of principal influence ( $\beta$ , beta) is one of the basic parameters used in the influence function method since it has a major impact on the distribution of the deformations on the surface. It is measured in degrees from the horizontal and the

average value determined for the Appalachian coalfields is  $\beta=67$  deg. The parameter required for these calculations is the tangent of this angle (i.e.  $\tan\beta = 2.31$ ). The angle of influence is related to the radius of influence as shown in the equation:

$$\tan\beta = \frac{h}{r}$$

where

$h$  = the overburden depth

$r$  = the radius of influence

This value should be determined for each site by fitting a calculated subsidence profile to a measured subsidence profile. If this is not possible, the influence angle can be approximately set as the complementary angle to the angle of draw.

### Supercritical Subsidence Factor Tables

The supercritical subsidence factors used in the calculations are presented in Tables 1.7.1 and 1.7.2.

Table 1.7.1: Calculation of maximum subsidence factors ( $S_{max}/m$ ) for longwall panels

W/h	Percent Hardrock in the Overburden							
	10%	20%	30%	40%	50%	60%	70%	80%
0.6	0.64	0.59	0.51	0.42	0.34	0.26	0.21	0.16
0.7	0.69	0.63	0.55	0.46	0.36	0.28	0.22	0.18
0.8	0.71	0.65	0.57	0.47	0.38	0.29	0.23	0.18
0.9	0.72	0.66	0.58	0.48	0.38	0.30	0.23	0.19
1.0	0.73	0.67	0.58	0.49	0.39	0.30	0.24	0.19
1.1	0.74	0.68	0.59	0.49	0.39	0.31	0.24	0.19
1.2	0.74	0.68	0.59	0.49	0.39	0.31	0.24	0.19
1.3	0.74	0.68	0.60	0.49	0.40	0.31	0.24	0.19
1.4	0.75	0.69	0.60	0.50	0.40	0.31	0.24	0.19
1.5	0.75	0.69	0.60	0.50	0.40	0.31	0.24	0.19
1.6	0.75	0.69	0.60	0.50	0.40	0.31	0.24	0.19
1.7	0.75	0.69	0.60	0.50	0.40	0.31	0.24	0.19
1.8	0.75	0.69	0.60	0.50	0.40	0.31	0.24	0.19
1.9	0.76	0.69	0.60	0.50	0.40	0.31	0.24	0.19
2.0	0.76	0.69	0.60	0.50	0.40	0.31	0.24	0.19

Table 1.7.2: Calculation of maximum subsidence factors ( $S_{max}/(m R^*)$ ) for high extraction room-and-pillar panels

W/h	Percent Hardrock in the Overburden							
	10%	20%	30%	40%	50%	60%	70%	80%
0.6	0.52	0.48	0.42	0.35	0.28	0.22	0.17	0.13
0.7	0.57	0.53	0.46	0.38	0.30	0.24	0.19	0.15
0.8	0.60	0.55	0.48	0.40	0.32	0.25	0.19	0.15
0.9	0.61	0.56	0.49	0.41	0.32	0.25	0.20	0.16
1.0	0.62	0.57	0.49	0.41	0.33	0.26	0.20	0.16
1.1	0.62	0.57	0.50	0.41	0.33	0.26	0.20	0.16
1.2	0.63	0.58	0.50	0.42	0.33	0.26	0.20	0.16
1.3	0.63	0.58	0.51	0.42	0.34	0.26	0.20	0.16
1.4	0.64	0.58	0.51	0.42	0.34	0.26	0.21	0.16
1.5	0.64	0.59	0.51	0.42	0.34	0.26	0.21	0.16
1.6	0.64	0.59	0.51	0.42	0.34	0.26	0.21	0.16
1.7	0.64	0.59	0.51	0.43	0.34	0.27	0.21	0.16
1.8	0.64	0.59	0.51	0.43	0.34	0.27	0.21	0.17
1.9	0.64	0.59	0.51	0.43	0.34	0.27	0.21	0.17
2.0	0.64	0.59	0.52	0.43	0.34	0.27	0.21	0.17

### Horizontal Strain Factor

The value of this factor is directly related to the magnitude of the calculated strains and curvatures over an undermined area. It can be empirically estimated by the average ratio of measured strain and curvature over a set of surface points.

The average value determined for the Appalachian coalfields is:

$$Bs = (0.35 \pm 0.05) \frac{h}{\tan\beta}$$

where  $h$  is the excavation depth and  $\tan\beta$  is the influence angle. The horizontal strain factor is expressed in units of length. The horizontal strain coefficient is unitless and its default value is 0.35.

**Note:** The higher the value for this coefficient, the larger the predicted strains and displacements.



# Chapter 3: The Influence Function Method

## 3.1 Overview of the Influence Function Method

Influence function methods for subsidence prediction have the ability to consider any mining geometry, to negotiate superposition of the influence from a number of excavated areas having different mining characteristics and, also, to calculate horizontal strains as well as other related deformation indices. The function utilized in SDPS is the bell-shaped Gaussian function. This method assumes that the influence function for the two-dimensional case is given by:

$$g(x, s) = \frac{S_o(x)}{r} \exp \left[ -\pi \frac{(x - s)^2}{r^2} \right]$$

where:

- r = the radius of principal influence = h / tan(beta);
- h = the overburden depth;
- beta = the angle of principal influence;
- s = coordinate of the point P, where subsidence is considered;
- x = coordinate of the infinitesimal excavated element; and
- So(x) = convergence of the roof of the infinitesimal excavated element.

Subsidence at any point P(s), therefore, can be expressed by the following equation:

$$S(x, s) = \frac{1}{r} \int_{-\infty}^{+\infty} s_o(x) \exp \left[ -\pi \frac{(x - r)^2}{r^2} \right]$$

where:

- So(x) = m(x) a(x);
- m(s) = extraction thickness; and
- a(x) = roof convergence (subsidence) factor.

The influence function formulation can thus be applied to calculate surface deformations (subsidence, strain, slope, curvature, displacements) above longwall and room-and-pillar panels, given the geometry of the excavation, information on the overburden geology, as well as the location of the prediction points on the surface.

More specifically, the required data include:

- the geometry of the mine plan and the associated properties (extraction thickness, subsidence factor for supercritical conditions)

- the location (coordinates) of the points on the surface for which prediction of the deformation indices (subsidence, strain, slope, curvature, horizontal displacement) is to be performed
- the empirical parameters that numerically represent the behavior of the overburden

The typical steps required to calculate surface deformations using the influence function method, are shown below. The corresponding flowchart is also shown in Figure 3.1.1. Figure 3.1.2 presents a schematic diagram for creating the input data. Figure 3.1.3 presents typical distributions for the deformation indices that can be calculated by the influence function method. Table 3.1.1 shows all the indices that can be calculated by the influence function method.

- ✓ Load the Influence Function Program
- ✓ Input Data
- ✓ Mine Plan Data
  - Prediction Point Data
  - Empirical Parameters
- ✓ Select calculation options
  - Subsidence
  - Horizontal Strain
  - Horizontal Displacement
  - Slope
  - Curvature
- ✓ Save Project File
- ✓ Calculate Surface Deformations
- ✓ Load Graphing Program
- ✓ View Calculated Deformations

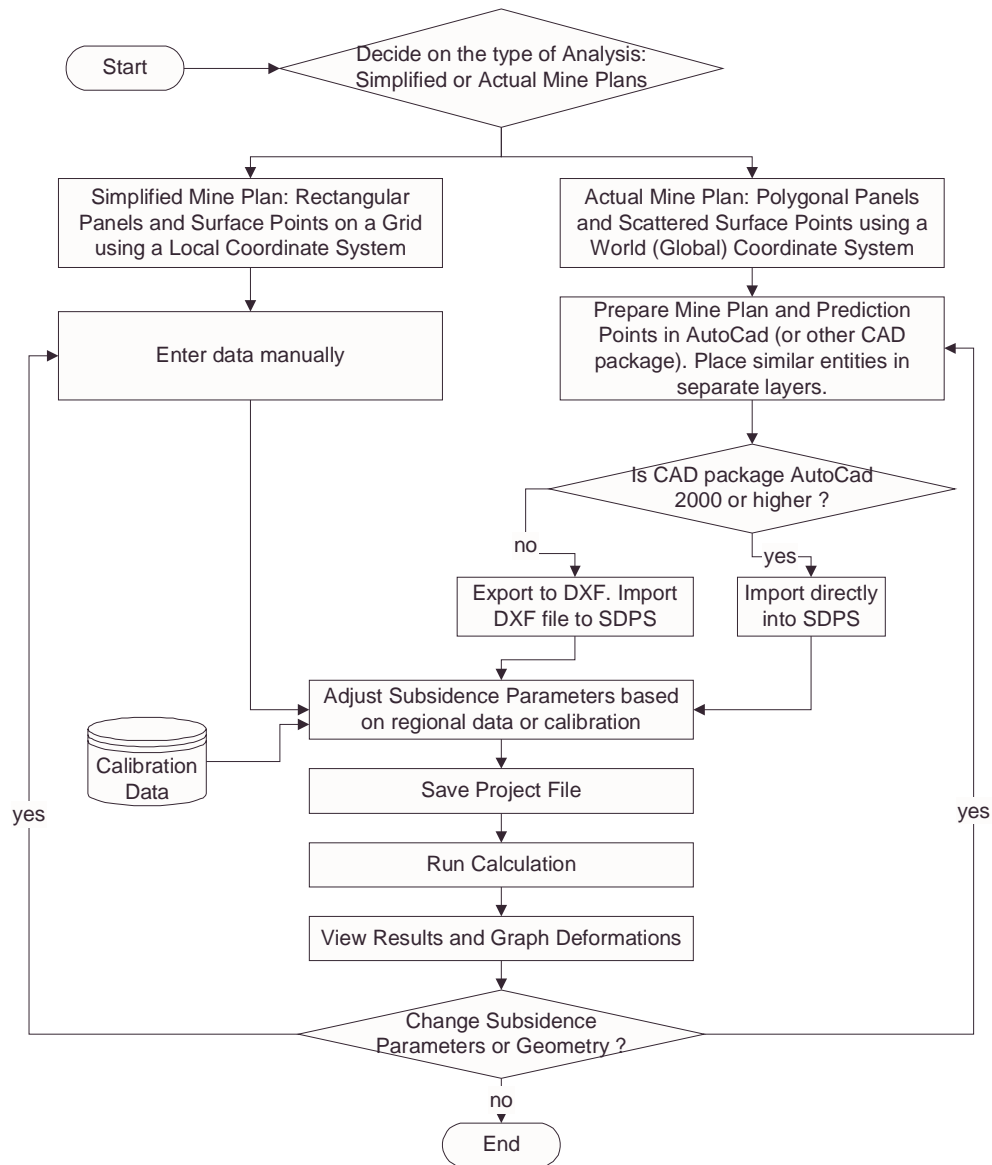


Figure 3.1.1: Flowchart diagram for using the influence function module

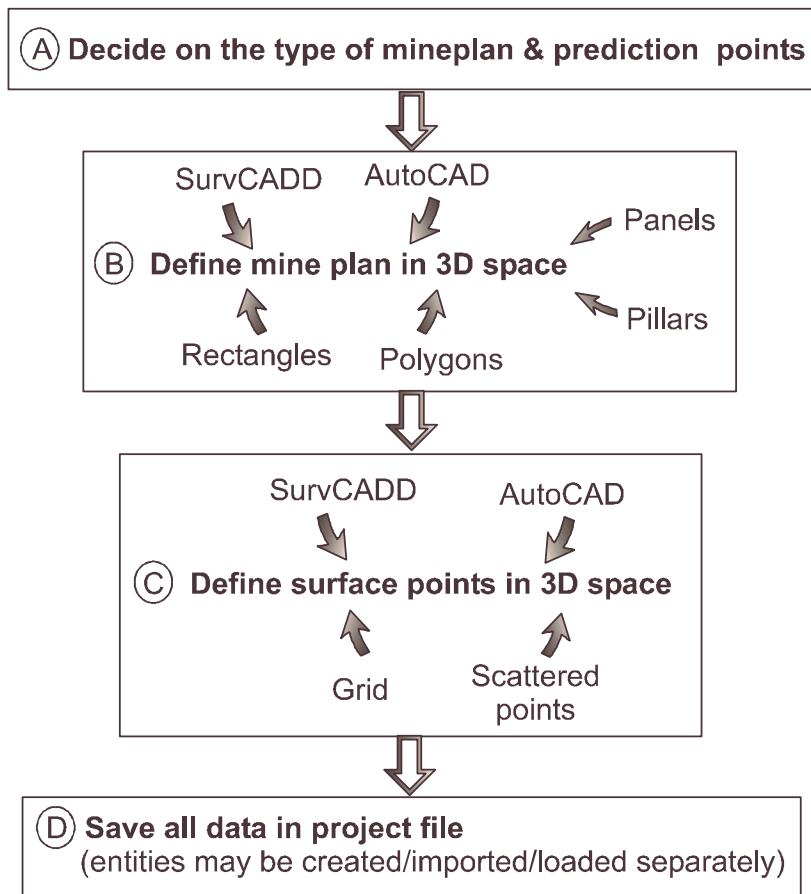
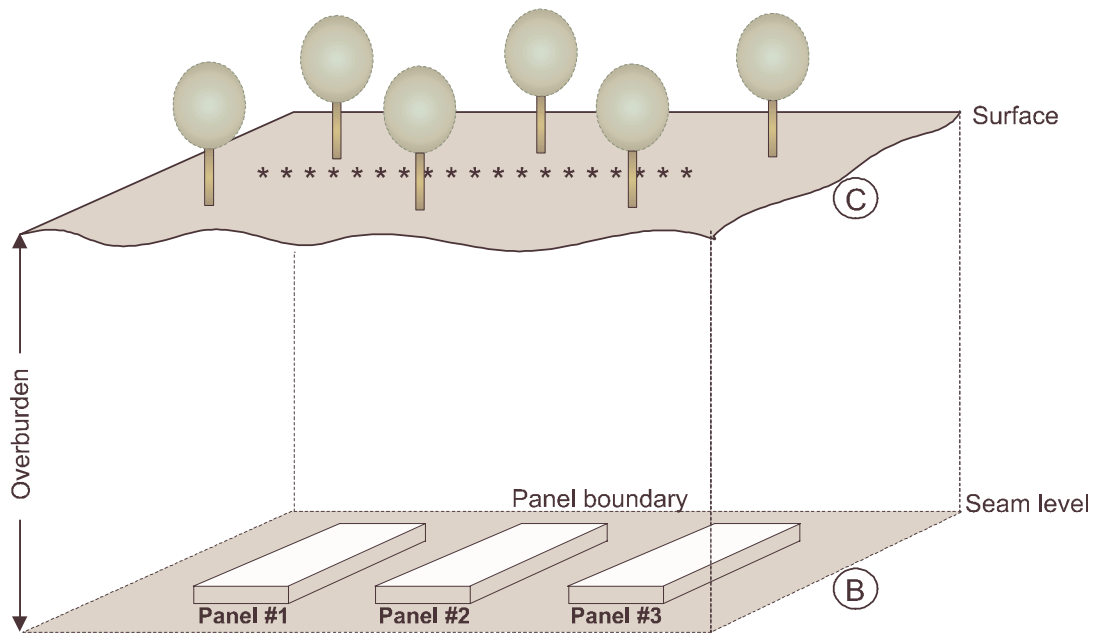


Figure 3.1.2: Steps in defining a project file

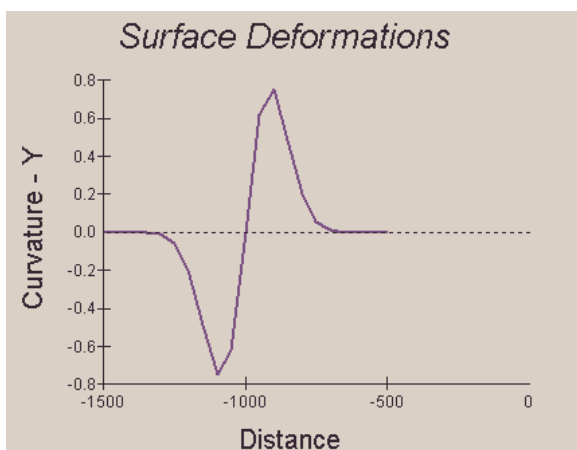
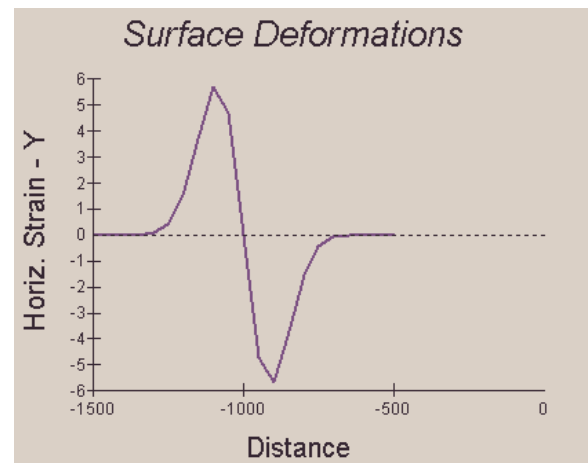
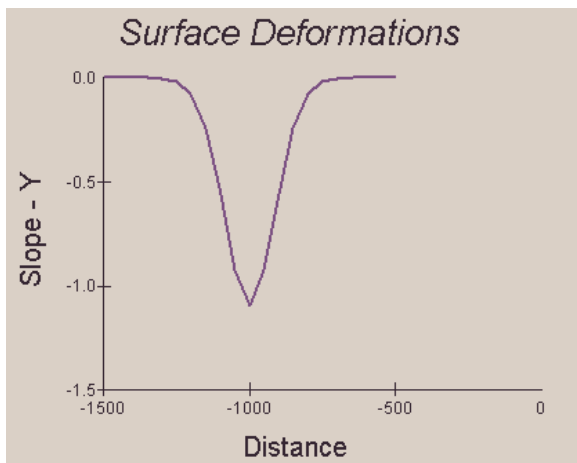
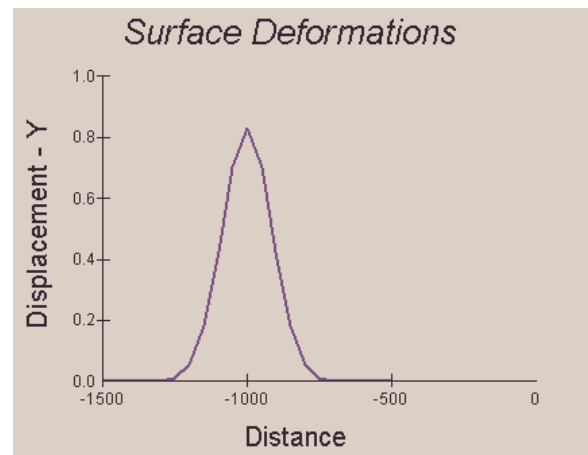
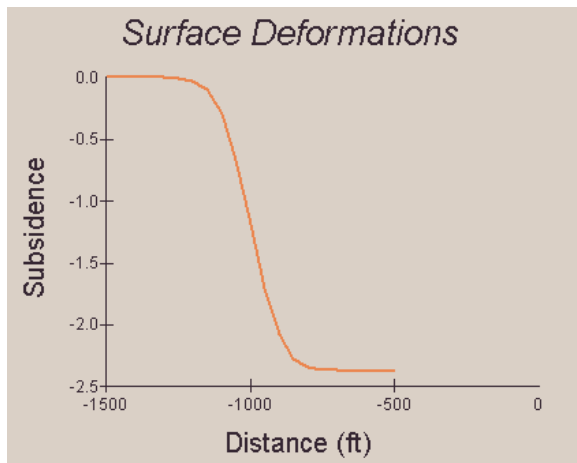


Figure 3.1.3: Typical deformation distributions

Table 3.1.1: Identification codes for deformation indices

Number	Deformation Index Name	Code	Units
1	Subsidence	SU	ft or m
2	Slope in the X-direction	TX	%
3	Slope in the Y-direction	TY	%
4	Directional Slope	TA	%
5	Maximum (Total) Slope	TM	%
6	Angle <sup>1</sup> of Maximum Slope	TE	deg
7	Horizontal Displacement in the X-direction	VX	ft or m
8	Horizontal Displacement in the Y-direction	VY	ft or m
9	Directional Horizontal Displacement	VA	ft or m
10	Maximum (Total) Horizontal Displacement	VM	ft or m
11	Angle <sup>1</sup> of Maximum Horizontal Displacement	VE	deg
12	Curvature in the X-direction	KX	1/ft or 1/m <sup>2</sup>
13	Curvature in the Y-direction	KY	1/ft or 1/m <sup>2</sup>
14	Directional Curvature	KA	1/ft or 1/m <sup>2</sup>
15	Maximum Principal Curvature	K1	1/ft or 1/m <sup>2</sup>
16	Minimum Principal Curvature	K2	1/ft or 1/m <sup>2</sup>
17	Maximum Curvature	KM	1/ft or 1/m <sup>2</sup>
18	Angle <sup>1</sup> of Maximum Principal Curvature	KE	deg
19	Horizontal Strain in the X-direction	EX	- <sup>3</sup>
20	Horizontal Strain in the Y-direction	EY	- <sup>3</sup>
21	Directional Horizontal Strain	EA	- <sup>3</sup>
22	Maximum Strain	EM	- <sup>3</sup>
23	Maximum Principal Strain	E1	- <sup>3</sup>
24	Minimum Principal Strain	E2	- <sup>3</sup>
25	Angle <sup>1</sup> of Maximum Principal Strain	EE	deg

<sup>1</sup> This angle is calculated in degrees from the positive x-axis in a counter-clockwise direction. It gives the direction of the maximum value of the corresponding index on the x-y plane.

<sup>2</sup> expressed in tenths of ppm (divide by 10.000 to obtain result)

<sup>3</sup> expressed in millistrains (divide by 1000 to obtain result)

## 3.2 Definition of the Mine Plan in the Influence Function Program

Mine plan data describe the extraction area under consideration using various conventions. An extraction area is always defined in three-dimensional space by specifying the X,Y,Z coordinates of the points defining that area. Mine panels and pillars are referred to as excavation parcels. A parcel can be either active or not active. A parcel, which is not active, is not deleted from the file, but it does not participate in the calculations.

### Geometry and Boundary Adjustment:

The geometry of a mine plan is determined by the geometry of the excavation panels adjusted by the edge effect. This parameter represents the distance between the actual rib of the excavation and the position of the inflection point, as determined by panel geometry and site characteristics. The location of the inflection point, which defines the transition between horizontal tensile and compressive strain zones, is very important for the application of the influence function method. The distance of the inflection point from the rib using either an average and a conservative estimate as a function of the width-to-depth ratio of a panel can be estimated using this graph.

Thus, the magnitude of the edge effect can be determined as follows:

- ✓ from the graph estimating the location of the inflection point for the conservative or average estimate (Figure 3.1.1),
- ✓ by clicking on the *Subs.Parm* button in the rectangular mine plan form of the influence function program,
- ✓ by analyzing subsidence curves measured at a specific site or region.

### Panel Representation:

- ✓ Simple mine layouts can usually be approximated using sets of rectangular extraction areas. In this case, the input required for every parcel includes the parcel number; the coordinates of the west, east, south, and north borders; the seam elevation; the extraction thickness (mining height); and the average supercritical subsidence factor (in percent) associated with it. These coordinates can be specified in a local or a global coordinate system with axes parallel to the parcel sides. In the Influence function module, this option is implemented as **Rectangular Mine Plans**.
- ✓ Complex mine layouts can usually be approximated by a closed polygon (i.e. a piece-wise linear shape). In this case, the input required for every point within a parcel includes the point reference number; the northing (Y), easting (X), and elevation (Z); the extraction thickness (mining height); and the supercritical subsidence factor (in percent) associated with it. The mine plan editor can

provide access to all points in a parcel, add new points, and add new parcels provided that the current parcel is defined by three or more points. The points should be entered in a counter-clockwise fashion. The location of each point should be adjusted to reflect the edge effect, or the relative position of the inflection point. The maximum number of parcels and points per parcel can be adjusted within the limits of the available memory. In the Influence function module, this option is implemented as Polygonal Mine Plans.

### **Warning:**

Pillars can not exist outside extracted areas. If a pillar is defined outside an extracted area the results are unpredictable. Currently, the parcel definition module of the program can not check for such inconsistencies. Examples of erroneous panel definitions are given in Appendix 3.

### **Notes:**

- ✓ If no adjustments are made to the geometry of the mine plan, the program assumes that the inflection point is over the rib of the excavation.
- ✓ The user must specify whether each parcel represents an extracted panel or a pillar within an extracted panel. A pillar is mathematically represented as a parcel with a negative subsidence factor. Setting the pillar option on a parcel will reset the subsidence factor associated with this parcel. In that sense, an extraction area can be either positive (i.e. longwall panel) or negative (i.e. pillar in the middle of a panel). Thus, a mine plan that consists only of pillars (without an extraction boundary) will produce a mathematically positive! subsidence.
- ✓ It should be emphasized that the subsidence factor used here is the subsidence factor for supercritical conditions.
- ✓ The reason for supporting more than one format for input data is for the user's convenience. For example, certain panels or pillars can be easily represented as rectangles and can be entered as single entities, compared to four or more entries required if these panels are digitized point by point. Additionally, calculations for rectangular parcels are much faster compared to calculations for parcels defined by individual points.



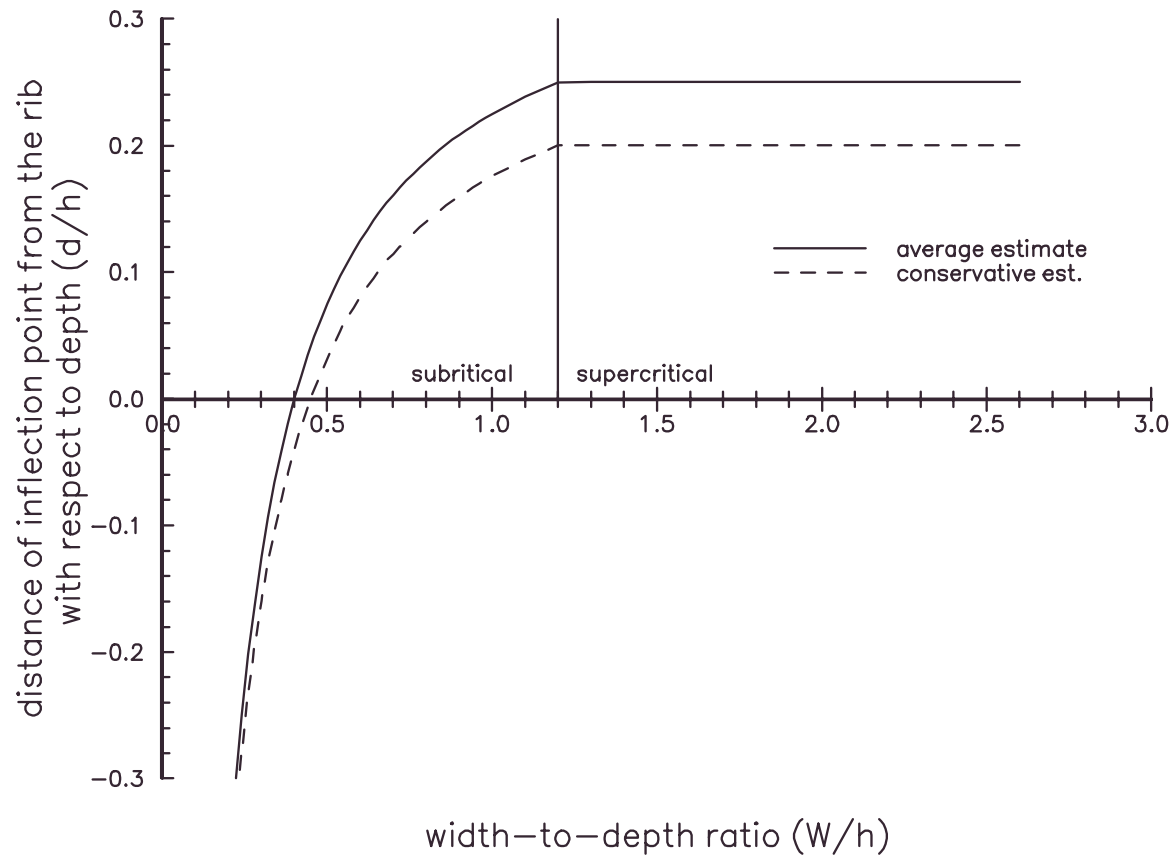


Figure 3.2.1: Determination of the offset of the inflection point.

## 3.3 Definition of the Prediction Points in the Influence Function Program

Prediction point data describe the surface points where the deformation indices will be calculated. Prediction points are always defined in three-dimensional space, by specifying the X,Y,Z coordinates of these points. A point can be either active or not active. A point which is not active is not deleted from the file but will not be included in the calculations.

### Scattered Points

A scattered point set may consist of any number of points that are randomly located on the surface. If such points can be specified as part of a grid, then the Grid Points option should be used. Required parameters for each point include:

- ✓ the point reference code which can be any alphanumeric string,
- ✓ the easting, northing and elevation of each point,
- ✓ the point status, i.e. active or not active (an inactive point will not be displayed in the View option and will not participate in any of the calculations)

### Grid Points

A grid point set may consist of any number of points in a window. This window is defined by minima and maxima in the X- and Y- directions as well as the cell size in each direction.

The grid can only be oriented parallel to the current coordinate system. If the grid needs to be oriented at an angle to the current coordinate system, the grid points should be generated by a different tool and imported as scattered points into the Influence Function module.

The user has two options regarding grid elevations.

- ✓ to consider a flat surface and specify a uniform elevation for all points, and
- ✓ to consider each point on an individual basis and specify individual point elevations.

# Surface Deformation Characteristics Above Undermined Areas: Experiences from the Eastern United States Coalfields

M. KARMIS, A. JAROSZ, P. SCHILIZZI & Z. AGIOUTANTIS\*

**SUMMARY** Damage resulting from surface movements due to underground mining may range from simple land settlement to severe structural damage. Since subsidence prevention is not feasible, it is important that accurate ground movement prediction techniques are developed, so that damage due to underground mining as well as the amount of coal lost due to the protection of surface structures can be minimized.

To facilitate the mitigation of the deleterious effects of subsidence in the Eastern U.S. region, empirical subsidence prediction techniques for longwall mining were developed from 45 case studies collected within the coalfield. From these subsidence prediction techniques a strain prediction model was also formulated. These subsidence and strain prediction methods can be used to predict ground movements as part of the mining plan and to evaluate the impacts of underground mining on the surface.

## 1 INTRODUCTION

Surface subsidence is rapidly gaining emphasis as an important environmental consequence of underground coal mining in the United States. Its impact has been witnessed in both rural and urban areas, and can be associated with active as well as abandoned mining operations. The damage associated with this phenomenon may include land settlement and fracturing, structural damage to surface buildings or facilities and disruption or contamination of ground water supplies.

As the need for energy increases, coal production will undoubtedly be accelerated, and since over 99 percent of all subsidence recorded in the United States arises from underground mining, it is evident that the incidence of subsidence will increase. With this increase in production and as underground mining moves into more populous areas, the prediction of surface subsidence, horizontal displacements, strains, and associated damages will surely become a requisite.

To exemplify the significance of this problem, a recent U.S. Bureau of Mines report indicated that over 32,000 km<sup>2</sup> have been undermined in the United States in extracting coal, metals and nonmetallic ores. Over one-fourth of this area, or approximately 8100 km<sup>2</sup>, has been disturbed by subsidence, with underground mining of bituminous coal accounting for 7700 km<sup>2</sup> and metal and nonmetallic ores accounting for 68 km<sup>2</sup> of disturbed land. Thus, over 99 percent of all subsidence incidents are attributed to underground coal mining. Moreover, the Bureau of Mines estimates that an additional 10,000 km<sup>2</sup> will be undermined in the United States by the year 2000 (Chen et al., 1982), thus increasing considerably the number of areas in the country affected by subsidence.

Even though, under present technological and economic conditions, subsidence prevention is not feasible, it has been demonstrated in many coalfields that surface subsidence can be predicted and controlled, thus minimizing the deleterious effects of ground movement. Therefore, it is imperative that reliable methods of surface movement prediction and control be established for

the United States. With such techniques available, ground movements can be predicted as part of the mining plan, and if environmentally, economically or legally unacceptable situations are foreseen, remedial measures can be implemented.

## 2 TYPES OF MINING SUBSIDENCE EXPERIENCED IN THE UNITED STATES

Underground excavations disturb the natural equilibrium of the rock mass, causing redistribution of loads in the medium and thus producing horizontal and vertical displacements. Subsidence occurs when these displacements propagate from the mine opening, through the overlying strata, to the surface and can manifest two principle modes of ground settlement: sinkhole and trough subsidence (Figure 1).

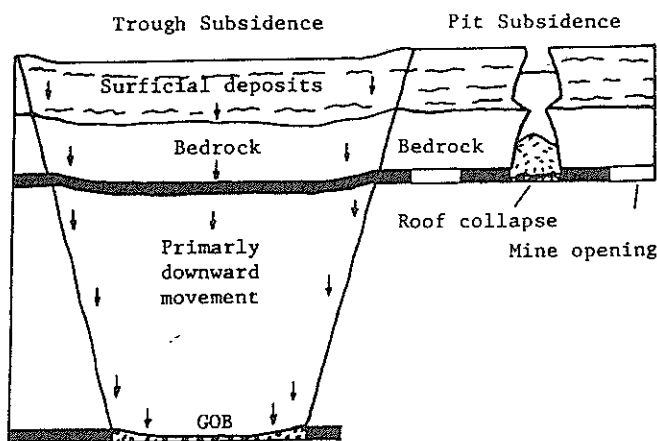


Figure 1 Trough and pit subsidence (after Wildanger et al., 1980).

### 2.1 Sinkholes, or Pit Subsidence

Sinkholes, or pit subsidence, are characterized by a sudden and sometimes violent collapse of the surface and usually occur above shallow, abandoned room and pillar mines with incompetent overburden; in rare instances, however, this type of subsidence

can also occur over active mines, given the proper mining and geological conditions. Pit subsidence is expressed by an abrupt drop in the surface and has vertical to bell-shaped walls. The washing of bedrock and surficial deposits into the mine void may cause the depth of sinkhole to exceed the mining height.

Obviously, the effects of pit subsidence can be serious. The damage caused is the result of a loss of support over all or part of the structure. Also, due to the uncertainty of mine and geologic parameters, the time, location and extend of such a subsidence event is very difficult to predict. Since the goal of subsidence and strain prediction is to minimize the cost of extracting coal in active mines that are below structures, the characteristics of trough subsidence have been studied more extensively than those of sinkholes.

## 2.2 Trough Subsidence

Trough subsidence is expressed by a gradual and general movement over an observed area with a subsidence basin being formed. Trough theory considers the phenomenon of subsidence to be represented by a complicated combination of material movement and interaction, as depicted in Figure 2. Caving occurs above the mine opening (zone a). The strata above the caving zone moves toward the excavation, experiencing fracturing (zone b) and beam bending phenomena (zone c). This representation of ground movement around a mining excavation is considerably complex to analyze and model; therefore, this concept is simplified by treating only the effects of underground excavation on the surface, or other strata levels within the bending zone.

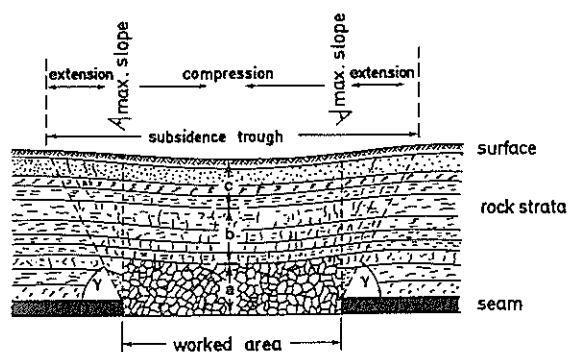


Figure 2 Strata movements above an extracted area (after Kratzsch, 1983)

Trough theory considers a zone of influence in which movement occurs and which spreads from the excavation to the surface, forming a subsidence trough. When an excavation is made at depth, the movement of the strata extends to the surface and manifests itself as vertical displacement (subsidence) and horizontal displacement within a zone of influence. The zone of influence is bounded by a plane that extends from the edge of extraction to the line on the surface where movement ceases. A vertical cross-section of the subsidence trough along with its associated parameters is shown in Figure 3. The angle defined by the vertical from the rib and the line of influence is the angle of draw (or limit angle).

## 3 DEVELOPMENT OF SUBSIDENCE PREDICTION METHODS

A number of different methods have been proposed for or applied to prediction of surface ground movements due to underground mining. These

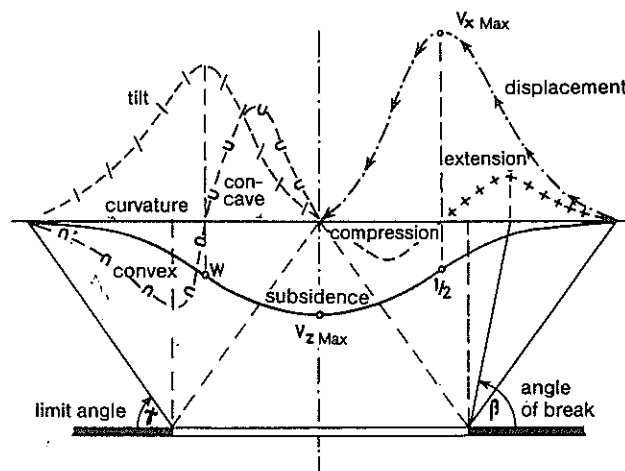


Figure 3 Components of ground movement (after Kratzsch, 1983)

approaches can be broadly divided into three groups. The first two are:

- Theoretical models based on the elastic, plastic, viscoelastic or other phenomenological models which are widely used in other engineering fields (Voight and Pariseau, 1970).
- Numerical methods, mostly used as solutions to complex situations involving the phenomenological methods.

Both these approaches assume that the strata in the overburden behaves in a specific and predictable manner. In using these models, considerable information describing the behavior of the overburden is required, which has often limited the applicability of these methods. Furthermore, in order to adapt their results to field data, a large number of adjusting coefficients may have to be determined.

The third approach can be defined as:

- Empirical or semi-empirical methods such as profile functions, influence functions, the zone area method (Brauner, 1973; Karmis et al., 1981b and 1983).

In this research, the latter approach was pursued since empirical methods are realistic, flexible, and easy to use. Their application, however, requires that a significant number of field measurements be made in order to determine the essential input parameters of the equations.

## 3.1 Data Collection and Analysis

During the initial stages of this research effort, a large number of subsidence case studies were collected from literature, the coal industry and government agencies. In total, data from 45 longwall panels and 70 room and pillar panels were collected. The limitations of the collected case studies data, i.e. accuracy of surveys, frequency of monitoring, lack of horizontal movement measurements, etc, led Virginia Polytechnic Institute and State University to the initiation of a detailed subsidence and strain monitoring program

above a number of active mines, located in three major coal producing counties of Virginia. The aim of this program was to enhance the data base with accurate and complete measurements of surface movements and to subsequently allow the refinement of the prediction techniques.

In this major monitoring effort, a total of sixteen room and pillar sections and seven longwall panels, in nine mines, were instrumented. Above each panel or section a number monument lines were installed. The lines were extended on either side of the panel well beyond the maximum expected area of influence. The final effort included approximately 1,200 stations over 35,000 feet of monitoring lines (Schilizzi et al., 1986).

This data bank was used to determine some basic ground movement relationships between the basic mining and subsidence parameters, in order to allow the evaluation of the various prediction methods for the Appalachian coal region.

Analysis of the subsidence information has revealed some interesting subsidence characteristics for Appalachian longwall panels. The observed angles of draw varied considerably; however, the angle of draw appears to approach a constant value of approximately 30 degrees at width-to-depth (W/h) ratios in excess of 1.2 (Figure 4). The range of maximum subsidence factors for the collected case studies is shown in Figure 5. It shows two lines constructed from the data. Line (1) represents the average values  $S_{max}/m$ , whereas line (2) is an envelope line, covering all data points. The figure also shows that this parameter asymptotes to a constant value at a width-to-depth ratios greater than 1.2. These results suggest that critical conditions are reached for W/h ratios of about 1.2,

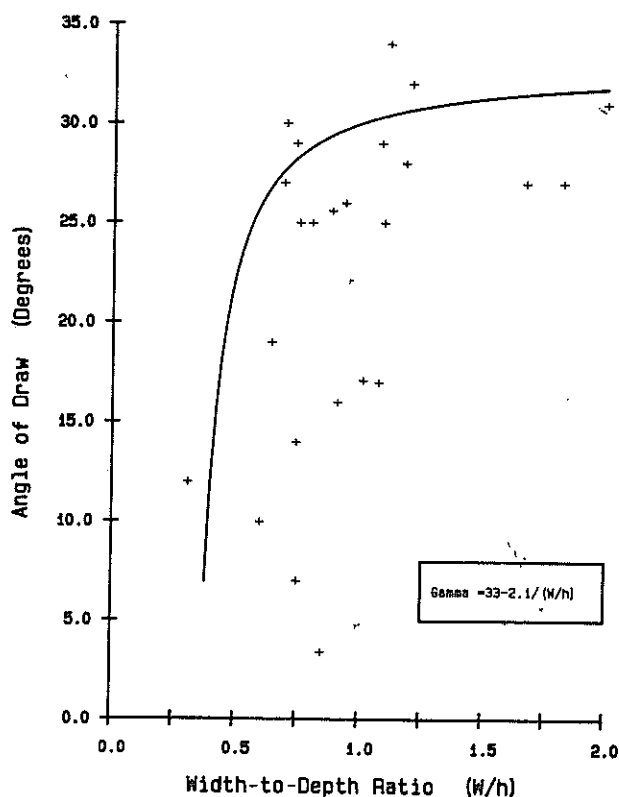


Figure 4 Observed angles of draw for various case studies

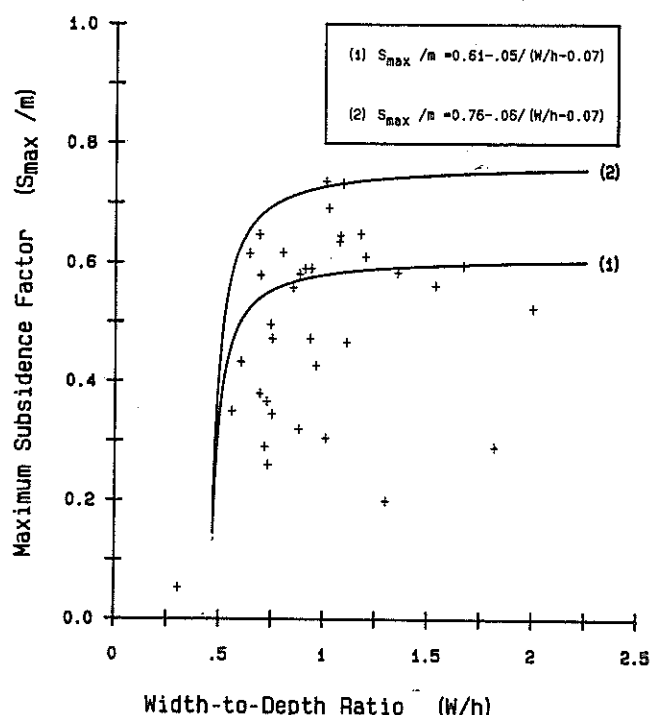


Figure 5 Influence of W/h ratio on maximum subsidence factor

as confirmed by the relationship between the position of the inflection point and the width-to-depth ratio of the panel shown on Figure 6.

According to the collected data and their dispersion, it was hypothesized that two factors influenced the subsidence: geology of the overburden and geometry of the panel. In order to establish the relationship between geology (lithology) and subsidence, the subsidence factor was plotted against the percent of hardrock (percent of limestone and sandstone) in the overburden for critical and supercritical panels only (Figure 7). Since the effect of panel geometry was thus eliminated, a relationship between subsidence and geological conditions was established. Once this correlation was possible, a complete relationship between subsidence and panel geometry was developed for varying lithologies (Figure 8).

To determine characteristic subsidence profiles, different empirical or semi-empirical methods were tested and adopted. Data collected during the monitoring program were primarily used, because of their completeness and accuracy.

### 3.2 Profile Function Methods

A profile function method defines the distribution of subsidence or strain values on the surface along a profile, orthogonal to the boundary of (theoretically) an infinitely long underground excavation. In general, a function which is tangent or asymptotic to two horizontal lines is required. The parameters to be used for this equation must be determined from field data.

The advantage of such a method is that it can be implemented easily through the use of a computer, or of pre-calculated tables. The main disadvantage is that it cannot negotiate excavations of complex shape or significant variations in mining

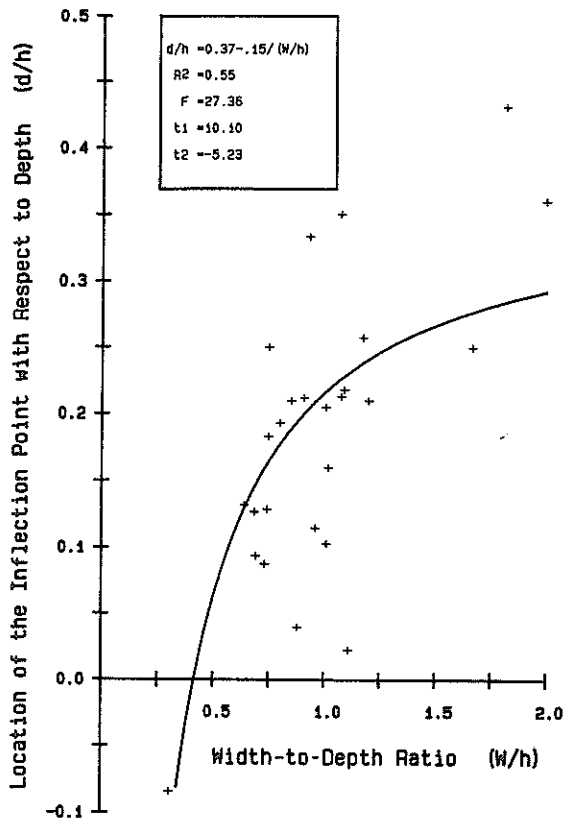


Figure 6 Effect of W/h ratio on inflection point location

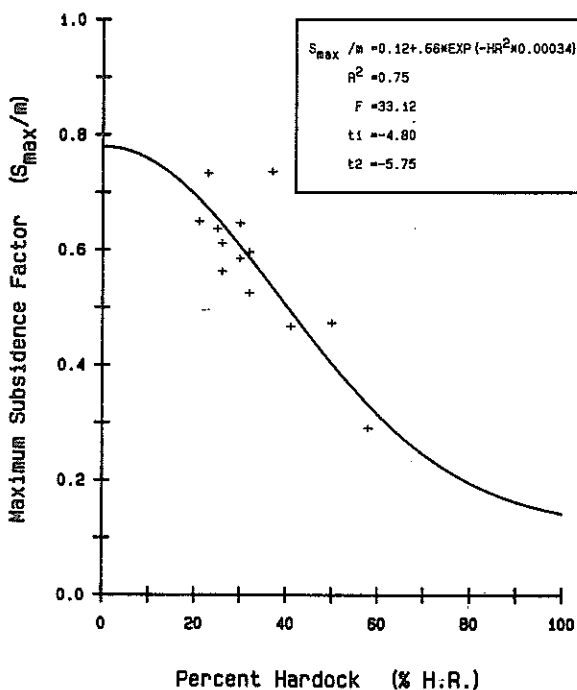


Figure 7 Effect of lithology on maximum subsidence factor

Parameters such as mining height, percent of extraction, and depth of the excavation (Brauner, 1973; Karmis et al., 1981a).

In this approach, a number of accepted profile functions were fitted to the subsidence profiles

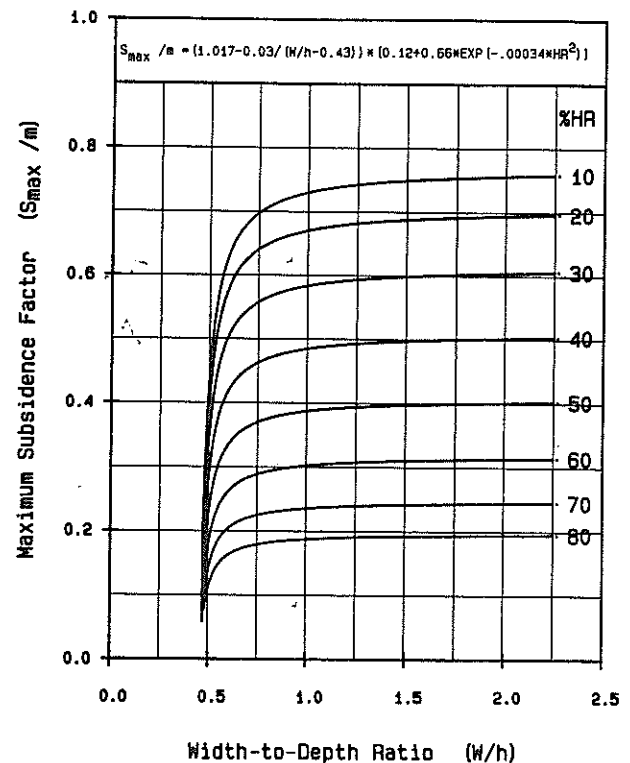


Figure 8 Nomograms for maximum subsidence prediction

developed from collected case studies. This analysis demonstrated that the hyperbolic tangent function given by the following equation, provided the best fit curve (Karmis et al., 1981b and 1984):

$$S(x) = 0.5 S_{\max} [1 - \tanh(cx)/B] \quad (1)$$

where,

- $S(x)$  = subsidence at a given point on the surface;
- $S_{\max}$  = maximum subsidence (obtained from a table [Table 1] or nomogram [Figure 8]);
- $c$  = constant, calculated as 1.8 for critical or supercritical panels and 1.4 for subcritical panels;
- $x$  = distance from the inflection point to the point in question; and,
- $B$  = distance from the inflection point to  $S_{\max}$  (which can be assessed from tables or nomograms [Figure 6] as a function of panel geometry and width-to-depth ratio).

The latter equation can be used in conjunction with predictions of  $S_{\max}$  (Figure 8) and position of the inflection point (Figure 6) to allow for complete subsidence pre-calculation.

### 3.3 Influence Function Methods

This approach to subsidence prediction was initially developed by Dutch and German engineers (Bals, 1932) and has been extensively used in the Central and Eastern European coalfields. An influence function describes the distribution of vertical ground movement, i.e. subsidence, on the surface or other levels of the overburden, caused by an infinitesimal underground excavation. Considering the two dimensional situation:

$$dS(x_1, z) = f(x_1 - x_2, z) dV \quad (2)$$

where,

$dS(x_1, z)$  = subsidence at point  $P(x_1, z)$ ;  
 $dV$  = infinitesimal underground excavation (void);  
 $f(x_1 - x_2, z)$  = influence function;  
 $x_1$  = coordinate of surface point;  
 $x_2$  = coordinate of infinitesimal excavation; and,  
 $z$  = vertical distance from excavation to prediction point  $P(x_1, z)$ .

The Budryk-Knothe influence function method (Knothe, 1957), developed in Poland, was selected for this research as the most appropriate function for use in the Eastern U.S. coalfields. Initially, a two-dimensional situation was considered for the analysis of data obtained from panels of an almost orthogonal shape and with uniform mining conditions i.e. mining height, percent extraction, depth. The equation used is as follows:

$$f(x, z) = -\frac{1}{r} \exp\left(-\pi \frac{x^2}{r^2}\right) \quad (3)$$

where,

$r$  = the radius of influence ( $r = z/\tan(b)$ );  
 $b$  = angle of influence; and,  
 $x, z$  = coordinates of surface point on a system where the origin is located at the infinitesimal excavation.

For the three-dimensional approach:

$$f(x, y, z) = \frac{1}{r^2} \exp\left[-\pi \frac{(x^2 + y^2)}{r^2}\right] \quad (4)$$

where,

$r$  = the radius of influence; and,  
 $x, y, z$  = coordinates of a surface point on a system where the origin is located at the infinitesimal excavation.

Subsidence at any point will be:

$$S(x, y, z) = \frac{S_{\max}}{r^2} \iint_A \exp\left[-\frac{\pi}{r^2} (x^2 + y^2)\right] dx dy \quad (5)$$

where,

$S(x, y, z)$  = subsidence at a point having coordinates  $x, y, z$ ;  
 $S_{\max}$  = maximum subsidence for supercritical excavation;  
 $r$  = the radius of influence; and,  
 $A$  = the area of excavation.

The above integral was transformed and solved in polar coordinates, for polygonal excavations.

For this method, as with most mathematical models, the inflection point of the subsidence profile is located above the rib of the excavation. In practice, however, the inflection point is displaced at a distance,  $d$ , from the rib. In order to accommodate this, the outer boundaries of the excavation have been adjusted accordingly.

### 3.4 Zone Area Method

This method was initially developed in Britain for irregular longwall or room and pillar panels (Marr, 1975). It assumes that movement at a specific point on the surface is affected by the excavation of a circular underground area which is further sub-divided into a series of angular rings. To determine the amount of movement caused by each ring, the extracted area of the ring is calculated and multiplied by the zone factor of the respective

ring. Appropriate zone factors for Appalachia have been calculated from the field data (Goodman, 1980; Karmis et al., 1981b and 1984). The same procedure is followed for all rings, and the superimposed results will yield total movement.

### 4 DEVELOPMENT OF STRAIN PREDICTION METHODS

One of the most damaging manifestations of surface subsidence is the development of horizontal strains. As noted previously, subsidence measured in Appalachia is smaller than that found in certain other coalfields, such as the U.K. However, the strains experienced in the U.S. often appear to be greater than those predicted for British conditions. Thus, an effort was directed toward the identification of the cause of these higher strains and toward the subsequent formulation of an acceptable strain prediction model for Appalachia.

As a first step, the relationship between strain and curvature had to be determined. Factor B was used to calculate horizontal strain as a function of curvature, i.e.:

$$\text{Horizontal Strain} = -B * \text{Curvature} \quad (6)$$

In the original stages of this research a direct relationship between strain and curvature was sought which could describe B independent of any other mining parameters (Karmis et al., 1983). As more case studies were made available through this project, it became apparent that such a relationship will be difficult to establish (Figure 9). As a result, a different approach was adopted, based on the work of Awershin (1947), Budryk (1953) and Akimov and Zemicev (1970), which suggested that the magnitude of the horizontal strain factor (B) is a function of the excavation depth or the radius of principal influence ( $r$ ).

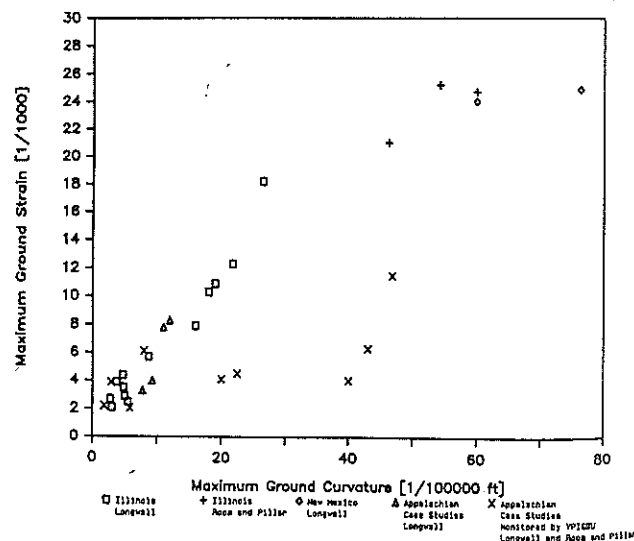


Figure 9 Maximum ground strain and curvature data

For each of the collected case studies, factor B was determined by comparing the measured strains and the fitted curvature profiles.

Using the established values of parameter B and the corresponding values of excavation depth ( $h$ ), radius of influence ( $r$ ), and angle of principal influence ( $b$ ), a statistical relationship was found (Figure 10) as expressed by the equation:

$$B = (0.35 \pm 0.05) r \quad (7)$$

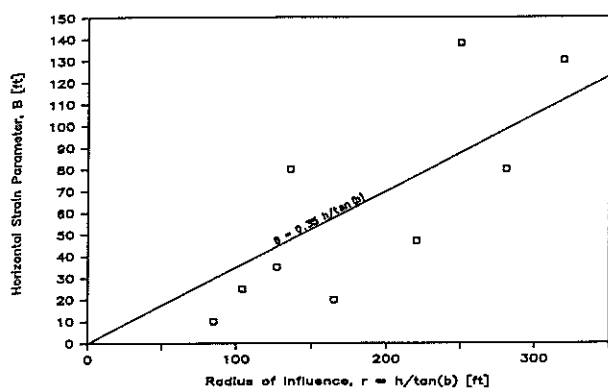


Figure 10 Effect of radius of influence on the horizontal strain parameter

or

$$B = (0.35 \pm 0.05) h/\tan(b) \quad (8)$$

where,

$r$  = radius of the principal influence;  
 $h$  = depth of the excavation; and,  
 $b$  = angle of the principal influence.

## 5 DEVELOPMENT OF COMPUTER SOFTWARE

The development of a comprehensive software package was necessary in order to facilitate the analysis of the field measurements. All field data were stored in an 880-line memory incorporated in the surveying instrument, and then transferred to magnetic diskettes for further processing on an HP micro-computer system. Stored field data included coordinates, sometimes on a localized system, elevations and the values of subsidence and strain for individual stations on the monitoring lines for each date.

Computer software for the application of the prediction methods under consideration was developed for two widely used personal computer systems.

For the profile function, the program is rather simple and involves the calculation of subsidence values along a line orthogonal to the rib of the excavation. The parameters used for this calculation depend on the given geologic conditions, width-to-depth ratio and mining height, and must be obtained from tables or nomograms and entered manually. The origin of the coordinates can be adjusted manually if necessary.

For the application of the influence function method, a number of programs were developed, each of them for specific conditions. For general cases involving complex mining conditions, where the mining section under consideration must be divided into polygons of uniform conditions, the influence function equation was converted to polar coordinates and was used in the program in this form. The computer program calculates subsidence at any point along a polygonal line or on a grid. For mine sections of irregular shape or where areas of different mining height, extraction ratio or seam elevation exist, the section is separated into homogeneous polygonal sub-sections. Subsidence and other related indices of deformation, in any given direction, caused by each of these sub-sections is calculated and their total value is determined by superposition. This procedure, however, requires considerable computational time for each point.

For simple conditions, however, where areas of different mining height, extraction ratio or seam elevation can be described by rectangular homogeneous sub-sections, different programs have been written for considerably faster execution on a microcomputer, yielding comparable results. Furthermore, a program using the two dimensional approach has been written for single panels of uniform overall parameters.

The program for the zone area method was initially developed for mainframe computers (Karmis et al., 1982); however, it is currently being adapted for use with personal computers.

It should be noted that these programs also produce data compatible with commercially available plotting and contouring software packages. Mine plan coordinates and the corresponding parameters can be entered manually or by a digitizer or by a plotter with digitizing capabilities.

## 6 APPLICATION OF PREDICTION METHODS

In this paper, data obtained from three case studies are presented to demonstrate and compare the prediction methods. The first two are from room and pillar mining operations, whereas the last one is from a longwall case study.

In the first example, the two dimensional approach was used. Predicted and fitted subsidence curves, using the profile and influence function methods, are presented in Figure 11.

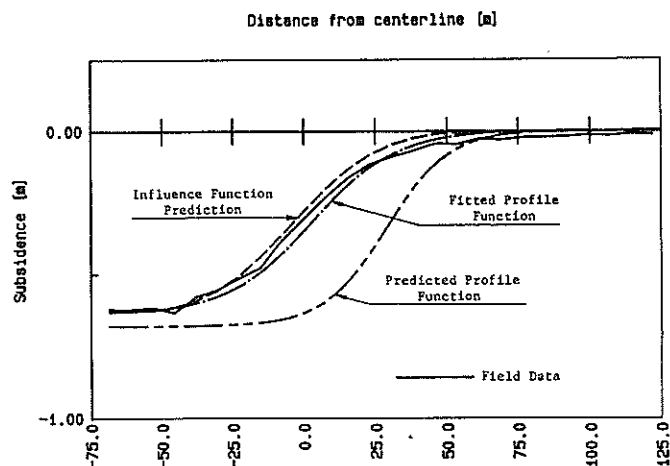


Figure 11 Example #1: Field data and prediction curves

In the second example (Figure 12), a three dimensional influence function approach was used to take into account a number of pillars left in place for roof control purposes. This case demonstrates the accuracy which can be obtained through adjustment of the influence function parameters, especially for subsidence predictions.

In the last example (Figure 13), a three dimensional influence function method was used for a longwall operation with considerable variation in overburden depth. Subsidence and horizontal strain values, calculated using this technique, show excellent correlation with the corresponding measured values.



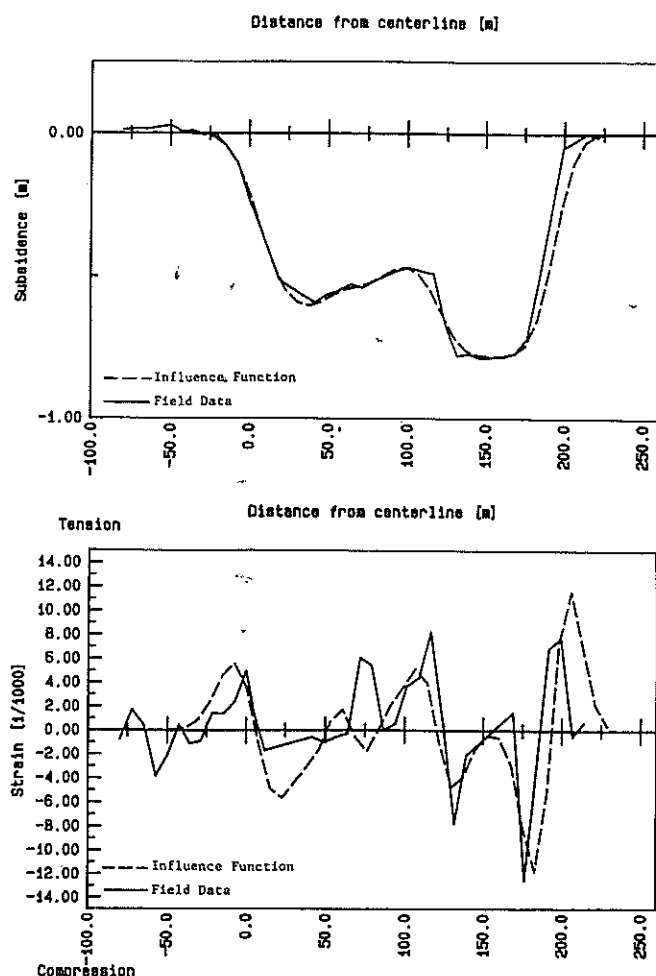


Figure 12 Example #2: Field data and prediction curves for subsidence and horizontal strain

## 7 CONCLUSIONS

The expansion of underground mining into more populous areas, and the resultant increase in the potential for surface and structural damage, have rendered the formulation of accurate surface deformation models an important requisite. To meet this demand, accurate subsidence and strain prediction techniques have been formulated for the Eastern U.S. coalfield. The semi-empirical subsidence prediction techniques discussed in this paper were developed from a substantial number of case studies collected within the Appalachian coalfield. Using the subsidence model as a base, the strain model was formulated using empirically and mathematically derived relationships. These models can greatly facilitate mine planning and allow the amount of coal lost due to the protection of surface structures to be minimized.

## 8 ACKNOWLEDGEMENTS

This research is based upon work sponsored by the Office of Surface Mining, Reclamation and Enforcement, the U.S. Department of the Interior and the Powell River Project. Any opinions, findings, conclusions or recommendations expressed in this paper are those of the authors and do not necessarily reflect the views of the sponsors. Finally, the cooperation, encouragement, and discussions offered by the technical personnel of

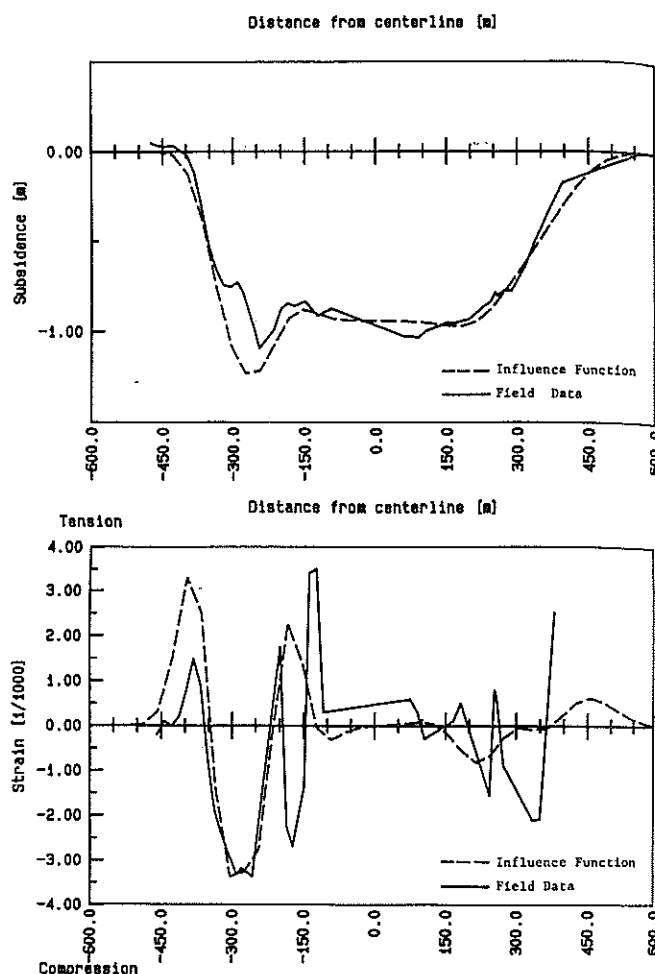


Figure 13 Example #3: Field data and prediction curves for subsidence and horizontal strain

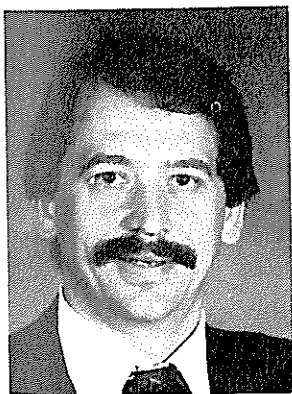
numerous coal companies involved in this project are gratefully acknowledged.

## 9 REFERENCES

1. Akimov, A. and B. Zemicev, 1970, Subsidence of the Rock Strata Caused by the Underground Excavation of Coal and Lead Ores, Nedra Publishing, Moscow, (in Russian).
2. Awershin, S. G., 1947, Subsidence of the Rock Strata Caused by Underground Excavation, Ugletekhizdat Press, Moscow, (in Russian), 245 p.
3. Bals, R., 1932, "A Contribution to the Problem of Precalculating Mining Subsidence," *Mitteilungen aus dem Markscheidewesen*, Vol. 42/43, pp. 98-111 (in German).
4. Brauner, G., 1973, "Subsidence Due to Underground Mining (in two parts)," U.S.B.M. Info. Circ. 8571, 8572.
5. Budryk, W., 1953, "Determination of the Magnitude of Horizontal Strains," Archives of Mining and Metallurgy, Vol. I, Part 1, (in Polish).

6. Chen, C. Y., D. E. Jones and D. K. Hunt, 1982, "Government Regulation of Surface Subsidence due to Underground Mining," Proceedings, International Symposium on the State of the Art of Ground Control in Longwall Mining and Mining Subsidence, Honolulu, Hawaii, pp. 245-252.
7. Goodman, G., 1980, "Computer Modeling of Mining Subsidence Using the Zone Area Method," M.S. Thesis, VPI&SU.
8. Karmis, M., C. Haycocks, I. Eitani and B. Webb, 1981a, "A Study of Longwall Subsidence in the Appalachian Coal Region Using Field Measurements and Computer Modeling Techniques," Proceedings, 1st Conference for Ground Control in Mining, West Virginia University, July 27-29, pp. 220-229.
9. Karmis, M., C. Haycocks, B. Webb and T. Triplett, 1981b, "The Potential of the Zone Area Method for Mining Subsidence Prediction in the Appalachian Coalfield," Proceedings, Workshop on Surface Subsidence Due to Underground Mining, Morgantown, West Virginia, November 30-December 2, pp. 48-62.
10. Karmis, M., G. Goodman, C. Haycocks and T. Triplett, 1982, "The Development and Testing of a Regional Subsidence Prediction Model," Proceedings, 17th Inter. Symposium on Computer Applications to the Mineral Industry, APCOM, Denver, Colorado, pp. 240-252.
11. Karmis, M., T. Triplett, C. Haycocks and G. Goodman, 1983, "Mining Subsidence and Its Prediction in the Appalachian Coalfield," Proceedings, 24th U.S. Symp. on Rock Mech., College Station, Texas, June, pp. 665-675.
12. Karmis, M., G. Goodman and G. Hasenfus, 1984, "Subsidence Prediction Techniques for Longwall and Room and Pillar Panels in Appalachia," Proceedings, Second International Conference on Stability in Underground Mining, Lexington, Kentucky, August 6-8, pp. 541-553.
13. Knothe, S., 1957, "Observations of Surface Movements Under Influence of Mining and the Theoretical Interpretation," Proceedings, European Congress on Ground Movement, The University of Leeds, April 9-12.
14. Kratzsch, H., 1983, "Mining Subsidence Engineering," Springer-Verlag, Berlin, Heidelberg, New York.
15. Marr, J. E., 1975, "The Application of the Zone Area System to the Prediction of Mining Subsidence," Min. Eng., Vol. 135, No. 176, pp. 53-62.
16. Schilizzi, P., M. Karmis and A. Jarosz, 1986, "Development of Subsidence Prediction Technology from an Extensive Monitoring Program," Proceedings, 2nd Workshop on Surface Subsidence Due to Underground Mining, Morgantown, West Virginia, June 9-11, in press.
17. Voight, B. and W. Pariseau, 1970, "State of Predictive Art in Subsidence Engineering," Journal of the Soil Mechanics and Foundations Div., Proc., ASCE, Vol. 96, No. SM2.
18. Wildanger, E. G., J. Mahar and A. Nieto, 1980, "Sinkhole-type Subsidence Over Abandoned Coal Mines in St. David, Illinois," Illinois Abandoned Mined Lands Reclamation Council, 88 P.

\* (Paper C1570 originally presented at the Fourth Australia - New Zealand Conference on Geomechanics, Perth, May 1984)



M KARMIS

Michael Karmis is Professor of Mining Engineering at Virginia Polytechnic Institute and State University, where he has been a member of the faculty since 1978. Previously he was with the faculty of the National Technical University of Athens, Greece. Dr Karmis is a graduate of the University of Strathclyde, Glasgow, Scotland, where he received the B.Sc. (Honors) and Ph.D. degrees in Mining Engineering.

Dr Karmis' research interest is in the area of rock mechanics and ground control and he is particularly interested in the application of such principles to the design and optimization of mining systems. He has authored or co-authored numerous technical papers and reports on this subject.

Dr Karmis is a Fellow of the Institution of Mining and Metallurgy, a Member of many professional societies, a Chartered and Professional Engineer, and serves as an independent consultant to the mining industry.



A P JAROSZ

Andrzej P Jarosz has been a Research Associate at the Department of Mining and Minerals Engineering, Virginia Polytechnic Institute and State University, since 1984. Previously he worked for the Mining and Metallurgy Academy in Cracow, Poland, as a faculty member and for the Central Mining Institute in Katowice, Poland, as head of the Mine Pillar Control Laboratory.

Dr Jarosz is a graduate of the Mining and Metallurgy Academy, Cracow, Poland, where he received his M.S. (Honors) and Ph.D. degrees in Mining Surveying.

Dr Jarosz's research interest is in the areas of subsidence monitoring and prediction as well as the practical applications of ground control principles in mining. He has authored or co-authored many technical papers on this subject.



P P G SCHILIZZI

Paul P G Schilizzi received his education at the National Technical University, Athens, Greece, and graduated in July, 1980, with a Diploma in Mining and Metallurgical Engineering. Mr Schilizzi attended graduate school in the Department of Mining and Minerals Engineering, Virginia Polytechnic Institute and State University, where he completed his M.S. degree in July, 1982. He received an assistantship to continue his education leading to a Ph.D. degree in the same department and completed his work for this degree in January, 1987.



Z AGIOUTANTIS

Zacharias Agioutantis graduated from the National Technical University, Athens, Greece, in November, 1982, with a Diploma in Mining and Metallurgical Engineering. He was then admitted to the graduate program at Virginia Polytechnic Institute and State University, Blacksburg, Virginia, under an assistantship, and received his M.S. degree in Mining Engineering. Since September, 1984, he has been pursuing a Ph.D. degree at the same school while working on different research projects. His research work is reflected in several publications in the fields of Rock Mechanics and Ventilation.

# SDPS

## Surface Deformation Prediction System for Windows version 6.0

### Quick Reference Guide and Working Examples

by

Dr. Zacharias Agioutantis and Dr. Michael Karmis  
Department of Mining and Minerals Engineering  
Virginia Polytechnic Institute and State University  
Blacksburg, Virginia 24061-0239

This software package is the property of the Department of Mining and Minerals Engineering, and the Virginia Center for Coal and Energy Research, Virginia Polytechnic Institute and State University. It has been licensed and may be distributed only to O.S.M.R.E. and State Regulatory Agencies. The SDPS software can be purchased by individuals and/or companies through Carlson Software.

November 16, 2008

## 3.2 Applying the Influence Function Method to Calculated Dynamic Deformations

An understanding of the difference between final, or static, subsidence and dynamic subsidence must be established in order to properly assess almost any mine subsidence issue. In general, the dynamic subsidence differs from the final subsidence in that it is the subsidence movements that occur as mining progresses toward, beneath, and past a point on the surface. In contrast, static or final subsidence relates to the degree of subsidence that occurs at a given point on the surface after the mining has passed the point and no further subsidence-related movements are expected to occur. The distinction between dynamic and static states of subsidence is very important because the distribution of strains, and therefore damage potential, for each condition is significantly different. When evaluating an area to be undermined, it is important that mining engineers assess the damage potential from both dynamic and static subsidence. A basic diagram depicting the concept of a moving "wave" of subsidence, accompanied by both tensile and compressive strains, is presented in Figure 3.12.

The main and residual phases of subsidence are believed to often constitute approximately 90% of the total subsidence.

The methodology discussed by Jarosz *et al.* (1990) and based on Knothe (1953), has been implemented into SDPS to enable the prediction of dynamic subsidence experienced by surface points as longwall mining approaches, passes, and moves away. The basic time-subsidence function proposed by Knothe (1953) is:

$$\dot{S}(t) = c [S^f(t) - s(t)] \quad (3.10)$$

where:

$S^f(t)$  = the final subsidence

$c$  = a time coefficient; and

$S(t)$  = subsidence at time  $t$ .

Using the relationship by Knothe (1953), and an influence function for final subsidence

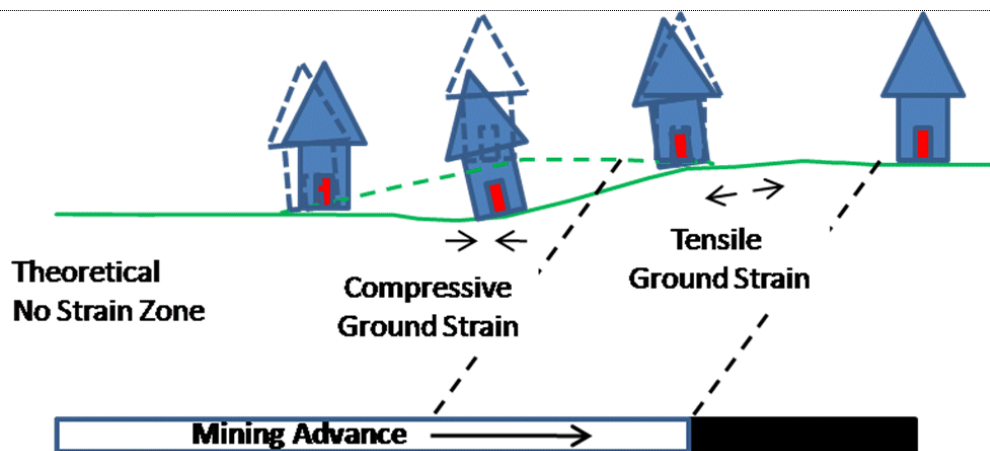


Figure 3.12: Compressive and tensile strains due to dynamic subsidence

at a point above a panel, the following equation for calculating subsidence development due to undermining by a longwall panel was developed. The equation assumes that the longwall panel has a constant width and that the extraction advances at a constant rate.

$$\begin{aligned}
S(x_t, x_o, y_1, y_2, z, \Delta t) = & S^f(x_t, x_o, y_1, y_2, z) - \\
& - \exp\left(\frac{u_z^2}{4\pi}\right) \exp\left(\frac{u_z x_t}{r_z}\right) S^f\left(x_t + \frac{r_z u_z}{2\pi}, x_o + \frac{r_z u_z}{2\pi}, y_1, y_2, z\right) + \\
& + \Delta S^f(x_t, x_o, y_1, y_2, z)[1 - \exp(-c\Delta t)]
\end{aligned} \tag{3.11}$$

where:

$$x_t = x_o + vt$$

$x_o$  = the starting x-coordinate for the advancing panel,

$v$  = the rate of advance of mining assumed to be constant,

$t$  = the time since mining began,

$x_1, x_2$  = x-coordinates for the advancing panel,

$y_1, y_2$  = y-coordinates for the advancing panel, i.e. they define the width of the advancing panel, which is assumed to be constant,

$z$  = the depth of mining,

$\Delta t$  = time since excavation has stopped ( $\Delta t = 0$  for advancing faces),

$S^f$  = final subsidence at time  $t$ ,

$S$  = subsidence at time  $t$ ,

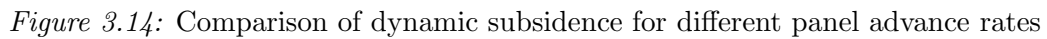
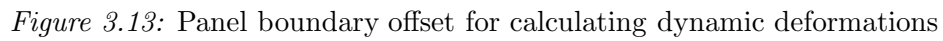
$$u_z = -\frac{c_z r_z}{v},$$

$c_z$  = time coefficient for horizon  $z$ ,

$r_z$  = the radius of influence at horizon  $z$  (i.e. ground surface), and

$\frac{r_z u_z}{2\pi}$  = the magnitude of translation used to calculate surface effects due the advancing longwall panel (see figure 3.13).

The first part of equation [3.11] represents final, asymptotic subsidence at a point. Subsidence development at the point while the face is moving (constant velocity) is represented by the first two parts of the equation. Finally, the residual subsidence, or the subsidence development between the time at which the face stops and the time when the maximum subsidence is reached, is represented by the entire equation (Jarosz *et al.*, 1990). To calculate the subsidence due to the advancing longwall at a given point, the methodology proposed by Jarosz *et al.* (1990) evaluates the effects of extraction at an offset panel location. For any actual panel location, the method calculates the predicted effects of subsidence from a panel position offset a distance equal to  $\frac{r_z u_z}{2\pi}$  in the opposite direction of mining advance (second part of equation [3.11]). The offset distance is referred to as the magnitude of translation. Prediction of subsidence due to an advancing longwall panel involves numerous calculations of predicted subsidence for translated panel positions corresponding to each actual panel location. The calculations reduce the final subsidence for each face location according to the influence of the offset (or translated) panel location.



40

Also, it should be noted that accurate prediction of the end of the main phase of subsidence is particularly important for subsidence mitigation activities and for planning development of surface structures on recently undermined land.

### 3.3 Definition of a Mine Plan in the Influence Function Program

Mine plan data describe the extraction area under consideration using various conventions. An extraction area is always defined in three-dimensional space by specifying the X,Y,Z coordinates of the points defining that area. Mine panels and pillars are referred to as excavation parcels. A parcel can be either active or not active. A parcel, which is not active, is not deleted from the file, but it does not participate in the calculations.

#### 3.3.1 Geometry and Boundary Adjustment

The geometry of a mine plan is determined by the geometry of the excavation panels adjusted by the edge effect. This parameter represents the distance between the actual rib of the excavation and the position of the inflection point, as determined by panel geometry and site characteristics. The location of the inflection point, which defines the transition between horizontal tensile and compressive strain zones, is very important for the application of the influence function method. The distance of the inflection point from the rib using either an average and a conservative estimate as a function of the width-to-depth ratio of a panel can be estimated using this graph.

Thus, the magnitude of the edge effect can be determined as follows:

- from the graph estimating the location of the inflection point for the conservative or average estimate (Figure 3.15),
- by selecting the *Edge Effect Management* tab in the *Rectangular Mine Plan* window of the influence function program and clicking on *Automatic Adjustment*,
- by analyzing subsidence curves measured at a specific site or region.

#### 3.3.2 Panel Representation

Simple mine layouts can usually be approximated using sets of rectangular extraction areas. In this case, the input required for every parcel includes the parcel number; the coordinates of the west, east, south, and north borders; the seam elevation; the extraction thickness (mining height); and the average supercritical subsidence factor (in percent) associated with it. These coordinates can be specified in a local or a global coordinate system with axes parallel to the parcel sides. In the Influence function module, this option is implemented as **Rectangular Mine Plans**.

Complex mine layouts can usually be approximated by a closed polygon (i.e. a piece-wise linear shape). In this case, the input required for every point within a parcel includes the



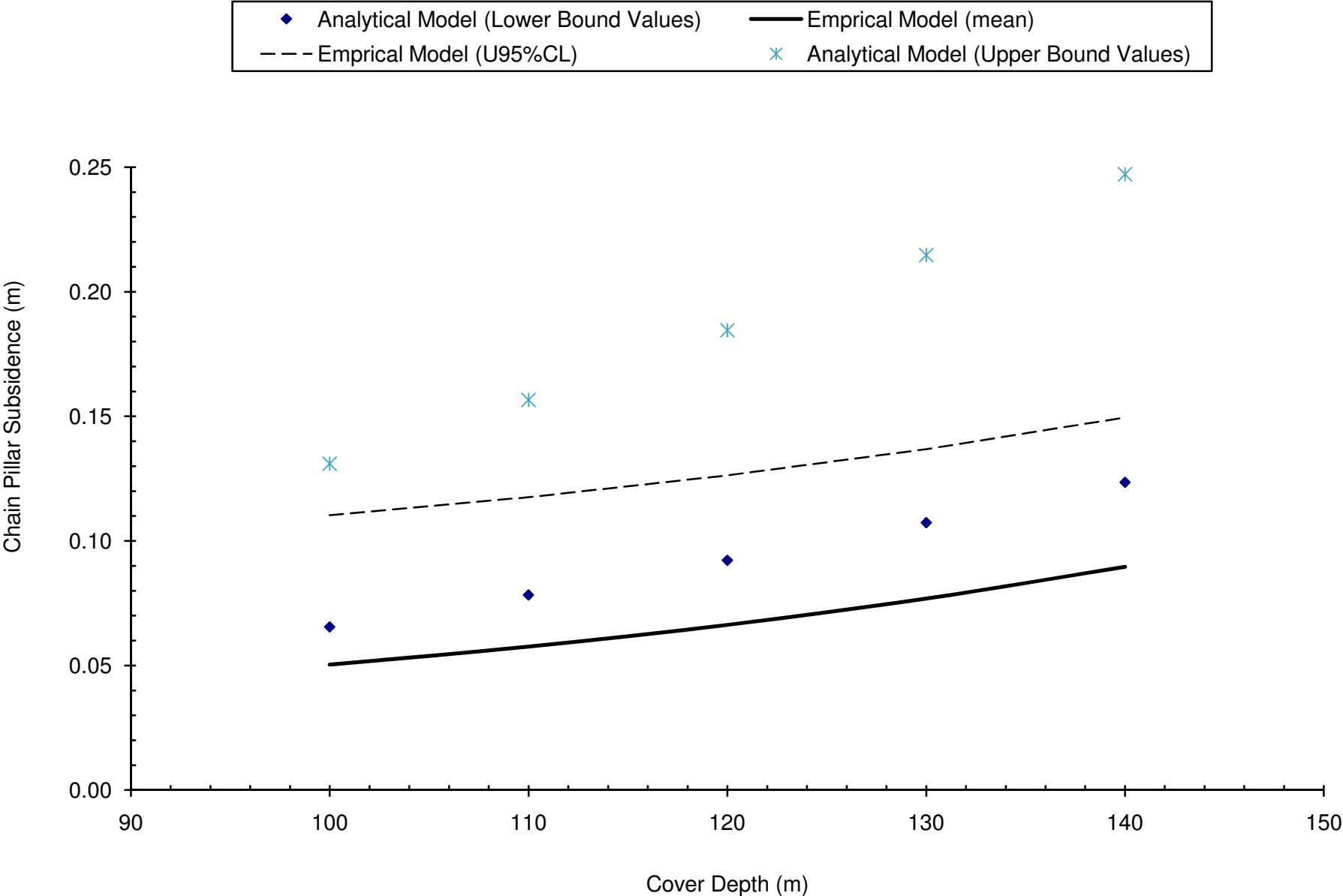


## **APPENDIX C – Inter Panel Barrier Pillar Stability Calculations**

## UNSW Pillar Design Spreadsheet

## Abel Mine - Upper Donaldson Seam (Area 2)

INPUT DATA						
Depth of Cover (m)	100	110	120	130	140	150
Development Height (m)	2.5	2.5	2.5	2.5	2.5	2.5
Pillar Length - centres (m)	500.0	500.0	500.0	500.0	500.0	500.0
Pillar Width - centres (m)	30.0	30.0	30.0	30.0	30.0	30.0
Roadway Width for <u>maximum</u> pillar dimension	5.5	5.5	5.5	5.5	5.5	5.5
Roadway Width for <u>minimum</u> pillar dimension	5.5	5.5	5.5	5.5	5.5	5.5
Cut-Through Angle (degrees)	90	90	90	90	90	90
Average Panel Span (m) (rib-rib width)	160.5	160.5	160.5	160.5	160.5	160.5
SG (tonnes/m <sup>3</sup> )	2.5	2.5	2.5	2.5	2.5	2.5
Conversion (tonnes to N)	10000	10000	10000	10000	10000	10000
Abutment Angle (°)	21	21	21	21	21	21
INTERMEDIATE CALCULATIONS						
Maximum Rib to Rib Pillar Length (w <sub>2</sub> )	494.5	494.5	494.5	494.5	494.5	494.5
Minimum Rib to Rib Pillar Width (w <sub>1</sub> )	24.5	24.5	24.5	24.5	24.5	24.5
w, Minimum Rib to Rib Pillar Width (ie w <sub>1</sub> sinθ)	24.5	24.5	24.5	24.5	24.5	24.5
Minimum Pillar Width/Height Ratio	9.8	9.8	9.8	9.8	9.8	9.8
Extraction Ratio (%)	19.2%	19.2%	19.2%	19.2%	19.2%	19.2%
Abutment Angle (Radians)	0.367	0.367	0.367	0.367	0.367	0.367
Cut-Through Angle (Radians)	1.571	1.571	1.571	1.571	1.571	1.571
Is the Panel Super-Critical?	Yes	Yes	Yes	Yes	Yes	Yes
D (Peng & Chiang Loading Factor)	51.300	53.804	56.196	58.491	60.699	62.829
R (Pillar 2nd Abutment Component)	0.93	0.91	0.90	0.88	0.87	0.86
Dimensionless Pillar 'Rectangularity'	1.91	1.91	1.91	1.91	1.91	1.91
Width/Height Ratio Exponent	1.00	1.00	1.00	1.00	1.00	1.00
Effective Width Factor (Omega)	1.91	1.91	1.91	1.91	1.91	1.91
Effective Width Interim	46.69	46.69	46.69	46.69	46.69	46.69
Effective Pillar Width (m)	46.69	46.69	46.69	46.69	46.69	46.69
Effective Pillar Loading Height (m)	100.00	110.00	120.00	130.00	140.00	150.00
RESULTS						
Tributary Area Loading (MPa)	3.10	3.40	3.71	4.02	4.33	4.64
Pillar Strength (UNSW Squat Pillar 1999)	38.97	38.97	38.97	38.97	38.97	38.97
Pillar Strength (UNSW w/h<5)	N/A	N/A	N/A	N/A	N/A	N/A
Safety Factor under FTA Loading (Squat Pillar)	12.59	11.45	10.49	9.69	8.99	8.39
Safety Factor under FTA Loading (w/h<5)	N/A	N/A	N/A	N/A	N/A	N/A
No. SAs, n	2	2	2	2	2	2
Single Abutment Loading (3D) - full	1.98	2.40	2.85	3.35	3.88	4.46
Single Abutment Loading (3D) - pillar	1.84	2.19	2.56	2.96	3.38	3.82
Single Abutment Loading (3D) - solid	0.14	0.21	0.29	0.39	0.50	0.64
Cell Sensitivity (MPa)	0	0	0	0	0	0
Total Pillar Loading with Single Abutment Loading	4.93	5.59	6.28	6.98	7.71	8.46
Safety Factor (under Single Abutment Loading)	7.90	6.97	6.21	5.58	5.05	4.61
Total Pillar Loading @ nA	7.06	8.20	9.42	10.72	12.10	13.55
Safety Factor @ nA	5.52	4.75	4.14	3.64	3.22	2.88
Total Pillar Loading under Double Abutment Loading	7.06	8.20	9.42	10.72	12.10	13.55
Safety Factor (under Double Abutment Loading)	5.52	4.75	4.14	3.64	3.22	2.88
Subsidence Predictions						
Notes: Mining Height (m)	2.5	2.5	2.5	2.5	2.5	2.5
Effective w/h	9.80	9.80	9.80	9.80	9.80	9.80
FTA Sp/T	0.012	0.013	0.013	0.014	0.015	0.015
FTA Sp(m)	0.031	0.032	0.034	0.035	0.036	0.038
FTA Sp/T (U95%)	0.060	0.061	0.061	0.062	0.063	0.063
FTA Sp (U95%)	0.151	0.152	0.154	0.155	0.156	0.158
nA Sp/T	0.020	0.023	0.027	0.031	0.036	0.042
nA Sp First (m)	0.050	0.058	0.066	0.077	0.090	0.105
nA Sp/T (U95%)	0.044	0.047	0.051	0.055	0.060	0.066
nA Sp First (U95%)	0.110	0.118	0.126	0.137	0.150	0.165
Max ER Subs	0.48	0.48	0.48	0.48	0.48	0.48
nA Sp Final (m)	0.060	0.069	0.080	0.092	0.107	0.126
nA Sp Final (U95%)	0.12	0.13	0.14	0.15	0.17	0.19
nA Sp Final (L95%)	-0.050	-0.048	-0.047	-0.045	-0.042	-0.039
Ecoal(GPa)	4.00	4.00	4.00	4.00	4.00	4.00
Efloor(GPa)	10.00	10.00	10.00	10.00	10.00	10.00
Eroof(GPa)	10.00	10.00	10.00	10.00	10.00	10.00
Poissons Ratio floor/roof	0.25	0.25	0.25	0.25	0.25	0.25
Shape Factor, I	1.500	1.500	1.500	1.500	1.500	1.500
virgin stress (MPa)	2.50	2.75	3.00	3.25	3.50	3.75
final vertical stress (MPa)	7.06	8.20	9.42	10.72	12.10	13.55
final pillar stress	7.06	8.20	9.42	10.72	12.10	13.55
Mean Pillar Compression (m)	0.003	0.003	0.004	0.005	0.005	0.006
Mean Roof Compression (m)	0.031	0.037	0.044	0.051	0.059	0.067
Mean Floor Compression (m)	0.031	0.037	0.044	0.051	0.059	0.067
Mean Total Compression (m)	0.065	0.078	0.092	0.107	0.124	0.141
Ecoal(GPa)	2.00	2.00	2.00	2.00	2.00	2.00
Efloor(GPa)	5.00	5.00	5.00	5.00	5.00	5.00
Eroof(GPa)	5.00	5.00	5.00	5.00	5.00	5.00
Poissons Ratio floor/roof	0.25	0.25	0.25	0.25	0.25	0.25
Shape Factor, I	1.500	1.500	1.500	1.500	1.500	1.500
virgin stress (MPa)	2.50	2.75	3.00	3.25	3.50	3.75
final vertical stress (MPa)	7.06	8.20	9.42	10.72	12.10	13.55
final pillar stress	7.06	8.20	9.42	10.72	12.10	13.55
Mean Pillar Compression (m)	0.006	0.007	0.008	0.009	0.011	0.012
Mean Roof Compression (m)	0.063	0.075	0.088	0.103	0.118	0.135
Mean Floor Compression (m)	0.063	0.075	0.088	0.103	0.118	0.135
WC Total Compression (m)	0.131	0.157	0.185	0.215	0.247	0.282



## UNSW Pillar Design Spreadsheet

Abel Mine - Upper Donaldson Seam								
INPUT DATA								
Depth of Cover (m)	90	98	105	97	100	105	103	100
Development Height (m)	2.5	2.5	2.5	2.5	2.5	2.5	2.5	2.5
Pillar Length - centres (m)	905.5	905.5	905.5	805.5	805.5	50.0	50.0	50.0
Pillar Width - centres (m)	22.0	22.0	22.0	26.5	26.5	29.0	29.0	26.5
Roadway Width for <u>maximum</u> pillar dimension	5.5	5.5	5.5	5.5	5.5	5.5	5.5	5.5
Roadway Width for <u>minimum</u> pillar dimension	5.5	5.5	5.5	5.5	5.5	5.5	5.5	5.5
Cut-Through Angle (degrees)	90	90	90	90	90	90	90	90
Average Panel Span (m) (rib-rib width)	120	120	120	89	89	140	140	105.5
SG (tonnes/m <sup>3</sup> )	2.5	2.5	2.5	2.5	2.5	2.5	2.5	2.5
Conversion (tonnes to N)	10000	10000	10000	10000	10000	10000	10000	10000
Abutment Angle (°)	21	21	21	21	21	21	21	21
INTERMEDIATE CALCULATIONS								
Maximum Rib to Rib Pillar Length (w <sub>2</sub> )	900.0	900.0	900.0	800.0	800.0	44.5	44.5	44.5
Minimum Rib to Rib Pillar Width (w <sub>1</sub> )	16.5	16.5	16.5	21.0	21.0	23.5	23.5	21.0
<b>w, Minimum Rib to Rib Pillar Width (ie w<sub>1</sub>sinθ)</b>	<b>16.5</b>	<b>16.5</b>	<b>16.5</b>	<b>21.0</b>	<b>21.0</b>	<b>23.5</b>	<b>23.5</b>	<b>21.0</b>
Minimum Pillar Width/Height Ratio	6.6	6.6	6.6	8.4	8.4	9.4	9.4	8.4
Extraction Ratio (%)	25.5%	25.5%	25.5%	21.3%	21.3%	27.9%	27.9%	29.5%
Abutment Angle (Radians)	0.367	0.367	0.367	0.367	0.367	0.367	0.367	0.367
Cut-Through Angle (Radians)	1.571	1.571	1.571	1.571	1.571	1.571	1.571	1.571
Is the Panel Super-Critical?	Yes	Yes	Yes	Yes	Yes	Yes	Yes	Yes
D (Peng & Chiang Loading Factor)	48.667	50.784	52.567	50.525	51.300	52.567	52.064	51.300
R (Pillar 2nd Abutment Component)	0.84	0.82	0.80	0.89	0.89	0.91	0.91	0.89
Dimensionless Pillar 'Rectangularity'	1.96	1.96	1.96	1.95	1.95	1.31	1.31	1.36
Width/Height Ratio Exponent	1.00	1.00	1.00	1.00	1.00	1.00	1.00	1.00
Effective Width Factor (Omega)	1.96	1.96	1.96	1.95	1.95	1.31	1.31	1.36
Effective Width Interim	32.41	32.41	32.41	40.93	40.93	30.76	30.76	28.53
Effective Pillar Width (m)	32.41	32.41	32.41	40.93	40.93	30.76	30.76	28.53
Effective Pillar Loading Height (m)	90.00	98.00	105.00	97.00	100.00	105.00	103.00	100.00
RESULTS								
Tributary Area Loading (MPa)	3.02	3.29	3.52	3.08	3.18	3.64	3.57	3.54
Pillar Strength (UNSW Squat Pillar 1999)	24.55	24.55	24.55	31.82	31.82	30.27	30.27	26.47
Pillar Strength (UNSW w/h<5)	N/A	N/A	N/A	N/A	N/A	N/A	N/A	N/A
<b>Safety Factor under FTA Loading (Squat Pillar)</b>	<b>8.13</b>	<b>7.47</b>	<b>6.97</b>	<b>10.33</b>	<b>10.02</b>	<b>8.32</b>	<b>8.48</b>	<b>7.47</b>
<b>Safety Factor under FTA Loading (w/h&lt;5)</b>	<b>N/A</b>	<b>N/A</b>	<b>N/A</b>	<b>N/A</b>	<b>N/A</b>	<b>N/A</b>	<b>N/A</b>	<b>N/A</b>
No. SAs, n	2	2	2	2	2	2	2	2
Single Abutment Loading (3D) - full	2.37	2.81	3.23	2.16	2.30	2.53	2.43	2.57
Single Abutment Loading (3D) - pillar	1.98	2.30	2.59	1.93	2.04	2.30	2.22	2.28
Single Abutment Loading (3D) - solid	0.39	0.51	0.63	0.23	0.26	0.23	0.21	0.29
Cell Sensitivity (MPa)	0	0	0	0	0	0	0	0
Total Pillar Loading with Single Abutment Loading	5.00	5.58	6.11	5.01	5.22	5.94	5.79	5.82
<b>Safety Factor (under Single Abutment Loading)</b>	<b>4.91</b>	<b>4.40</b>	<b>4.02</b>	<b>6.35</b>	<b>6.10</b>	<b>5.09</b>	<b>5.23</b>	<b>4.55</b>
Total Pillar Loading @ nA	7.76	8.91	9.97	7.41	7.78	8.70	8.44	8.68
<b>Safety Factor @ nA</b>	<b>3.16</b>	<b>2.76</b>	<b>2.46</b>	<b>4.29</b>	<b>4.09</b>	<b>3.48</b>	<b>3.59</b>	<b>3.05</b>
Total Pillar Loading under Double Abutment Loading	7.76	8.91	9.97	7.41	7.78	8.70	8.44	8.68
<b>Safety Factor (under Double Abutment Loading)</b>	<b>3.16</b>	<b>2.76</b>	<b>2.46</b>	<b>4.29</b>	<b>4.09</b>	<b>3.48</b>	<b>3.59</b>	<b>3.05</b>
Subsidence Predictions								
Notes: Mining Height (m)	2.5	2.5	2.5	2.5	2.5	2.5	2.5	2.5
Effective w/h	6.60	6.60	6.60	8.40	8.40	9.40	9.40	8.40
FTA Sp/T	0.012	0.013	0.013	0.012	0.013	0.013	0.013	0.013
FTA Sp(m)	0.031	0.032	0.033	0.031	0.032	0.033	0.033	0.033
FTA Sp/T (U95%)	0.060	0.061	0.061	0.060	0.061	0.061	0.061	0.061
FTA Sp (U95%)	0.151	0.152	0.153	0.151	0.152	0.153	0.153	0.153
nA Sp/T	0.022	0.025	0.028	0.021	0.022	0.024	0.024	0.024
<b>nA Sp First (m)</b>	<b>0.055</b>	<b>0.062</b>	<b>0.071</b>	<b>0.052</b>	<b>0.055</b>	<b>0.061</b>	<b>0.059</b>	<b>0.061</b>
nA Sp/T (U95%)	0.046	0.049	0.052	0.045	0.046	0.048	0.048	0.048
<b>nA Sp First (U95%)</b>	<b>0.115</b>	<b>0.122</b>	<b>0.131</b>	<b>0.112</b>	<b>0.115</b>	<b>0.121</b>	<b>0.119</b>	<b>0.121</b>
Max ER Subs	0.64	0.64	0.64	0.53	0.53	0.70	0.70	0.74
nA Sp Final (m)	0.066	0.075	0.085	0.063	0.066	0.073	0.071	0.073
nA Sp Final (U95%)	0.13	0.13	0.14	0.12	0.13	0.13	0.13	0.13
nA Sp Final (L95%)	-0.049	-0.048	-0.046	-0.050	-0.049	-0.048	-0.048	-0.048
Ecoal(GPa)	4.00	4.00	4.00	4.00	4.00	4.00	4.00	4.00
Efloor(GPa)	10.00	10.00	10.00	10.00	10.00	10.00	10.00	10.00
Eroof(GPa)	10.00	10.00	10.00	10.00	10.00	10.00	10.00	10.00
Poissons Ratio floor/roof	0.25	0.25	0.25	0.25	0.25	0.25	0.25	0.25
Shape Factor, I	1.500	1.500	1.500	1.500	1.500	1.500	1.500	1.500
virgin stress (MPa)	2.25	2.45	2.63	2.43	2.50	2.63	2.58	2.50
final vertical stress (MPa)	7.76	8.91	9.97	7.41	7.78	8.70	8.44	8.68
final pillar stress	7.76	8.91	9.97	7.41	7.78	8.70	8.44	8.68
Mean Pillar Compression (m)	0.003	0.004	0.005	0.003	0.003	0.004	0.004	0.004
Mean Roof Compression (m)	0.031	0.036	0.041	0.033	0.035	0.020	0.019	0.019
Mean Floor Compression (m)	0.031	0.036	0.041	0.033	0.035	0.020	0.019	0.019
<b>Mean Total Compression (m)</b>	<b>0.065</b>	<b>0.076</b>	<b>0.087</b>	<b>0.070</b>	<b>0.074</b>	<b>0.044</b>	<b>0.042</b>	<b>0.042</b>
Ecoal(GPa)	2.00	2.00	2.00	2.00	2.00	2.00	2.00	2.00
Efloor(GPa)	5.00	5.00	5.00	5.00	5.00	5.00	5.00	5.00
Eroof(GPa)	5.00	5.00	5.00	5.00	5.00	5.00	5.00	5.00
Poissons Ratio floor/roof	0.25	0.25	0.25	0.25	0.25	0.25	0.25	0.25
Shape Factor, I	1.500	1.500	1.500	1.500	1.500	1.500	1.500	1.500
virgin stress (MPa)	2.25	2.45	2.63	2.43	2.50	2.63	2.58	2.50
final vertical stress (MPa)	7.76	8.91	9.97	7.41	7.78	8.70	8.44	8.68
final pillar stress	7.76	8.91	9.97	7.41	7.78	8.70	8.44	8.68
Mean Pillar Compression (m)	0.007	0.008	0.009	0.006	0.007	0.008	0.007	0.008
Mean Roof Compression (m)	0.062	0.072	0.082	0.067	0.071	0.040	0.039	0.038
Mean Floor Compression (m)	0.062	0.072	0.082	0.067	0.071	0.040	0.039	0.038
<b>WC Total Compression (m)</b>	<b>0.130</b>	<b>0.153</b>	<b>0.174</b>	<b>0.139</b>	<b>0.148</b>	<b>0.088</b>	<b>0.085</b>	<b>0.084</b>

## UNSW Pillar Design Spreadsheet

Abel Mine - Upper Donaldson Seam				
INPUT DATA				
Depth of Cover (m)	100	103	101	100
Development Height (m)	2.5	2.5	2.5	2.5
Pillar Length - centres (m)	500.0	500.0	500.0	500.0
Pillar Width - centres (m)	27.0	28.0	28.0	28.0
Roadway Width for <u>maximum</u> pillar dimension	5.5	5.5	5.5	5.5
Roadway Width for <u>minimum</u> pillar dimension	5.5	5.5	5.5	5.5
Cut-Through Angle (degrees)	90	90	90	90
Average Panel Span (m) (rib-rib width)	160.5	160.5	160.5	160.5
SG (tonnes/m <sup>3</sup> )	2.5	2.5	2.5	2.5
Conversion (tonnes to N)	10000	10000	10000	10000
Abutment Angle (°)	21	21	21	21
INTERMEDIATE CALCULATIONS				
Maximum Rib to Rib Pillar Length (w <sub>2</sub> )	494.5	494.5	494.5	494.5
Minimum Rib to Rib Pillar Width (w <sub>1</sub> )	21.5	22.5	22.5	22.5
<b>w, Minimum Rib to Rib Pillar Width (ie w<sub>1</sub>sinθ)</b>	<b>21.5</b>	<b>22.5</b>	<b>22.5</b>	<b>22.5</b>
Minimum Pillar Width/Height Ratio	8.6	9.0	9.0	9.0
Extraction Ratio (%)	21.2%	20.5%	20.5%	20.5%
Abutment Angle (Radians)	0.367	0.367	0.367	0.367
Cut-Through Angle (Radians)	1.571	1.571	1.571	1.571
Is the Panel Super-Critical?	Yes	Yes	Yes	Yes
D (Peng & Chiang Loading Factor)	51.300	52.064	51.556	51.300
R (Pillar 2nd Abutment Component)	0.89	0.90	0.90	0.91
Dimensionless Pillar 'Rectangularity'	1.92	1.91	1.91	1.91
Width/Height Ratio Exponent	1.00	1.00	1.00	1.00
Effective Width Factor (Omega)	1.92	1.91	1.91	1.91
Effective Width Interim	41.21	43.04	43.04	43.04
Effective Pillar Width (m)	41.21	43.04	43.04	43.04
Effective Pillar Loading Height (m)	100.00	103.00	101.00	100.00
RESULTS				
Tributary Area Loading (MPa)	3.17	3.24	3.18	3.15
Pillar Strength (UNSW Squat Pillar 1999)	32.53	34.55	34.55	34.55
Pillar Strength (UNSW w/h<5)	N/A	N/A	N/A	N/A
<b>Safety Factor under FTA Loading (Squat Pillar)</b>	<b>10.25</b>	<b>10.66</b>	<b>10.87</b>	<b>10.98</b>
<b>Safety Factor under FTA Loading (w/h&lt;5)</b>	<b>N/A</b>	<b>N/A</b>	<b>N/A</b>	<b>N/A</b>
No. SAs, n	2	2	2	2
Single Abutment Loading (3D) - full	2.26	2.29	2.20	2.16
Single Abutment Loading (3D) - pillar	2.02	2.06	1.99	1.95
Single Abutment Loading (3D) - solid	0.24	0.23	0.21	0.20
Cell Sensitivity (MPa)	0	0	0	0
Total Pillar Loading with Single Abutment Loading	5.19	5.30	5.17	5.10
<b>Safety Factor (under Single Abutment Loading)</b>	<b>6.27</b>	<b>6.52</b>	<b>6.69</b>	<b>6.77</b>
Total Pillar Loading @ nA	7.69	7.82	7.58	7.46
<b>Safety Factor @ nA</b>	<b>4.23</b>	<b>4.42</b>	<b>4.56</b>	<b>4.63</b>
Total Pillar Loading under Double Abutment Loading	7.69	7.82	7.58	7.46
<b>Safety Factor (under Double Abutment Loading)</b>	<b>4.23</b>	<b>4.42</b>	<b>4.56</b>	<b>4.63</b>
Subsidence Predictions				
Notes: Mining Height (m)	2.5	2.5	2.5	2.5
Effective w/h	8.60	9.00	9.00	9.00
FTA Sp/T	0.013	0.013	0.013	0.013
FTA Sp(m)	0.032	0.032	0.032	0.031
FTA Sp/T (U95%)	0.061	0.061	0.061	0.061
FTA Sp (U95%)	0.152	0.152	0.152	0.151
nA Sp/T	0.022	0.022	0.021	0.021
<b>nA Sp First (m)</b>	<b>0.054</b>	<b>0.055</b>	<b>0.054</b>	<b>0.053</b>
nA Sp/T (U95%)	0.046	0.046	0.045	0.045
<b>nA Sp First (U95%)</b>	<b>0.114</b>	<b>0.115</b>	<b>0.114</b>	<b>0.113</b>
Max ER Subs	0.53	0.51	0.51	0.51
nA Sp Final (m)	0.065	0.066	0.064	0.063
nA Sp Final (U95%)	0.13	0.13	0.12	0.12
nA Sp Final (L95%)	-0.049	-0.049	-0.049	-0.049
Ecoal(GPa)	4.00	4.00	4.00	4.00
Efloor(GPa)	10.00	10.00	10.00	10.00
Eroof(GPa)	10.00	10.00	10.00	10.00
Poissons Ratio floor/roof	0.25	0.25	0.25	0.25
Shape Factor, I	1.500	1.500	1.500	1.500
virgin stress (MPa)	2.50	2.58	2.53	2.50
final vertical stress (MPa)	7.69	7.82	7.58	7.46
final pillar stress	7.69	7.82	7.58	7.46
Mean Pillar Compression (m)	0.003	0.003	0.003	0.003
Mean Roof Compression (m)	0.032	0.034	0.032	0.032
Mean Floor Compression (m)	0.032	0.034	0.032	0.032
<b>Mean Total Compression (m)</b>	<b>0.068</b>	<b>0.071</b>	<b>0.068</b>	<b>0.067</b>
Ecoal(GPa)	2.00	2.00	2.00	2.00
Efloor(GPa)	5.00	5.00	5.00	5.00
Eroof(GPa)	5.00	5.00	5.00	5.00
Poissons Ratio floor/roof	0.25	0.25	0.25	0.25
Shape Factor, I	1.500	1.500	1.500	1.500
virgin stress (MPa)	2.50	2.58	2.53	2.50
final vertical stress (MPa)	7.69	7.82	7.58	7.46
final pillar stress	7.69	7.82	7.58	7.46
Mean Pillar Compression (m)	0.006	0.007	0.006	0.006
Mean Roof Compression (m)	0.064	0.067	0.065	0.064
Mean Floor Compression (m)	0.064	0.067	0.065	0.064
<b>WC Total Compression (m)</b>	<b>0.135</b>	<b>0.141</b>	<b>0.136</b>	<b>0.134</b>

